Novel Fibrous Catalyst in the Decomposition of Airborne Chemical Agents at Moderate Temperatures

Gabriela Nagy

Ph.D.

2011

Novel Fibrous Catalyst in the Decomposition of Airborne Chemical Agents at Moderate Temperatures

By

Gabriela Nagy

(MEng, MSc)

Thesis submitted in partial fulfilment for the award of Doctor of Philosophy in Chemistry at the Faculty of Health and Life Sciences, De Montfort University Leicester, United Kingdom

August 2011

Dedicated to my family

Acknowledgement

Abstract

Volatile organic compounds (VOCs) are an important source of air pollution. The reduction of VOCs concentration in air, including their catalytic oxidation is becoming increasingly important, not only because of their toxicity, and typical or unpleasant odour, but also because of their environmental impact (smog, greenhouse gases, acid rain, etc). Many effective catalysts (mostly noble metals or metal oxides deposited on different supports) have been developed and tested for the catalytic decomposition of different classes of VOCs. The main disadvantage of these catalysts is the high working temperatures (most of them above 500 °C) and sometimes high operating pressures. The need of fast, efficient and economical decontamination technologies was also recognized in the security sector, especially for the use in the clean-up phase after a chemical, biological, radiological or nuclear (CBRN) incident (deliberate or accidental) that affects the quality of air and water.

The aim of this research was to develop an alternative technology for the decomposition of airborne VOCs, based on the use of a novel heterogeneous modified polyacrylonitrile (PAN) fibrous catalyst, used as yarn or as knitted mesh, with or without the addition of H_2O_2 solution, and operating under mild conditions (moderate temperature and ambient pressure), contrary to most catalytic oxidation processes reported to date.

The efficiency of the modified PAN catalyst was first tested in static mode, for the decomposition of a variety of chemical agents. This study provided the first comprehensive experimental evaluation of the potential use of the novel catalyst for gas phase reactions. A fixed bed catalytic reactor (44 cm^3 volume) with temperature control and on-line analysis of gas samples was designed and constructed, enabling dynamic mode tests (at 45 °C and atmospheric pressure) on the efficiency of the fibrous catalyst in the decomposition of sulphur VOCs. The reaction products for the catalytic decomposition of ethyl mercaptan (EtSH) were identified and quantified and the conversion of reactant and turnover frequency for the catalyst were evaluated. The main product of this reaction was diethyldisulphide. It was determined that the physical form, but mainly the packing of the catalyst in reactor was responsible for differences in breakthrough time, which increased from 2.5 hours for catalyst used as threads to 29 hours for catalyst used as mesh.

Further, a novel laboratory scale decontamination unit comprising of an absorption column and a three-phase (gas-liquid-solid) catalytic reactor with temperature control and the possibility of on-line analysis of gas samples was developed. The designed unit ensured the simultaneous and continuous presence of organic pollutant, fibrous catalyst and H_2O_2 solution in the system, being suitable for the decontamination of a continuous flow of polluted air, at moderate or ambient temperature and atmospheric pressure. The operating conditions were optimized in order to achieve the best performance for the unit.

The efficiency of this system was evaluated for the decomposition of EtSH (93.3 mg/m^3 air) at 45 °C and at ambient temperature, and for a mixture of EtSH (93.3 mg/m^3 air) and dimethyl sulphide (DMS, 100 mg/m^3 air) at ambient temperature. Ethane sulphonic acid was identified and quantified for the oxidation of EtSH both at 45 °C and at ambient temperature and the mixture of ethane and methane sulphonic acids was identified for the oxidation of the mixture of EtSH and DMS. The system was operated in steady state, with the main reaction products being the sulphonic acids.

An amount of 20.1 g catalytic mesh (50% catalytic threads, [Fe] = 0.52 mmol Fe/g threads) was used in the presence of 100 mg/L H_2O_2 solution (2.4 mL/min) for a total of 1504 hours (about 62 days) as following: 415 hours in the decomposition of EtSH at 45 ˚C, 309 hours in the decomposition of EtSH at ambient temperature and 780 hours in the decomposition of the mixture of EtSH and DMS. A total of 45.12 L of air were treated, the total amount of VOCs passing through the unit was 252.67 mg EtSH and 140.4 mg DMS.

Table of contents

List of figures

List of tables

Abbreviations

[A] - Concentration of 'A'

AOP - Advanced oxidation process

CAS - Chemical Abstracts Service

CBRN - Chemical, biological, radiological or nuclear (incident)

CNM - Chloronitromethane

COD - Carbon oxygen demand

CP - Chloropicrin CCl_3NO_2

CWA - Chemical warfare agents

$d_{catalyst\ bed}$ - Density of the catalyst bed

DCE - 1 ,2-dichloroethane

DCM - Dichloromethane

DCNM - Dichloronitrometane

Defra - Department for Environment, Food and Rural Affairs

DES - Diethyl sulphide, $(C2H5)_2S$

DMDS - Dimethyl disulphide, $(CH_3)_2S_2$

DMS - Dimethyl Sulphide $(CH_3)_2S$

$d_{PP\ bed}$ - Density of polypropylene bed

$d_{catalyst\ bed}$ - Density of catalyst bed

EA - Environment Agency (UK)

EC - European Commission

ECD - Electron capture detector

EPA - Environmental Protection Agency (USA)

EtSH - Ethyl Mercaptan (Ethanethiol), C_2H_5SH

$EtSO_3H$ - Ethane sulphonic acid

FID - Flame Ionization Detector

FTIR - Fourier Transform Infra Red (spectroscopy)

GC - Gas Chromatograph

GC-MS - Gas Chromatograph – Mass Spectrometer

GFC - Glass fibre catalysts

HPA - Health Protection Agency

IC - Ion Chromatography

LPG - Liquefied petroleum gases

λ_{max} - Wavelength for which the absorption is maximal

m_{cat} - Mass of catalyst

$m_{control}$ - Mass of raw threads/mesh used as control

MeCN - Acetonitrile

$MeSO_3H$ - Methane sulphonic acid

m_{PP} - Mass of polypropylene

MT - Methanethiol

NHS –National Health Service

NO - Oxides of nitrogen

OSHA - Occupational Safety and Health Administration (USA Department of Labour)

P - Pollutant

PAN - Polyacrylonitrile

PEL - Permissible Exposure Limits

PP - Polypropylene

ppm - Parts per million

ppmv - Parts per million (volumetric)

Pt/FC/C - Pt/fluorinated carbon/ceramic

RP-HPLC - Reversed Phase High Performance Liquid Chromatography

RSH - Mercaptan

R_t - Retention time

SEM - Secondary electron multiplier

SPME - Solid Phase Micro Extraction

SV - Space velocity

T - Residence time

TCE - Trichloroethylene

TOF - Turnover Frequency for the catalyst

TPD - Temperature programmed desorption

UV - Ultra violet

v/v - Volume/volume

V_{cat} - Volume of catalyst

V_{liquid} - Volume of liquid

VOC - Volatile organic compound

V_{PP} - Volume of polypropylene

w/w - Weight/weight

X - Conversion of reactant

Chapter 1. Introduction

1.1. Background

Clean air means life, as air is the number one element that sustains our lives! Without air, the average human being would only live about three minutes. It was estimated that the average adult takes about 14 breaths per minute, with a tidal volume of 0.5 L, totalling about seven litters per minute or approximately 10 m^3 of air per day. At an average air temperature of 20 °C, this means about 12 kg of air every day (Tidal volume, 2011). Because of these facts alone, the importance of the air we breathe and its quality must never be treated indifferently.

Air pollution is a constant problem and can affect the quality of our lives, reducing the life expectancy by seven to eight months for average people. This can increase to 9 years for people who are especially sensitive and are exposed to the worst pollution, an 11.2% reduction considering that in the UK the average life expectancy is around 80 years (NHS, 2011; HPA, 2010).

There are different sources of air pollution and they may be anthropogenic (man-made) or natural. Generally any substance that people introduce intentionally or by accident into the atmosphere, that has damaging effects on living things and the environment is considered air pollution. The levels of anthropogenic pollution are regulated (EA, 2011). The main anthropogenic sources are: burning of fossil fuels in electricity generation, transport, industry and households; industrial processes and solvent use, (e.g. in chemical and mineral industries); agriculture and waste treatment.

Toxic (known as hazardous) air pollutants are those compounds that are known or suspected to cause serious health or adverse environmental effects (EPA, 2011). Volatile organic compounds (VOCs) are an important source of pollution, and thus the reduction of VOCs concentration in air is becoming increasingly important, not only because of their toxicity, and typical or unpleasant odour, but also because of their environmental impact (smog, greenhouse gases, acid rain, etc). VOCs containing reduced sulphur such as thiols and thioethers are released mostly from biological activities, but also a number of manufacturing processes, such as papermaking and petroleum refining (Kachina *et al.,* 2006). Different techniques are available for the reduction of VOC emissions to air, grouped into two main categories: *destruction techniques* aiming to decompose the VOCs (thermal, catalytic, or biological oxidation), and *recovery techniques* aiming to separate and reuse the recovered VOCs (condensation, adsorption and absorption).

Concentrating on the catalytic oxidation as a method of reduction of VOCs concentrations in air, work has been done on the development and testing of effective

catalysts for the catalytic decomposition of different classes of VOCs. Most of the reported research is based on noble metals (Pt and Pd) deposited on different supports, such as: *alumina* (Gonzales-Velasco *et al.,* 1998; Aranzabal *et al.,* 2000; Sinquin *et al.,* 2001; Chu *et al.,* 2001; Chauhan, *et al.,* 2003), *zeolites* (López-Fonseca *et al.,* 2003), *glass fibres* (Balzhinimaev *et al.,* 2003; Balzhinimaev *et al.,* 2010) or metal oxides deposited on supports such as MnO/Fe_2O_3 (Chu *et al.,* 2003). All of these catalysts operate at temperatures above 500 °C (some of them at elevated pressures, too), with very few reported to be effective at temperatures lower than 200 °C. The only catalysts that are efficient at low temperatures are those based on wood and coal ash (Kastner *et al.,* 2002; Kastner *et al.,* 2003), operating at 25 °C.

A novel catalyst based on modified polyacrylonitrile (PAN) fibres has been developed at De Montfort University (Huddersman and Ishtchenko; 2007 and 2008), and is currently used in wastewater treatment trials. However, this catalyst has never been tested towards the decontamination of air.

The need of fast and efficient decontamination technologies was also recognized in the security sector, especially for the use in the clean-up phase within the recovery phase after a chemical, biological, radiological or nuclear (CBRN) incident (deliberate or accidental) that affects the quality of the air and water. Regardless of their origin (deliberate or accidental), any incident involving unidentified substances is considered a CBRN incident that requires fast and efficient methods and technologies to minimize the effect of the chemical release on the public and environment. Protective equipment and filters based on different absorbers (mostly activated carbon or activated carbon

impregnated with metal ions) are used along with biofilters in order to protect the emergency response team and to decontaminate the affected air (Home Office, 2008; Strategic National Guidance, 2008; Communities, 2011).

Therefore, the development of environmentally friendly and cost-effective air treatment technologies for reducing the level of VOCs in air, including the development of new catalysts for their catalytic oxidation is a timely research topic.

1.2. Research aim and objectives

The aim of this research was to test the capability of the novel modified PAN catalyst used as threads or as an open knitted mesh, with and without addition of H_2O_2 solution, to decompose a range of air borne toxic VOCs and other chemical agents, and to theoretically incorporate the catalyst into gas-liquid-solid flow reactors which can be fitted into modified ISO containers to provide mobile decontamination units (for use in the case of a CBRN incident), operating at moderate temperature (4–45 °C) and ambient pressure.

In order to achieve this aim, the following objectives were set:

1. To design and construct a fixed bed catalytic reactor suitable for the dynamic study of gas phase decomposition of VOCs, with temperature control and on-line analysis of gas samples.

2. To investigate the catalyst efficiency in the decomposition of selected VOCs in both static and dynamic studies, using the designed reactor, with and without the addition of H_2O_2 solution into the system.

3. To optimize the experimental conditions and to identify the reaction products of VOC decomposition.

4. To design and construct a laboratory scale decontamination unit incorporating a three-phase catalytic reactor, suitable for the dynamic study of VOCs decomposition in gas–solid–liquid system, with temperature control and on-line analysis of the gas samples.

5. To optimize the operating parameters for the laboratory scale decontamination unit and to identify and quantify the reaction products for the decomposition of ethyl mercaptan (EtSH) and dimethyl sulphide (DMS), singly and as mixtures.

6. To investigate the potential use of the proposed decontamination unit in emergency responses, and to evaluate the cost implications of the decontamination of air using a commercial size unit (scale-up based on the laboratory scale design).

1.3. Research methodology

The preliminary studies involving different organic compounds as surrogate pollutants and catalyst as threads or mesh, were carried out at 45 °C, in static mode, using crimp sealed glass vials as reaction vessel. The change in the gas composition was monitored

by periodic sampling and gas chromatographic (GC) analysis. Control experiments with raw PAN threads or mesh were performed for comparison. The compound for which the decomposition was maximal in static experiments (i.e. EtSH) was used in further dynamic studies in the designed gas-solid fixed bed catalytic reactor. The studies were performed at 45 °C, using the catalyst both as threads and as mesh. The composition of the gas effluent was monitored in time by periodic GC analysis. The reaction products were identified and quantified. The conversion of reactant and the turnover frequency for the catalyst were evaluated for both cases and compared.

The influence of addition of H_2O_2 into the system was initially studied at 45 °C, with catalyst as mesh, in the laboratory scale decontamination unit incorporating the designed three phase catalytic reactor, operated either in scrubber or slurry regime. The gas effluent was monitored by periodic GC analysis to determine breakthrough of reactant and to quantify both reactant and gas phase reaction products. The liquid effluent was analysed periodically using gas chromatography–mass spectrometry (GC-MS) and ion chromatography (IC); oxidation products were identified and quantified. The consumption of H_2O_2 was continuously monitored by visible spectroscopy (VIS). The performance of the unit was evaluated and the design of the decontamination unit was modified until the best efficiency was achieved. This was evaluated with respect to the presence of very low concentrations of both reactant and reaction products identified in the gas phase effluent and steady state consumption of H_2O_2 and production of advanced oxidation products in the liquid phase. In the final version of the laboratory scale decontamination unit, in order to improve the mass transfer of the organic pollutant from the gas to the liquid phase, the contaminated air and the H_2O_2 solution

flow through an absorption column before entering the catalytic reactor. The performance of this unit was evaluated towards the decomposition of a single pollutant (i.e. EtSH) at 45 °C and at ambient temperature, and towards a mixture of two VOCs (EtSH and DMS) at ambient temperature.

A simplified cost estimation for the commercial scale-up of the final version of the laboratory scale decontamination unit was calculated taking into account capital costs, daily running costs and costs with chemicals used in the regeneration of the catalyst.

1.4. Main contributions of the thesis

The main contributions of this research work can be summarized as follows:

- A detailed evaluation of the factors that affect the performance of the novel fibrous modified PAN catalyst in the gas phase decomposition of several airborne VOCs without addition of H_2O_2 is provided. This study offers the first comprehensive experimental evaluation of the potential use of the modified PAN catalyst for gas phase reactions.

- A laboratory scale fixed bed catalytic reactor with temperature control and on-line analysis of the gas samples was designed and constructed. The reactor is suitable for the decontamination of an air flow contaminated with sulphur VOCs (i.e. EtSH),

using the novel modified PAN catalyst in dry conditions (without addition of H_2O_2 solution), at moderate temperature and atmospheric pressure.

- The performance of the designed catalytic reactor towards the decomposition of a single pollutant (EtSH) in the air stream at 45 °C and atmospheric pressure was evaluated by elucidating the nature and quantifying the oxidation products.

- A novel laboratory scale decontamination unit comprising of an absorption column and a three-phase (gas-liquid-solid) catalytic reactor with temperature control and the possibility of on-line analysis of gas samples was designed, constructed and developed. The designed unit ensures the simultaneous and continuous presence of organic pollutant, fibrous catalyst and H_2O_2 solution in the system, and is suitable for decontamination of a continuous flow of polluted air, at moderate or ambient temperature and atmospheric pressure.

- A comprehensive evaluation of the factors that influence the efficiency of the decontamination unit and guidelines for the optimal operating process conditions are provided in order to achieve the best performance for the modified PAN/H_2O_2 solution catalytic system in the lab-scale decontamination unit.

- The performance for the proposed decontamination unit was evaluated for the decomposition of a single pollutant (i.e. EtSH) at 45 °C and at ambient temperature and of a mixture of sulphur VOCs in the air stream, at ambient temperature, by elucidating the nature and quantifying the oxidation products. All studies were performed at atmospheric pressure.

- A step-by-step procedure to be followed in case of emergency response in a CBRN incident with air contamination, and guidelines for optimal operational process parameters are provided in the form of a flow chart. The treatment is assumed to be performed in a portable decontamination unit (scaled up version of the designed laboratory scale decontamination unit), incorporating a 33 m^3 catalytic reactor housed in a 20 ft long ISO container.

1.5. Thesis structure

The thesis is structured into nine chapters, with two extra sections: one allocated to references and one to appendices. A brief description of each chapter is presented below:

Chapter 2. Literature review: This chapter provides an overview of the scientific work published with regard to available methods used in the decontamination of air from VOCs, aiming to provide a relevant context of the research. After a short introduction on the VOC topic and the methods available for the reduction of VOCs concentration in air, the review concentrates on the catalytic oxidation of different classes of VOCs, reaction conditions and catalysts used. The Fenton and Fenton-like processes for liquid phase catalysis, with their advantages and limitations are also presented before introducing the novel modified fibrous catalyst tested in this research.

Chapter 3. Materials, instruments and methods: Describes the instruments used for the analysis of gas and liquid samples during the study, presenting at the same time the sample collection, preparation and analysis procedure, materials used and operating conditions for the instruments.

Chapter 4. Preliminary study for the catalytic decomposition of airborne VOCs: This chapter presents the results of a preliminary study for the catalytic decomposition of four airborne VOCs in static experiments, using the novel fibrous catalyst as threads or as mesh, and oxygen from air as oxidant. In the final part the effect of addition of H_2O_2 into the system is also presented.

Chapter 5. Gas-solid catalytic decomposition of airborne EtSH: This chapter presents the results of dynamic mode experiments with EtSH as model air pollutant, the novel catalyst (as threads or as knitted mesh) and oxygen from air (of ambient or increased humidity) as oxidant, indicating at the same time the reaction products of the catalytic process.

Chapter 6. Gas-liquid-solid catalytic decomposition of airborne EtSH: This chapter presents the results of the dynamic study of the catalytic decomposition of EtSH as surrogate air pollutant, the novel catalyst (as knitted mesh) and H_2O_2 solution as additional oxidant. As advanced oxidation products were identified and quantified, it was concluded that in the presence of H_2O_2, the modified PAN catalyst proves to be more effective in the advanced oxidation of organic pollutants than in the presence of O_2 from air alone. The study was performed in a three phase catalytic reactor designed for this purpose, operated in either scrubber or slurry regime, and then modified in order

to improve its performance. The reasoning behind switching from one operational regime to the other and then redesigning the decontamination unit is also presented here, along with the unit performance evaluated at 45 °C and at ambient temperature.

Chapter 7. Gas-liquid-solid catalytic decomposition of a mixture of VOCs in air: This chapter presents the evaluation of the performance for the laboratory scale decontamination unit for a simulated 'real life' contamination that would require an emergency response. The study was performed at ambient temperature, with a simulated 'real' contaminated air flow (50:50 v/v mixture of EtSH and DMS with air), the novel catalyst (as knitted mesh) and H_2O_2 solution.

Chapter 8. Portable decontamination unit for emergency responses, based on the modified PAN/H_2O_2 catalytic system: The chapter introduces some aspects regarding the emergency response procedures in the case of a CBRN incident, and presents a simplified cost estimation for the potential scale-up of the laboratory scale unit to a portable decontamination unit incorporating the catalytic reactor housed in a modified 20 ft long ISO container. Recommendations for possible cost reductions are also made.

Chapter 9. Conclusions and recommendations: This last chapter provides a summary of the findings resulting from this work and makes some recommendations for further research.

Chapter 2. Literature review

2.1. Volatile organic compounds

Volatile organic compounds (VOCs) are defined as any organic compound having an initial boiling point less than or equal to 250 °C measured at a standard atmospheric pressure of 101.3 kPa, that can affect the environment and human health by doing damage to visual or audible senses. According to EC Directive 1999/13/EC (Solvent Emissions Directive), VOCs are functionally defined as organic compounds having at 293.15 K (i.e., 20°C) a vapour pressure of 0.01 kPa (0.075 mm Hg) or more, or having a corresponding volatility under particular conditions of use (European Solvents Industry Group, 2008). Although VOCs include both naturally occurring and anthropogenic (man-made) chemical compounds, only the anthropogenic VOCs are regulated, especially for indoor air quality. Indoor VOCs concentration can reach higher values due to accumulation and thus they pose a greater danger to humans, as the effect of repeated exposure even to low concentrations of VOCs develops slowly and is usually chronic rather than acute.

Many hydrocarbons and substituted derivatives including nitrogenous, chlorinated, and sulphurated compounds are categorised as VOCs. Volatile organic compounds containing reduced sulphur such as thiols and thioethers are released mostly from biological activities and a number of manufacturing processes, such as papermaking and petroleum refining (Kachina *et al.,* 2006). Sewage and industrial wastewater plants are examples of places of their pronounced anthropogenic generation. These compounds are also found in the industries that manufacture or utilize organic solvents: petrochemical, pulp or coating industry; they have a strong unpleasant odour and very low perceptibility thresholds, some of them being also toxic. Some VOCs, such as mercaptans, sulphides or amines, are not extremely toxic but may have offensive odours even at extremely low concentration.

Ethyl Mercaptan (Ethanethiol, EtSH) has a strongly disagreeable odour that humans can detect in minute concentrations. The threshold for human detection is as low as one part in 2.8 billion parts of air. Its odour resembles that of leeks or onions. With a vapour pressure of 442 mmHg at 20 °C (Lide, 1992), EtSH is intentionally added to butane and propane to impart an easily noticed smell to these odourless fuels, that otherwise pose a threat of fire and explosion. If inhaled, EtSH is irritant and harmful (Jou *et al.,* 2001), the admissible limit in air is 25 mg/m^3 air (10 ppmv) (OSHA, 2008).

Acetonitrile (MeCN) is a chemical compound manufactured at industrial scale and is used as a solvent in the production of pharmaceuticals, perfumes, pesticides, plastics and as a non-aqueous solvent for inorganic salts. It is also used in the photographic industry, in the extraction and refining of copper, in the textile industry, in lithium

batteries, for the extraction of fatty acids from animal and vegetable oils, and in analytical chemistry laboratories. Acetonitrile is also a byproduct of acrylonitrile production (Micaroni *et al.,* 2004; Zhuang *et al.,* 1999*)*. Acetonitrile is toxic and flammable. The levels causing toxicity in humans are unknown but OSHA set the admissible limit in air to 40 ppmv (70 mg/m^3 air) (OSHA, 2008)*,* as MeCN is metabolized into the extremely harmful and toxic compound, hydrogen cyanide (Micaroni *et al.,* 2004*)*. Acetonitrile is a common pollutant in water, but is also found in air because of its high volatility (73 mmHg at 20 °C) (Lide, 1992). It is widely used as a solvent, and mixed with water is used as a mobile phase in Reversed Phase High Performance Liquid Chromatography (RP-HPLC). It is irritant and toxic by inhalation, ingestion or skin absorption (Addamo *et al.,* 2005*)*.

Chloropicrin (CP) is a very volatile (vapour pressure: 18.3 mm Hg at 20 °C), colourless oily liquid with a strong, sharp, highly irritating odour, being also a strong lachrymator (Wade *et al.,* 2002*)*. Its main use today is in pre-plant soil fumigation and wood treatment, as a warning agent in commercial fumigants, and in organic synthesis. CP has been used as an insecticide since 1917 and as a soil fumigant since 1920 (Spokas *et al.,* 2006; Wilson *et al.,* 1999; Zheng *et al.,* 2003). It was also used as a "tear gas" by military forces during World War I *(*Muir *et al.,* 2002; Burk and Flowerree, 1991). At that time it was considered by the US military to be among the top four chemical warfare agents, the others being chlorine, mustard gas and phosgene. After World War II, however, the importance of chloropicrin for military use decreased dramatically. Chloropicrin is considered less toxic than phosgene, but more toxic than chlorine. For this reason, many combinations were made from these gases with other substances

intended to assist them in their action. CP requires a higher degree of concentration to cause a suffocative action than could readily be obtained in field use. It was frequently used in conjunction with phosgene against the enemy, hoping that the prompt irritant effect of the chloropicrin would prevent the wearing of the gas mask, thus rendering the soldier an easy prey to the accompanying phosgene. Protective equipment was developed for use in contaminated atmosphere, gas masks with layers of micro fibres and activated carbon for adsorption of a large range of chemical warfare gases, including chloropicrin (Cole *et al.,* 2007).

The odour is a distinctive warning property of this liquid compound, and it can be detected at very low levels. The symptoms people can experience after exposure to air contaminated with chloropicrin are presented in Table 1 (Huebner, 2008*).*

Table 2.1. Symptoms after exposure to different concentrations of chloropicrin

1 ppm (v/v)	Irritation with pain in the eyes
4 ppm (v/v)	Incapacitates exposed individuals
20 ppm (v/v)	Definite bronchial or pulmonary lesions

Chloropicrin can also be found in potable water after disinfection treatment with disinfectants like chlorine, chloramines and ozone, as a disinfection byproduct. Chloropicrin is toxic to aquatic animals and to mammals (Cole *et al.,* 2007), and can easily enter the troposphere where is photolysed to phosgene (which will hydrolyze to carbon dioxide and hydrogen chloride), another toxic compound.

Environmentally benign and cost-effective air pollution control technology for reduced sulphur compounds is still a hot topic of research, e.g., in pulp and paper industry. Dimethyl sulphide (DMS) and ethyl mercaptan (EtSH) are two common contaminants of Earth's atmosphere, their oxidation leading to the formation of tropospheric SO_2, which eventually becomes H_2SO_4, one of the main components in acid rain (Babich and Stotzky, 1978; Sarbak, 1996; Bentley and Chasteen, 2004). Reduced sulphur compounds have also found their use as chemical warfare agents (CWAs). For example, the main component of the well-known vesicant yperite, or mustard gas, is bis(2-chloroethyl) sulphide (Vorontsov *et al.,* 2001).

Reduction of VOCs concentration in air is becoming more and more important, not only because of their toxicity, and typical or unpleasant odour, but also because of their environmental impact (smog, greenhouse gases). There are two types of techniques used in industry in order to reduce the emission of VOCs to air: (i) destruction techniques and (ii) recovery techniques (Allen and Blaney, 1985; and Straitz, 1993).

(i) Destruction techniques. Oxidation of VOCs is widely applied and the process is performed in installations called incinerators. This can be done by:

1. **Thermal oxidation (incineration)**, which requires very high temperatures (up to 1000 °C) and sophisticated equipment; the method is suitable for a very broad range of VOC concentrations, from 10 to 10000 ppm. Thermal oxidizers have the broadest applicability of all the VOC control devices and can be used for almost any VOC compound, usually providing destruction efficiencies that exceed 95-99%. The main limitation of thermal oxidizers is the large amount of fuel required

to heat the gas stream to the temperature necessary for high-efficiency VOC destruction.

2. **Catalytic oxidation**, when due to the presence of the catalyst, the oxidation reactions can be performed at temperatures in the range of 250 °C to 575 °C. Common types of catalysts include noble metals (i.e. platinum and palladium) and ceramic materials. Working at substantially lower temperatures than thermal oxidizers, VOC destruction by catalytic oxidizers usually exceeds 95-99%. The catalytic process is more suitable for lower concentrations of VOCs and is usually implemented as a cyclic process. The main disadvantage of catalytic systems is that the catalyst can be sensitive to poisoning by sulphur, chlorines and other oxidation products and that the catalyst has to be replaced often. There are other methods, such as plasma oxidation, plasma-catalytic oxidation, photocatalytic oxidation or ozonisation, used more for research studies at laboratory scale than for large scale removal of VOCs from air.

3. **Biological oxidation** - is a relatively new control method in the air pollution control field. VOCs can be removed by forcing them to absorb into an aqueous liquid or moist media inoculated with microorganisms that consume the dissolved and/or adsorbed organic compounds. The bio-absorbers consist of an irrigated packed bed that hosts the microorganisms (biofilters). They work at temperatures not higher than 40 °C in order to avoid harming the organisms. Biological oxidation systems are used primarily for very low concentration VOCs in air (sometimes less than 100 ppmv). The overall VOC destruction efficiencies are

often above 95%. One limitation of this technique is the type of VOC; the method is not suitable for certain compounds that are toxic to the microorganisms.

(ii) Recovery techniques. These techniques are used for economical purposes, and are being used more and more in industry. The most important methods are:

1. **Condensation** - by chilling or pressurisation - efficient low gas flows containing VOCs with boiling points above 40 °C and relatively high concentrations (>5000 ppm). The concentration of VOCs is reduced to the level equivalent to the vapour pressures of the compounds at the operating temperature. The removal efficiencies are in the 90 to 99% range depending on the vapour pressures of the specific compounds.

2. **Adsorption**, where VOC molecules are physically bound to the high surface area presented by carbon, zeolite, or organic polymer used as the adsorbent. The gas stream, rich in VOCs is often cooled prior to entry into the adsorption system, because the effectiveness of adsorption improves at lower temperatures. When the adsorbent is approaching saturation with organic vapour, the bed is isolated from the gas stream and desorbed. Low-pressure steam, hot air or nitrogen is often used to remove the adsorbed organic compounds, thus regenerating the adsorbent bed and allowing its reuse. The concentrated stream from the desorption cycle is treated to recover the organic compounds. This method is suitable for high concentrations of VOCs in air.

3. **Absorption**, where the air stream is put in contact with a liquid solvent in a scrubber, designed to provide a liquid-vapour contact area necessary to facilitate mass transfer (method suitable for VOC concentrations in the range 500-5000 ppm) (Van der Braken, 2008). The liquid containing the absorbed VOCs is then treated in order to recover the organic compounds. Wet scrubbers using oxidizing chemicals such as ClO_2, NaOCl, H_2O_2 or ozone can also be used to treat off-gases; this is a destructive method, the VOCs will not be recovered.

The work presented here is directed to a destruction technique, aiming to extensively oxidize the organic pollutants, if possible to mineralise them.

2.2. Catalytic oxidation of volatile organic compounds

Direct combustion has been, up to now, the conventional incineration treatment for any VOC, but temperatures exceeding 800–1000 °C are required to obtain complete decomposition and make it very expensive. In addition, the presence of chlorine or other heteroatom in VOC molecules tends to yield a large amount of highly toxic products of incomplete combustion. The catalytic oxidation (incineration) at less severe conditions (lower temperature) is a promising alternative for removal of halocarbon traces. These systems use catalysts based on precious metals and operate typically at 200 to 350°C. Compared to thermal oxidation units, the catalytic units are much smaller in size and weight and their overall performance is greater. These benefits, together with low

oxides of nitrogen (NO) emissions, make catalytic systems a very attractive solution to VOC emission control (Noordally *et al.,* 1994).

Catalysts reported for destructive oxidation of chlorinated VOC mostly consist of transition metal oxides and noble metals on acidic supports (Agarwal *et al.,* 1992; Bickle *et al.,* 1994; Rossin and Farris, 1993; Balzhinimaev *et al.,* 2010). Most research has been focused on platinum catalysts with very little work reported on combustion of halogenated VOC over supported palladium (Aranzabal *et al.,* 2006). Since Pd is significantly less expensive and more abundant than platinum and rhodium its use is being continuously explored as a potential substitute for the more expensive metals. In addition to high activity, these oxidation catalysts have to minimise the formation of hazardous incomplete oxidation products under operating conditions, such as HCl, Cl_2, and other chlorinated hydrocarbons. The preferred product is HCl, as it can be readily scrubbed downstream of the catalytic oxidiser preventing its exit from the stack.

The catalytic decomposition of various classes of VOCs, including chlorinated compounds, hydrocarbons, sulphides, mercaptans, amines, etc., was investigated by different research groups (Spivey, 1987; Noordally *et al.,* 1994; Alkaraz *et al.,* 1998; Iliev *et al.,* 1999; Poplawski *et al.,* 2000; Schneider *et al.,* 2000; Sinquin *et al.,* 2001; Chauhan, *et al.,* 2003; Balzhinimaev *et al.,* 2003; Balzhinimaev *et al.,* 2010).

Gonzales-Velasco *et al.* (1998) used alumina supported noble metal catalysts (Pt and Pd) for the complete catalytic oxidation of 1,2-dichloroethane (DCE) and trichloroethylene (TCE), compounds which are well known chlorinated volatile organic compounds. Their experiments were performed at conditions of lean hydrocarbon

concentration (around 1000 ppmv) in air, between 250 °C and 550 °C and at atmospheric pressure, with the authors claiming total destruction of these compounds. The authors concluded that palladium catalysts were more active than platinum catalysts in the oxidation of both chlorinated volatile organic compounds; DCE being completely destroyed at 375 °C, whereas TCE required 550 °C. HCl was the only chlorine-containing product in the oxidation of DCE in the range of 250 – 400 °C. Oxidation reactions were carried out in a conventional fixed-bed flow reactor consisting of a 12 mm internal diameter stainless steel tube located inside an electrical furnace.

Protonic zeolites (H-ZSM-5, H-MOR and chemically dealuminated H-Y zeolite) have also been used as catalysts in the oxidation reaction of DCE, dichloromethane (DCM) and TCE as individual chlorohydrocarbons and of their binary mixtures in conventional fixed bed flow reactors (López-Fonseca *et al.,* 2003). The studies showed that the catalytic activity is related to the presence of strong Bronsted acidity. The chemically dealuminated H-Y zeolites and H-MOR zeolites proved to be the most active catalysts in the oxidation of chlorinated VOCs, with carbon monoxide, carbon dioxide, hydrogen chloride and and chlorine being the most common reaction products. Vinyl chloride, methyl chloride and tetrachloroethylene, were produced as by-products in the combustion of DCE, DCM and TCE. When binary mixtures of these compounds were studied, competition for adsorption on the active sites occurred and the ignition temperature for the oxidation increased compared to that of the single compounds; this reduced the rate of production of chlorinated by-products and increased the selectivity towards the deep oxidation chlorinated product (HCl).

The oxidation of mixtures of VOCs with a similar composition to that expected from groundwater air strippers was also investigated using Pd/Al_2O_3 and Pt/Al_2O_3 catalysts at temperatures from 200 to 550°C (Aranzabal *et al.*, 2000). DCE proved to be the easiest to oxidize, followed by dichloromethane and 1,1- dichloroethylene and TCE.

Aranzabal *et al.* (2006) investigated the same reactions to elucidate the reaction mechanism. Their experiments were conducted in a in a similar manner and the outlet composition was analysed by a gas chromatograph equipped with an electron capture detector (ECD), the most sensitive detector for analysing chlorinated compounds. The conditions of the experiments were varied (large range of temperatures: 200°C to 500°C, initial concentration of chlorinated compounds to be oxidized, residence time for the gas flow through the reactor) for their effect on catalytic activity. Their study showed that DCE is first decomposed by dehydrochlorination to vinyl chloride and HCl, followed by direct oxidation to CO and CO_2. The proposed reaction model, in correlation with the experimental data obtained is presented below:

$$C_2H_4Cl_2 \quad \rightarrow \quad C_2H_3Cl + HCl \qquad\qquad\qquad (2.1)$$

DCE$\qquad\qquad\qquad$ Vinyl chloride

$$C_2H_3Cl + (x + \tfrac{1}{2})\, O_2 \quad \rightarrow \quad 2CO_x + HCl + H_2O \qquad (x = 1, 2) \qquad (2.2)$$

$$CO + \tfrac{1}{2}\, O_2 \quad \rightarrow \quad CO_2 \qquad\qquad\qquad\qquad\qquad (2.3)$$

The formation of Cl_2 can also be expected due to high concentration of O_2 in the reaction environment:

$$2\,HCl \;+\; \tfrac{1}{2}\,O_2 \;\rightarrow\; \quad H_2O \;+\; Cl_2 \qquad\qquad\qquad (2.4)$$

Zhang reported the use of a novel low-temperature oxidation catalyst, Pt/fluorinated carbon/ceramic (Pt/FC/C), for extensive oxidation of benzene as a model reaction to examine the effectiveness of the catalyst for the deep oxidation of volatile organic compounds at temperatures below 200 °C (Zhang *et al.*, 1997). They compared their results with those from conventional Pt/alumina catalysts. For equivalent platinum loading, the group reported that the activity of the Pt/FC/C is comparable to that of the Pt/alumina catalyst in dry feed conditions. However, when water vapour is present in the feed stream, they conclude that the Pt/FC/C catalyst shows significantly higher activity than the Pt/alumina catalyst. The reason for this behaviour is that under humid conditions, benzene oxidation on the Pt/alumina catalyst is substantially inhibited by the adsorption of water vapour on both the alumina support and on the Pt sites. The effect of humidity on the alumina is more significant than the effect of humidity on the Pt sites. For the Pt/FC/C catalyst, the support hydrophobicity prevents the adsorption of water on the support. The adsorption of water vapour on the Pt sites results in only a slight decrease in activity, suggesting that the Pt/FC/C catalyst is more suitable for deep oxidation of VOCs when the feed gas contains a significant amount of humidity.

According to the work reported by Sinquin *et al.* (2001), the $LaMnO_{3+\delta}$ perovskite shows interesting performances in the total catalytic destruction of chlorinated C_2 hydrocarbons selectively to CO_x (mainly CO_2) and HCl at temperatures above 500–550 °C. The saturated chlorinated VOCs are easier to decompose than the unsaturated ones, with elimination of HCl through dehydrochlorination reactions. The production of

higher chlorinated C_2 by-products is explained by successive chlorination and dehydrochlorination reactions. The addition of water decreases the amount of chlorinated by-products and enhances the formation of carbon oxides, especially CO_2. To prevent the destruction of the catalyst, the oxygen must be in excess at all times (Sinquin *et al.,* 2001).

Lately, a new generation of highly efficient oxidation catalysts based on glass-fibre support containing extra-low amounts of noble metals (Pt or Pd in concentration of up to 0.01–0.02 mass %) were developed and used in many catalytic reactions. These glass fibre catalysts (GFC) were tested in different oxidation reactions, including oxidation of VOCs. The high performance of GFCs is explained by the ability of the glass fibres to stabilize the transient metals in the glass bulk in a highly dispersed form (Balzhinimaev *et al.,* 2003; Balzhinimaev *et al.,* 2010). These novel catalysts are characterised by specific heat/mass transfer properties, original geometry, high flexibility and high mechanical strength. They show great potential in solving various environmental problems, such as: purification of automotive exhausts, decomposition of VOCs in waste gases, including chlorinated VOCs, dioxins, sulphurated VOCs, including SO_2 oxidation for purification of industrial waste gases. The Pt/GFC catalyst proved efficient in the deep oxidation of chlorinated hydrocarbons (chlorobenzene, DCE, etc.) with reported almost complete conversion of initial Cl-VOCs into CO_2, water and HCl (no CO and Cl_2 formation) and no harmful oxidation by-products (phosgene, dioxins).

As mentioned above, catalytic incineration is one of the cost-effective technologies able to solve the troublesome VOCs. The major parameters affecting catalytic incineration of

VOCs include catalyst types, VOC types, VOC concentration, operating temperature, space velocity and O_2 concentration (Chu *et al.,* 2003). In general, the operating temperature of catalytic incineration depends on catalyst type, VOC types, concentration of VOCs and space velocity (inverse of residence time of VOCs in the catalytic reactor). Therefore, residence time would decrease as space velocity increases and the conversion of VOCs would drop.

Some sulphur containing VOCs, may deactivate the catalyst (Pt is commonly used in the catalytic incineration process) and reduce the advantage of catalytic incineration. Chu *et al.,* (2001) studied the catalytic incineration of dimethyl sulphide (($CH_3)_2S$, DMS) over a Pt/Al_2O_3 fixed bed catalytic reactor, at temperatures between 110 °C – 400 °C, with different initial concentrations of DMS and O_2 and a range of space velocities for the reaction mixture. The results show that the conversion of DMS increases as the inlet temperature increases and the space velocity decreases. The higher the DMS concentration, the lower its conversion. Increasing O_2 concentration in the feed stream leads to a higher degree of DMS decomposition. Their study also shows that DMS has a poisoning effect on the Pt/Al_2O_3 catalyst, especially at lower temperatures. They also studied the catalytic incineration on a mixture of DMS with EtSH and concluded that the conversion of DMS is significantly suppressed by the existence of EtSH.

Again, Chu and Lee (1998) used the same Pt/Al_2O_3 catalyst to catalytically convert ethanol (C_2H_5OH) in mixtures with dimethyl disulphide (($CH_3)_2S_2$, DMDS). The oxidation reaction was carried out in a fixed bed catalytic reactor, for which the operating parameters were varied (temperature at inlet for mixture of gases, pollutant

and O_2 concentration, catalyst size, etc). The study showed that the conversions of C_2H_5OH and DMDS increase as the inlet temperature increases and the space velocity decreases. The higher the C_2H_5OH concentration, the higher its conversion. However, the reverse is true for DMDS. Variation in O_2 concentration has no effect on the amount of C_2H_5OH decomposed, but increases the amount of $(CH_3)_2S_2$ decomposed. DMDS has a poisoning effect on the Pt/Al_2O_3 catalyst, especially at lower temperatures. They concluded that the conversion of ethanol was significantly suppressed by the existence of DMDS at temperatures lower than 300 °C.

The catalytic incineration of DMS and DMDS was also studied in a MnO/Fe_2O_3 fixed bed catalytic reactor, again by the same scientist (Chu *et al.*, 2003). Their paper provides information on the influence of the operating parameters including: inlet temperature, space velocity, VOC concentration and O_2 concentration, on the decomposition rate of DMS and DMDS. The results show again that the conversion of VOCs increases as the inlet temperature increases and the space velocity decreases. The higher the concentration of VOCs, the lower their conversion. Also, they found that the O_2 concentration has no affect on the conversion of DMS and DMDS, and that these two VOCs have poisoning effect on the MnO/Fe_2O_3 catalyst, especially at lower temperatures. The experiments also showed that a higher temperature is required to accomplish the same DMS conversion compared to that of DMDS.

The TiO_2-assisted photocatalytic degradation of gas-phase DMS was reported by Gonzales-Garcia *et al.* (2004). The group detected surface and gas-phase reaction intermediates and final products and tried to explain the deactivation of the catalyst

taking these compounds into account. A reaction mechanism is suggested based on both, intermediates found in this study and previous mechanisms reported by other authors for the gas-phase heterogeneous photocatalytic degradation of similar S containing compounds (Voronstov *et al.*, 2001). They concluded that DMS photocatalytic degradation in the presence of irradiated TiO_2 proceeds towards total mineralization with formation of CO_2. Intermediate reaction products identified are compounds as: CH_3OH, $H_3CS(O)CH_3$ and $H_3CS(O)_2CH_3$ (and most probably CH_4, H_2CO, H_3CSSCH_3, and SO_4^{2-}) that cause the catalyst deactivation. The reaction mechanism proposed by the authors is presented in Figure 2.1 below (scheme adapted from Voronstov *et al.,* 2001):

Figure 2.1. Proposed mechanism for the photocatalytic degradation of DMS with TiO₂ catalyst

The photocatalytic destruction of gaseous diethyl sulphide was also studied by Vorontsov and his collaborators, using again TiO_2 catalyst (Vorontsov *et al.,* 2001).

Using initial concentrations of DES in the order of hundreds of ppm, the photooxidation reaction was performed in a fixed bed flow reactor, under ambient conditions. $(C_2H_5)_2S_2$, CH_3CHO, CH_3CH_2OH, C_2H_4, and CO_2 were detected as major products in the gaseous effluent from the reactor. Trace products identified in the gas phase included CH_3COOH, $C_2H_5SC(O)CH_3$, and SO_2. The catalyst showed deactivation within a range of 100–300 min. The products extracted from the catalyst's surface in isopropanol included $(C_2H_5)_2S_2$, $(C_2H_5)_2S_3$, $(C_2H_5)_2SO$, $(C_2H_5)_2SO_2$, and $C_2H_5SCH_2CH_2OH$. The experiments showed that at relatively low light intensities, an increase in humidity from less than 1% to ~20% resulted in an increase in the amount of DES converted. However, at higher light intensities, similar increase in humidity had an adverse effect on the conversion of DES. Additions of H_2O_2 in the reactor feed stream increased the rate of DES destruction and altered the product distribution throughout the reaction time. The authors suggest that the distribution of products show that the two main pathways of the degradation are the oxidation of S and C atoms and cleavage of the C-S bond, similar to the reactions presented in Scheme 2.1. The products of complete oxidation (SO_2 and CO_2) were detected in minute quantities; most of the products corresponded to C-S bond cleavage and partial oxidation.

Kozlov *et al.,* (2003) studied the gas-phase heterogeneous photocatalytic oxidation of DES in a batch reactor at room temperature, using detection of gaseous products and FTIR identification of surface species. Acetaldehyde and ethylene were detected as gaseous intermediates and diethyl sulphone and carboxylates were detected on the surface of TiO_2 as intermediate products. The authors found that DES is oxidized completely and the final products of its oxidation are CO_2 and water (in gas phase) and

sulphate and carbonate species on the catalyst's surface. To detect the deactivation of the catalyst in the batch system, the authors performed a set of experiments using the same catalyst several times, and they observed that DES disappeared almost completely from the gas phase in about 50 min of reaction. The production of CO_2 corresponded to almost stoichiometrically complete oxidation of DES according to the equation:

$$(C_2H_5)_2S + 8O_2 \quad \rightarrow \quad 4CO_2 + 4H_2O + H_2SO_4 \qquad\qquad (2.5)$$
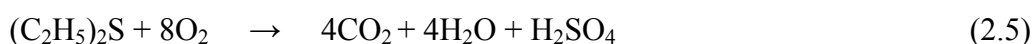
In this study the accumulation of surface sulphates detected by FTIR was found responsible for the TiO_2 photocatalyst deactivation in the process of DES oxidation.

Volatile organic sulphur compounds (VOSCs) play a major role in the global sulphur cycle (a combination of biological, chemical and geochemical processes). Even though VOSCs have important environmental functions, they are linked with global warming, acid precipitation, and cloud formation. Two major components of the VOSC group are DMS and methanethiol (CH_3SH, MT). These compounds and the products derived from their photochemical oxidation in the atmosphere are also involved in the pollution process. DMS and MT are the two compounds formed in large amounts by living systems (e.g. algae, bacteria, plants), especially in marine environments. Oxidation of DMS in the atmosphere by hydroxyl and nitrate radicals produces many degradation products including CO_2, COS, dimethyl sulphoxide, dimethyl sulphone, organic oxyacids of sulphur, and sulphate. These materials have important roles in the complex processes that constitute the organic sulphur cycle. Bentley and Chasteen present in their study the cycle of dimethyl sulphide in nature: water-atmosphere. This is shown in Figure 2.2 below (adapted from Bentley and Chasteen, 2004):
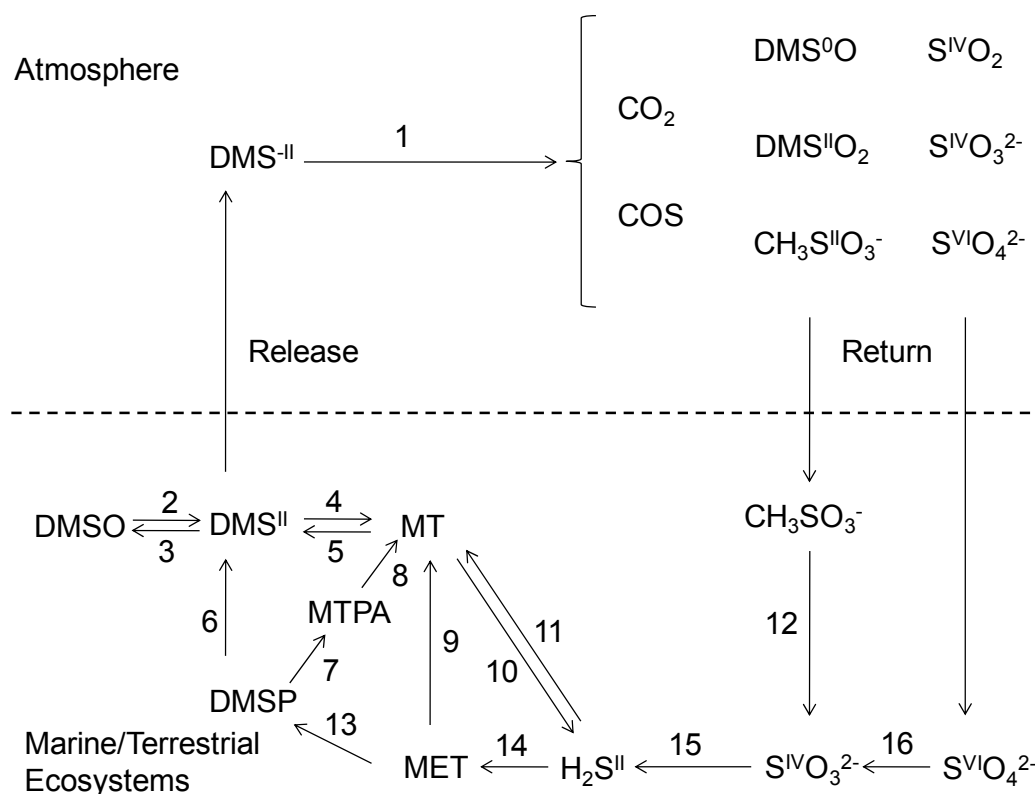
Legend: (1)- Photochemical oxidation; (2)- DMS dehydrogenase; (3)- DMSO reductase; (4)- Thiol transmethylation; (5)- DMS monooxygenase; (6)- DMSP-lyase; (7)- Demethylation; (8)- Demethiolation; (9)- MET gamma-lyase; (10)- MT oxidase; (11)- Thiol transmethylation; (12)- Methanesulfonate monooxygenase; (13)- Several enzymes and intermediates; (14)- MET biosynthetic pathway; (15) and (16)- Sulfate reducing organisms; (DMS)- Dimethyl sulphide; (DMSO)- Dimethyl sulphoxide; $(DMSO_2)$- Dimethyl sulphone; (MT)- Methanethyol; (MET)- L-methyonine; (MTPA)- 3-methylthiopropionic acid; (DMSP)- Dimethylsulphoniopropionate.

Figure 2.2. Diagram of dimethyl sulphide natural cycle in environment

This cycle involves the transformation of sulphur from its highest oxidation state, +VI in SO_4^{2-}, to its lowest oxidation state, −II, in DMS; this operation occurs in marine/terrestrial ecosystems. The reduced sulphur is then transported to the atmosphere (as DMS), where it undergoes re-oxidation. The highly oxidized sulphur compounds, (oxidation states +IV and +VI), are removed through precipitation or dry deposition.

Analytical determination of DMS and MT sampled from the gas phase is performed by gas chromatography (GC) (Lawrence *et al.,* 2000), with gas instruments equipped with capillary columns and pulsed flame photometric, photoionization or mass selective detectors (Hill and Smith, 2000). However, the best detectors are the sulfur chemiluminescence, and mass selective detectors (Wardencki, 1998). Determination of DMS and MT from liquid phase also involves GC for detection but the liquid phase sampling is often carried out using the solid phase microextraction (SPME) technique (Lestremau *et al.,* 2003). This sampling technique uses a small diameter fibre on which the compound to be analysed (DMS) is adsorbed from the solution and then is later desorbed in the hot injector of a gas chromatograph.

Anna Kachina *et al.,* (2006) studied the photocatalytic oxidation of ethyl mercaptan over titanium dioxide in a continuous flow tubular reactor at temperatures from 373 to 453 K. The temperature influence on the reaction pathway and reaction kinetics was studied. Sulphur dioxide, carbon monoxide, carbon dioxide, acetic acid and water were identified as by-products.

The use of waste materials (wood and coal fly ash) as inexpensive catalysts to remove reduced sulphur compounds (H_2S, MT, EtSH) from polluted gases was investigated by some scientists (Kastner *et al.,* 2002; Kastner *et al.,* 2003). Coal ash is reported to have high concentrations of metal oxides, such as Al_2O_3 (14–20%, w/w), Fe_2O_3 (8–14%, w/w), and TiO_2 (1–1.6%, w/w) that could act as catalysts (Mallik and Chaudhuri, 1999). The wood and coal fly ash proved to catalytically oxidize H_2S, MT and EtSH at low temperatures (23−25 °C), with elemental sulphur (for H_2S) and dimethyl disulfide (for

MT) and DEDS (for EtSH) as end reaction products. As wood ash has a higher surface area compared to coal ash, this had a higher initial H_2S removal rate (0.16 vs 0.018 mg/g/min) under similar conditions. Elemental sulphur was made responsible for the catalyst deactivation as it deposited on the catalyst and reduced its surface area. Catalyst regeneration (hot water washing at 85 °C) was not very effective, and only increased its performance slightly. The performance of the catalyst improved when the inlet gas stream had a pollutant composition closer to that of a real industrial plant (400-500 ppmv H_2S); in this case the concentration of H_2S was reduced to 200 ppmv at a residence time of 4.5 s (50% removal efficiency for approximately 4.6 hours) at 25 °C.

Currently, wet scrubbers using oxidizing chemicals, such as ClO_2, NaOCl or ozone are utilized to treat off-gas treatment of VOCs (Kastner and Das, 2002; Kastner *et al.,* 2002; Prage and Cocke, 2001; Kastner *et al.,* 2003; Chungsiriporn *et al.,* 2004; Chungsiriporn *et al.,* 2005). These systems proved effective against VOCs, including reduced sulphur compounds (e.g., methanethiol) but less effective against aldehydes and alkanes. Packed-bed wet scrubbers using chemical oxidizing agents can achieve usually efficiencies of 85-90% and even 98-99% for some VOCs, based on odour dilution to thresholds units, but very poor performance towards other VOCs, especially branched and straight chain aldehydes. The composition and concentration of VOCs in air vary widely depending on the pollution source, and thus the wet air scrubbing is not always the best alternative for air depollution. Little information is available on the kinetics of the ClO_2 reaction with air pollutants (Rav-Acha and Choshen, 1987; Hoigne and Bader, 1994), limiting wet scrubber design and optimisation. Unlike aldehydes, EtSH and DMDS react rapidly with ClO_2 and it was found that increasing pH significantly

increases the efficiency of the wet scrubber for removal of odour causing compounds. However, an increase in pH did not improve aldehyde removal.

At the same time, biofilters can also be used to remove VOCs from contaminated air. Literature reports that a biofilter system successfully removed aldehydes from a mixture of VOCs in air (Kastner and Das, 2005); the report was based on GC/MS analysis of inlet and outlet streams of air. Total aldehyde removal efficiencies ranged from 40 to 99% for the biofilter, and the chemical analysis indicated that the overall removal of VOCs increased, with aldehyde removal efficiencies significantly higher than that of chemical wet scrubbers. It is suggested that coupling a wet scrubber and biofilter in series could improve the overall VOC removal efficiencies. A wet scrubber would remove reduced sulphur compounds in the first stage and biofiltration unit would remove incompletely oxidized VOCs or untreated VOCs (eg aldehydes) in the next stage. Recently, a two-stage biofiltration system with a catalytic reactor (iron catalyst) followed by a conventional biofilter was used to remove H_2S and methyl ethyl ketone from an air stream under ambient temperature and pressure. H_2S was removed almost totally in the catalytic reactor (using O_2 from air) and thus the biofilter was protected from acidification (undesired process expected if H_2S was allowed to enter the biofilter). This combined system was demonstrated to have significant advantages over a biofilter alone for removal of such a mixture (Xiaobing *et al.,* 2003).

The oxidation of thiols into disulfides is an important reaction in the chemical and petroleum industries, as disulfides are used as intermediates in organic syntheses and at the same time they have various direct industrial applications, e.g. in the vulcanization

of rubbers and elastomers (Basu *et al.,* 1993; Menini *et al.,* 2011). The synthesis of disulfides from thiols use stoichiometric amount of oxidants, such as dichromates (López *et al.,* 1985; Shrini *et al.,* 2004), permanganates (Shaabani and Lee, 2001), and metal (nickel or chromium) peroxides (Nakagawa *et al.,* 1980; Firouzabadi *et al.,* 1986). The disadvantage of these processes is that they generate large amounts of by-products, which are usually toxic, and thus they require complicated clean-up procedures. In order to overcome these disadvantages, the use of molecular oxygen as oxidant was intensively studied in the last decade.

Oxidative coupling of mercaptans to disulfides is of interest from biological, synthetic and oil-sweetening point of view. At the same time, thiols are widely distributed in petroleum products from where they should be removed before its processing, as they are corrosive, they poison the metal catalysts, have unpleasant odour and produce environmental pollution. The removal of mercaptans from petroleum is usually referred to as 'sweetening'. The compounds of different elements, such as manganese (Golchoubian and Hosseinpoor, 2007), copper (Hashemi *et al.,* 2004), cerium (Silveira and Mendes, 2007), nickel (Saxena *et al.,* 2007), vanadium (Han and Hill, 2007) or cobalt (Nemykin et al., 2007) have been used as catalysts for the aerobic oxidation of thiols into disulfides, in ambient conditions. The most studied catalysts for this reaction, that had also found their application in the petroleum and in the synthetic industry are the cobalt phthalocyanine complexes. These catalysts are usually expensive, and the reactions require strong alkaline conditions.

The oxidation of thiols in alkaline media is the most widely used procedure for the extraction and removal of thiols from liquefied petroleum gases (LPG) in the refining industry. In the Merox process (Van de Vusse, 1958; Wallace *et al.,* 1964; Harkness *et al.,* 1970; Basu *et al.,* 1993; Mayer, 2003), the mercaptans present in petroleum are oxidized with air to disulfides in the presence of water-soluble cobalt phthalocyanines and caustic soda. The end oxidation products are disulphides (Wallace and Shriesheim, 1965; Leitão and Rodrigues, 1989; Leitão and Rodrigues, 1990).

The chemical reactions involved in the Merox process are:

$$2RSH + 2\,NaOH \;\rightarrow\; 2NaSR + 2\,H_2O \tag{2.6}$$

$$4NaSR + O_2 + 2H_2O \;\rightarrow\; 2RSSR + 4NaOH \tag{2.7}$$
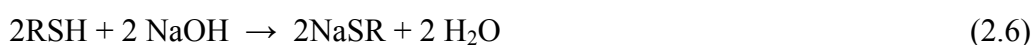
The net overall Merox reaction can be expressed as:

$$4\,RSH + O_2 \rightarrow 2RSSR + 2H_2O \quad \text{(in alkaline conditions)} \tag{2.8}$$

Lately a new process for the oxidation of thiols under mild alkali conditions was developed and tested at laboratory scale (Menini *et al.,* 2011). The process is based on the use of inexpensive Co–Fe magnetic materials as efficient heterogeneous catalysts, high boiling solvents and oxygen from air as oxidant. The use of weakly basic solvents enhances the reaction rate by activating the substrate and thus eliminating the need of an alkaline co-catalyst that proved to be corrosive and waste generating. With this type of catalyst, disulfides can be obtained in high yields at low catalyst loading (0.008% molar). One of the main benefits of this process is that the catalyst does not undergo

leaching and can be recovered at the end of the reaction by applying an external magnetic field.

With stronger oxidants than air (e.g. Fenton's reagent), thiols can be oxidized further than disulphides, to the corresponding sulphonic acids (Cremlyn, 1996), according to the reactions (2.9). This oxidation proceeds via the relatively unstable sulphenic and sulphinic acids, which are too susceptible to further oxidation to be isolated.

$$R\text{-SH} \xrightarrow{[O]} R\text{-SOH} \xrightarrow{[O]} R\text{-S(O)-OH} \xrightarrow{[O]} R\text{-S(O)}_2\text{-OH} \quad (2.9)$$

Mercaptan $\quad$ Sulphenic $\quad$ Sulphinic $\quad$ Sulphonic acid
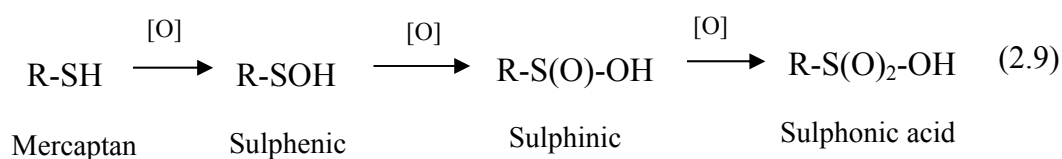
Advanced oxidation processes (AOPs) are used for the destruction of synthetic organic chemicals in wastewater, apart from disinfection and deactivation of pathogenic microorganisms that are difficult to degrade biologically. A typical AOP involves two stages: the formation of a strong oxidant (such as the hydroxyl radicals) and the reaction of these oxidants with the organic pollutants in the system. AOPs are mediated by free-radical reactions and include the application of ozone, hydrogen peroxide, and ultraviolet light, either individually or in combination O_3/UV; H_2O_2/UV; and O_3/H_2O_2/UV (Oppenländer, 2003; Parsons, 2004).

All AOPs have in common the generation of the hydroxyl radical (HO•), which is extremely reactive, and possesses a very high oxidation potential, being able to destroy compounds that cannot be oxidized by conventional oxidants such as chlorine, ozone, potassium permanganate, or oxygen.

In AOPs, the rate of the oxidation reaction depends on: radical concentration, pollutant concentration, and oxygen concentration (Parsons, 2004). The radical concentration can be affected by many factors, such as: temperature, pH, presence of ions, type of pollutant, presence of scavengers (e.g. bicarbonate ion), etc. A variety of methods are available to produce hydroxyl radicals in the aqueous phase. The most widely used on a commercial scale are combinations of oxidants such as H_2O_2/O_3, O_3/UV, H_2O_2/UV or $O_3/H_2O_2/UV$.

The AOPs can be divided in two groups: UV based processes (such as UV/O_3, $UV/O_3/H_2O_2$) and H_2O_2 based processes (such as H_2O_2/UV, H_2O_2/O_3, Fenton and photo – Fenton reaction). TiO_2 and iron are some of the compounds that are used as catalysts in AOPs, as they enhance the decomposition of H_2O_2 (Oppenlander, 2003).

Table 2 presents the oxidation potential of different oxidizing agents. The table shows that the hydroxyl radical is the most active oxidant after fluorine, with an oxidation potential of 2.8 V. These radicals are non selective in their mode of attack and are able to operate at normal temperature and pressure, being able to oxidize almost all dissolved materials present in wastewater, without restriction to specific classes or groups of compounds. The process is very complex since a large number of reactions can possibly occur, and thus it is very difficult to predict all of the oxidation products. If enough HO• are present in the system, the process continues until the initial compound will be completely mineralized to simple, relatively harmless inorganic compounds, such as carbon dioxide and water (Parsons, 2004).

Table 2.2. Oxidation power of common oxidizing species

Species	Oxidation Potential, V
Fluorine	3.03
Hydroxyl radical	2.80
Atomic oxygen	2.42
Ozone	2.07
Hydrogen Peroxide	1.78
Perhydroxyl radical	1.70
Permanganate	1.68
Hypobromous acid	1.59
Chlorine dioxide	1.57
Hypochlorous acid	1.49
Chlorine	1.36

(Adapted from Parsons, 2004)

The main benefits that make AOPs (liquid phase) more attractive than other treatment techniques such as stripping, adsorption onto activated carbon, chemical coagulation, filtration or ion exchange is that the dissolved organic pollutants are decomposed rather than transferred or concentrated into a different phase. One of the advantages of the AOPs is that they don't generate secondary waste materials, therefore there is no need to dispose of them, and thus the cost of the wastewater treatment is reduced. Also, sometimes it is not necessary to oxidize the pollutants completely since only partial oxidation is sufficient to reduce their toxicity, or to make them more susceptible to further biological decomposition (Parsons, 2004; Oppenlander, 2003).

Literature shows few examples of AOPs used for degradation of acetonitrile (MeCN) residues. Lichtin and Avudaithai (1996) described a comparative study to degrade MeCN in the vapour phase and in aqueous solutions using photocatalysis with TiO_2, in stirred batch reactors, continuous oxygen supply and UV irradiation, concluding that MeCN is more reactive in vapour phase than in liquid phase. TiO_2 was reported as the most used catalyst for the photodegradation of MeCN in vapour phase, using different sources of irradiation (Zhuang *et al.,* 1999; Addamo *et al.,* 2005).

The photo-oxidation of MeCN was studied in gas-solid and gas-liquid regimens (Addamo *et al.,* 2005), using TiO_2 catalyst and a 500W medium-pressure Hg lamp (with emission at 365 nm) as source of irradiation. In the gas–solid regime, CO_2 and HCN were the main reaction products identified, supporting the hypothesis claiming breakage of the C–C bond in acetonitrile during the photo oxidation process (Zhuang *et al.,* 1999). Methanoate ions and nitrate ions were identified on the surface of the used catalysts; this can be attributed to the partial oxidation of the organic moiety of the molecule. The overall reaction for the photo-oxidation of acetonitrile in gas-solid regime with TiO_2 as catalyst is:

$$CH_3CN + \frac{3}{2}O_2 \xrightarrow{\quad TiO_2, hv \quad} CO_2 + HCN + H_2O \qquad (2.10)$$

In the liquid–solid regime, the acetonitrile photodegradation process produced cyanate and carbonate ions and very small amounts of cyanide, nitrite, nitrate, and methanoate ions. Based on this finding, the authors assumed that the catalyst irradiation for both regimes determines the acetonitrile photoadsorption on TiO_2 surface sites proposing a

mechanism when the reaction between adsorbed acetonitrile and phototoproduced •OH radicals is able to perform C–C bond breakage with the production of cyanide radicals and methanol:

$$TiO_2 \xrightarrow{\text{hv}} TiO_2\,(H^+, e^-) \tag{2.11}$$

$$O_2 + e^- \rightarrow \ •O_2^- \tag{2.12}$$

$$•O_2^- + H_2O \rightarrow \ HO_2• \ + OH^- \tag{2.13}$$

$$OH^- + v^+ \rightarrow \ •OH \tag{2.14}$$

$$CH_3CN_{(ads)} + \ •OH \rightarrow CH_3OH + CN• \tag{2.15}$$
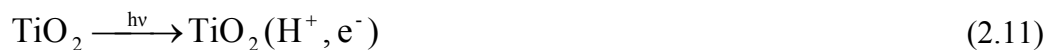
In the gas–solid regime, the CN• radicals reacted with water adsorbed on the catalyst, facilitating the formation of HCN, whereas methanol was photo-oxidised to CO_2:

$$CN• + H_2O \rightarrow HCN + \ •OH \tag{2.16}$$

$$CH_3OH + 6 \ •OH \rightarrow CO_2 + 5H_2O \tag{2.17}$$

In contrast, in the liquid–solid regime, most of the cyanide radicals were transformed into cyanate ions, which desorbed from the surface to the aqueous solution. The remaining cyanide radicals produced cyanide ions, which were also released to the solution:

$$CN• + 2OH^- + h^+ \rightarrow CNO^- + H_2O \tag{2.18}$$

$$CN\bullet + OH^- \rightarrow CN^- + \bullet OH \tag{2.19}$$

The cyanide ions produced through reaction (2.19) underwent photocatalytic oxidation, leading to cyanate, also photo-oxidized to carbonate and nitrate ions:

$$CNO^- + 10\ OH^- + 8\ H^+ \rightarrow CO_3^{2-} + NO_3^- + 5\ H_2O \tag{2.20}$$
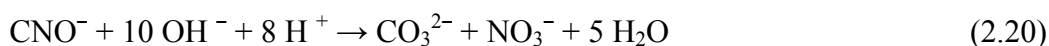
Methanol (not detected, probably due to its fast oxidation), formed according to (2.15), was oxidised to methanal, methanoate, and carbonate ions, although only the last two species were detected:

$$CH_3OH + 2\ \bullet OH \rightarrow HCOH + 2H_2O \tag{2.21}$$

$$HCOH + 3OH^- + 2H^+ \rightarrow HCOO^- + 2H_2O \tag{2.22}$$

$$HCOO^- + 3OH^- + 2H^+ \rightarrow CO_3^{2-} + 2H_2O\bullet \tag{2.23}$$
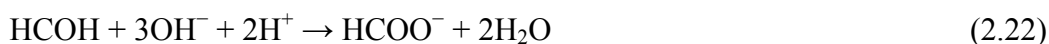
The production of cyanide in the gas phase photo oxidation of acetontrile is a drawback of this process, HCN being very toxic, thus, a further step devoted to the elimination of HCN must be added to the photoprocess.

The degradation of acetonitrile in liquid phase was also studied with H_2O_2 in both Fenton and photo-Fenton processes (Micaroni *et al.,* 2004). Among these options, photolysis proved to be the most effective (100% degradation of 20% aqueous MeCN solution in 30 hours).

Chloropicrin (CP) is toxic to aquatic animals and to mammals, but since it is only slightly soluble in water it will not move rapidly in aquatic environments. It also has a higher density than water (1.65 g/mL) and consequently it will sink to the bottom of the surface water. The half-life of chloropicrin in water exposed to light was 31.1 hours with carbon dioxide, bicarbonate, chloride, nitrate and nitrite being the breakdown products (Duguet *et al.,* 1988).

Cervini-Silva *et al.* (2000) studied the decomposition of chloropicrin in the presence of reduced ferruginous smectite (SWa-1) in liquid phase. The dechlorination of CP in the presence of Fe(II)-bearing clays leads to the formation of dichloronitromethane, chloronitromethane, and nitromethane, suggesting that CP and the iron baring clay participate in two electron pathways and decompose according to scheme:

$$C\text{-}Cl(Cl_2)NO_2 + e^- \rightarrow C\text{-}Cl(Cl)_2NO_2^- \rightarrow {}^\bullet CCl_2NO_2 + Cl^- \xrightarrow{H^+}$$

$$\rightarrow CHCl_2NO_2 \xrightarrow{H^+} CH_2ClNO_2 \tag{2.24}$$

$$CH_2Cl\text{-}NO_2 \xrightarrow{2e^-} CH_2{=}NO_2^- + Cl^- \xrightarrow{H^+} CH_3NO_2 \xrightarrow{reduction} Products \tag{2.25}$$

$$Cl_3C\text{-}NO_2 \rightarrow Cl_2CH\text{-}NO_2 \rightarrow ClCH_2\text{-}NO_2 \rightarrow CH_3\text{-}NO_2 \tag{2.26}$$
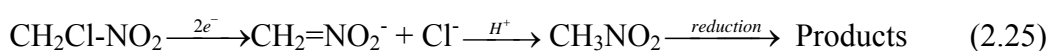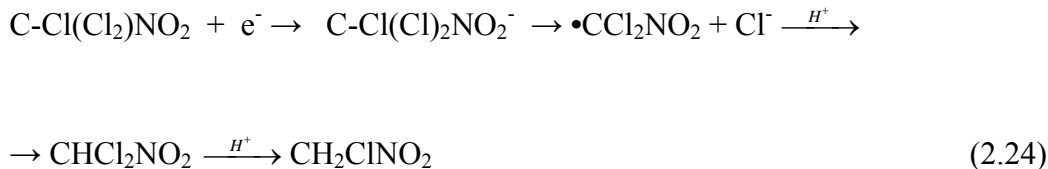
Having a high vapour pressure (23.8 mm Hg at 25 °C), chloropicrin can enter the troposphere during application as soil fumigant or through subsequent evaporation from the soil (Howard, 1990). Chloropicrin is efficiently photolysed in the atmosphere. The half-life of chloropicrin in air exposed to simulated sunlight was 20 days, the

photoproducts being phosgene (which will hydrolyse to carbon dioxide and hydrogen chloride), nitric oxide, chlorine, nitrogen dioxide and dinitrogen tetroxide.

Moilanen *et al.* (1978) photolysed chloropicrin in gas phase using a 275-W RS Sunlamp, and found that nitrosyl chloride (NOCl) and phosgene (Cl_2CO) were produced when chloropicrin was photolysed in air. They observed no reaction in nitrogen. Additionally, when the reaction was performed with $^{18}O_2$, all of the photoproducts were found to be labelled. Based on these results, they proposed that chloropicrin reacts with oxygen to form a trioxalone intermediate that then dissociates to produce NOCl and Cl_2CO. They further suggested that O_2 catalyses this process and propose the mechanism presented in Figure 2.3 (scheme adapted from Moilanen *et al.*, 1978):
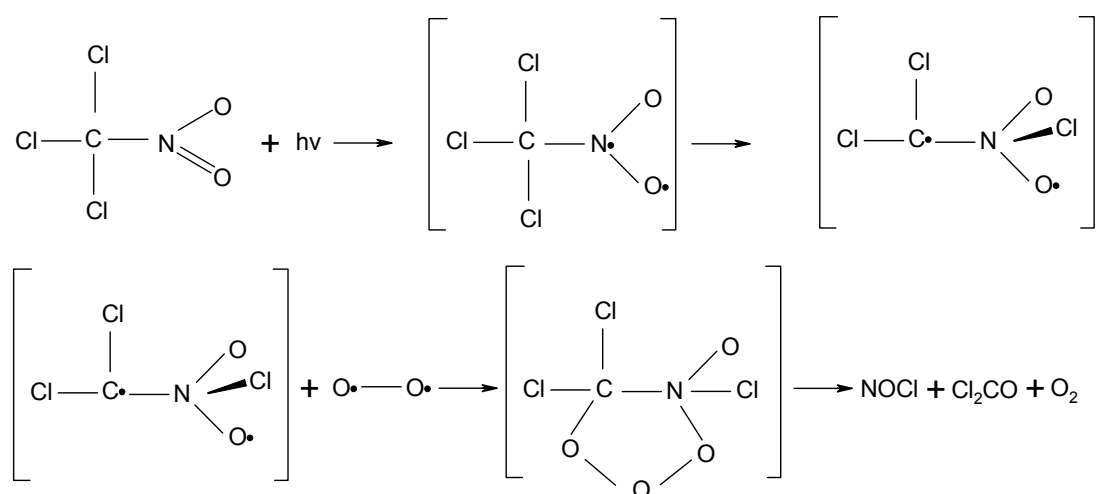
Figure 2.3. Photodegradation of chloropicrin in gas phase with air

In cryogenic matrices, chloropicrin undergoes photolysis at a wide range of photolysis wavelengths, whether or not oxygen is present, giving the same reaction products

(Wade *et al.,* 2002). When $^{18}O_2$ is present, ^{18}O-labeled photoproducts are not observed in cryogenic matrices, leading to the view that CP initially undergoes cleavage of the C-N bond to produce $NO_2\bullet$ and $CCl_3\bullet$ radicals which will react to form phosgene and nitrosyl chloride, according to the reactions:

$$CCl_3NO_2 \quad \rightarrow \quad Cl_3C\bullet + \bullet NO_2 \qquad\qquad (2.27)$$

$$Cl_3C\bullet + \bullet NO_2 \quad \rightarrow \quad Cl_2CO + NOCl \qquad\qquad (2.28)$$

These compounds can be washed off by rain drops and moisture in the atmosphere, leading to CO_2, HCl, nitric oxide, Cl_2, NO_2 and nitrogen tetroxide.

2.3. Fenton and Fenton-like processes

In 1894 H.J. Fenton observed and reported that the oxidation of maleic acid with hydrogen peroxide is promoted by the ferrous iron (Fenton, 1894). Only about forty years later, in 1934, Haber and Weiss revealed that the hydroxyl radical was the effective oxidative agent in the Fenton reaction (Haber and Weiss, 1934). Since then, the mechanism of the reaction and the generated species in the Fenton's process are under intense research and controversial discussions (Walling, 197; Siegel and Siegel, 1999), and has not been totally elucidated.

The Fenton's process comprises of the reduction of hydrogen peroxide by a transition metal catalyst. As transition metals have various oxidation states, they are able to

undergo both oxidation and reduction reactions. A typical example is iron that can easily change its oxidation state from +2 to +3 and back to +2. Ferrous iron (Fe^{2+}) is the main ion used in Fenton's chemistry, but other ions such as ferric iron (Fe^{+3}), Cu^{2+}, Zn^{2+}, Mn^{2+}, Co^{2+}, etc., can also be used; in this case the process is called 'Fenton-like'(Tony *et al.,* 2009). When ferric iron is used, the overall oxidation rate for the Fenton-like process is slower than that of the Fenton reaction as the reaction is limited by the conversion of Fe^{+3} to Fe^{+2} (process much slower than the conversion of Fe^{+2} to Fe^{+3}). It is very common that the metal ions are immobilised on different supports for the Fenton-like system (Chou and Huang, 1999; Xiong *et al.,* 2000; Ishtchenko *et al.,* 2003; Pigantello *et al.,* 2006; Chi Tangyie and Huddersman, 2007; Lee *et al.,* 2009).

The Fenton process has various forms and can be divided into the 'dark' Fenton and the photo–Fenton process. The 'dark' Fenton process uses an oxidizing agent (mainly H_2O_2 or/and O_3) and a catalyst (a metal salt or oxide - mainly iron). In addition, the photo–Fenton process involves irradiation with sunlight or artificial light source (Parsons, 2004; Venkatadri *et al.,* 1993; Kavitha and Palanivelu, 2004; Hermosilla *et al.,* 2009).

Fenton's reagent treatment consists of the mixture of iron salts and hydrogen peroxide. The use of a Fe^{+2}/H_2O_2 couple as the oxidation process in wastewater treatment has a variety of advantages. H_2O_2 is considered to be an environmentally friendly compound, although, it has some negative effects, since it decomposes slowly into water and oxygen. Besides that, iron is highly abundant transition metal naturally occurring in the environment with different oxidation numbers. It is also non-toxic and easy to remove (Pigantello, 1992).

The major reactions involved in the Fenton process are presented in the reactions (2.29) to (2.35). The reactions present only the interactions between the species involved in reaction (2.29). The reactions show that the iron acts as a catalyst decomposing H_2O_2 (Parsons, 2004; Oppenlander, 2003).

$$Fe^{2+} + H_2O_2 \rightarrow Fe^{3+} + OH^{\bullet} + OH^- \tag{2.29}$$

$$Fe^{2+} + OH^{\bullet} \rightarrow Fe^{3+} + OH^- \tag{2.30}$$

$$H_2O_2 + OH^{\bullet} \rightarrow HOO^{\bullet} + H_2O \tag{2.31}$$

$$Fe^{3+} + H_2O_2 \rightarrow Fe-OOH^{2+} + H^+ \tag{2.32}$$

$$Fe-OOH^{2+} \rightarrow HOO^{\bullet} + Fe^{2+} \tag{2.33}$$

$$Fe^{2+} + HOO^{\bullet} + H^+ \rightarrow Fe^{3+} + H_2O_2 \tag{2.34}$$

$$Fe^{3+} + HOO^{\bullet} \rightarrow Fe^{2+} + O_2 + H^+ \tag{2.35}$$
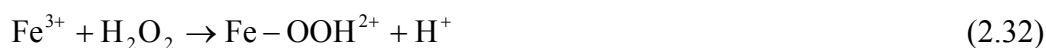
Reactions (2.30) and (2.31) show that there are also competing reactions in the Fenton's process that consume OH•. Fe^{2+} is continuously consumed during the process, so Fe^{3+}, which is generated in reactions (2.29) and (2.30), reacts with the remaining H_2O_2 to form peroxo-complexes. The peroxo-complex, in turn, decomposes slowly into Fe^{2+} and HO_2• in accordance with reaction (2.33). The oxidation potential of HOO• is approximately twice lower than that of OH•, so the OOH• radicals generated during

reactions (2.31) and (2.33) reduce the oxidation power of the system. The rate constant for the reaction (2.33) is much smaller than the rate constant for the reaction (2.29) indicating that Fe^{2+} is consumed rapidly but produced slowly. In conclusion, the higher the concentration of Fe^{2+} the more OH• is produced (Benitez *et al.,* 1999; Chamarro *et al.,* 2001).

The efficiency of the Fenton process strongly depends on the concentrations of Fe^{2+} and H_2O_2 and the pH value of the reaction. The rate of decomposition of H_2O_2 by Fe^{2+} is highly influenced by the pH (Fenton's process requires acidic pH, ideally pH=3), H_2O_2 concentration, Fe^{2+} concentration, $[H_2O_2]/[Fe^{2+}]$ ratio, and complexation of Fe^{2+} by inorganic and organic ligands (Pigantello, 1992). The catalyst is usually added as a ferrous salt such as $FeSO_4$. When Fe(II) is used as a catalyst, the hydroxyl radicals are immediately produced by the rapid reaction between the ferrous salt and the hydrogen peroxide (reaction (2.29)).

It is also possible to add ferric salt, such as $FeCl_3$. When iron Fe(III) is used instead of Fe(II), the process is called Fenton-like (Parsons, 2004). During the Fenton-like process, the production of OH• occurs in a two stages process with the slow reaction between ferric iron and H_2O_2. Only the first two stages of the process are presented in reactions (2.36) and (2.37) since further reactions can occur in the same way as before (see reactions (2.29) – (2.35)).

$$Fe^{3+} + H_2O_2 \rightarrow Fe^{2+} + HOO^{\bullet} + H^+ \qquad (2.36)$$

$$Fe^{2+} + H_2O_2 \rightarrow Fe^{3+} + OH^{\bullet} + OH^- \qquad (2.37)$$
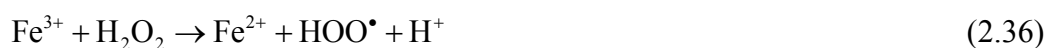
Advantages and disadvantages of the Fenton process:

Advantages:

- Relatively inexpensive reagents: H_2O_2 and iron salts, iron is highly abundant and non toxic compound;

- The Fenton's process is easy to operate; works well at room temperature and atmospheric pressure, making it very attractive for industrial applications;

- H_2O_2 is easy to transport and handle and is environmentally benign in diluted form;

- The use of Fenton's reagent leads to complete mineralization of some organic compounds to CO_2, H_2O, inorganic ions, with low chemical costs and energy requirements comparing to technologies that use UV and O_3.

Disadvantages:

- Large amounts of H_2O_2 are required;

- For the homogeneous systems, a large amount of ferric oxyhydroxide sludge is produced, which has to be removed; this increases the costs of operation;

- Possible generation of toxic by–products if complete mineralisation is not achieved;

- Necessity to work at low pH values; the pH adjustment increases the treatment cost;

- Usually the pH of the effluent needs to be adjusted (neutralized) before discharge into surface waters (e.g. rivers); this also increases the operational costs.

2.4. Novel heterogeneous catalyst

The development of supported Fenton catalysts (transition metal cations or transition metal oxides immobilized on different supports) has recently become important in the field of advanced oxidation processes as they overcome some of the disadvantages of the homogeneous Fenton's process (Parsons, 2004). A range of heterogeneous solid catalysts, including activated carbon impregnated with iron and copper oxide have been used to degrade recalcitrant organic compounds in liquid phase (Georgi and Kopinke, 2005; Ramírez *et al.,* 2007). Examples: the Nafion/Fe structured membrane catalyst used in the photo-assisted immobilized Fenton degradation of azo dyes, (Fernandez *et al.,* 1998; Fernandez *et al.,* 1999; Parra *et al.*, 2004; Gumy *et al.*, 2005). As this is a very expensive catalyst for practical use, low cost supports such as the C structured fabric (Yuranova *et al.,* 2004), activated carbon (Ramirez *et al.,* 2007), mesoporous silica SBA-15 (Calleja *et al.,* 2005; Martinez *et al.,* 2005; Martinez *et al.,* 2007), structured silica fibres (Bizzi *et al.,* 2003), resins (Cheng *et al.,* 2004; Liou *et al.,* 2005), zeolite (Sarbak, 1996; Fajerwerg and Debellefontaine, 1996; Centi *et al.,* 2000; Maurya *et al.,* 2002; Noorjaha *et al.,* 2005; Kusic *et al.,* 2006), ashes (Flores *et al.,* 2008), and clay (Chirchi and Ghorbel, 2002; Feng *et al.,* 2006; Chen and Zhu, 2007; Feng *et al.,* 2003; Liou *et al.,* 2004; Carriazo *et al.,* 2005) have been used for the immobilization of active iron species. Modified polyacrylonitrile fibres were also used to prepare transition metal impregnated catalysts (Tereschenko *et al.,* 2000; Ishtchenko, 2002; Ishtchenko *et al.,* 2003a; Huddersman and Ishtchenko, 2007 and 2008; Huddersman, 2009; Han *et al.,* 2009; Han *et al.,* 2010(a); Han *et al.,* 2010(b); Dong *et al.,* 2010; Han *et al.,* 2011).

The novel heterogeneous catalyst used in this research is based on a complex thread consisting of polyacrylonitrile (PAN) fibre filaments (DralonL: copolymer of acrylonitrile 92.3%, methylmethacrylate 6.2% and itaconic acid 1.5%), knitted together with one or two support threads of inert polypropylene (PP) in order to improve the mechanical and hydrodynamic properties of the resulting mesh. The resulting mesh, which can have different proportions of active threads:PP scaffold, (for the catalyst used in this work the ratio DralonL:PP was normally 50:50) was then chemically modified with hydrazine and hydroxylamine under alkaline conditions, according to the method and procedure described by Ishtchenko (Ishtchenko *et al.,* 2003a), and then improved by Huddersman and Ishtchenko (2007), to incorporate chelating functional groups onto the surface of the catalyst. The main reactions that take place between PAN and the modifying solution of hydrazine and hydroxylamine in alkaline conditions are shown in Figure 2.4. below (Karaivanova and Badev, 1986; Ishtchenko *et al.,* 2003a).
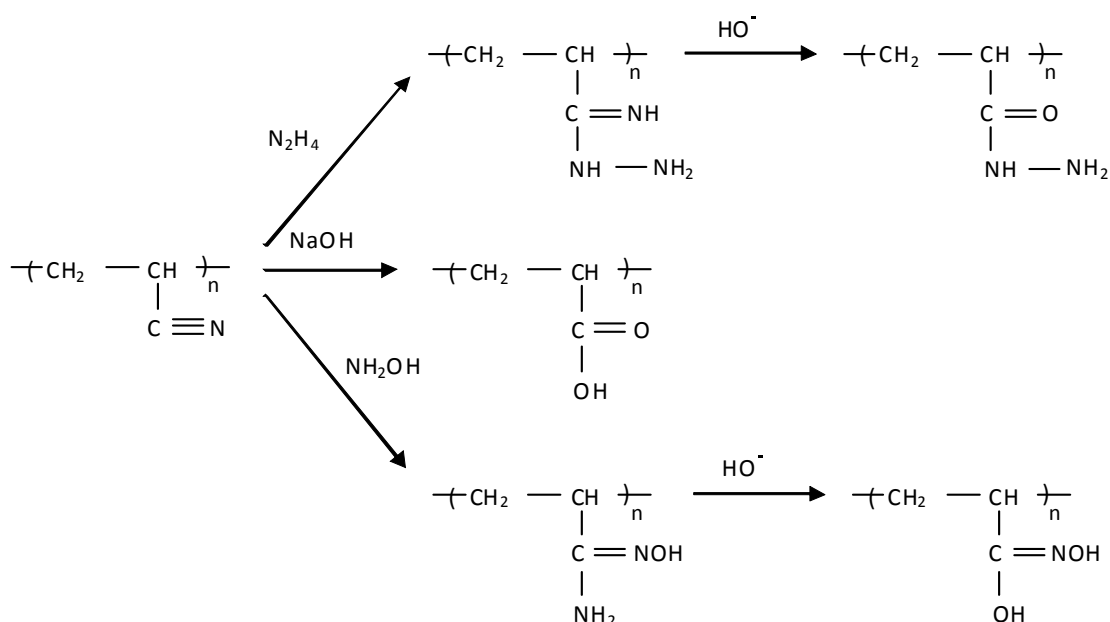
Figure 2.4. Main reactions of PAN threads with hydrazine, hydroxylamine and NaOH

The changes in the PAN threads could be identified after FTIR analysis of unmodified and modified (after each modification step) PAN threads, as shown in Figure 2.5. The interpretation of these FTIR spectra confirmed the formation of functional groups able to strongly ligate transition metal cations, such as Fe^{3+} during the impregnation step (step 3) of the catalyst production process (Chi Tangyie, 2008). These cations (Fe^{3+}) represent the active catalytic sites for the decomposition of H_2O_2 in the heterogeneous Fenton-like process.
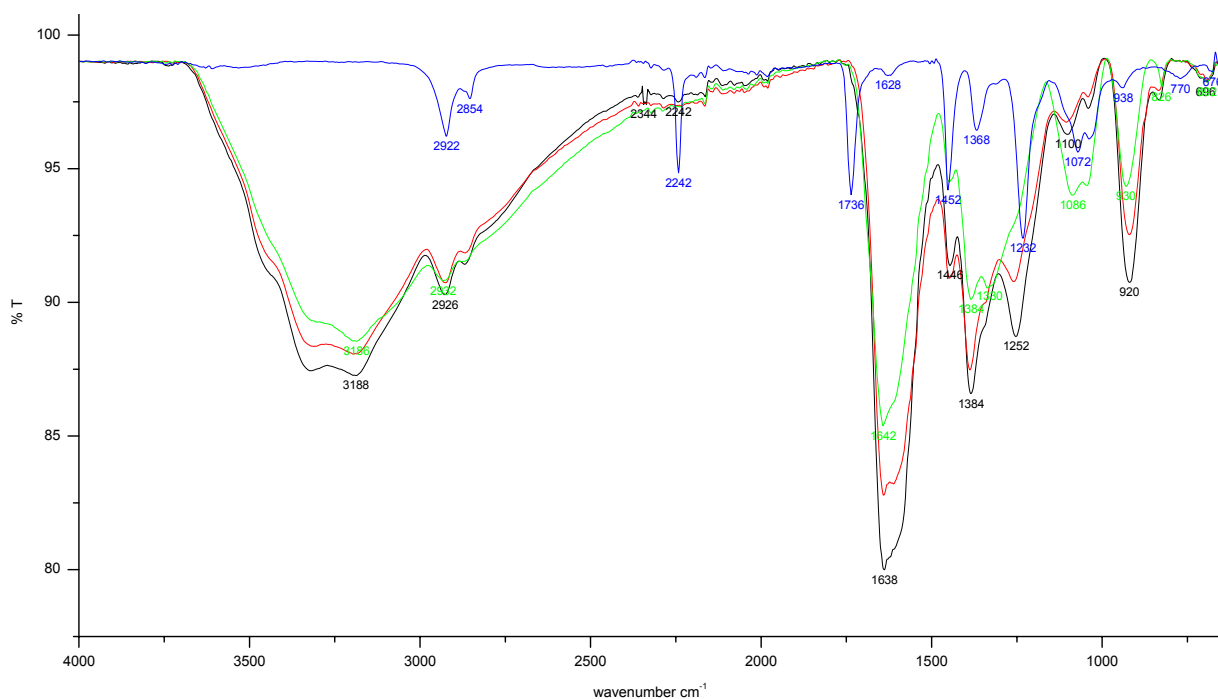
Figure 2.5. Overlaid baseline corrected FTIR-ATR spectra of unmodified PAN (blue) and modified PAN after modification step 1 (black), step 2 (red) and step 3 (green), (Chi Tangyie, 2008)

These ligating functional groups were proposed after interpretation of the above spectra and assignment of the different IR bands to the corresponding functional groups, as presented in table Table 2.3. (Chi Tangyie, 2008).

Table 2.3. Principal IR bands in PAN and modified PAN

Wavenumber (cm^{-1})	Assignment	Functional group
3400	υ(OH)	O-H hydroxyl group H-bonded stretch
3324	υ(NH$_2$)	N-H stretch in primary amine (-NH$_2$)
3210-3190	υ(NH)	N-H stretch of imino compounds (=N-H)
2924	υ(CH$_2$)	C-H asymmetrical stretch of methylene (CH$_2$)
2850	υ(CH)	C-H symmetrical stretch
2242	υ(C≡N)	C≡N saturated
1733	υ(C=O)	C=O as in esters
1640	υ(C=O)	as in amide -CONH$_2$
1613	δ(NH$_2$)	N-H, primary amine bend
1650-1580	υ(C=N, N-H)	C=N (includes C=N inoximes and imidines), N-H bends mixed
1540	υ(COO$^-$)	Acid salts
1445	δ(CH$_2$)	C-H bend of methylene
1384	δ_s(CH), δ_s(NH)	CH$_3$ bending mode
1236	υ(C-N), υ(C-C),	C-N, C-C, mixed
1106	υ(N-N)	N-N stretch of hydrazide group
1080	υ(C-O)	C-O stretch in C-O-Fe
1070, 1100	υ(C-O)	C-O stretch of primary alcohol, secondary alcohol
1130-1080,	υ(SO$_4^{2-}$)	Inorganic sulfate usually accompanied by a peak at 680-610 cm^{-1}
1036	υ(C-O)	C-O stretch in C-O-C
938	δ_r(CH)	Vinyl out of plane bend
920	υ(NOH)	N-O bend of Oxime, usually accompanied by N-O stretch at 1240–1215 cm^{-1}, C=N stretch at 1690-1620 cm^{-1}, and bonded OH stretch at 3300-3150 cm^{-1}
828	υ(NO$_3$)	Nitrate usually accompanied by a peak at 1410-1340 cm^{-1}
695	υ(O=C-N)	Bending motion of O=C-N group in amides

The ligating functional groups proposed are (Chi Tangyie, 2008):

amidoxime group

amide group

carboxyl group

alcohol group

hydroxamic acid group

imido hydrazide group

oxo hydrazide group
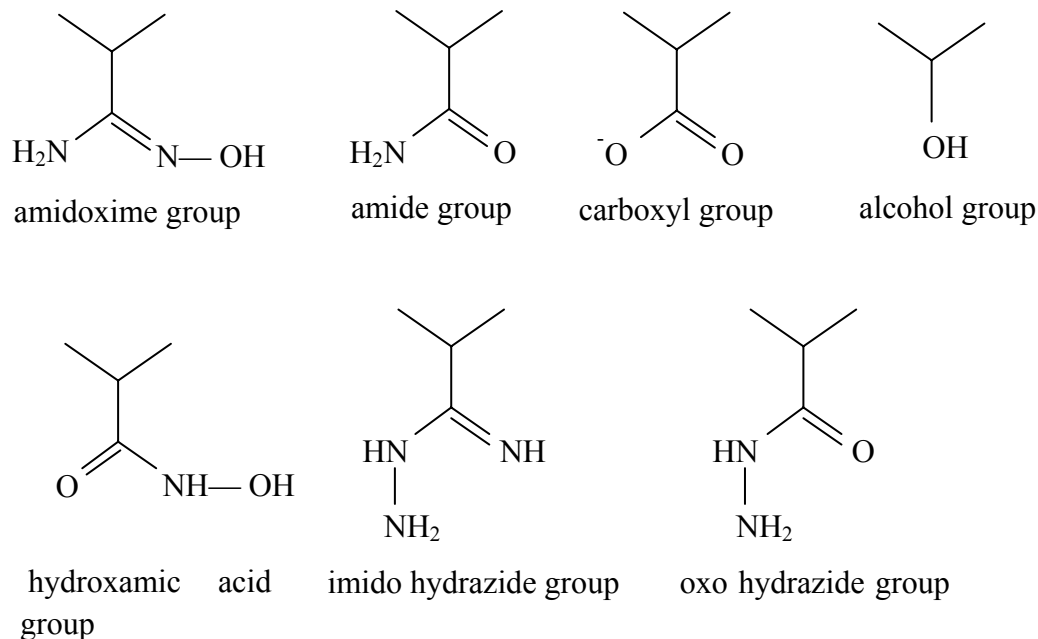
The heterogeneous fibrous catalyst produced is slightly acid, and even though the modification procedure reduces the mechanical strength by half in comparison to original fibre, strength indices are still within acceptable limits for exploitation of the catalyst in industrial applications. The good mechanical strength (tensile strength value of 18.7 MPa) and hydrodynamic properties, along with the fact that exposing the catalyst to acetone and solutions of acids and bases over a pH range of 2–12 showed negligible iron leaching from the fibres and the ability to decompose H_2O_2 in solution, make this catalyst an excellent choice for the wastewater treatment industry (Ishtchenko *et al.,* 2003b). This catalyst has proved to be very efficient for oxidizing organic compounds in aqueous phase reactions, in the presence of air and/or H_2O_2 as auxiliary oxidants. The catalytic activity was investigated towards different compounds, such as: phenol in addition to (i) the anthraquinone dyes: acid blue 45, carminic acid and reactive blue 19, and (ii) the azo-dye drimarine red K_4B_c (Ishtchenko, 2002; Ishtchenko *et al.,* 2003a), 4-nonylphenol (Chi Tangyie and Huddersman, 2007), real textile effluent

from a dyeing and finishing factory (Ishtchenko *et al.,* 2003a), effluent from the photographic industry (Yang *et al.,* 2006), and it shows potential towards the decomposition of leachate with high initial values of chemical oxygen demand (COD).

2.5. Summary

Scientific literature reports many studies published on the development and testing of effective catalysts for the gas phase catalytic decomposition of different classes of VOCs from air. Most of the reported research is based on noble metals (Pt and Pd) or metal oxides deposited on different supports. The main disadvantage of these catalysts is the operational parameters for the catalytic oxidation processes, as most of the reported catalysts operate at high temperatures (usually above 500 °C, very few at temperatures lower than 200 °C), some of them also requiring high pressures. The only catalysts that are efficient at low temperatures (operating at 25 °C) are those based on wood and coal ash; they have a high content of metal oxides such as Al_2O_3, Fe_2O_3 and TiO_2 (Kastner *et al.,* 2002; Kastner *et al.,* 2003).

Recognizing the importance of cost effective catalytic oxidation processes, the research work presented in this thesis aims to develop an alternative decontamination technology, based on the use of a novel heterogeneous fibrous catalyst used as threads or as an open knitted mesh, with or without the addition of H_2O_2 solution, and operating at moderate temperature and ambient pressure.

Chapter 3. Materials, instruments and methods

3.1. Introduction

This chapter presents the materials (catalyst, model pollutants and chemicals) used in this research, along with the instruments used for the identification and quantification of reactants and reaction products during the monitoring of the oxidation reactions. The methodology of sample preparation, analysis and calibration of instruments are also described herein.

3.2. Materials

3.2.1. Catalytic system

As mentioned in Chapter 2.4., in the presence of H_2O_2 solution, the novel fibrous catalyst used in this work is analogous to a heterogeneous Fenton-like catalyst. As the active sites of the catalyst are the Fe^{+3} ions strongly bound to the chemically modified

PAN fibres, the catalyst can be used as threads or as mesh, depending on the application. The use of catalyst as mesh is more common for the treatment of liquid samples (e.g. wastewater treatment), when the packing of the catalyst in the reactor takes advantage of the mechanical strength and good hydrodynamic characteristic of the catalyst. The mesh offers the option of a smooth, unobstructed flow of the liquid through the catalytic mesh, keeping at the same time the sample in intimate contact with the active sites. The use of the catalyst as fibres would offer the option of tighter packing of the catalyst in the reactor, for applications that do not require the mechanical strength of the polypropylene (PP) scaffolding. Figure 3.1. (a and b) shows the appearance of the catalyst as knitted mesh and as catalytic threads.

(a)   (b)

Figure 3.1. PAN fibre based catalyst: (a)-knitted mesh, (b)-catalytic threads

In this study, the catalyst was used in both physical forms: (i) **as fibres**, prepared by modification and impregnation of raw threads of polyacrylonitrile (Dralon L) resulting in catalytic threads having different iron contents (specified in the following sections, for each individual study presented), and (ii) **as mesh**, prepared by modification and impregnation of knitted mesh (different ratios DralonL:PP scaffold), resulting in

catalytic mesh with different iron content (again, specified in the following sections, for each individual study presented). The catalyst samples tested in this work were provided for use, after production and characterisation with regard to the iron content, which was determined by atomic absorption spectroscopy (AAS) after appropriate sample preparation. They were produced in different batches (at laboratory scale or at pilot scale), and thus they had different iron content; Table 3.1. presents a summary of the iron content on the catalyst, depending on the physical form of the sample used.

Table 3.1. Iron content and physical form of the catalyst used in the experimental work

Catalyst form	PAN:PP scaffold ratio	Fe content (mmol Fe/g thread)	Sample
Threads	-	0.083	KDHG1, E1
		0.165	GJ1
Mesh	70:30[*]	0.065	A
	50:50[**]	0.52	B

[*]produced in the laboratory
[**]produced at pilot scale

Control experiments with raw PAN fibres, modified fibres (after modification step 1 and 2 in the catalyst production process), or raw PAN-PP mesh were performed for comparison.

For the experiments involving H_2O_2, this was purchased from Sigma-Aldrich, UK, as stabilized aqueous solution (30 wt. %, density 1.11 g/mL at 25 °C). The solution was kept in the refrigerator at all times and was diluted to the required concentration before each experiment.

3.2.2. Choice of model pollutant system

Careful planning of experiments and design of the experimental rigs ensure a good start and minimize the inevitable problems that occur during the work in laboratory. First, in order to plan the experiments, the model pollutant system was chosen, this consisted of the mixtures air/dimethyl sulphide (DMS), air/ethyl mercaptan (EtSH), air/acetonitrile (MeCN), air/chloropicrin (CP), and air/EtSH/DMS. All these organic compounds were purchased as 'analytical grade' from Sigma-Aldrich, UK, except MeCN, which was purchased from Fisher Scientific, UK, as HPLC gradient grade.

The admissible limits in air (in closed rooms) are regulated by the USA Department of Labour, Occupational Safety and Health Administration (OSHA, 2008), and are presented below, along with the physical properties of these compounds (Lide, 1992):

Physical properties of Dimethyl Sulphide (DMS, CAS number: [75-18-3]):

Molecular formula: C_2H_6S; Molecular mass: M = 62.13 g/mole

Appearance: colourless to light yellow liquid

Vapour density: 2.14 (vs. air), Vapour pressure: 340 mmHg (20 °C)

Density: 0.846 g/mL (at 25 °C); measured to be 0.900 g/mL at 4 °C

Normal boiling temperature: 38°C; Normal melting temperature: - 98 °C

Solubility: slightly soluble in water (2% w/w), soluble in alcohol, ether

Odour threshold: 0.001 ppm;

OSHA admissible limit in air: 10 ppmv (20 mg/m^3 air)

Physical properties of Ethyl Mercaptan (EtSH, CAS number: [75-08-1]):

Molecular formula: C_2H_6S; Molecular mass: M = 62.13 g/mole

Appearance: colourless to light yellow liquid

Vapour density: 2.14 (vs. air), Vapour pressure: 442 mmHg (at 20 °C)

Density: 0.8391 g/mL (at 25 °C)

Normal boiling temperature: 36 °C; Normal melting temperature: -144.4 °C

Solubility in water: 0.68 g/100 mL at 20 °C, soluble in organic solvents

Odour threshold: 0.002 ppm

OSHA admissible limit in air: 10 ppmv (25 mg/m^3 air)

Physical properties of Acetonitrile (MeCN, CAS number: [75-05-8]):

Molecular formula: CH_3CN; Molecular mass: M = 41.05 g/mole

Appearance: clear, colourless liquid

Vapour density: 1.4 (vs. air), Vapour pressure: 73 mmHg (20 °C)

Density: 0.7766 g/mL (at 25 °C)

Normal boiling temperature: 81.6 °C; Normal melting temperature: -45.7 °C

Solubility in water: miscible in all proportions

OSHA admissible limit in air: 40 ppmv (70 mg/m^3 air)

Physical properties of Chloropicrin (CP, CAS number: [76-06-2]):

Molecular formula: CCl_3NO_2; Molecular mass: M = 164.38 g/mole

Appearance: Heavy, colourless, liquid with a sharp odour

Vapour density: 5.87 (vs. air), Vapour pressure: 18.3 mmHg (at 20 °C)

Density: 1.66 g/mL (at 25 °C)

Normal boiling temperature: 112 °C; Normal melting temperature: -64.5 °C

Solubility in water: 1.6 g/L at 25 °C

OSHA admissible limit in air: 0.1 ppmv (0.7 mg/m^3 air)

3. 3. Analysis of gas samples

3.3.1. Instruments

For the analysis of gas samples, two instruments were used: a Gas Chromatograph (GC) Perkin Elmer Series 8600 (for analysis of DMS, EtSH and MeCN in static experiments and EtSH in dynamic experiments) and a Gas Chromatograph – Mass Spectrometer (GC-MS) Varian series 2000 for the analysis of CP samples (static experiments).

Gas Chromatography is an analytical technique widely used to separate, identify and quantify the components of gas or liquid samples that can be vaporized without decomposition. The GC consists of an injection block, a column (housed in an oven with controllable temperature), and a detector. An inert gas such as helium (also called carrier gas or mobile phase), flows continuously through the system. A very small amount of liquid or gas sample (for capillary columns the sample is about 1 μL or less) is injected into the instrument and is volatilized in the hot injection chamber. Then, it is swept by the stream of inert carrier gas through the heated column which contains the

stationary phase (a microscopic layer of high-boiling liquid or polymer usually impregnated on a high surface area inert solid support like high purity fused silica or alumina), inside a piece of glass or metal tubing called column. As the mixture travels through the column, its components interact with the stationary phase and are separated based on the strength of this interaction. Each component of the sample will elute (leave the column) at a different time, known as the retention time (recorded by the instrument in minutes). Just before each compound exits the instrument, it passes through a detector, that sends an electronic message to the recorder (computer or printer), which records the chromatographic peak. The comparison of retention times is what gives GC its analytical usefulness. There are different types of detectors used in gas chromatography; the most common is the Flame Ionization Detector (FID), which is a very robust detector, highly sensitive to hydrocarbons. The disadvantage of this detector is that it destroys the samples.

Sometimes mass spectrometers are attached to the end of the GC and used as detectors (GC-MS), when the identification of the organic compounds is based not only on the retention time, but also on the mass spectra recorded on the instrument.

The Perkin Elmer Series 8600 GC is equipped with a FID detector, capillary column (Zebron ZB1) and gas sample loop (0.5 cm^3 volume), and is connected to a PC through a data acquisition interface. Helium at a constant pressure of 15 psi was used as carrier gas.

The characteristics of the ZB1 column used are:

Stationary phase: 100% Dimethylpolysiloxane on fused silica

Dimensions: length: 30 m

internal diameter: 0.32 mm

Film thickness: 5 micrometer

Temperature limits: minimum: - 60 °C,

maximum: 340/360 °C

The operating conditions for the GC were:

- Oven temperature: T_{oven} = 70 °C – isothermal (for analysis of DMS, EtSH, MeCN in static experiments)

- Oven temperature profile: T_1 = 70 °C for 3 minutes, then temperature ramp at 15°C/min to T_2 = 200 °C, isothermal at 200 °C for 1.4 minutes (for analysis of EtSH in dynamic mode, identification of diethyl disulphide (DEDS) as reaction product)

- Injector temperature: T_{inj} = 100 °C, split ratio 30:1

- Detector temperature: T_{det} = 225 °C

The retention times were: R_t = 3.25 minutes (for DMS), R_t = 2.36 minutes (for MeCN), R_t = 2.82 minutes (for EtSH), and R_t = 10.65 minutes (for DEDS). DEDS 99% purity (CAS number 110-81-6, density 0.993 g/mL at 25 °C, solubility in water: 0.36 g/L at 25 °C) from Sigma-Aldrich, UK, was used for calibration.

The GC-MS used for analysis of chloropicrin consists of a Gas Chromatograph Varian Star 3400CX (capillary column SGE BP1) linked to Mass Spectrometer Varian Saturn 2000 (detector). Helium at a constant pressure of 10 psi was used as carrier gas.

The characteristics of the SGE BP1 column used are:

Stationary phase: 100% Dimethylpolysiloxane on fused silica
                      suitable for most organic compounds

Dimensions: length: 30 m
                      internal diameter: 0.25 mm
                      Film thickness: 0.25 micrometer

Temperature limits: minimum: - 60 °C,
                      maximum: 340/360 °C

The working conditions for the GC during chloropicrin samples (gas) analysis were:

- Oven temperature profile: $T_1 = 35$ °C for 2 minutes, then temperature ramp at 20 °C
  /min to $T_2 = 220$ °C, isothermal at 220 °C for 1.5 min.

- Injector temperature: $T_{inj} = 175$ °C, split ratio 50:1

- Detector: Mass Spectrometer model Varian 2000

The working conditions for the Varian Saturn 2000 Mass Spectrometer were:

- Ionization mode: 'auto'

- Trap temperature: 220 °C

- Mainfold temperature: 100 °C

- Transfer line temperature: 275 °C

- Number of filaments: 2

- Axial modulation voltage: 4.0 V

- Emission current: 10 microampers

In these conditions CP was identified according to the mass spectra recorded (that was compared with the spectra of CP available in the instrument's library), and had a retention time of $R_t = 3.15$ minutes.

3.3.2. Calibration of instruments

The calibration of instruments was performed with gas samples having the same temperature as the samples involved in the static experiments. In all cases, the sample preparation for calibration followed the same procedure:

- **Preparation of a master gas mixture**: a master gas mixture was prepared by injecting 1 µL of liquid organic compound (0.5 µL for chloropicrin) in a 60 mL crimp sealed vial, kept at 45°C in thermostated oven before pollutant injection. The concentrations of the master gas mixtures were: **DMS**: 15000 mg DMS/m^3 air; **EtSH**: 14000 mg EtSH/m^3 air; **MeCN***: 13100 mg MeCN/m^3 air, **DEDS**: 16550 mg DEDS/m^3 air and **CP***: 13833 mg CP/m^3 air.

- **Preparation of gas samples:** volumes between 0.01 – 2 mL master gas mixture prepared as above, were injected into the already warm crimp sealed vials (60 mL), followed by vigorous shaking of the vial for homogenisation. For calibration in the lower range of concentration, repeated dilution of the gas samples was used to achieve the desired concentration. The injected volumes ensured the final concentrations used for calibration for each organic compound.

- **Sample collection for GC analysis**: All samples (DMS, EtSH, DEDS, MeCN) were kept at constant temperature (45°C) in a thermostated oven at all times during calibration, except for the time needed to inject the sample into the GC. 0.5 mL of gas sample was collected with a gas tight syringe (kept warm in the thermostated oven) and injected into the GC.

- **Sample collection for GC-MS analysis:** For chloropicrin, all vials were kept on a water bath at 50°C and the sample collection and injection into the GC-MS was made using the Solid Phase Micro Extraction (SPME) technique, with a SPME fibre MW 80-500, 30 μm polydimethylsiloxane manufactured and purchased from Supelco Company. The following procedure was applied: chloropicrin sample was collected by inserting the needle containing the SPME fibre in the crimp sealed vial (kept at 50 °C on a water bath), and exposing the absorbent fibre to the CP/air mixture for 15 minutes. After 15 minutes, the fibre was withdrawn inside the SPME device's needle and was transferred to the GC injector, where it was exposed for 2 minutes at 175 °C for CP desorption and analysis. CP was identified according to its mass spectra and the library of compounds available on the GC-MS instrument.

- **Collection of data:** For each compound at least five different concentrations were prepared according to this procedure. Peak areas at the corresponding retention times were recorded and plotted as a function of pollutant concentration in air. Each measurement had more replicates; the average values of peak area were recorded. The calibration curves were linear with R^2 between 0.9998 – 0.9892. The calibration equations were used to determine the concentration of pollutant in the gas samples.

3.4. Analysis of liquid samples

The liquid effluent from the dynamic experiments with hydrogen peroxide solution was analyzed periodically in order to identify and quantify any dissolved unreacted reactants (EtSH or DMS), oxidation products such as DEDS, sulphonic acids, organic acids and residual H_2O_2. For this purpose three analytical techniques were used: GC-MS - for identification of dissolved EtSH, DMS and DEDS, Ion Chromatography (IC) for the identification of advanced oxidation products (organic acids, ethane sulphonic acid and methane sulphonic acid), and visible spectroscopy (VIS) for the determination of the residual H_2O_2 in the liquid effluent.

3.4.1. GC-MS analysis of liquid effluent

GC-MS analyses of liquid effluent were performed on the same instrument (Gas Chromatograph Varian Star 3400CX linked to Mass Spectrometer Varian Saturn 2000 working as detector) used for the analysis of the gaseous CP sample (see section 3.3.1. above). The same capillary column SG-BP1 was used. The working conditions for the MS were the same as presented in section 3.3.1; the working conditions for the GC were:

- Oven temperature profile: T_1 = 32 °C for 3 minutes, then ramp at 20 °C/min to 180°C, isothermal at 180 °C for 1.5 min.

- Injector temperature: T_{inj} = 250 °C, split ratio 50:1

- Detector: Mass Spectrometer model Varian 2000

- Carrier gas: Helium at a constant pressure of 10 psi

The retention times were: 1.23 min (EtSH), 1.67 min (DMS) and 8.19 min (DEDS).

The compounds were identified according to their mass spectra and with the MS library available on the instrument. The instrument was calibrated for these compounds and the limit of quantification was determined to be 0.5 mg/L for these compounds. The calibration curve was linear with R^2 between 0.9917 and 0.9991.

3.4.2. IC analysis of liquid effluent

Ion-exchange chromatography (or ion chromatography, IC) is a process that allows the separation of ions and polar molecules from a liquid sample, based on their charge. The sample (usually a volume of 20 µL) mixes with the mobile phase (eluent) that flows continuously through the system and passes the column (that contains the stationary phase), where the actual separation takes place. The retention of the individual components of the sample is predominantly controlled by ionic interactions between the ions of the solute and the counter ions that are situated in, or on, the stationary phase (Fritz and Gjerde, 2000). For example, to separate organic acids, the negatively charged acid ions need to be selectively retained. This means that the stationary phase must contain immobilized positively charged cations as counter ions for retention of the acid ions. Similarly, to separate cations, the stationary phase must contain immobilized anions as counter ions with which the cations can interact. Usually a conductivity

detector is used to detect the changes in the electrical conductivity of the individual components of the sample and to send the signal to the recorder. Ion suppression is necessary when the mobile phase has a high conductivity and thus the contribution of the eluted ions to the total signal is insignificant in comparison to the background signal form the mobile phase (noise). The suppressor simultaneously lowers background conductivity from the eluent and enhances the analyte conductivity (Dionex, 2008).

The IC analyses were performed on an Ion Chromatograph Metrohm Modular MIC-2 advanced system (with computer controlled Metrohm IC-Net 2.3 software), equipped with a 20 µl injection loop and operated in isocratic mode, with the column temperature set at 30 °C. The operating conditions of the IC system were:

a) Identification of organic acids (formic acid and acetic acid):

- Column: Metrosep 5.1005.200 'Organic acids' column (250 mm x 7.8 mm, polystyrene/divinylbenzene copolymer packing material of 10 μm particle size)
- Eluent: H_2SO_4 solution (0.38 mM) at 0.5 mL/min
- Detection: Suppressed conductivity detector operated in positive mode at a full scale of 100 μS and range of 1 μS
- Suppressor: Cation Self-Regenerating Suppressor, using as regenerant a solution of 100 mM LiCl and double distilled water
- Pressure column: 2.1 MPa

v

In these conditions the retention times were: 13.39 minutes for formic acid and 14.87 minutes for acetic acid. The instrument was calibrated for these organic acids for

concentrations between 0.01 – 5 mg/L. The calibration curve is linear for this range of concentration, with $R^2 = 0.9991$ (acetic acid) and $R^2 = 0.9991$ (formic acid).

b) Identification of sulphonic acids (ethane and methane sulphonic acid)

- Column: Metrohm Ionpac column AS4A-SC, SN 23623 (250 mm x 4 mm, packed with ethylvinylbenzene crosslinked with 55% divinylbenzene microporous resin bead functionalized with very hydrophilic quaternary ammonium groups, particle size 13-μm diameter)

- Eluent: solution of Na_2CO_3 (2.5 mM) and $NaHCO_3$ (2mM) at 0.5 mL/min

- Detection: Suppressed conductivity detector operated in positive mode at a full scale of 300 μS and range of 1 μS

- Suppressor: Anion Self-Regenerating Suppressor using as regenerant a solution of 100 mM H_2SO_4 and double distilled water

- Pressure column: 2.5 MPa

In these conditions the retention times were 3.48 min for ethane sulphonic acid ($EtSO_3H$) and 3.52 min for methane sulphonic acid ($MeSO_3H$). The instrument was calibrated for $EtSO_3H$ for concentrations between 0.107 – 5.35 mg/L. The calibration curve was linear with $R_2 = 0.9991$. The calibration equation was used for quantification of $EtSO_3H$ during dynamic experiments. In the dynamic experiment with mixture of EtSH and DMS as simulated 'real effluent', the two sulphonic acids ($MeSO_3H$ and $EtSO_3H$) eluted together as one peak with a retention time of 3.49 minutes and the two peaks could not be separated (different mobile phases were tested).

3.4.3. VIS analysis of liquid effluent

UV/Vis spectroscopy is a routinely used analytical technique for the quantitative determination of different analytes, such as transition metal ions, highly conjugated organic compounds, and biological macromolecules. Determination is usually carried out in solutions. Solutions of transition metal ions can be coloured (i.e., absorb visible light) because d electrons within the metal atoms can be excited from one electronic state to another. The colour of metal ion solutions is strongly affected by the presence of other species, such as certain anions or ligands. Each compound absorbs the UV/Vis light at different wavelengths, and usually the working wavelength is the wavelength where the absorption is the maximum (λ_{max}). This can be taken from references (published tables), or more accurately, determined by performing a scan of absorption for the analyte within a wavelength interval (Skoog *et al.*, 2006). The quantification of the analytes is based on the Lambert-Beer law that states that the absorbance of a solution is directly proportional to the concentration of the absorbing species in the solution and the path length. Thus, for a fixed path length, UV/Vis spectroscopy can be used to determine the concentration of the absorber in a solution. The instrument needs to be calibrated for different concentrations of the analyte at λ_{max} (within the expected concentration range).

Analysis of hydrogen peroxide concentration

Reagents: ammonium metavanadate (99%, Sigma-Aldrich, UK) and H_2SO_4 solution (diluted from H_2SO_4 95.0-98.0%, density: 1.840 g/mL at 25 °C, Sigma-Aldrich, UK).

Instrument: Hach Lange DR 3800 visible spectrophotometer, with a working wavelength range between 320 and 1100 nm (wavelength used for analysis: 450 nm).

Procedure: The analysis of H_2O_2 concentration in the liquid effluent was performed by measuring the absorbance of a solution containing H_2O_2, ammonium metavanadate and sulphuric acid at 450 nm (maximum absorbance for the complex with H_2O_2), on a Hach Lange DR 3800 visible spectrophotometer, using a method developed by Abdul Galil *et al.*, (2007), and modified at De Montfort University, Leicester. The sample preparation for this analysis is simple: 1 mL of a 0.01M solution of ammonium metavanadate is mixed with 1 mL of 2M sulphuric acid solution and then 0.6 mL of a solution containing H_2O_2 of unknown concentration is added. The liquor is mixed for homogenisation and after 2 minutes (colour stabilisation time) the absorbance is measured at 450 nm. Zero reading was measured using the same procedure (with double distilled water instead of H_2O_2 solution). The instrument was calibrated for H_2O_2 solutions of 10, 25, 50, 100 and 200 mg/L concentration. The calibration curve was linear with $R^2 = 0.9983$. The calibration equation was used for quantification of hydrogen peroxide in the liquid effluent during the dynamic experiments.

Chapter 4. Preliminary study for the catalytic decomposition of airborne VOCs

4.1. Introduction

This chapter presents the results of a preliminary study for the catalytic decomposition of different airborne VOCs in static experiments, using the novel fibrous catalyst and oxygen from air as oxidant. The purpose of this study was to determine whether the catalytic system with air as oxidant is efficient in the removal of the studied VOCs from the air samples and, if yes, to determine the most suitable compound to be transferred to dynamic mode experiments for further studies at laboratory scale and for cost estimations for an eventual commercial scale-up.

Four organic compounds, namely DMS, EtSH, MeCN and CP were used in this study, in batch experiments, using crimp sealed glass vials (60 mL volume) as reaction vessel. The static experiments consisted of keeping the closed vials containing known amounts of catalyst and organic compound in a thermostated oven at 45 °C for different periods of time and analysing (by GC or GC-MS) the headspace composition periodically, looking for changes in the organic compound concentration (and eventually for

oxidation products). The samples were introduced into the GC using an airtight syringe or by solid phase micro extraction technique (SPME) for the GC-MS.

The concentration of pollutant (P) in air is expressed in ppm mass per volume: quantity of P [mg] in 1 m^3 of air (mg (DMS/EtSH/MeCN/CP)/m^3 air), according to equation 4.1.:

$$C_p = \frac{m_p\,(mg)}{V_{air}\,(mg)} = \frac{\rho_p\,(mg/L) \cdot V_p\,(mL)}{V_{air}\,(m^3)} \qquad (4.1)$$

where: - C$_P$: concentration of pollutant in air (mg/m^3 air)

- m$_P$: mass of pollutant (mg)
- V$_{air}$: volume of air (m^3)
- ρ$_P$: density of pollutant (mg/mL) (at 4°C for DMS; 25°C EtSH, MeCN, CP)
- V$_P$: volume of pollutant used to prepare the sample (mL)

4.2. Static experiments methodology, sample collection and analysis

The methodology presented in this section is the general methodology used in all the experiments performed in static mode in this research. The experimental conditions (physical form, mass and iron content of catalyst used, control experiments, etc.) are given for each compound tested, as they are different for each case.

Experiment methodology: master gas mixtures were prepared for each pollutant, according to the procedure described in section 3.3.2., Calibration of Instruments. Each experiment was performed in a number of replicates to check for reproducibility. A

known mass of catalyst or control (mesh or yarn) was introduced in a 60 mL glass vial at room temperature. After crimp sealing, the vials were introduced in a thermostated oven at 45 °C (water bath for chloropicrin) for 15 minutes to ensure that the same temperature was reached in the vials. 0.5 or 1 mL master gas mixture was then injected in each vial, this volume giving a theoretical initial concentration of pollutant in each vial. After injection, the vials were shaken to increase the homogeneity of the gas mixture inside the vial. The first analysis was made as soon as possible to determine the real initial concentration of the pollutant used in the experiment, which was then recorded as concentration at time t = 0. The experiments usually lasted for 2 – 4 hours with a final analysis after 5 hours in for one set of experiments. The vials were kept at 45 °C at all times except for the time needed to fill the syringe for the analysis.

Sample collection and analysis: for the experiments with DMS, EtSH and MeCN, samples were collected using an air tight syringe, kept at 45 °C at all times except for the time needed for sample collection (1 mL) and injection into the GC for analysis (every 30 minutes or every hour). The peak area at the corresponding retention times was recorded, converted into concentrations and plotted as a function of time. The samples were shaken regularly to ensure a better contact of the organic compound with the mesh/fibres inside the vials. For the experiments with chloropicrin, samples were collected using the SPME technique and procedure described in section 3.3.2., and analysed on the GC-MS Varian series 2000 (see section 3.3.1).

Experimental conditions for the preliminary tests: The amount of catalyst or control used varied between 0.1g and 0.46 g; this introduced a maximum error of 2% in the

volume, when considering the volume of the gas sample in the 60 mL vial. This was verified by measuring the volume of water that filled an empty vial and a vial containing the largest amount of catalyst/control. The specific experimental conditions for each organic compound tested are presented individually in the corresponding section.

4.3. Static experiments with DMS

4.3.1. Experimental conditions

DMS: initial concentration: 240 - 280 mg DMS/m^3 air (1 mL master gas mixture of concentration 15000 mg DMS/m^3 air injected in the 60 mL crimp sealed vials).

Catalyst:

1. 0.458 g catalytic mesh (70% Dralon L and 30% PP scaffold (% w/w)) with [Fe] = 0.065 mmol Fe/g threads; molar ratio Fe:DMS = 86.3:1

2. 0.1 g catalytic threads with [Fe] = 0.165 mmol Fe/g thread; molar ratio: Fe:DMS = 68.3:1

Control: same amounts of raw/modified mesh or raw fibres

4.3.2. Results and discussion for static experiments with DMS

The experiments with catalyst as mesh or threads (and the corresponding control experiments) were performed in 3 replicates in order to check for reproducibility. The experiments followed the methodology described in section 4.2. and lasted for 2 hours, with sample analysis every 30 minutes. For the experiments with catalyst as threads, a final analysis at 4 hours was also performed. The variation of DMS concentration with time for these experiments is presented in Figure 4.1. and Figure 4.2. The experimental points are the average value of three individual experiments. As the results are very similar, the standard deviation included in the figures is not noticeable.
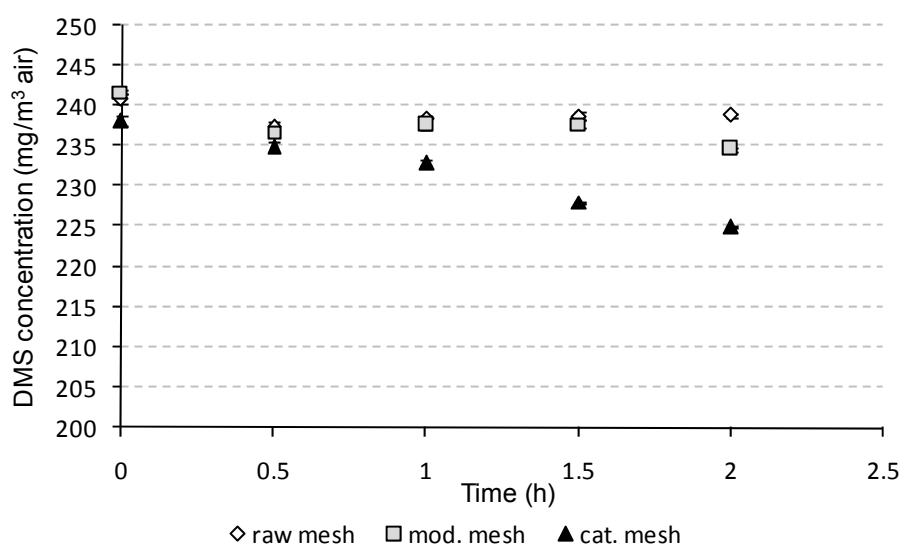
Figure 4.1. Variation of DMS concentration with time during static experiments with raw (◇), modified (▢) and catalytic mesh (▲)

The decrease in DMS concentration in time was calculated to be: 0.46% for raw mesh, 3.72% for modified mesh and 4.7% for the catalytic mesh. Figure 4.1. shows that the

catalytic mesh, from this modification batch, has very little activity in the decomposition of gaseous DMS over two hours.
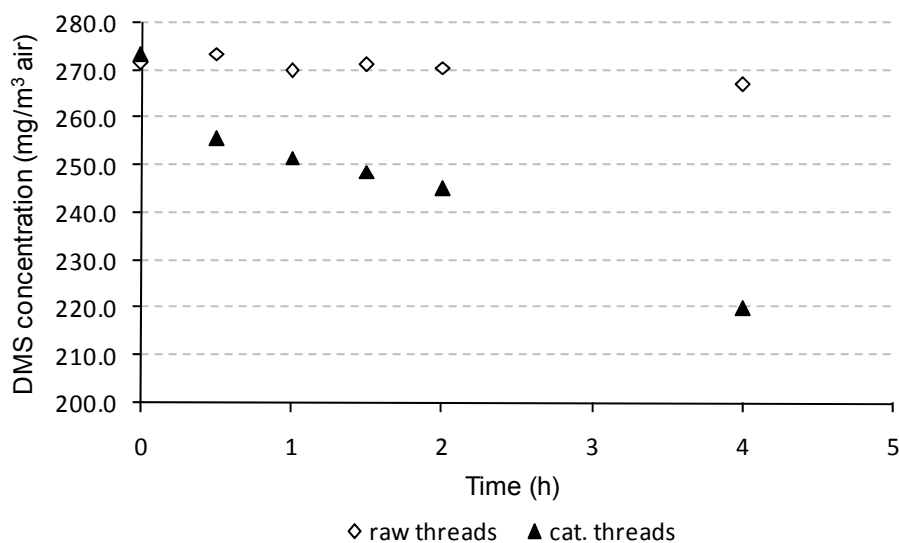
Figure 4.2. Variation of DMS concentration with time during static experiments with raw (◊) and catalytic threads (▲)

Figure 4.2. shows that during the 4 hours, the reduction in DMS concentration was 18-20% when using catalytic fibres, while in the control experiments with raw fibres the decrease was only ~2% (attributed to adsorption of DMS on threads). The decrease in DMS concentration was more pronounced when the catalyst was used as threads than when the catalyst was used as mesh. The process was still slow, with a DMS removal of max 11% after the first 2 hours. The Fe content of the catalyst was much higher for the threads (0.165 mmol Fe/g threads) than for the catalytic mesh (0.065 mmol Fe/g threads), but the molar ratio Fe:DMS in the vials was higher for the experiments with the catalyst as mesh (86.3:1) than for threads (68.3:1). The better results can be attributed to the distribution of the catalyst in the vials; the diffusion of DMS to the threads should be faster as the threads are more dispersed within the vial than the mesh.

4.3.3. Conclusions for static experiments with DMS

The decrease in pollutant concentration during control experiments with unmodified fibres/mesh was attributed to a process of pollutant adsorption on the fibres/mesh.

DMS adsorption is almost negligible on the unmodified mesh (70% Dralon L, and 30% PP scaffold, w/w) and approximately 2% on the raw Dralon L fibres. Adsorption was measured to be ~3.3 μg DMS adsorbed per g raw fibres.

Modified mesh after modification step 2 (i.e. after treatment with hydrazine and hydroxylamine and alkali to remove the cyano group of PAN) was also used as control in the experiments with DMS. A reduction in DMS concentration of ~3.7% was observed, not very different than when using catalytic mesh. Modified fibres were not used as control for the experiments with catalytic threads.

The decrease in DMS concentration was more significant when the catalyst was used as threads, even though the molar ratio Fe:DMS in the vials was higher when the catalyst was used as mesh. This could be due to a better contact between the catalyst and DMS, and probably a faster diffusion of DMS to the active centres, as the threads were more dispersed within the vial than the mesh.

4.4. Static experiments with MeCN

For this study, two sets of experiments were performed: with MeCN initial concentration of 108 mg/m^3 air and 215 mg/m^3 air. The catalyst used was prepared by modification and impregnation of raw threads of Dralon L, resulting in catalytic threads with iron content of 0.165 mmol Fe/g threads. Control experiments were performed with raw threads. The amount of MeCN was doubled (keeping all other experimental conditions the same) in order to check the effect of substrate concentration on the removal of MeCN from gas samples.

4.4.1. Experimental conditions

MeCN: initial concentration: 108 mg MeCN/m^3 air and 215 mg MeCN/m^3 air (0.5 mL and 1 mL of master gas mixture of concentration 13100 mg MeCN/m^3 air injected in the 60 mL vials).

Catalyst: 0.1 g catalytic fibres with [Fe] = 0.165 mmol Fe/g threads (molar ratio: Fe:MeCN = 103.4:1 and 51.7:1 respectively)

Control: 0.1 g raw fibres

4.4.2. Results and discussion for static experiments with MeCN

The experiments with MeCN and catalytic threads were performed following the experimental procedure presented in section 4.2. Control experiments with raw threads of PAN fibres were run to check for sorption of MeCN. Experiments were performed in three replicates to check for reproducibility. The experiments lasted for 4 hours, with sample analysis every 30 minutes for the first hour and then every hour.

The variation of MeCN with time for these experiments is presented in Figure 4.3. (110 mg MeCN/m^3 air) and Figure 4.4. (215 mg MeCN/m^3 air) below. The experimental points are the average value of the three individual experiments, with error bars indicating the standard deviation from this value, showing good reproducibility of the results.
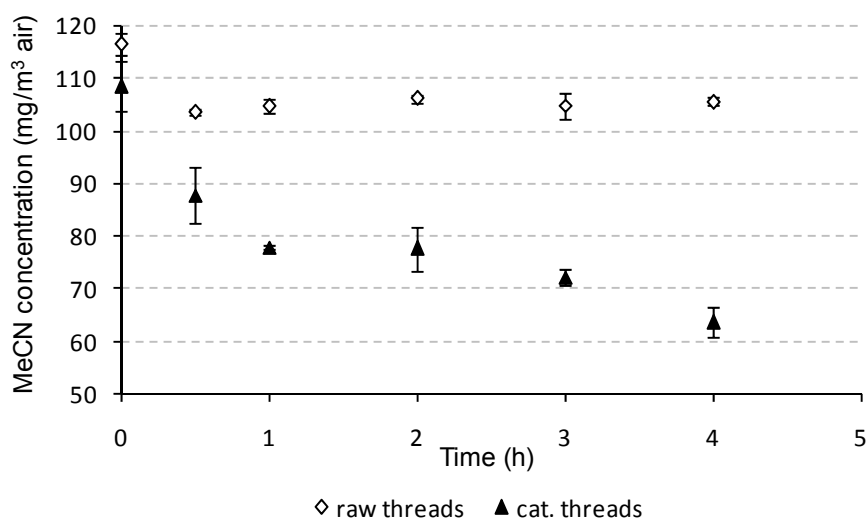
Figure 4.3. Variation of MeCN concentration with time in static experiments with raw (◊) and catalytic (▲) threads; initial MeCN concentration: 110 mg/m^3 air
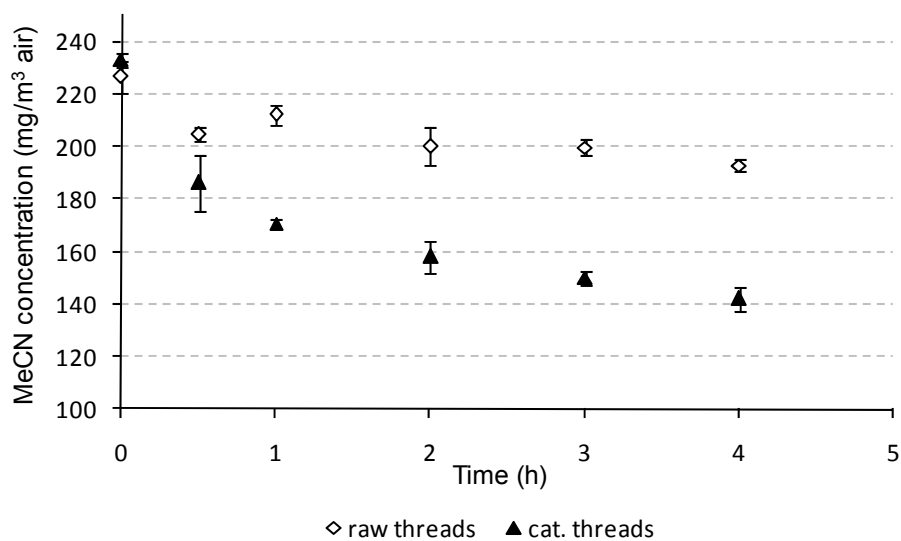
Figure 4.4. Variation of MeCN concentration with time in static experiments with raw ($\Diamond$) and catalytic ($\blacktriangle$) threads; initial MeCN concentration: 225 mg/m^3 air

The results show a decrease in MeCN concentration with time for both control and experiments with catalytic threads.

For the control experiments, MeCN concentration was reduced by ~9% when the initial concentration was 110 mg MeCN/m^3 air, and by ~15% when the initial concentration was 225 mg MeCN/m^3 air. This decrease in concentration can be attributed to adsorption of MeCN on the PAN fibres.

For experiments with catalytic threads, the decrease in MeCN concentration was about 40% in both cases. No reaction products were identified during the experiments with catalytic threads; this could be due to the lack of suitability of the GC method used for analysis, or because the reaction products were strongly held on the catalyst. The catalytic threads were not investigated at the end of the experiments.

The results show that the novel catalyst (as threads) is efficient in the removal of MeCN from air samples, but the process is slow. Adsorption of MeCN on raw PAN fibres depends on the initial amount of pollutant in the air sample. As the same amount of raw fibres adsorb almost double the amount of MeCN when the MeCN concentration in the vial is doubled, it can be concluded that adsorption of MeCN on raw PAN fibres is proportional to the amount of MeCN used in the static experiments and that the sites for sorption on the control had not been saturated after the 4 hours.

4.4.3. Conclusions for static experiments with MeCN

The static experiments with MeCN show that the novel catalyst is suitable for removal of MeCN from air samples, but the process is slow. Working even with relatively low MeCN initial concentrations and a big excess of catalyst, removal was only ~40% after 4 hours. The control experiments show that adsorption of MeCN on raw PAN fibres is proportional to the amount of MeCN used in the static experiments.

4.5. Static experiments with CP

4.5.1. Experimental conditions

CP: initial concentration: 227 mg CP/m^3 air (1 mL master gas mixture of 13833 mg CP/m^3 air injected in the 60 mL vials).

Catalyst: 0.35 g catalytic mesh with [Fe] = 0.52 mmol Fe/g threads (molar ratio: Fe:CP = 1080.7:1, large excess of iron)

Control: same amount of catalyst and CP, inert atmosphere of N_2 (ensured by flushing the vials with N_2 for 10 minutes before crimp sealing)

Temperature: the vials were kept at 50°C on a water bath, at all times during the experiments.

4.5.2. Results and discussion for static experiments with CP

The experiments with catalyst and chloropicrin in air and control experiments in N_2 atmosphere lasted for 5 hours, with sample collection and analysis every hour and were performed in 3 replicates to check for reproducibility.

The results for the experiments with chloropicrin and catalyst in air and control experiments in N_2 atmosphere are presented in Figure 4.5.
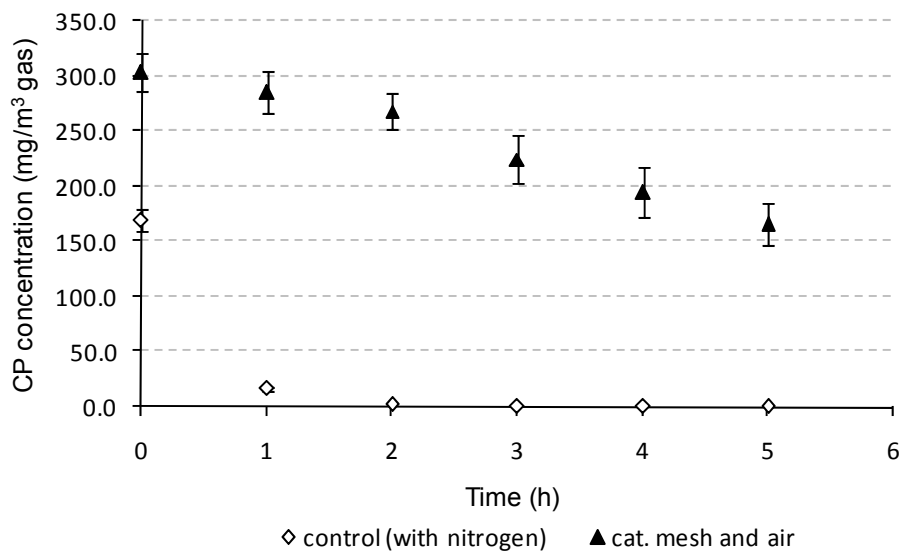
Figure 4.5. Variation of CP concentration with time in static experiments with catalyst and air (▲) and control experiments in inert atmosphere of N_2 (◊).

A decrease of about 46 % in the CP concentration was observed for the experiments with catalytic mesh and air, during the 5 hours. No reaction product was identified during sample analysis. Chloropicrin can be photolyzed in air, leading to phosgene and nitrosyl chloride, and further to CO_2, HCl, nitric oxide, Cl_2, NO_2 and nitrogen tetroxide in the presence of air humidity (Moilanen *et al*, 1978). None of these compounds were identified by GC-MS analysis. This could be due to unsuitability of GC column, or analysis conditions, or it can be assumed that CP is only adsorbed on the catalytic fibres and not actually decomposed.

For the control experiments, CP concentration decreased by 90-95% within the first hour and to 0 mg CP/m^3 air after 2 hours, but again, no reaction products were identified during the analyses.

Surprisingly, CP was removed faster in inert atmosphere of N_2 than in air, where O_2 is present. This could be attributed to competitive adsorption of chloropicrin and oxygen from air on the catalyst. When both oxygen and CP are present in the system, they compete for adsorption on the active sites of the catalyst. The adsorption of O_2 seems to be faster than that of CP considering that Fe is in great excess and that there is still CP identified in the system after 5 hours. When oxygen is not present in the system, CP does not have competitors in adsorption on the catalyst; therefore the removal of CP is faster. The results also suggest that N_2 is not adsorbed on the catalyst and/or that it is not effective in competing CP for catalyst sites. This theory needs to be further investigated by trying to identify compounds present on the catalyst at the end of both experiments.

To check whether there is a decrease in CP concentration in N_2 atmosphere (in the absence of catalyst), due to decomposition of CP, 0.5 mL of CP master gas mixture prepared as presented in section 3.3.2. was injected in a crimp closed vial containing only nitrogen. Following the experimental procedure described above, the CP concentration was monitored over a 4 hour time period, with sample collection and analysis every hour. The CP concentration was stable in time, at its initial value of ~125 mg CP/m^3 air. This test proves that in the experimental conditions used, without external irradiation with light of specific wavelengths, CP does not decompose to phosgene and nitrosyl chloride. Literature mentions that in the atmosphere and in cryogenic matrices, CP undergoes photolysis over a wide range of photolysis wavelengths, whether or not oxygen is present, giving phosgene and nitrosyl chloride as reaction products along with other smaller compounds (Wade *et al*, 2002).

4.5.3. Conclusions for static experiments with CP

In the experimental conditions used, the catalyst is not efficient in the decomposition of chloropicrin from air samples.

As no reaction products were identified during the GC-MS analyses, adsorption of CP on the catalytic fibres is likely to be responsible for the decrease in CP concentration. The used catalyst needs to be tested for identification of CP or any reaction products adsorbed on it.

CP and oxygen compete for adsorption on the active centres of the catalyst, as control experiments in N_2 atmosphere showed a faster removal of CP from the vials than for the experiments with air.

If CP is only adsorbed on the catalyst, this process is also slow. Only less than 50% of the CP used in the experiments was removed from the system in 5 hours of experiment.

In N_2 atmosphere, when there is no competition between CP and O_2 for adsorption on active centres, the removal of CP is faster (total removal within 2 hours). The theory of only adsorption of CP on catalytic fibres needs to be further investigated.

4.6. Static experiments with EtSH

The catalytic decomposition of EtSH was studied in static experiments with catalyst as mesh or as fibres and control experiments were performed with raw (unmodified) and modified fibres/mesh. The influence of addition of hydrogen peroxide (H_2O_2) into the system was also studied; in this case the control experiments were performed with EtSH and H_2O_2, without catalyst.

4.6.1. Experimental conditions

(i). Experiments without addition of hydrogen peroxide into the system

EtSH: initial concentration: 230 mg EtSH/m^3 air (1 mL of master gas mixture of concentration 14000 mg EtSH/m^3 air injected in the 60 mL vials).

Catalyst: 0.1 g (sample KDHG1, GJ1, E1) and 0.2 g (sample GJ1) of catalytic threads with [Fe] = 0.083 mmol Fe/g fibres (sample KDHG1 and E1), or [Fe] = 0.165 mmol Fe/g fibres (sample GJ1). Molar ratio: Fe:EtSH = 36.8:1 (sample KDHG1 and E1), and 73.2:1 or 146.4:1 (sample GJ1).

Control: ~0.1 and 0.2 g raw fibres and modified fibres after modification step 1 (with hydrazine and hydroxylamine) and step 2 (further modification with NaOH) in the production process for the catalyst.

(ii). Experiments with addition of H_2O_2 into the system

EtSH: initial concentration: 230 mg EtSH/m^3 air (1 mL of master gas mixture of concentration 14000 mg EtSH/m^3 air injected in the 60 mL vials).

Catalyst: 0.13 g catalytic mesh (50% catalytic threads – 50% PP scaffold) with [Fe] = 0.52 mmol Fe/g thread. Molar ratio Fe:EtSH = 300.4:1.

H_2O_2: 4 μL H_2O_2 (30% w/w), was added into the vial at the same time as EtSH. Molar ratio [Fe]:[H_2O_2] of 1:0.522.

Control: same amount of EtSH and H_2O_2 solution, no catalyst in the vials.

4.6.2. Results and discussion for static experiments with EtSH

4.6.2.1. Experiments with EtSH and no addition of H_2O_2 into the system

In order to study the effect of the iron content of the catalyst on the catalyst activity, several experiments with EtSH and catalytic threads from different production batches were performed according to the procedure presented in section 4.1. Three catalyst samples were tested: sample KDHG1 and E1 with [Fe] = 0.083 mmol Fe/g threads (different production batches) and sample GJ1 with [Fe] = 0.165 mmol Fe/g threads. The experimental conditions are those presented in section 4.6.1.(i). The experiments usually lasted for 4 hours, with headspace analysis every 30 minutes, but in some cases a final analysis was performed after 24 hours. The results are summarized below.

1. Static experiments with EtSH, raw/catalytic fibres (sample KDHG1)

The catalyst used ($[Fe] = 0.083$ mmol Fe/g threads) was prepared by modification and impregnation of raw threads of Dralon L and control experiments with raw threads were performed in the same conditions. The results are presented in Figure 4.6. (a) and (b).

Figure 4.6. Variation of EtSH concentration with time in static experiments with raw (◊) and catalytic (▲) threads; (catalyst sample KDHG1, $m_{cat} = 0.1$ g, $[Fe] = 0.083$ mmol Fe/g threads): (a) actual concentrations, (b) relative concentrations (C_t/C_0)

The decrease in EtSH concentration is max. 4.3% for in the control experiments and 4.9% when catalytic fibre was used. Considering the very small change in concentration over the 4 hours, it can be concluded that the catalyst sample KDHG1 was not effective in the decomposition of EtSH in these conditions. This might be due to storage conditions, as sample KDHG1 was used after being previously stored in open air for months before use (see also (3) within this section for a possible explanation according to the FTIR spectra of the catalyst sample).

2. Static experiments with EtSH, raw/catalytic fibres (sample GJ1)

The catalyst ([Fe] = 0.165 mmol Fe/g threads) used was prepared by modification and impregnation of raw threads of Dralon L and control experiments with raw threads were performed in the same conditions. The results are presented in Figure 4.7.

Figure 4.7. Variation of EtSH concentration with time in static experiments with raw (◊) and catalytic (▲) threads; (catalyst sample GJ1, m_{cat} = 0.1 g, [Fe] = 0.165 mmol Fe/g threads)

As seen in Figure 4.7. , the decrease in EtSH concentration during the 4 hours is ~4.9% for the unmodified threads (control), and ~ 92% for the catalytic fibres. The amount of Fe on the fibres is double for catalyst sample GJ1 compared with sample KDHG1, ensuring more active sites on the catalyst. Also, sample GJ1 was freshly prepared before use. It can be concluded that in this case, the catalytic threads show good activity in the removal of EtSH from air samples.

3. Static experiments with EtSH, raw/catalytic fibres (sample E1)

A freshly prepared sample of catalytic threads (sample E1) with the same iron content of [Fe] = 0.083 mmol Fe/g thread as sample KDHG1 was tested in order to determine whether the amount of Fe on the catalytic fibres has an influence on the removal of EtSH from air samples. Again, experiments with same amount of raw threads were run as control. The results are presented in Figure 4.8.
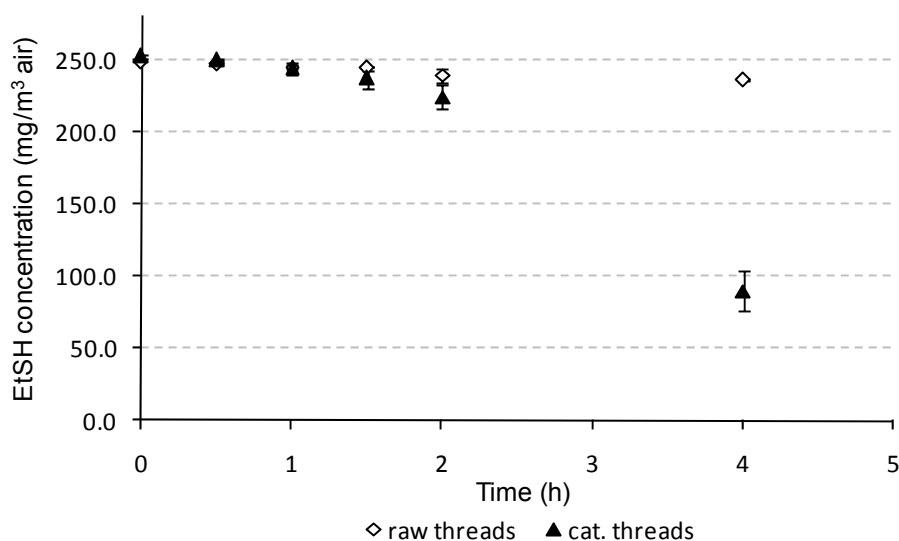
Figure 4.8. Variation of EtSH concentration with time in static experiments with raw ($\Diamond$) and catalytic ($\blacktriangle$) threads; (catalyst sample E1, m_{cat} = 0.1 g, [Fe] = 0.083 mmol Fe/g threads)

In this case, the decrease in EtSH concentration during the 4 hours is ~4.9% for the control experiments and 64.3% when catalytic fibres were used. The results for the experiments with samples E1 and KDHG1 should be similar, as the same amount of catalyst was used and the iron content of the two catalyst samples was the same ([Fe] = 0.083 mmol Fe/g threads), but sample KDHG1 showed practically no catalytic activity. Sample KDHG1 was stored for some time before usage, while sample E1 was freshly prepared before use. They also come from different batches.

To elucidate why the catalyst samples perform so differently, FTIR analysis of the three catalysts was performed, and the overlaid and baseline corrected spectra of the three catalyst samples are shown in Figure 4.9. The FTIR analysis was performed on a Perkin Elmer Spectrum One FTIR Spectrometer, with a microscope system. The instrument is equipped with KBr crystal, mylar beam splitters and ZnSe top plate for ATR measurement. The yarn samples were pressed against the crystal with a force of 80 units and each sample was scanned 8 times with a resolution of 4 cm^{-1}. The analysis for each sample was performed in three replicates to check for accuracy. Interpretation of FTIR spectra took into account the available information on the catalyst (Chi Tangyie, 2008), as presented in section 2.4. (see Figure 2.5., Table 2.3. and the functional groups proposed in the same section), and is presented below (Kuptsov and Zhizhin, 1998; Coates, 2000; Chi Tangyie, 2008).
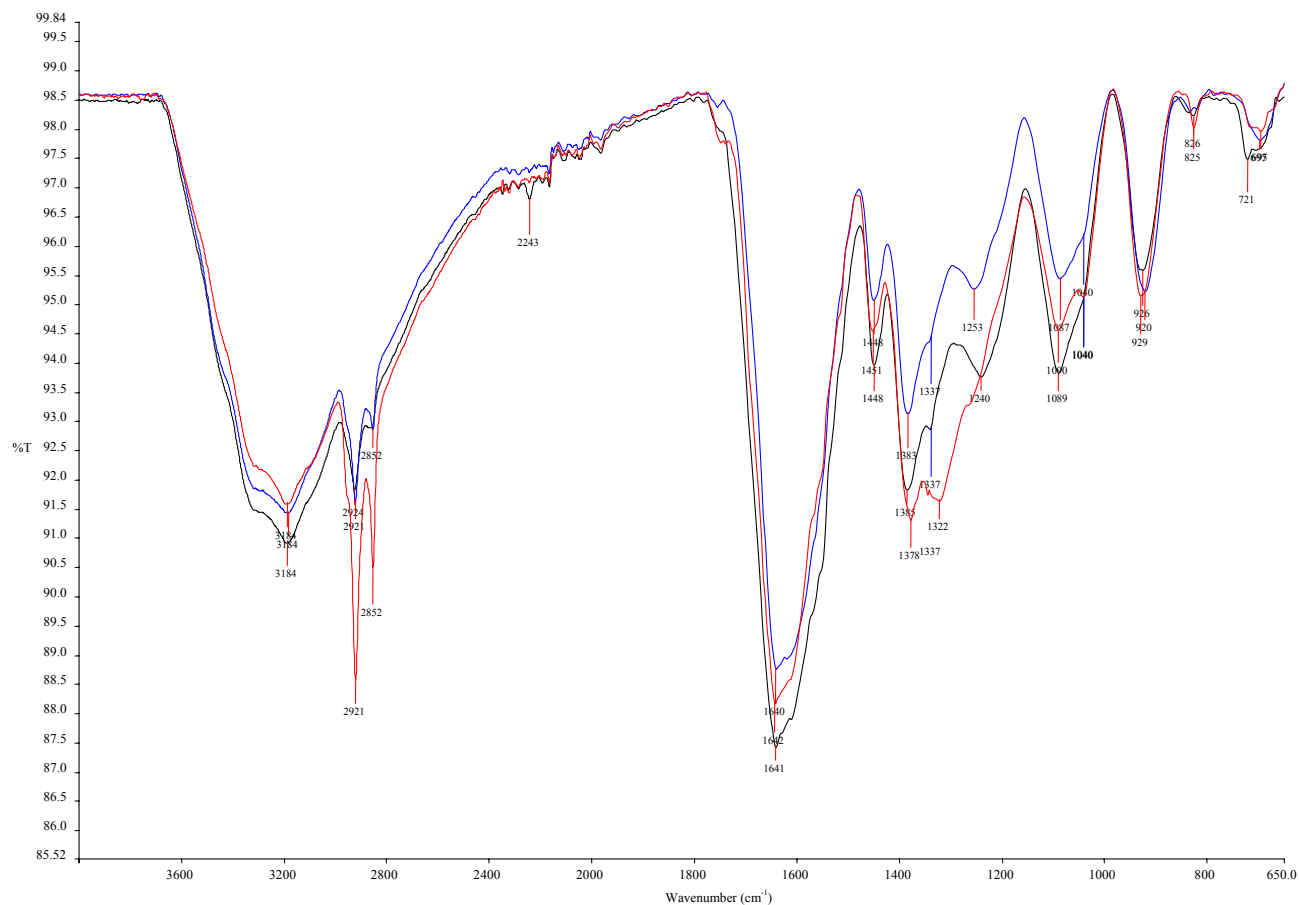
Figure 4.9. FTIR spectra for catalytic samples KDHG1 (red), GJ1 (blue) and E1 (black)

At a first glance, the spectra for all three samples KDHG1, GJ1 and E1 look similar. However, there are some differences, which are pointed out below:

The band at wavenumber 2243 cm^{-1} corresponds to the -cyano (-C≡N) functional group. The fact that this peak is still noticeable for sample E1 indicates an incomplete surface conversion of the -cyano groups during the modification procedure, with potential effect on the amount of iron ligated during the impregnation step (step 3 in the catalyst production). This is in good accordance with the lower iron content of sample E1 (0.083

mmol Fe/g threads) when compared to that of sample GJ1 (0.165 mmol Fe/g threads) for which the -C≡N peak is not present in the FTIR spectra.

All three samples have a wider band at wavenumber 1378-1383 cm^{-1}, with a shoulder at 1337 cm^{-1}. These bands correspond to the -C–N stretch of amine or amide group, bending of the N–H bond in amine, and also to the symmetric carboxylate stretch. The spectra for sample KDHG1 has an additional shoulder at wavenumber 1322 cm^{-1}, which is of medium intensity, attributed to bending of -N–H bond in amines or to vibrations of -O–H in alcohols. This shoulder is unusual for a freshly prepared catalyst (see Figure 2.5), and therefore could be due to aging of the catalyst or due to unknown organic compounds adsorbed on the surface of the catalyst during long storage.

The peak at wavenumber 1087-1089 cm^{-1} could correspond to stretches in the –C-O bond in the group C–O–Fe group. The fact that the spectra of sample KDHG1 has a visible shoulder at wavenumber 1040 cm^{-1} indicates again structural changes at the surface level, that could be attributed to potential adsorption of organic pollutants on the catalyst. Another possibility could be that exposing the catalyst to the open environment during lengthy storage facilitates the formation of FeO on the catalyst, reducing the amount of active iron on the catalyst and thus its efficiency.

Therefore, when comparing the performances of catalyst samples KDHG1 and E1 ([Fe]=0.083 mmol Fe/g thread for both samples), it is likely that sample KDHG1 was less active in the removal of EtSH from gas samples due to surface modifications that

occurred during storage, as the catalyst was used after long storage in open atmosphere and without previous washing.

When comparing the performance of the two catalyst samples JG1 and E1 (both were freshly prepared before use), the better performance of sample GJ1 could be attributed to the higher content of iron on the catalytic threads (0.165 mmol Fe/g thread for GJ1 vs. 0.083 mmol Fe/g thread for E1). The incomplete surface conversion of the -C≡N groups in sample E1 (as mentioned above) could be responsible for the lower iron content of catalyst sample E1.

4. Static experiments with EtSH and double amount of raw/catalytic fibre

To determine whether increasing the amount of catalytic fibres has any effect on the decomposition of EtSH, a set of experiments was run with double amount of raw PAN fibres (control) and catalyst sample GJ1, as this performed the best in the previous tests (m_{cat} = 0.2 g threads, [Fe] = 0.165 mmol/g threads). The experiments followed the same procedure described in section 4.1. and lasted for 5 hours, with headspace analysis every 30 minutes for the first hour and then every hour. The last headspace analysis was performed after 5 hours as the decrease in EtSH concentration after 4 hours was considerable, but not total. The results of these experiments are shown in Figure 4.10.
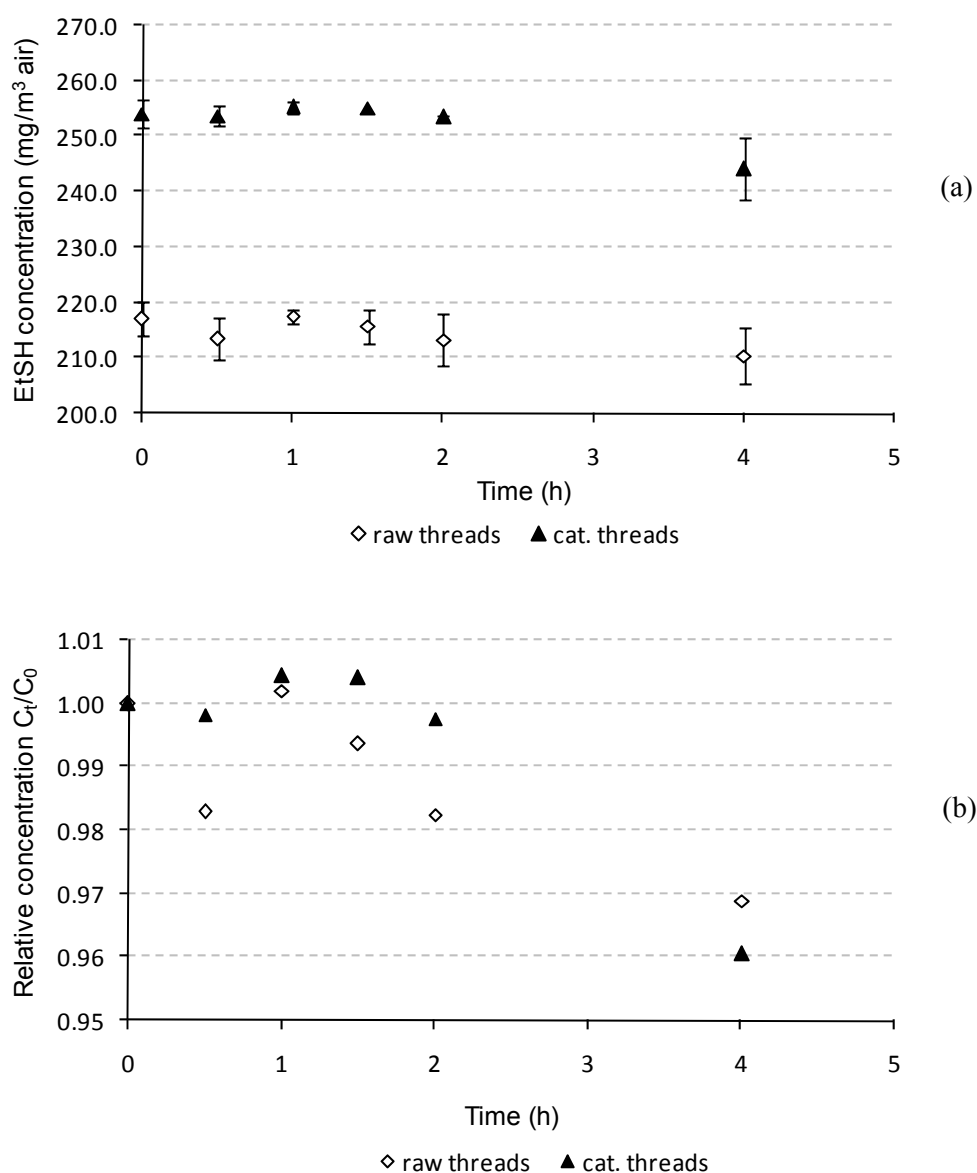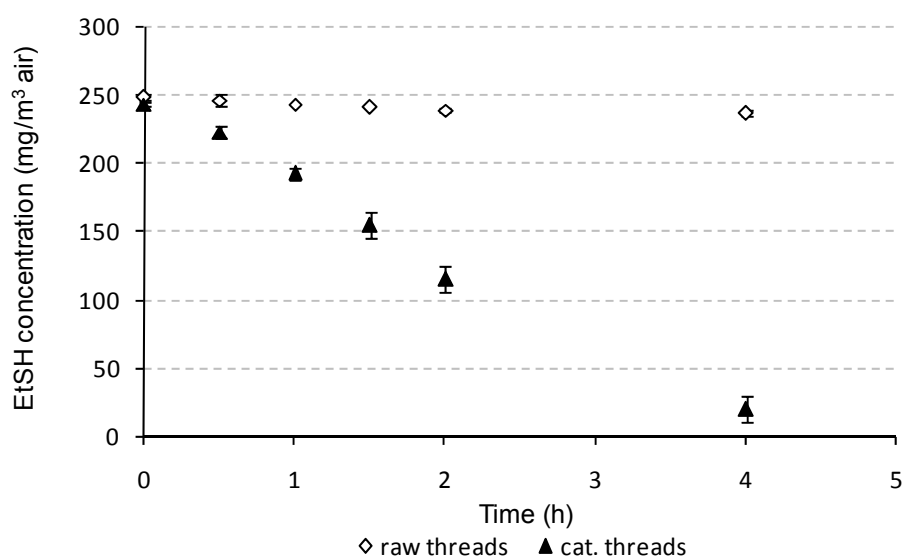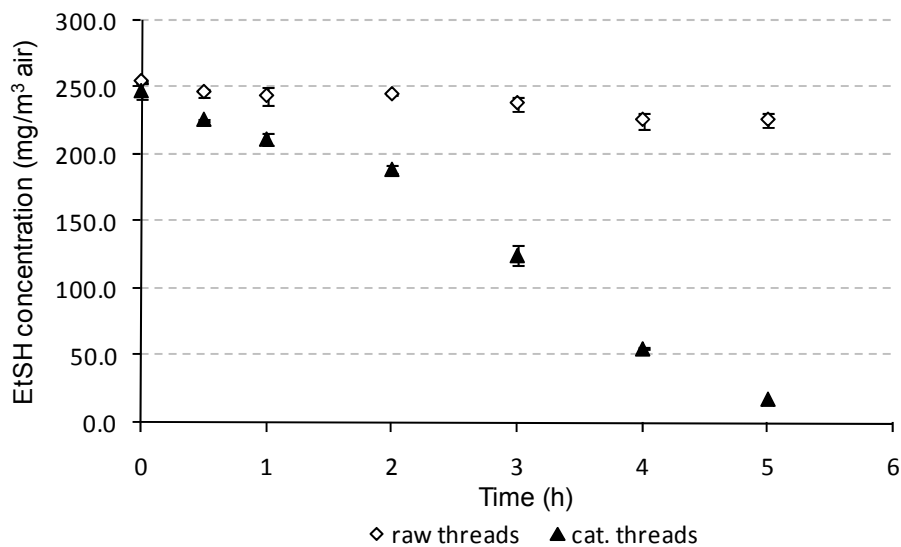
Figure 4.10. Variation of EtSH concentration with time in static experiments with double amount of raw (◊) and catalytic (▲) threads; (catalyst sample GJ1, m_{cat} = 0.2 g, [Fe] = 0.165 mmol Fe/g threads)

In the first 4 hours of the experiment the decrease in EtSH concentration was approximately 11% for the control (raw threads) and approximately 78% for the catalytic fibre. After 5 hours there was no further reduction in EtSH concentration for the control experiment, while for the experiment with catalytic fibres EtSH concentration had decreased further, showing a total removel of ~93%.

Figure 4.11. shows a comparison between the reductions in EtSH concentration during experiments with catalyst GJ1, normal and double amount of fibres.
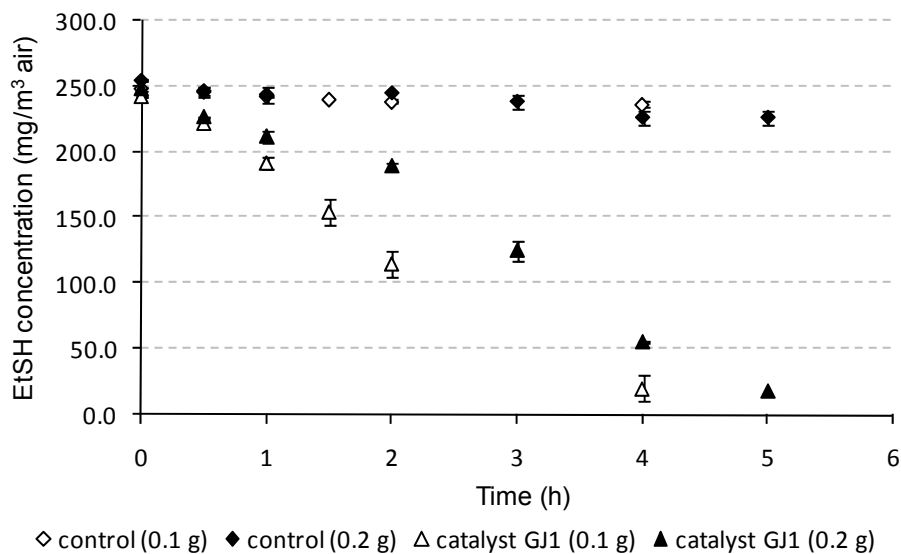
Figure 4.11. Variation of EtSH concentration with time; comparison between experiments with 0.1 and 0.2 g threads: control (◊ and ♦) and catalyst sample GJ1 (△ and ▲)

From these experiments (see also Table 4.1) one can conclude that the adsorption of EtSH on the raw fibres depends on the amount of fibre used, as the amount of EtSH adsorbed doubled (from ~5% to ~11%) when the amount of fibres doubled. The amount of catalytic threads used does not significantly influence the removal of EtSH in static experiments. Double amount of catalytic fibres ensures double amount of active sites, but the removal rate of EtSH is not influenced, showing that the amount of iron on the catalyst was already in excess, and the rate of reaction is limited by other factors.

Table 4.1. Summary of conditions and conclusions for the static experiments with EtSH

Nr	Catalyst sample	Sample form	[Fe] (mmol/g thread)	Amount Sample (g)	EtSH (initial conc.) (mg/m^{3}air)	Molar ratio Fe:EtSH	EtSH removal (%) 4 h	EtSH removal (%) 5 h	Notes
1	Raw DralonL	fibre	-	0.1	217	-	~3.5	-	Catalyst produced using raw threads of Dralon L; the catalyst was stored open, in a drawer, before use.
	KDHG1	fibre	0.083	0.1	254	36.8:1	~4	-	
2	Raw DralonL	fibre	-	0.1	248.4	-	4.9	-	Catalyst produced from raw threads of Dralon L and used as freshly prepared.
	GJ1	fibre	0.165	0.1	242.8	73.2:1	91.7	-	
3	Raw DralonL	fibre	-	0.1	248.2	-	4.9	-	Catalyst produced from raw threads of Dralon L and used as freshly prepared
	E1	fibre	0.083	0.1	252.3	36.8:1	64.3	-	
4	Raw DralonL	fibre	-	0.2	254.9	-	~11	~11	Doubling the amount of raw fibers doubles the amount of EtSH adsorbed on them
	GJ1	fibre	0.165	0.2	247.8	146.4:1	~78	~93	

4.6.2.2. Experiments with EtSH and addition of H_2O_2 into the system

The influence of addition of hydrogen peroxide into the system for the catalytic oxidation of EtSH was first investigated in static mode experiments. The experiments lasted for three hours and were performed according to the procedure described in section 4.2. and the experimental conditions presented in section 4.6.1.(ii). Headspace analyses were performed every 30 minutes, in the same conditions presented in the sections above.

Control experiments were performed with EtSH and hydrogen peroxide, but without catalyst. Later sections of this work present the identification of diethyl disulphide (DEDS) as reaction product for the catalytic oxidation of EtSH in the presence of the novel catalyst and oxygen from air. As the experiments with EtSH and H_2O_2 were performed after the identification of DEDS as reaction product and they are static experiments, these results are included in this chapter. DEDS and EtSH were both monitored during the dynamic experiments, and thus the GC was calibrated against DEDS, according to the procedure described in section 3.3.2. The formation of DEDS shows that the catalyst was able not only to remove EtSH from air by sorption, but to also catalyse its oxidation to the disulphide.

A set of three experiments with catalyst as mesh and the same number of control experiments were performed using the conditions presented in section 6.1. The results are presented in Figure 4.12.
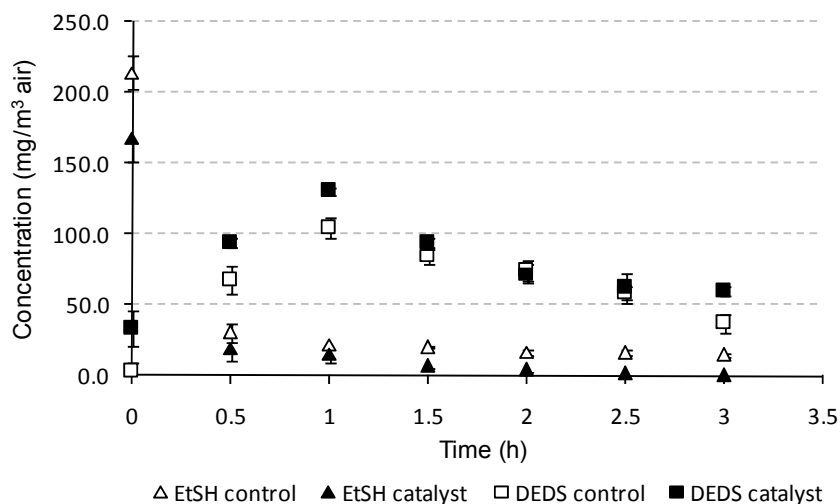
Figure 4.12. Variation of EtSH and DEDS concentrations with time in static experiments with EtSH and H$_2$O$_2$

Figure 4.12. shows that EtSH concentration decreases in time and DEDS is formed as a reaction product for both control and experiments with catalytic mesh. The control experiments show that EtSH is oxidized to DEDS in the presence of H$_2$O$_2$ even without catalyst, but the oxidation is slightly slower in this case, as after 3 hours there still is unoxidized EtSH in the vial. In the presence of catalyst and H$_2$O$_2$ solution EtSH concentration is reduced to zero after 2 hours and the amount of DEDS is slightly higher at all times during the experiment (compared to the experiment with H$_2$O$_2$ alone).

In all cases, additional peaks were noticed on the chromatograms (besides those corresponding to EtSH and DEDS), indicating that in the presence of H$_2$O$_2$, EtSH undergoes a more advanced oxidation process.

In the control experiments two new peaks were noticed (retention times R_T = 1.68 minutes and R_T = 2.11 minutes), while in the experiments involving the novel catalyst four new peaks were noticed (R_T = 1.68 minutes, R_T = 2.0 minutes, R_T = 2.11 minutes,

and R_T = 4.92 minutes). In all cases the new peaks were first seen at time t = 0.5 hours

and the peak intensities were stable with time.

Two examples of these chromatograms (time t = 2 hours) are presented in Figures 4.13

and 4.14.
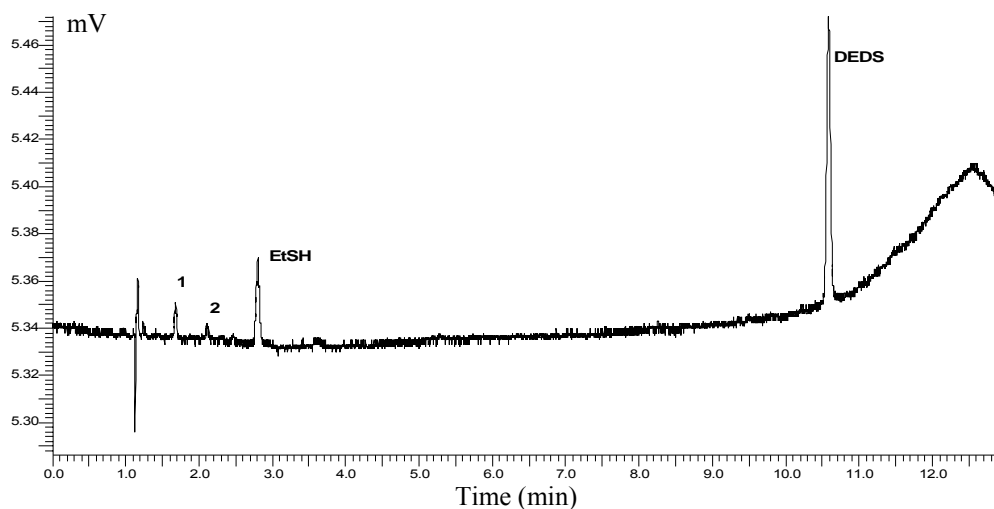
Figure 4.13. Chromatogram for control experiment with EtSH and H$_2$O$_2$ in static mode (t=2 hours). Retention times are: peak 1: 1.68 minutes, peak 2: 2.11 minutes, EtSH: 2.87 minutes and DEDS: 10.65 minutes.
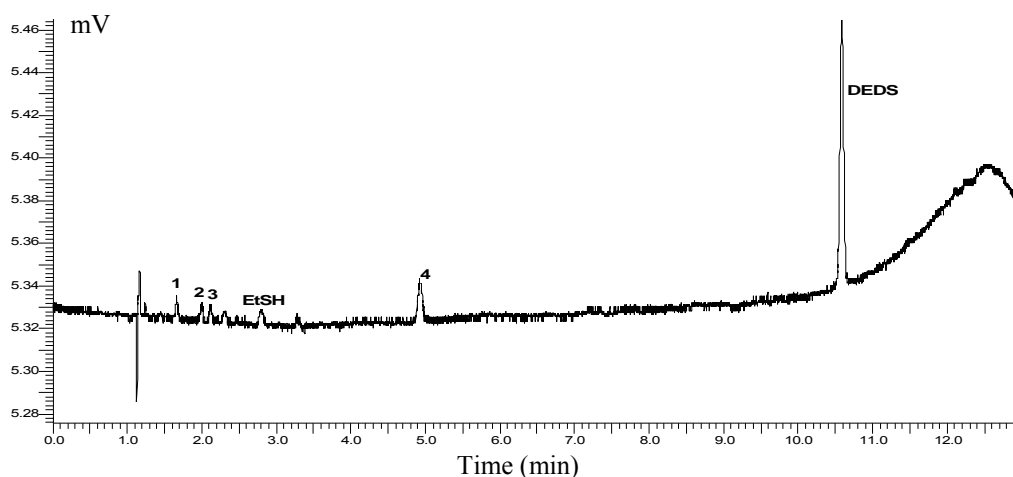
Figure 4.14. Chromatogram for experiment with EtSH, catalyst and H$_2$O$_2$ in static mode (t=2 hours). Retention times are: peak 1: 1.68 minutes, peak 2: 2.0 minutes, peak 3: 2.11 minutes, EtSH: 2.87 minutes, peak 4: 4.93 minutes and DEDS: 10.65 minutes.

The new peaks were not associated to any compounds as analyses on GS-MS were unsuccessful due to the unsuitability of the fibre used in the solid phase micro extraction technique (SPME) employed for sample collection and injection into the instrument.

The static experiments with EtSH, catalyst and H_2O_2 show that when H_2O_2 is added into the system, EtSH undergoes an advanced oxidation process and as a result, four additional peaks are visible on the chromatograms. During the control experiments, only two new peaks appear in addition to that corresponding to DEDS, indicating that the system catalyst/H_2O_2 is more effective in the oxidation of EtSH than H_2O_2 alone.

4.6.3. Conclusions for experiments with EtSH

EtSH was the organic compound involved in most of the experiments presented in this work. Before diethyl disulphide was identified as a reaction product, the experiments were focused on monitoring the disappearance of EtSH. Later, for the experiments with H_2O_2 added into the system, a reaction product (DEDS) was also monitored. For the static experiments with EtSH, it can be concluded that:

Adsorption of pollutant on raw fibres/mesh

Adsorption on the raw fibres is more pronounced for EtSH than for DMS. Approximately 5% EtSH removal was measured using 0.1 g raw fibres (7.5 µg EtSH adsorbed per g Dralon L fibres).

Using double the mass of raw fibres doubles the amount of EtSH adsorbed, indicating that 7.5 μg EtSH/g Dralon L fibres is the maximum value for EtSH adsorption in these experimental conditions.

Use of catalytic fibres/mesh

The novel catalyst (as fibres or mesh) was effective in the decomposition of EtSH from air samples, in static phase experiments.

Threads are more disperse in the vials than mesh, thus the pollutant access to the active sites and the decomposition rate is faster when using catalyst in the form of fibres.

Increasing the Fe content of the catalyst increases the reaction rate as shown by comparison between results of experiments with samples GJ1 ([Fe]=0.165 mmol Fe/g threads) and E1 ([Fe=0.083 mmol Fe/g threads). The lower iron content of sample E1 could be due to the incomplete conversion of the –CN functional group during the modification of PAN with hydrazine and hydroxylamine in alkaline conditions (see section 4.6.2.1(3) and Figure 4.9.) Even though sample KDHG1 had the same amount of iron on the threads as sample E1 ([Fe]=0.083 mmol Fe/g threads), its performance in the removal of EtSH from air was worse than that of sample E1. This could be attributed to surface modifications that occurred during lengthy storage.

 The experimental conditions ensured an excess of Fe in the system at all times. Doubling the amount of catalytic fibres does not influence the decomposition rate of EtSH. Experiments with 0.1 and 0.2 g catalyst (sample GJ1, [Fe] = 0.165 mmol Fe/g

threads) show that [Fe] on the catalyst was already in excess; the rate of reaction is limited by other factors.

As concluded from the FTIR spectra, poor modification leads to lower iron content on the catalyst, which affects its performance (the efficiency of catalyst sample E1 was lower than that of sample GJ1) in the removal of EtSH from air.

Storage of the catalyst before usage may influence its activity. It was observed that the catalyst freshly prepared had a higher catalytic activity than the catalyst stored in open atmosphere. The best results were observed when using freshly prepared catalyst.

Addition of hydrogen peroxide into the system

When H_2O_2 is added into the system, EtSH undergoes an advanced oxidation process and as a result, four additional peaks are visible during GC analysis of the gas samples, associated to unidentified reaction products. DEDS remains the main reaction product in the oxidation of EtSH in these conditions.

During control experiments, only two new peaks appear in the chromatograms in addition to DEDS, indicating that the system catalyst/H_2O_2 is more effective in the oxidation of EtSH than H_2O_2 alone.

The method of introducing H_2O_2 into the system should be changed to spraying it onto the catalyst; this would improve the contact between the catalyst and H_2O_2 as with the previous method moisture could be seen on the vial walls.

Chapter 5. Gas-solid catalytic decomposition of airborne EtSH

5.1. Introduction

This chapter presents the results of dynamic mode experiments with EtSH as model air pollutant, the novel catalyst (as threads or as knitted mesh) and oxygen from air (of ambient or increased humidity) as oxidant.

The purpose of this study was to determine whether the catalyst/air system is efficient in the oxidation of a continuous flow of air contaminated with EtSH, at moderate temperature and ambient pressure, without any additional oxidant, and to determine the oxidation products. The conversion of reactant (i.e. EtSH) and the turnover frequency for the catalyst were also calculated, as they provide valuable information on the efficiency of the catalytic process.

The used catalyst was investigated in order to determine possible causes of deactivation, looking for reactants or reaction products adsorbed on the catalyst or for changes in the functional groups on the catalyst that could explain its deactivation.

5.2. Experimental setup and experiment methodology

The experimental rig used in the work presented in this chapter was designed to incorporate a fixed bed catalytic reactor (made of glass) with on-line GC analysis of the gas samples. The experimental rig, with and without foil wrapping (heat insulator) is presented in Figure 5.1. and Figure 5.2., with a closer view of the reactor in Figure 5.3. The schematic for the experimental setup is presented in Figure 5.4.

The experiments consisted of the passage of a mixture of air and EtSH, in known concentration, through the catalyst bed placed in a thermostated tubular reactor, followed by the GC analysis of the out stream gas using the Perkin Elmer GC presented in section 3.3.1., linked to a PC for on-line analysis of the samples.

Figure 5.1. Dynamic experimental rig used for the oxidation of EtSH in dry conditions, wrapped in foil for better heat insulation

Figure 5.2. Dynamic experimental rig used for the oxidation of EtSH in dry conditions, with full view of the heating system
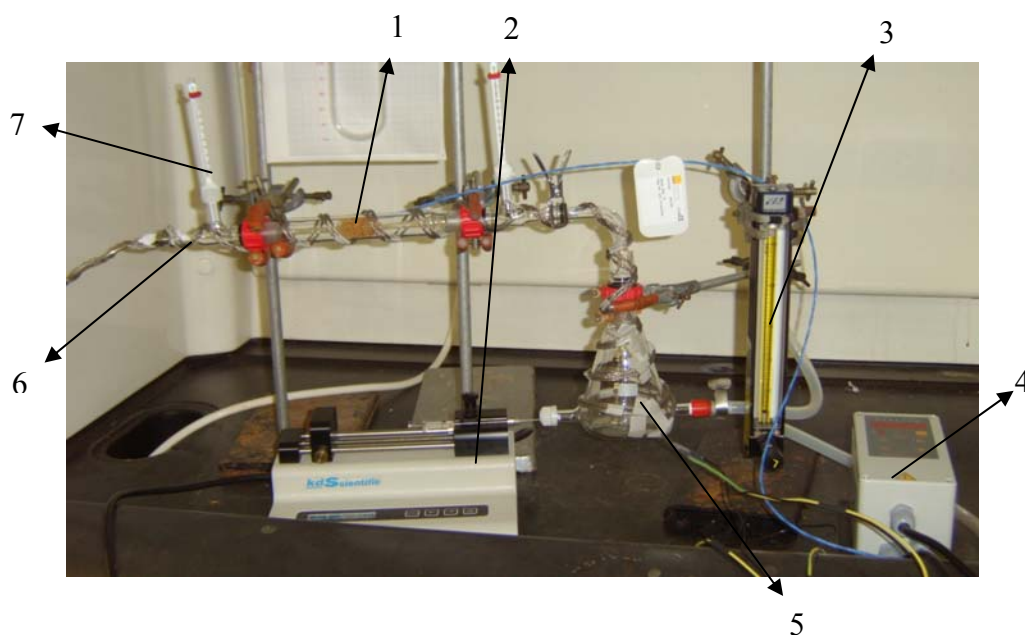
Legend: 1-loaded catalytic reactor, 2-syringe pump, 3-flow meter, 4-temperature controller, 5-mixing vessel/evaporator, 6-heating cable, 7-thermometer

Figure 5.3. Close up view of the dynamic experimental rig
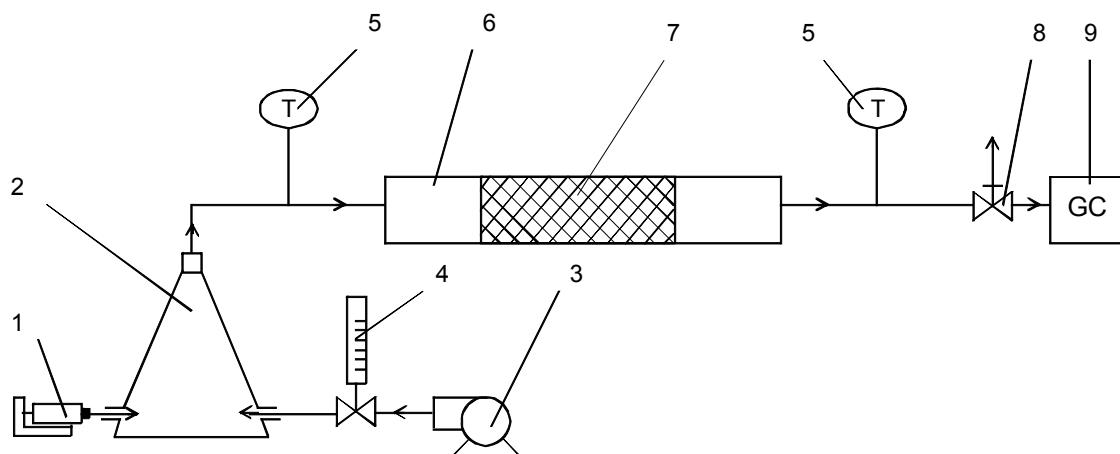
Legend: 1-syringe pump, 2-mixing vessel/evaporator, 3-air compressor, 4-flow meter, 5-thermometer, 6-catalytic reactor, 7-catalyst, 8-gas-sample loop, 9-gas chromatograph

Figure 5.4. Schematic of the experimental rig used for the oxidation of EtSH in dry conditions

Using the syringe pump with adjustable flow rate (1) (model KDS100, KD Scientific Inc., UK), EtSH was sent as a liquid to the mixing vessel/evaporator (2), a glass vessel kept at a temperature slightly above the normal boiling temperature of EtSH or other VOC (in this case the temperature was 45 °C). EtSH was instantly vaporised in the evaporator, and then it mixed with the ambient air sent to the same evaporator (2) using an air compressor (3) (Jun-Air 6-25, 25 L tank, work cycle 50%; Jun-Air International, Denmark). The mixing vessel/evaporator was heated by the heating cable (HTS, Sigma Aldrich, UK) that kept the temperature of the setup constant. The air flow was measured and controlled by the flow meter (4) (Fisher Scientific, UK). The desired ratio air/pollutant was achieved by altering the air flow and using different flow rates for the syringe pump. The reaction mixture passed into the catalytic reactor (6), where it came into contact with the catalyst (7) and where the catalytic oxidation took place. The temperature was kept constant (45-47 °C) throughout the experimental rig using a

temperature controller Horst MC1 in conjunction with a HST Heating cable (5.5 m, 125 W) and a Pt100/250 °C temperature sensor (positioned outside the reactor, in intimate contact with the reactor wall at the middle of catalyst bed length), and by wrapping the rig in aluminium foil for better thermal insulation. The temperature was measured at the beginning and end of the catalytic reactor with thermometers (5). The catalytic reactor consisted of a glass tube with the dimensions: length x internal diameter = 140 mm x 20 mm and thus internal volume of 44 cm^3. The out stream gas flow was constantly passed through the sample loop (8) of the GC (9), which was connected to a PC through a data acquisition interface, facilitating the on-line analysis of the samples. The gas effluent was periodically analysed to check for changes in its composition. The analysis consisted of sending the content of the gas sampling loop through the GC column and recording the peak areas of the compounds in the sample. The GC was calibrated for the compounds in the gas sample according to the procedure and conditions presented in section 3.3.1.

Space velocity and residence time:

Space velocity (SV) represents how quickly the sample passes through the reactor (Fogler, 1992), and is related to the **residence time (T)** in a chemical reactor (in this case the catalyst bed). When SV and the T are calculated at the same conditions,

$$SV \ (h^{-1}) = 1/T \tag{5.1}$$

$$T \ (h) = \frac{\text{Volume of catalyst bed (cm}^3)}{\text{Flowrate of air mixture (cm}^3/h)} \tag{5.2}$$

5.3. Dynamic experiments with catalyst as threads

The experiments were performed in the experimental setup presented in section 5.2., following the procedure presented in the same section. The catalyst (m_{cat} = 2.5 g) was used as threads ([Fe] = 0.165 mmol Fe/g threads), and was distributed loosely and evenly in the reactor, occupying its entire volume (V_{cat} = 44 cm^3). The packing of the catalyst in the reactor is presented in Figure 5.5.

Figure 5.5. Packing of catalytic threads in the dynamic reactor

Using a syringe pump, EtSH was introduced continuously into the system at a rate of 1 μL/h (0.84 mg EtSH/h) and mixed with the air introduced at 50 cm^3/min (0.003 m^3/h). The flow rates for air and EtSH were calculated and adjusted accordingly after experimental trials, ensuring the desired EtSH concentration in the reactor feed (280 mg EtSH/ m^3 air) and a velocity of gas to give enough contact time for catalyst and pollutant for the catalytic reaction to take place. These conditions ensured a residence time of T_{gas} = 53 seconds (14.6×10^{-3} h) for the gas phase (SV = 68.2 h^{-1}). Control experiments were performed with the same amount of raw Dralon L fibres, keeping all other experimental conditions constant. All the experiments were performed at 45 °C.

The first experiment lasted for 78 hours, without interruptions. In the first day the GC method used for monitoring EtSH (R_t = 2.82 min) concentration in time was modified

from isothermal at 70° C to the conditions presented in section 3.3.1. The new method was developed in the first 6 hours from the start of the experiment, and permitted the identification of a reaction product (retention time R_t = 10.65 min), confirmed later to be diethyl disulphide (DEDS), by using commercial DEDS purchased from Sigma-Aldrich Company (DEDS 99% purity, CAS number 110-81-6, density 0.993 g/mL at 25 °C) and comparing the retention times. The GC was calibrated for DEDS in the range 1 – 272 mg DEDS/m^3 air, as presented in section 3.3.2.

The results of the first 78 hours of the first dynamic experiment with EtSH and air of ambient humidity are presented in Figure 5.6.
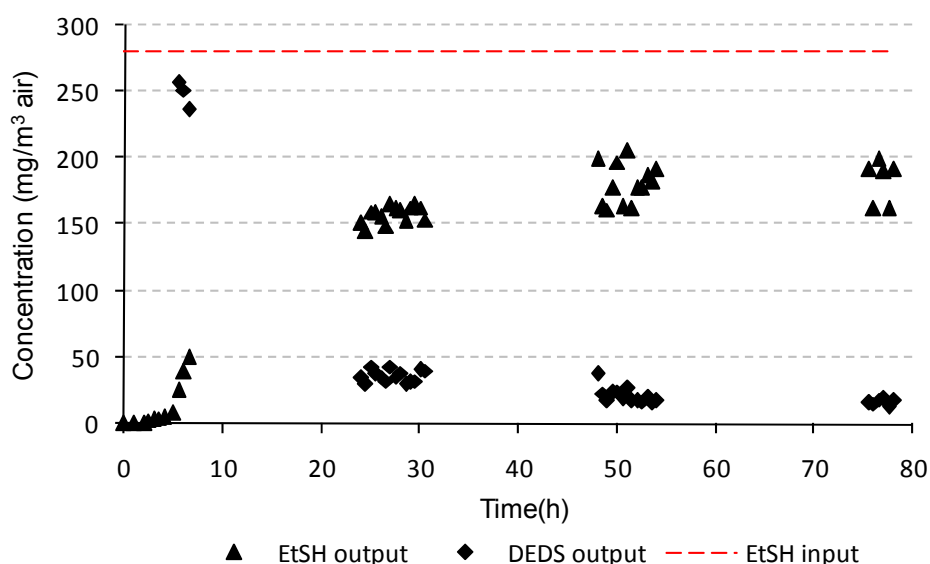
Conditions: air flow: 50 mL/min, EtSH flow: 1 μl EtSH/h, [EtSH]: 280 mg EtSH/ m^3 air, m$_{cat}$: 2.5 g catalytic threads, [Fe]: 0.165 mmol Fe/g threads, V$_{cat}$: 44 cm^3, temperature: 45 ˚C, residence time for EtSH: 53 seconds.

Figure 5.6. Variation of EtSH and DEDS concentration (gas effluent) with time during the first dynamic experiment with catalyst as threads (78 hours)

Replicate experiments showed that DEDS was produced almost instantaneously, being identified 5 minutes from the start of the experiment, but in the first experiment, as shown in Figure 5.6., DEDS was monitored only after its identification.

For the first experiment (see Figure 5.6.), breakthrough for EtSH was registered at 2.5 hours, whilst DEDS peak area was quite high (at 260 mg/m^3 air at 5.5 hours). DEDS concentration decreased with time, while EtSH concentration increased slowly a couple of hours after breakthrough. Over the 78 hours period, EtSH concentration continued to increase slowly, reaching a relatively stationary state at a concentration around 150 - 200 mg EtSH/m^3 air towards the end of the experiment. DEDS concentration decreased in time throughout the experiment, dropping to around 12-16 mg DEDS/m^3 air. The increase in EtSH concentration (reactant) and the decrease in DEDS concentration (reaction product) indicated that the catalyst started to deactivate. DEDS was identified as the only gaseous reaction product, but the GC method might have not been suitable for identification of other eventual reaction products.

The replicate experiments were shorter. The results for one replicate experiment (30 hours) are presented in Figure 5.7., with detail for the first hours shown in Figure 5.8. Figure 5.7. shows that the catalytic process was fast, DEDS being identified during the first analysis, which was performed after 5 minutes from the start of the experiment,. It can also be noted that the variation in the composition of the out stream of the reactor with respect to time follows the same pattern as in the first experiment. Breakthrough for EtSH occurs at 2.5 hours (clearly shown in figure 5.8.), the same time as for the first experiment.
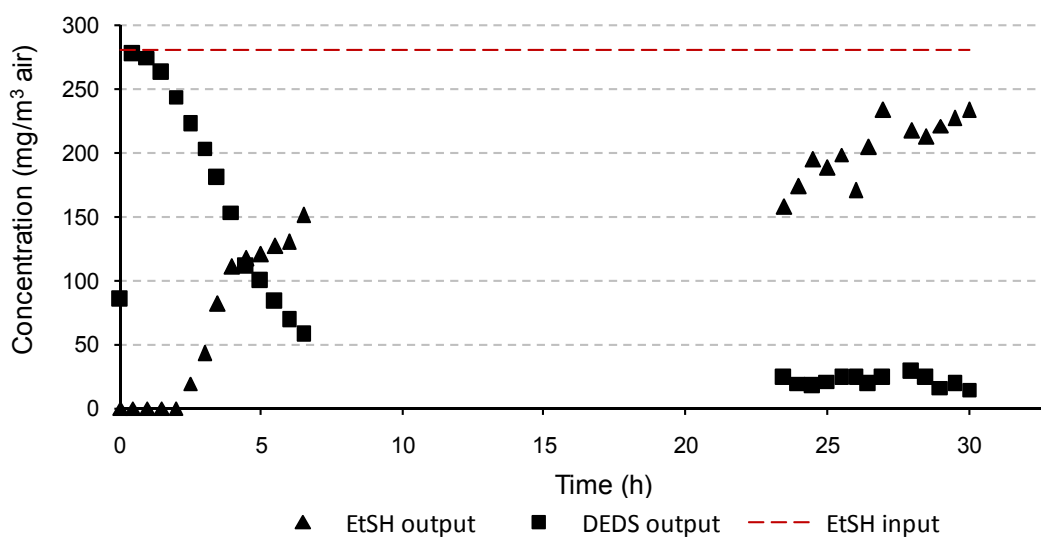
Conditions: air flow: 50 mL/min, EtSH flow: 1 μl EtSH/h, [EtSH]: 280 mg EtSH/ m^3 air, m_{cat}: 2.5 g catalytic threads, [Fe]: 0.165 mmol Fe/g threads, V_{cat}: 44 cm^3, temperature: 45 ˚C, residence time for EtSH: 53 seconds.

Figure 5.7. Variation of EtSH and DEDS concentration (gas effluent) with time during one replicate dynamic experiment with catalytic threads
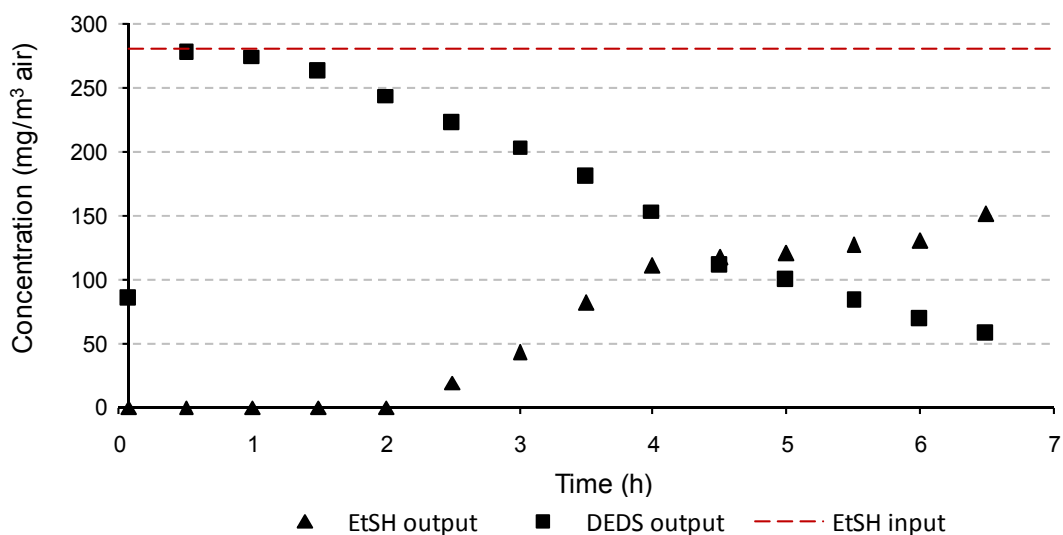
Figure 5.8. Variation of EtSH and DEDS concentration (gas effluent) with time during the first hours of one replicate dynamic experiment with catalytic threads

When a catalytic process is used to produce a chemical compound, the efficiency of the catalytic process is estimated taking into account different factors such as: costs with electricity and personnel, time, conversion, yield in compound of interest, etc, and the catalytic process is stopped when a balance of these factors is reached and the process is not efficient anymore. As this work focuses on the removal of VOCs (i.e. EtSH) from air, the catalytic process should be stopped when the exposure limit for the VOC is reached in the out stream of the reactor or after breakthrough. According to OSHA, the admissible limit in air for EtSH is 10 ppmv (25 mg/m^3 air), thus this catalytic process should be stopped very shortly after breakthrough.

Conversion (X) of reactant and **Turnover Frequency (TOF)** for the catalyst are two parameters which characterize the efficiency of a catalytic process:

$$X = \frac{n_0 - n_t}{n_0} = \frac{(c_0 - c_t) \cdot \Delta t}{c_0 \cdot \Delta t} = \frac{\int_0^t (c_0 - c_t) \cdot dt}{\int_0^t c_0 t} = \frac{\int_0^t (c_0 - c_t) \cdot dt}{c_0 \cdot t} \tag{5.3}$$

where: n = amount of EtSH (at time t = 0 and t = t)

c = concentration of EtSH (at time t = 0 and at time t = t)

$\Delta t = t - t_0$ (duration of experiment)

Plotting the variation of EtSH concentration in time and using numerical integration of experimental results with a mathematical software such as Origin (produced by OriginLab Corporation), makes it possible to calculate the conversion of EtSH at any time during the experiment. The conversion of EtSH was calculated at different times, for both the experiments presented above. The total amount of EtSH decomposed at a

certain time can be calculated by multiplying the conversion X with the total amount of EtSH introduced in the reactor by that time.

Turnover frequency (TOF) is specific to each catalyst and shows the amount of substrate (i.e. EtSH) that can be converted to product per catalytic site per unit time, and can be expressed according to the equation below:

$$TOF = \frac{[\text{EtSH decomposed}](\text{mol})}{[\text{Fe}](\text{mol}) \cdot \text{time}(\text{h})} \tag{5.4}$$

The calculated values of X (for EtSH) and values of TOF are presented in Table 5.1.

Table 5.1. Parameters calculated for the catalytic oxidation of EtSH in dynamic mode experiments with catalyst as threads

Experiment	Time (h)	EtSH decomposed (M = 62.13 g/mol)	Conversion X	TOF (h^{-1})
	3	0.0400 mmol (2.48 mg)	0.987	0.03273
1	24	0.2360 mmol (14.66 mg)	0.568	0.01859
	30	0.2714 mmol (16.86 mg)	0.535	0.01751
	78	0.4678 mmol (29.06 mg)	0.443	0.01452
	3	0.0399 mmol (2.48 mg)	0.985	0.03232
2	24	0.1856 mmol (11.53 mg)	0.572	0.01872
	30	0.2141 mmol (13.30 mg)	0.528	0.01728

The conversion (X)and the TOF were calculated at different times during the dynamic experiments and their variation with time is presented in Figure 5.9. (a) and (b) and Figure 5.10. (a) and (b).

(a)   (b)
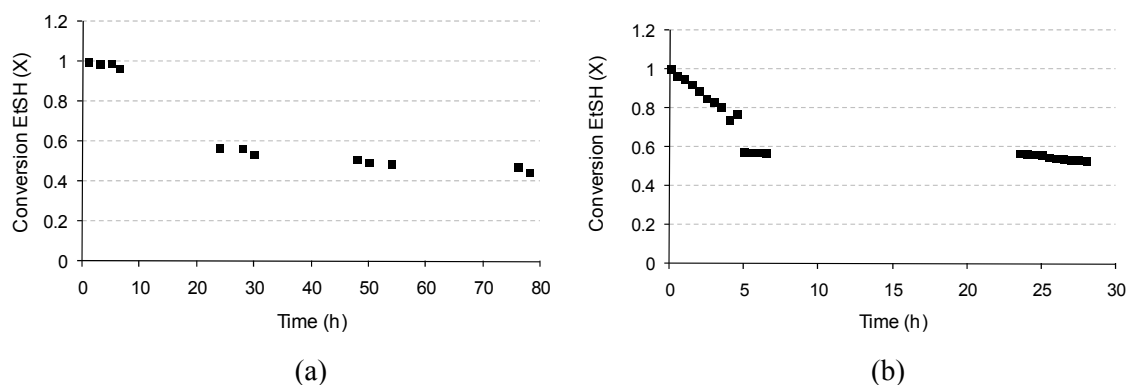
Figure 5.9. Variation of conversion of EtSH with time during dynamic experiments: (a) first experiment (78 hours), (b) replicate experiment (30 hours)

(a)   (b)
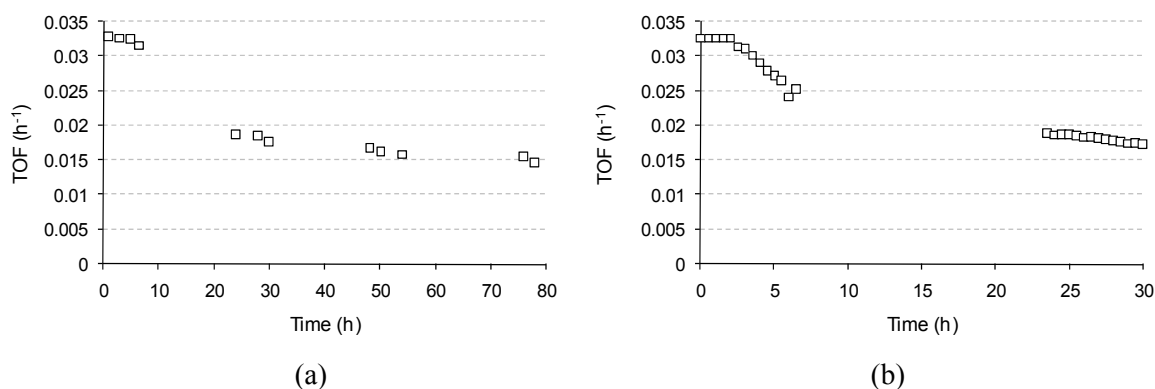
Figure 5.10. Variation of TOF with time during dynamic experiments: (a) first experiment (78 hours), (b) replicate experiment (30 hours)

Both conversion X and TOF decrease in time, another indication that the catalytic process becomes inefficient in time, due to the deactivation of the catalyst.

5.3.3. Control experiments with raw PAN fibers

A control experiment with raw threads of Dralon L (2.5 g) was performed for comparison, using the same experimental conditions as for the experiments with catalytic threads. The packing of raw threads in the reactor was similar to that for experiments with catalytic yarn. The variation of EtSH concentration during the control experiment is presented in Figure 5.11.
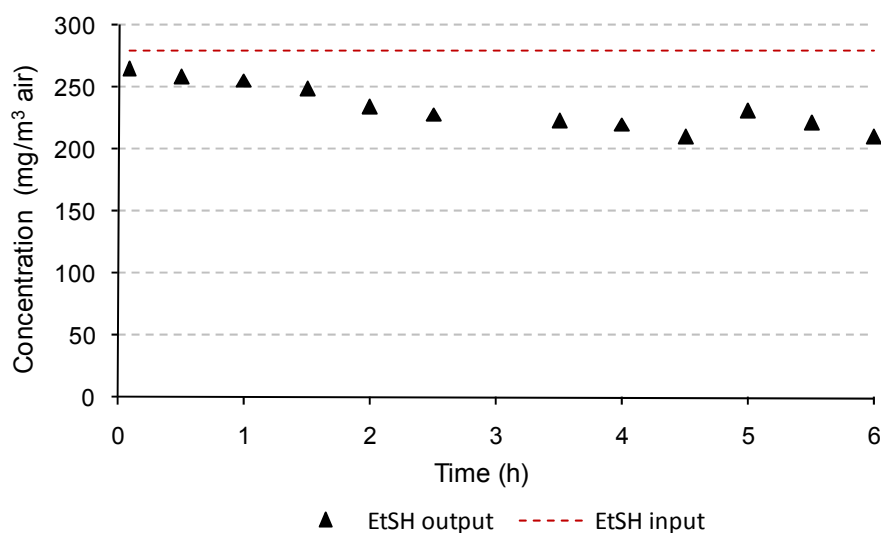
Conditions: air flow: 50 mL/min, EtSH flow: 1 μl EtSH/h, [EtSH]=280 mg EtSH/m^3 air, $m_{control}$=2.5 g raw threads, $V_{control}$=44 cm^3, temperature: 45 ˚C, residence time for EtSH: 53s.

Figure 5.11. Variation of EtSH concentration (gas effluent) with time during the control experiment

The results show a stabilization of EtSH peak at concentration 240 - 225 mg EtSH/m^3 air (theoretical concentration c = 280 mg EtSH/m^3 air) after 1.5 hours and no DEDS was identified in the gas effluent during sample analysis. This indicates that PAN threads do not decompose EtSH; the decrease in EtSH concentration was attributed to adsorption of EtSH on the raw threads.

5.3.4. Investigations of the used catalyst

The only reaction product identified in gas phase was DEDS, but other reaction products such as ethane sulphonic acid ($EtSO_3H$) or some intermediary oxidation products could have been formed and not detected by GC analysis, due to unsuitability of analysis method or physical properties of compounds (not volatile enough to be passed into gas phase or strongly sorbed on the catalytic fibres, causing poisoning of the catalyst). The used catalytic fibres were investigated for detection of chemical compounds sorbed on the fibres, as a possible cause of catalyst deactivation. The oxidation reactions for EtSH are presented below:

$$2C_2H_5\text{-SH} + 1/2O_2 \rightarrow C_2H_5\text{-S-S-}C_2H_5 + H_2O \qquad (5.5)$$
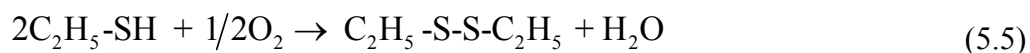
Ethyl mercaptan(EtSH)   Diethyl disulphide(DEDS*)*

$$C_2H_5\text{-SH} + \frac{3}{2}O_2 \rightarrow C_2H_5\text{-SO}_3H \qquad (5.6)$$

Ethyl mercaptan   Ethane sulphonic acid

The used catalytic threads were tested for any changes that might be responsible for the catalyst deactivation. The tests and their results are presented below:

5.3.4.1. GC analysis of the solvent used to wash the used catalytic threads

Samples of used catalyst (0.15 g threads) were washed either with water (5 mL) or ethanol (5 mL) at 45°C in crimp sealed vials to avoid losing any of the volatile compounds that might be present on the fibres. The vials were shaken regularly to

ensure a good contact of the catalyst with the washing liquid. The samples were then filtered and the washing liquid was tested for identification of any traces of EtSH and DEDS. The analyses were performed on a GC Focus II equipped with FID detector and capillary column. The operating conditions for the GC were:

- Column: Zebron capillary column ZB-5ms w/guardian, length 30 m (+5 m Guardian), internal diameter 0.25 mm, film thickness 25 μm

- Oven temperature profile: $T_1 = 34$ °C for 3 minutes, then ramp at 15 K/min to $T_2 = 200$ °C, isothermal for 2 minutes.

- Injector temperature: 200 °C

- Detector temperature: 325 °C

- Carrier gas: He at pressure 130 kPa

- Sample injected: 0.5 μL liquid, split mode with split ratio17.4:1

In these conditions, retention times are: 2.01 minutes for EtSH and 7.10 minutes for DEDS. The instrument was calibrated for EtSH and DEDS.

The results showed no trace of EtSH or DEDS in the liquid samples. GC analysis of head space did not identify EtSH or DEDS in the headspace above the liquid in the vials, thus this analysis suggested that neither of these two compounds was adsorbed on the catalyst, causing its deactivation.

5.3.4.2. Ion Chromatography of water used to wash used catalyst.

0.15 g of used catalytic threads was washed with water (5 mL) at 45°C in crimp sealed vials to avoid losing any volatile compounds present on the fibres. The vials were shaken regularly to ensure a good contact of the catalyst with the washing water. The samples were then filtered and the wash waters were tested for identification of traces of $EtSO_3H$, possible oxidation product for the advanced oxidation of EtSH.

The analyses were performed on a Metrohm Modular MIC-2 advanced IC system, with Metrohm IC-Net 2.3 software. The operating conditions of the IC system were:

- Column: IonPac NS1 10 µm, Analytical (250 mm x 4mm)

- Eluent (50:50 v/v):   4 mmol/L tetrabutylammoniumhydroxide (TBAOH) and 30% acetonitrile. The solutions were taken from different bottles (50:50 v/v), using a Y shaped plastic tubing connector

- Flow rate: 1.2 mL/min

- Injection loop: 20 µl

- Detection: Suppressed conductivity

- Suppressor: Anion self-regenerating suppressor

- Regenerant: 10 mmol/L sulphuric acid

In these conditions the retention time for ethanesulphonate ion is $R_t = 6.04$ minutes.

The results from the control analysis (27 ppm solution of $EtSO_3H$) and from the wash waters are presented in Figure 5.12 and Figure 5.13. respectively.
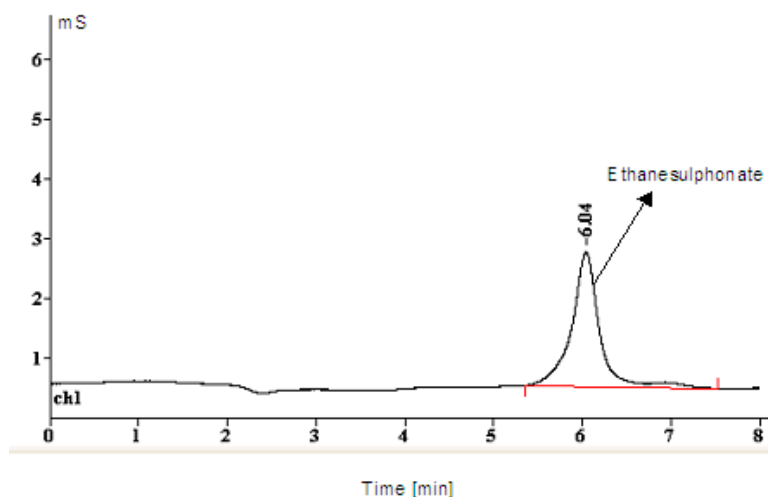
Figure 5.12. Ion chromatogram of ethane sulphonic acid (27 mg/L solution in water)
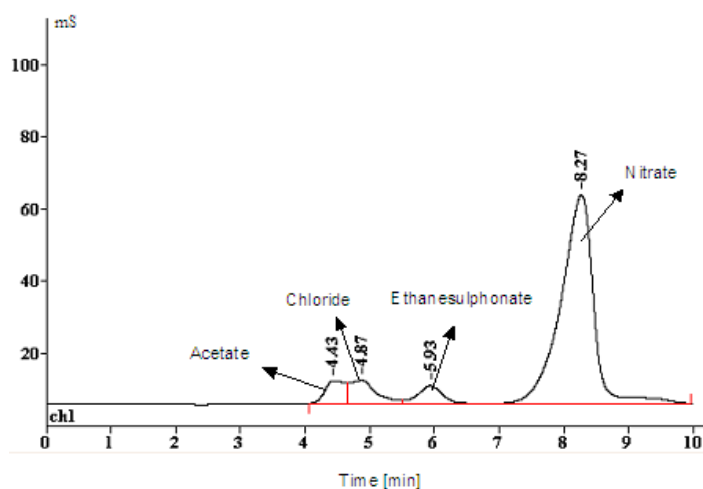
Figure 5.13. Ion chromatogram of wash water for catalytic threads used in dynamic mode experiments with EtSH, catalytic threads and air of ambient humidity

The IC analysis of samples collected after washing the used catalyst with water showed the presence of small amounts of $EtSO_3H$. This indicates that EtSH undergoes an advanced oxidation process (the process is slow as the main reaction product remains

DEDS). The additional ions identified in the samples originate from the catalytic threads, as modification and impregnation stages in the production of the catalyst involve the use of chemicals such as hydrazine chloride, hydroxylamine chloride, and calcium nitrate. The acetic acid detected in the solution is likely to originate from the oxidation of vinyl acetate copolymer, which was not completely hydrolysed during the modification process.

5.3.4.3. FTIR analysis of used and unused catalyst

FTIR analysis of catalytic threads was performed in order to identify structural changes of the catalyst during the catalytic reaction. The spectra are presented in Figure 5.14.
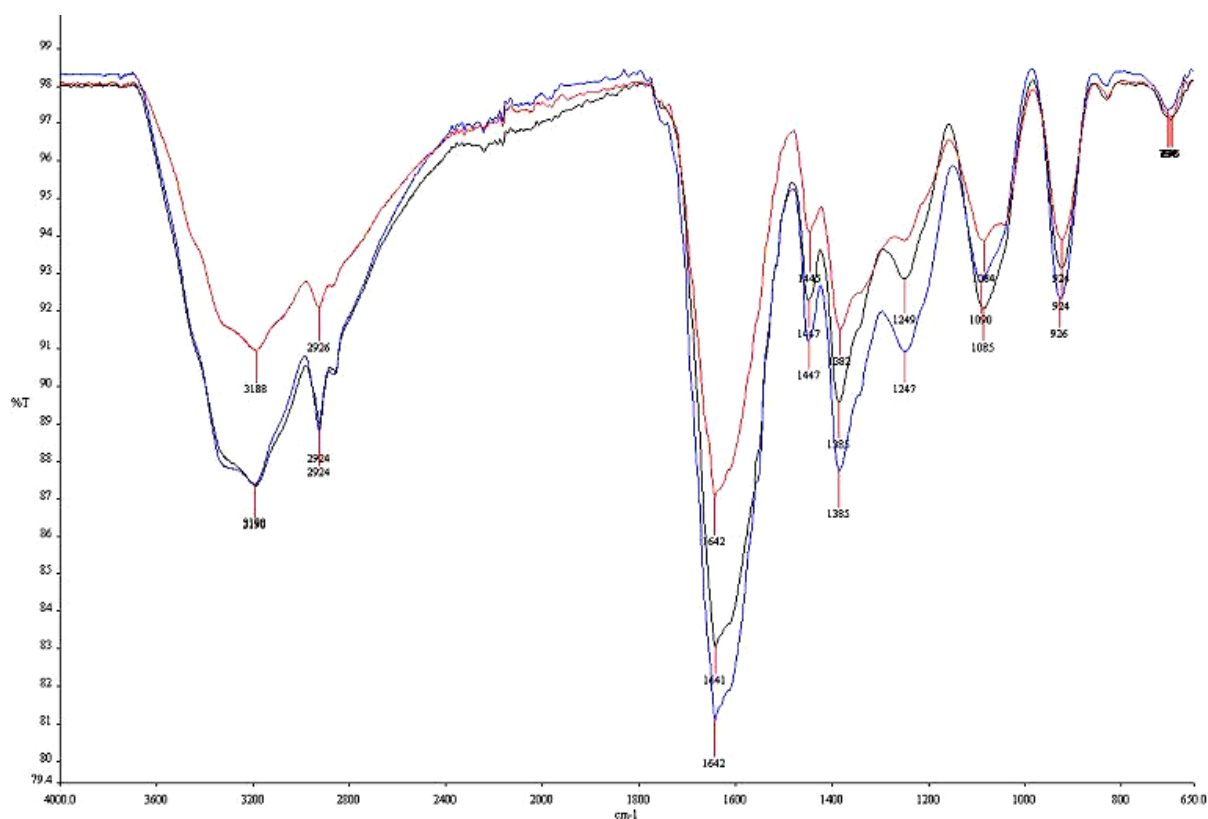
Figure 5.14. FTIR spectra of unused catalyst (black), catalyst used for 30 hours (red) and catalyst used for 78 hours (blue)

FTIR analysis showed no significant differences between unused and used catalyst threads. The stretching vibration in -SH functional group (mercaptan) is expected to produce an absorption peak at 2550 – 2600 cm^{-1} and the stretching vibration of the S-S group in disulphide (DEDS) at 500 – 540 cm^{-1} (the spectra was not recorded at these wavenumbers). At the same time, the S=O group has different characteristic absorption bands depending on the functional group: 1030 – 1060 cm^{-1} in sulphoxide, 1345 cm^{-1} in sulphonic acid and 1350-1450 cm^{-1} in sulphate (Infrared Spectroscopy, 2008; Kuptsov and Zhizhin, 1998; Coates, 2000).

The only significant change in the spectra is observed at 1050-1080 cm^{-1}, region that as mentioned above could correspond to the stretching vibration for S=O in a sulphoxide or sulphinic acid. If ethane sulphoxide or ethane sulphinic acid were produced during the catalytic process, these would be unstable and would further oxidize to sulphonic acid (no changes in the 1345 cm^{-1} region). The same region is characteristic to –OH bending vibration in alcohols and for –C–H bending vibrations in alkyl groups (–CH$_2$, –CH$_3$), already present in the spectra.

Peaks at wavenumber 2921 cm^{-1} and 2852 cm^{-1}, correspond to asymmetrical and symmetrical stretches of the –CH$_2$- group. Peaks at wavenumber 1382-1385 cm^{-1} correspond to –CH$_2$- scissoring bend and to the symmetric carboxylate stretch. No differences are observed at these wavenumbers in these regions.

As no significant differences between unused and used catalyst threads were noticed, it could be assumed that no structural changes occurred at the catalyst surface during the dynamic experiments.

5.3.4.4. Temperature Programmed Desorption Analysis (TPD)

Temperature programmed desorption analysis (TPD) of the used and unused catalyst threads were performed at University of Huddersfield, on a Hiden quadrupole mass spectrometer, model HPR20, using a secondary electron multiplier (SEM) detector and heated capillary inlet. Samples of catalytic fibres (25-30 mg) were heated to 30 °C, under flowing He at a flowrate of 20 mL/min. The samples were allowed to stabilize for 10 min at this temperature and then heated at 10 °C/min to a furnace temperature of 200-210 °C, and the following peaks (m/z) were monitored in time:

- 18 water
- 29 Ethyl   (component of all possible products)
- 62 EtSH   (parent/base peak)
- 122 $(EtS)_2$ (parent/base peak)
- 139 Et_2SO_4

All samples desorbed water as the only significant species. Plotting the water on the secondary axis, one can see that there appears to be a small amount of m/z 29 in all catalysts, even the unused sample. This may be due to traces of gaseous N_2 ($^{14}N^{15}N$) or possibly other fragments from the fibres, e.g. N_2H_4 from free hydrazine.

The TPD spectra for fresh and used catalytic threads are presented in Figure 5.15 and Figure 5.16.
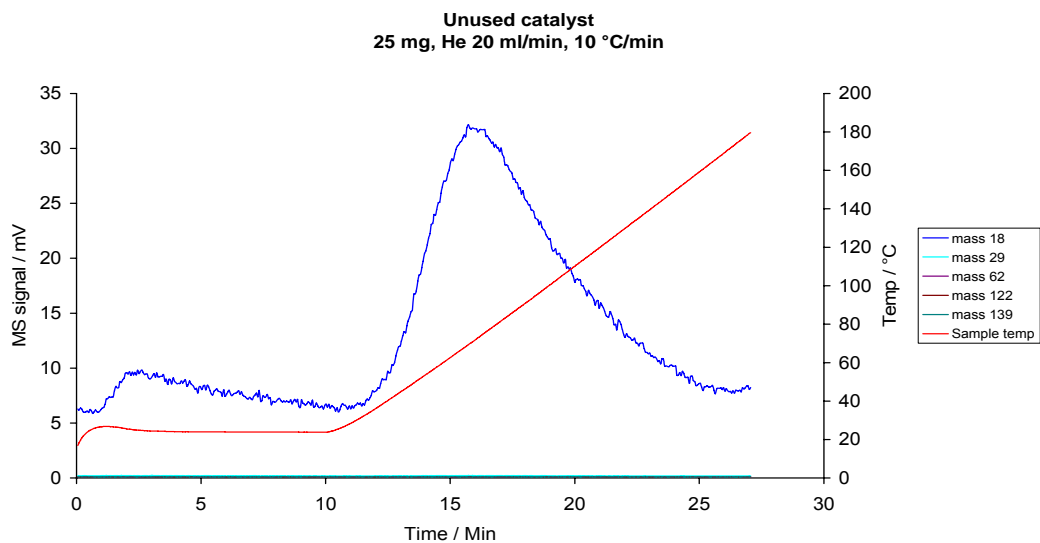
Figure 5.15. TPD spectra of unused catalytic threads
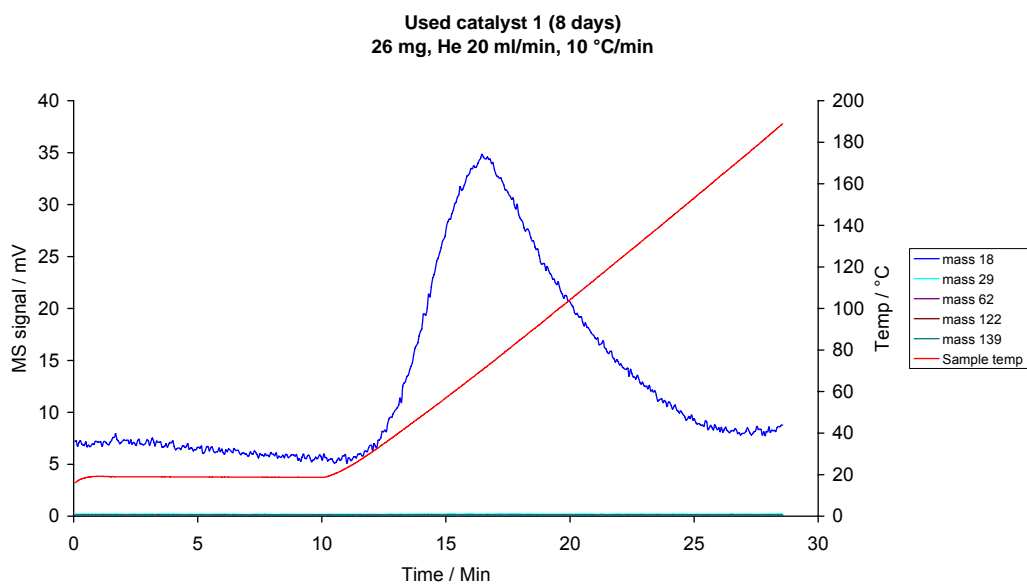
Figure 5.16. TPD spectra of catalytic threads used in catalytic oxidation of EtSH for 78 h

The absence of any significant peak for the m/z 29 (Ethyl) and all the other peaks monitored indicates that there were no compounds adsorbed on the catalytic threads (or adsorbed at levels below the limit of detection for the instrument), or that the

compounds adsorbed were strongly held on the fibres and they did not desorb at temperatures below 200 °C.

5.4. Dynamic experiments with catalyst as knitted mesh

Two separate sets of experiments were performed with catalyst as mesh: with air of ambient humidity and with air of increased humidity. The humidity of the air was increased by passing the air from the air compressor through water before being sent to the mixing vessel/evaporator. The experiments were performed at 45 °C, in the experimental setup and following the procedure presented in section 5.2. The catalyst was produced by modification and impregnation of raw PAN mesh, resulting in catalytic mesh consisting of 50% impregnated PAN yarn and 50% PP support, with an iron content of $[Fe] = 0.52$ mmol Fe/g threads. The catalytic mesh ($m_{cat} = 4.1$ g) was cut into discs of 20 mm diameter, and 15 identical discs were positioned (as a compact bed) in the middle of the reactor, in such a way that the catalyst bed covered the entire cross section of the reactor over a 6 cm length ($V_{cat} = 18.85$ cm^3). The packing of the catalyst in the reactor is presented in Figure 5.17.

Figure 5.17. Packing of catalytic mesh (discs) in the dynamic reactor

Using a syringe pump, EtSH was introduced continuously into the system at a rate of 1 µL/h (0.84 mg EtSH/h) and mixed with the air (of ambient or increased humidity) introduced at 50 cm^3/min (0.003 m^3/h). The flow rates for air and EtSH ensured an initial EtSH concentration of 280 mg EtSH/ m^3 air in the reactor feed, and a space velocity of SV = 159.5 h^{-1}. These conditions ensured a residence time of T$_{gas}$ = 22.6 seconds (6.27×10^{-3} h) for the gas phase.

5.4.1. Experiments with air of unmodified humidity

Three experiments with EtSH, catalyst as mesh and air of ambient humidity were performed, and the results, presented in Figure 5.18., show good reproducibility. The experiments lasted on average for 51 hours, without interruption, and the concentration of EtSH and DEDS in the gas effluent was monitored continuously during the day, without analysis during the night.

In these experimental conditions, breakthrough for EtSH occurred at time t = 29 hours from the start of the experiment. DEDS was identified as the only reaction product, and it was detected in the first half hour of the experiment, showing that EtSH is oxidized rapidly to DEDS.
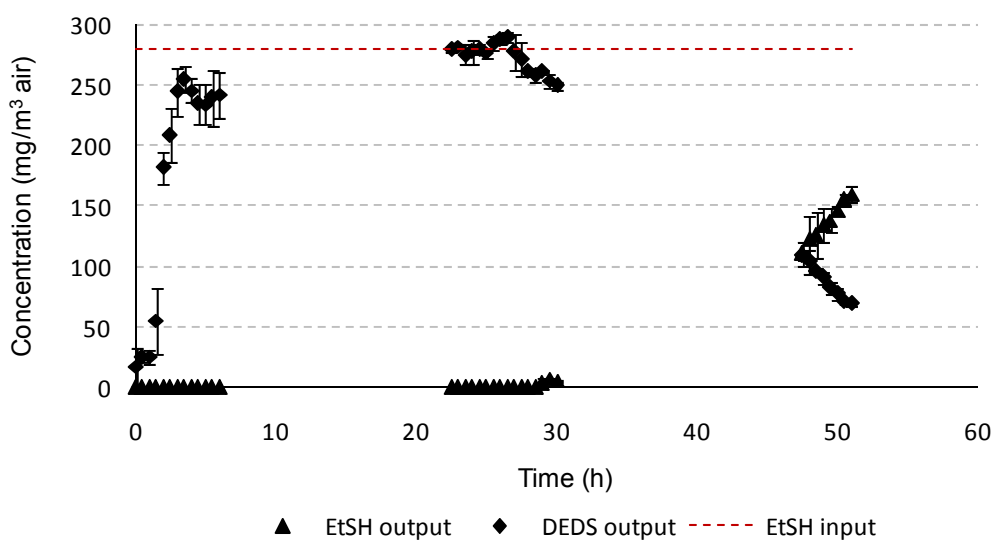
Conditions: air flow: 50 mL/min, EtSH flow: 1 μl EtSH/h, [EtSH]: 280 mg EtSH/m^3 air, m_{cat}: 4.054 g, [Fe]: 0.52 mmol Fe/g threads, V_{cat}: 18.85 cm^3, temperature: 45 ˚C, residence time for EtSH: 22.6 seconds.

Figure 5.18. Variation of EtSH and DEDS concentration (gas effluent) with time during the catalytic oxidation of EtSH in dynamic mode, using catalyst as mesh and air of unmodified humidity

Conversion of EtSH (X) and the TOF for the catalyst were calculated according to the equations 5.3 and 5.4. in section 5.3.2., using numerical integration of experimental data. The values for X and TOF at 30 hours (just after breakthrough) and at the end of the experiment (51 hours) are presented in Table 5.2.

From Figure 5.18. and Table 5.2. it can be concluded that after breakthrough (29 hours from the start of the experiment), the efficiency of the process decreases. Again, being interested in the removal of EtSH from air, the catalytic process should be stopped when the exposure limit for the EtSH (10 ppmv, 25mg/m^3 air) or that for the reaction product, DEDS, (10 ppmv, 25mg/m^3 air) is reached in the gas effluent.

Table 5.2. Parameters calculated for the catalytic oxidation of EtSH in dynamic mode experiments with catalyst as mesh and air of ambient humidity

Experiment	Time (h)	Conversion X	EtSH decomposed (M = 62.13 g/mole)	TOF (h^{-1})
1	30	0.9962	0.403 mmol (25.06 mg)	0.01276
	51	0.8972	0.6146 mmol (38.18 mg)	0.01149
2	29.5	0.996	0.3966 mmol (24.64 mg)	0.0128
	51	0.8788	0.6050 mmol (37.59 mg)	0.01125
3	30	0.9965	0.4035 mmol (25.07 mg)	0.0129
	51	0.8973	0.6178 mmol (38.38 mg)	0.01162

This study shows that experimental conditions, such as packing of the catalyst in the reactor and iron content on the catalyst, among others, influence the overall performance of the oxidation process. Using the catalyst as mesh (packed tightly in the middle of the reactor) it was possible to achieve a breakthrough time of 29 hours for EtSH ([Fe] = 0.52 mmol/g thread), compared to 2.5 hours when the catalyst was used as loosely packed yarn ([Fe] = 0.165 mmol/g thread). However, the values for the TOF calculated are only slightly lower than those calculated for the catalyst used as threads.

In both cases (i.e. catalyst used as threads and as mesh), the main reaction product identified was DEDS, with traces of EtSO$_3$H identified as adsorbed on the used catalyst. It is suggested that the oxidation of EtSH in dry conditions (without H$_2$O$_2$) proceeds

according to a free radical mechanism (see reactions (5.7) – (5.13) below) involving O_2 from air and Fe^{3+} immobilized on the catalyst. This is similar to the reaction path for the oxidation of thiols with oxygen from air, described by Capozzi and Modena (1974) and Ohno and Oae (1977).

$$Fe^{3+} + C_2H_5SH \longrightarrow Fe^{2+} + C_2H_5\text{-}S\bullet + H^+ \tag{5.7}$$

$$Fe^{2+} + O_2 \longrightarrow Fe^{3+} + O_2^{\bullet -} \tag{5.8}$$

$$C_2H_5\text{-}SH + O_2^{\bullet -} \longrightarrow C_2H_5\text{-}S\bullet + HOO^- \tag{5.9}$$

$$C_2H_5\text{-}SH + HOO^- \longrightarrow C_2H_5\text{-}S\bullet + HO\bullet + HO^- \tag{5.10}$$

$$C_2H_5\text{-}SH + HO\bullet \longrightarrow C_2H_5\text{-}S\bullet + H_2O \tag{5.11}$$

$$2C_2H_5\text{-}S\bullet \longrightarrow C_2H_5\text{-}S\text{-}S\text{-}C_2H_5 \tag{5.12}$$

$$H^+ + HO^- \longrightarrow H_2O \tag{5.13}$$
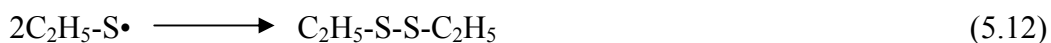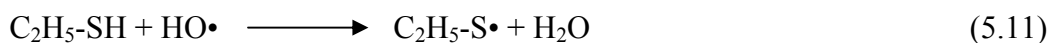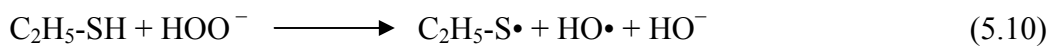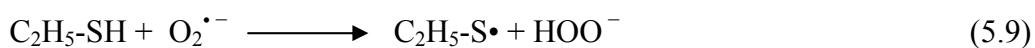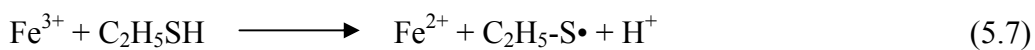
These reactions can be summarized in the schematic below:
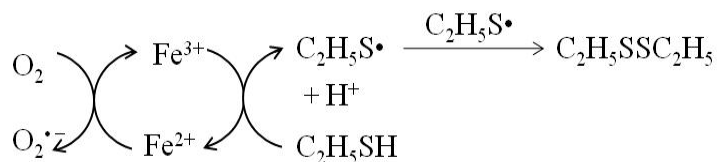
The results presented in this section are similar to those reported in the literature (Kastener *et al.*, 2002) when coal fly ash was used to oxidize reduced sulphur compounds (H_2S, and EtSH) from air. The scientists reported the oxidation of these gaseous pollutants in batch reactors and that of H_2S in a continuous flow packed reactor operated at 25 °C, with removal efficiencies of 50% (initial concentration of H_2S was 400 ppmv) over 4.6 hours, at a residence time of 4.6 s. Comparing these results with the

results presented in this chapter, the performance of the fibrous catalyst used as threads is slightly lower (100% removal of EtSH for 2.5 hours at a residence time of 53 s, initial concentration of pollutant 280 mg EtSH/m^3 air, or ~120 ppmv, operating temperature 45 °C). Contrary, the performance of the fibrous catalyst used as mesh is better than that of the reported system using coal fly ash, as 100% removal of ~120 ppmv EtSH was experienced over 29 hours, at a residence time of 22.6 s, in the system operated at 45 °C. Therefore, this fibrous catalyst shows potential in the use for removal (catalytic oxidation) of EtSH from air, at moderate temperatures and atmospheric pressure.

5.4.2. Experiments with air of increased humidity

In order to evaluate the effect of humidity of air on the catalytic oxidation of EtSH, the experimental conditions were altered by passing the air from the air compressor through water before sending it to the mixing vessel and then to the catalytic reactor. All other experimental conditions were the same as described in section 5.4.1. The experiments were conducted in replicates, showing good reproducibility (Figure 5.19.).
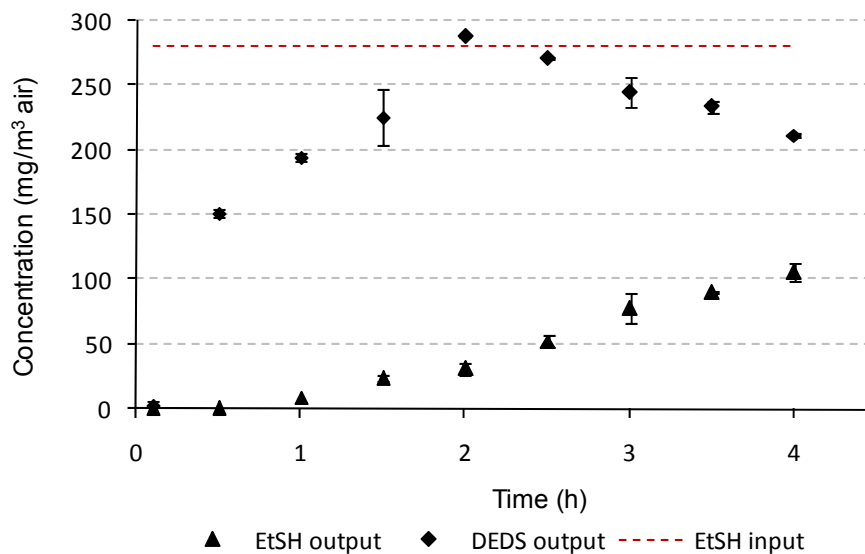
Conditions: air flow: 50 mL/min, EtSH flow: 1 μl EtSH/h, [EtSH]: 280 mg EtSH/m³ air, m_{cat}: 4.054 g, [Fe]: 0.52 mmol Fe/g threads, V_{cat}: 18.85 cm³, temperature: 45 ˚C, residence time for EtSH: 22.6 seconds.

Figure 5.19. Variation of EtSH and DEDS concentration (gas effluent) with time during the catalytic oxidation of EtSH with catalyst as mesh and air with increased humidity

Figure 5.19 shows breakthrough time for EtSH of 1 hour from the start of the experiment. The experiment was stopped after 4 hours, when EtSH concentration in the gas effluent reached one third of the initial concentration. These results indicate that increasing the humidity of the air reduces the catalyst efficiency towards the decomposition of EtSH in the experimental conditions presented. This might be due to water sorption on the active centres or, more likely, due to the fact that the moisture facilitates the formation of channels of preferential flow of the gas mixture, thus reducing the chances of physical contact between the catalyst and the gaseous pollutant (i.e. EtSH), and consequently the chances of a chemical reaction.

5.5. Conclusions

A fixed bed catalytic reactor made of glass was designed and incorporated into a laboratory scale experimental rig that offers the possibility of performing gas phase catalytic reactions with air contaminated with VOCs (i.e. EtSH) and the novel fibrous catalyst, at constant temperature and on-line GC analysis of gas samples.

The results of the investigations showed that the fibrous catalyst was active towards the decomposition of EtSH in dynamic mode, and under the experimental conditions used. The catalyst was active regardless of its physical form (threads or mesh) or procedure of modification and impregnation of raw threads/mesh used in its production.

The activity of the catalyst was influenced by the Fe content of the catalyst: the activity was higher for the catalyst in the form of mesh (0.52 mmol Fe/g thread), than for the catalyst used as threads (0.165 mmol Fe/g threads).

The theoretical residence time of the organic pollutant (i.e. EtSH) in the reactor was longer when the catalyst was used as threads (53 s compared to 22.6 seconds for catalyst used as mesh). This was due to the packing of the catalyst, as the catalytic threads were packed loosely in the reactor compared to the tight catalytic bed formed when the catalyst was used as knitted mesh.

The physical form, but mainly the packing of the catalyst in the reactor was responsible for differences in breakthrough time. In the experiments with air of ambient humidity,

breakthrough time increased from 2.5 hours (for catalyst used as threads) to 29 hours (for catalyst used as mesh).

The only reaction product identified in the gas phase during the experiments with air of either unmodified or increased humidity was DEDS. This was identified in the first half hour of the experiment.

The physical form of the catalyst, the Fe content, and the packing of the catalyst in the reactor influenced the conversion of EtSH (higher for the catalyst used as mesh) and TOF for the catalyst (slightly lower for catalyst used as mesh).

Control experiments with raw Dralon L threads showed no reaction product and a stabilization of EtSH concentration in the gas effluent at a slightly lower value than the initial theoretical one. This indicated that raw threads of PAN were not active in the decomposition of EtSH from contaminated air streams; the small decrease in concentration was attributed to adsorption of EtSH on the raw PAN fibres.

Increasing the humidity of the air fed into the reactor reduced the catalyst efficiency towards EtSH decomposition. Breakthrough time decreased from 29 hours (for air with unmodified humidity) to 1 hour (when the humidity of the air was intentionally increased by passing the air through water prior to sending it to the catalytic reactor).

Tests on the used catalytic threads revealed traces of $EtSO_3H$ in the wash water analysed by IC, indicating that a small fraction of the EtSH underwent a more advanced

oxidation process. All the other peaks registered during IC analysis were attributed to species originating from the catalyst.

The addition of H_2O_2 into the system needs to be investigated, as the catalyst, in the presence of H_2O_2 is analogous to a Fenton-like system, a more effective tool than oxygen from air in the advanced oxidation of many organic pollutants.

The novel fibrous catalyst packed in continuous flow reactors as threads or as mesh shows potential in the removal of EtSh from air streams, the performances of the system was comparable or even better that that of similar systems reported in the literature.

Chapter 6. Gas-liquid-solid catalytic decomposition of airborne EtSH

6.1. Introduction

This chapter presents the results of dynamic mode experiments with EtSH as model air pollutant, the novel catalyst (as knitted mesh) and H_2O_2 solution as oxidant. In the presence of H_2O_2, the modified PAN catalyst is analogous to a Fenton-like system, more effective in the advanced oxidation of many organic pollutants than O_2 from air.

As presented in Chapter 5, in the presence of the catalyst alone (without H_2O_2), the only reaction product identified and quantified was DEDS. During investigations on the used catalytic threads, traces of ethane sulphonic acid ($EtSO_3H$) were identified as deposited on the catalyst; this indicated that EtSH can be further oxidized in the presence of an additional oxidant, as oxygen from air is not a strong enough oxidizing agent. When H_2O_2 is added into the system, EtSH is expected to be further oxidized to $EtSO_3H$, organic acids (acetic and formic acid) and sulphuric acid, according to the scheme below:

$$C_2H_5\text{-}S\text{-}S\text{-}C_2H_5 \quad (DEDS)$$

$$C_2H_5SH + H_2O_2 \xrightarrow{Catalyst} \quad C_2H_5\text{-}SO_3H \quad (\text{ethane sulphonic acid})$$

$$CH_3\text{-}COOH + H_2SO_4$$
(acetic acid)

$$2\,HCOOH \longrightarrow CO_2 + H_2O$$
(formic acid)
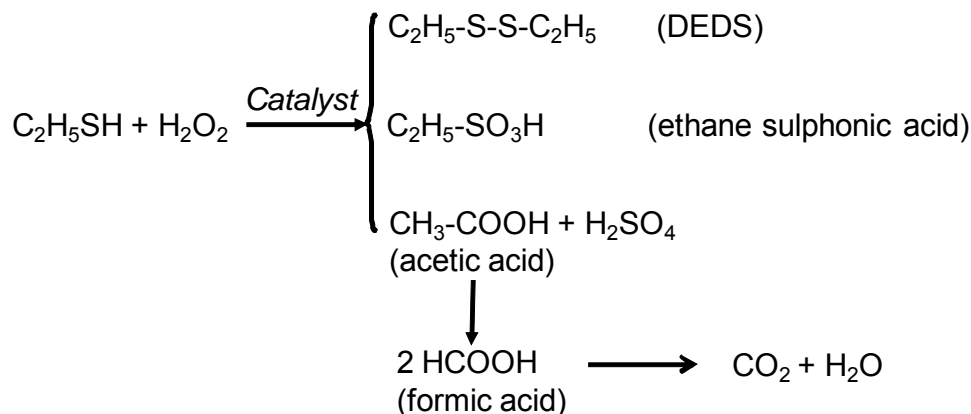
The oxidation of EtSH in the presence of the fibrous catalyst/H_2O_2 system proceeds through a free radical mechanism, with diethyl disulphide (DEDS) as first reaction product, as summarized in reactions (6.1) – (6.5):

$$Fe^{3+} + H_2O_2 \longrightarrow Fe\text{-}OOH^{2+} + H^+ \tag{6.1}$$

$$Fe\text{-}OOH^{2+} \longrightarrow HO_2^{\bullet} + Fe^{2+} \tag{6.2}$$

$$Fe^{2+} + H_2O_2 \longrightarrow Fe^{3+} + HO^{\bullet} + HO^- \tag{6.3}$$

$$C_2H_5\text{-}SH + HO^{\bullet} \longrightarrow C_2H_5\text{-}S\bullet + H_2O \tag{6.4}$$

$$2\,C_2H_5\text{-}S\bullet \longrightarrow C_2H_5\text{-}S\text{-}S\text{-}C_2H_5 \tag{6.5}$$
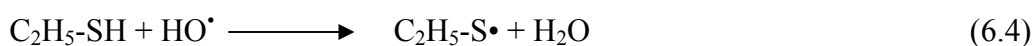
The Fe^{+3}/H_2O_2 system generates the powerful oxidizing agent HO•, capable to further oxidize DEDS to ethane sulphonic acid and organic acids through several intermediates. The reaction proceeds through three paths, as suggested by Savige and Maclaren (1966) and Field (1977).

$$C_2H_5-\overset{O}{\underset{}{S}}-S-C_2H_5 \xrightarrow{[O]} C_2H_5-\overset{O}{\underset{O}{S}}-S-C_2H_5 \xrightarrow{[O]} C_2H_5-\overset{O}{\underset{O}{S}}-\overset{O}{S}-C_2H_5 \xrightarrow{[O]} C_2H_5-\overset{O}{\underset{O}{S}}-\overset{O}{\underset{O}{S}}-C_2H_5$$

$$C_2H_5-\overset{O}{\underset{O}{S}}-S-C_2H_5$$

path A | Fe^{+3}/H_2O_2

$$\mathbf{C_2H_5-S-S-C_2H_5} \xrightarrow[Fe^{+3}/H_2O_2]{\text{path B}} C_2H_5-S-OH \xrightarrow{[O]} C_2H_5-\overset{O}{S}-OH \xrightarrow{[O]} C_2H_5-\overset{O}{\underset{O}{S}}-OH$$

path C | Fe^{+3}/H_2O_2

$$\xrightarrow{[O]} C_2H_5-S-S-OH \xrightarrow{[O]} C_2H_5-S-\overset{O}{S}-OH \xrightarrow{[O]} C_2H_5-S-\overset{O}{\underset{O}{S}}-OH \xrightarrow{[O]}$$

$$H_2SO_4$$

$$CH_3-CH_2-OH \xrightarrow{[O]} CH_3-CH=O \xrightarrow{[O]} \mathbf{CH_3COOH} \xrightarrow{[O]} \mathbf{CH_2O + CO_2 + H_2O}$$

$$\downarrow [O]$$

$$\mathbf{HCOOH}$$
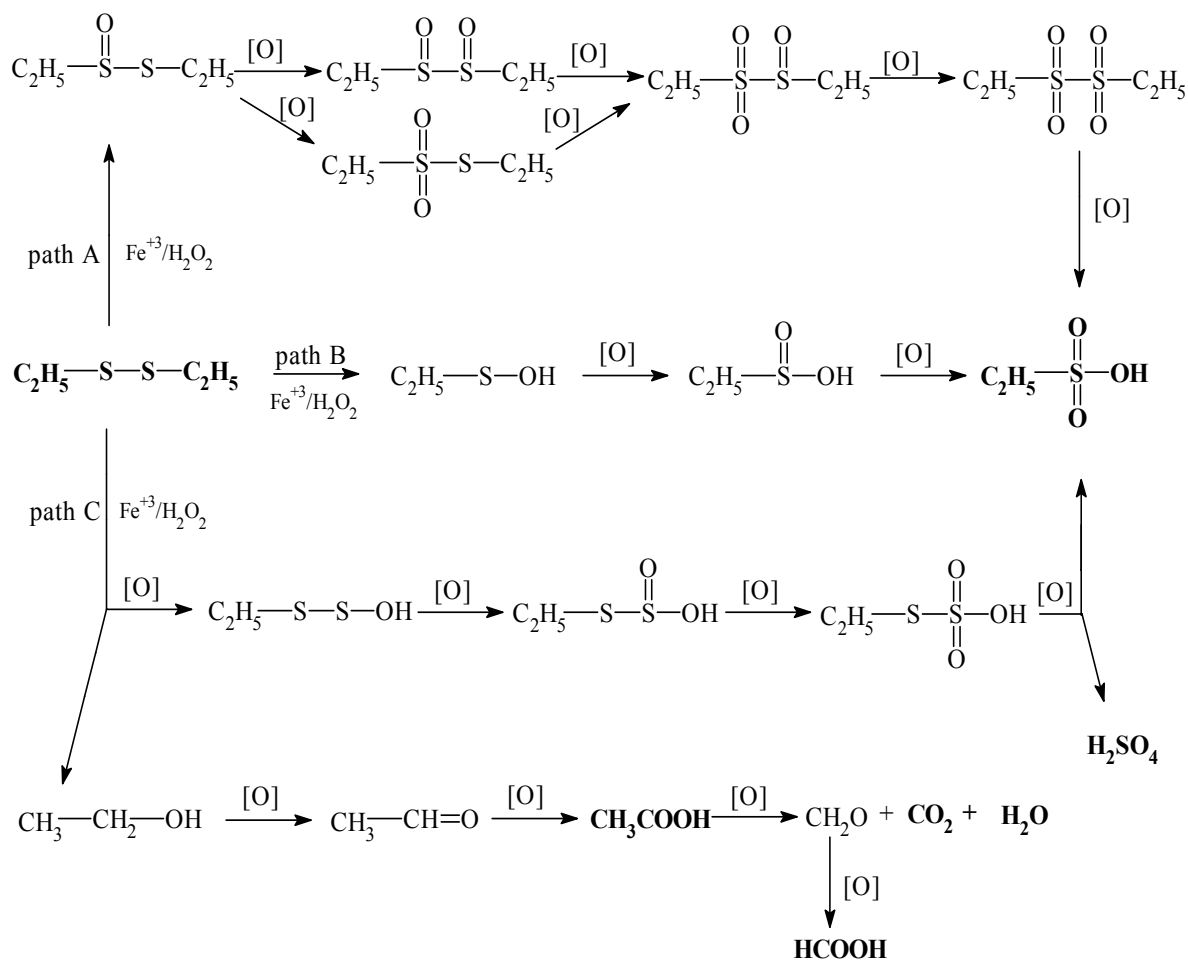
Path A and B involve the cleavage of the S-S bond in DEDS, leading to the formation of two molar proportions of the sulphonic acid, whereas path C requires the cleavage of the C-S bond and yields equimolar amounts of the sulphonic acid and sulphate. For path A, the cleavage of the S-S bond is homolitic and occurs in the final stage of the reaction, whereas for path B, S-S cleavage occurs at the beginning, leading to the formation of ethane sulphenic acid, which then undergoes further oxidation to form ethane sulphinic acid and finally ethane sulphonic acid. Path A is thus favoured by anhydrous conditions, while aqueous conditions should favour path B or C (Savige and Maclaren, 1966). It is believed that the oxidation of EtSH in the presence of the fibrous catalyst/H_2O_2 system

proceeds manly through path B, the cleavage of C-S bond requiring a higher dissociation energy (65 kcal/mole) than the S-S bond (54 kcal/mole) (Field, 1977). As a consequence, the main reaction product for the oxidation of EtSH is ethane sulphonic acid.

After preliminary studies on the most efficient way to introduce H_2O_2 into the system, a three-phase (gas-liquid-solid) catalytic reactor was designed, constructed and incorporated into an experimental setup with the possibility of on-line analysis of the gas effluent. The catalytic reactor could be operated in scrubber and slurry regimes, ensuring the simultaneous presence of catalyst, gas phase pollutant (i.e. EtSH) and H_2O_2 in the system. The reactor was tested in both operational modes, in different experimental conditions and was then modified in order to overcome the limitations of the initial design and to ensure the best performance of the experimental rig.

The purpose of this study was to determine whether the catalyst/H_2O_2 system is able to oxidize a continuous flow of air contaminated with EtSH to a more advanced stage than the system catalyst/O_2 from air (when DEDS was identified as reaction product), and to determine the advanced oxidation products.

6.2. Preliminary study on the effect of H_2O_2 added into the system

Using the experimental setup with the fixed bed flow reactor presented in section 5.2., Figure 5.1, two methods of introducing H_2O_2 into the system were investigated:

The first method was passing (bubbling) the air to be sent to the mixing vessel through an aqueous solution of H_2O_2 of 1200 mg/L concentration. The vessel containing the H_2O_2 solution was positioned between the flowmeter (3) and the mixing vessel/evaporator (5) (see Figure 5.3. in section 5.2). The concentration of H_2O_2 in the air was measured before the evaporator, using H_2O_2 strips (Fisher Scientific, UK). As the concentration was less than 0.5 ppmv, indicating that this method of introducing H_2O_2 into the system was not effective.

The second method tested was by spraying a 900 mg/L H_2O_2 solution directly onto the catalytic discs before introducing them into the catalytic reactor. Using this method, only a fixed amount of H_2O_2 was introduced into the system.

Following the methodology described in section 5.2., and keeping the temperature and the flowrates of air and EtSH at the same values as in the experiments in dry conditions, a first experiment with EtSH, catalyst and H_2O_2 was performed in dynamic mode. The catalytic discs (m = 4.150 g, 50% catalytic threads, [Fe] = 0.52 mmol Fe/g thread) were sprayed with a 900 mg/L H_2O_2 solution in water before they were introduced into the catalytic reactor. The mass gain for the catalyst was 0.9 g, and in these conditions the amount of H_2O_2 introduced into the system was 0.81 mg H_2O_2 or 0.0238 mmol H_2O_2. The molar ratio [Fe]: [H_2O_2] = 45.33:1 indicates a big excess of [Fe] in the system.

Even with this small amount of H_2O_2 introduced, because of the high proportion of water in the H_2O_2 solution, moisture droplets were noticed on the reactor walls at the beginning of the experiment (the catalytic reactor was kept at 45 °C). The moisture was

cleared in time by the continuous airflow and after 2.5 hours the reactor walls were free

of visible moisture. The results of this experiment are presented in Figure 6.1.
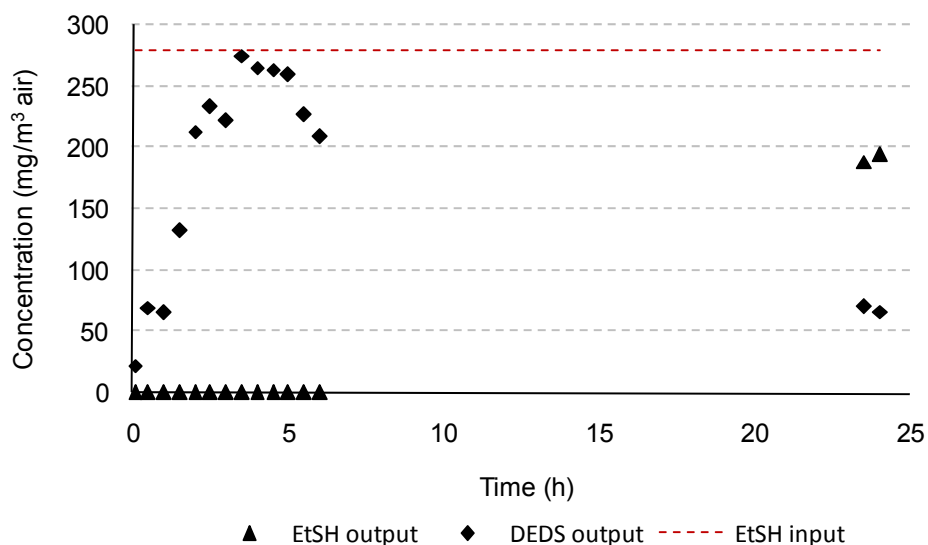
<u>Conditions:</u> air flow: 50 cm^3/min, EtSH flow: 1 μl EtSH/h, [EtSH]: 280 mg EtSH/ m^3 air, m$_{cat}$; 4.150 g, [Fe]: 0.52 mmoles Fe/g threads, H$_2$O$_2$: 0.9 g solution (900mg/L), V$_{cat}$: 18.85 cm^3, temperature: 45 °C, residence time of EtSH: 22.6 seconds.

Figure 6.1. Variation of EtSH and DEDS with time in the gas effluent during preliminary dynamic experiments with EtSH, catalyst as mesh and H$_2$O$_2$

Figure 6.1. shows that EtSH is oxidized fast to DEDS, with no EtSH identified in the

gas effluent. The DEDS concentration increased in time, and the new peaks noticed in

the GC spectra for the static experiments with H$_2$O$_2$ (see Figure 4.13. and Figure 4.14.

in section 4.6.2.2.) were also noticed at 2.5 hours, indicating that EtSH underwent an

advanced oxidation process with unidentified reaction products. DEDS concentration

reached a maximum at time 3.5 hours and decreased continuously after this. The

experiment was left running overnight and breakthrough for EtSH appeared during this

time, being confirmed on the first analysis made the next day (time 24 hours). After the

moisture was cleared from the system, and probably all the H$_2$O$_2$ was carried out by the

air flow, only the DEDS was identified as a reaction product, indicating that the process follows the same route as in the dynamic experiments with air of unmodified humidity, but the breakthrough was noticed earlier.

These preliminary results indicate that as H_2O_2 was not continuously added into the system, the advanced oxidation was only a temporary process, and thus a new way of continuously dosing H_2O_2 into the system needed to be investigated.

6.3. Design of an experimental rig with a three-phase catalytic reactor

In order to ensure continuous availability of H_2O_2 in the system, a new experimental setup was developed to incorporate a tri-phase catalytic reactor that insured the simultaneous presence of catalyst, organic pollutants (i.e. EtSH) and H_2O_2 solution in the system at all times. The design permits the operation of the reactor in both slurry (concurrent flow of gas and liquid phase) and scrubber (counter current flow of gas and liquid phase) regimes. The first design of the reactor incorporated an overflow tube, and considering the results of the test experiments, this design was modified to have an overflow at the side, and finally to incorporate an absorption column before the catalytic reactor. The absorption column enhances the mass transfer of EtSH from gas to the liquid phase, as the oxidation reactions were expected to take place in the liquid phase.

6.3.1. Experimental rig incorporating a catalytic reactor with overflow tube

6.3.1.1. Design and operational procedure

The schematic of the three-phase catalytic reactor is presented in Figure 6.2., and the operational procedure for the two regimes is presented below:

Legend:

1 – gas capillary

2 – catalytic reactor

3 – catalyst bed

4 – overflow tube

5 – glass grid

6 – gas distributor (sinter)

7 – valves

SP – syringe pump

P – peristaltic pump

GC – gas chromatograph

Regimes:

(1) – scrubber regime

(2) – slurry regime
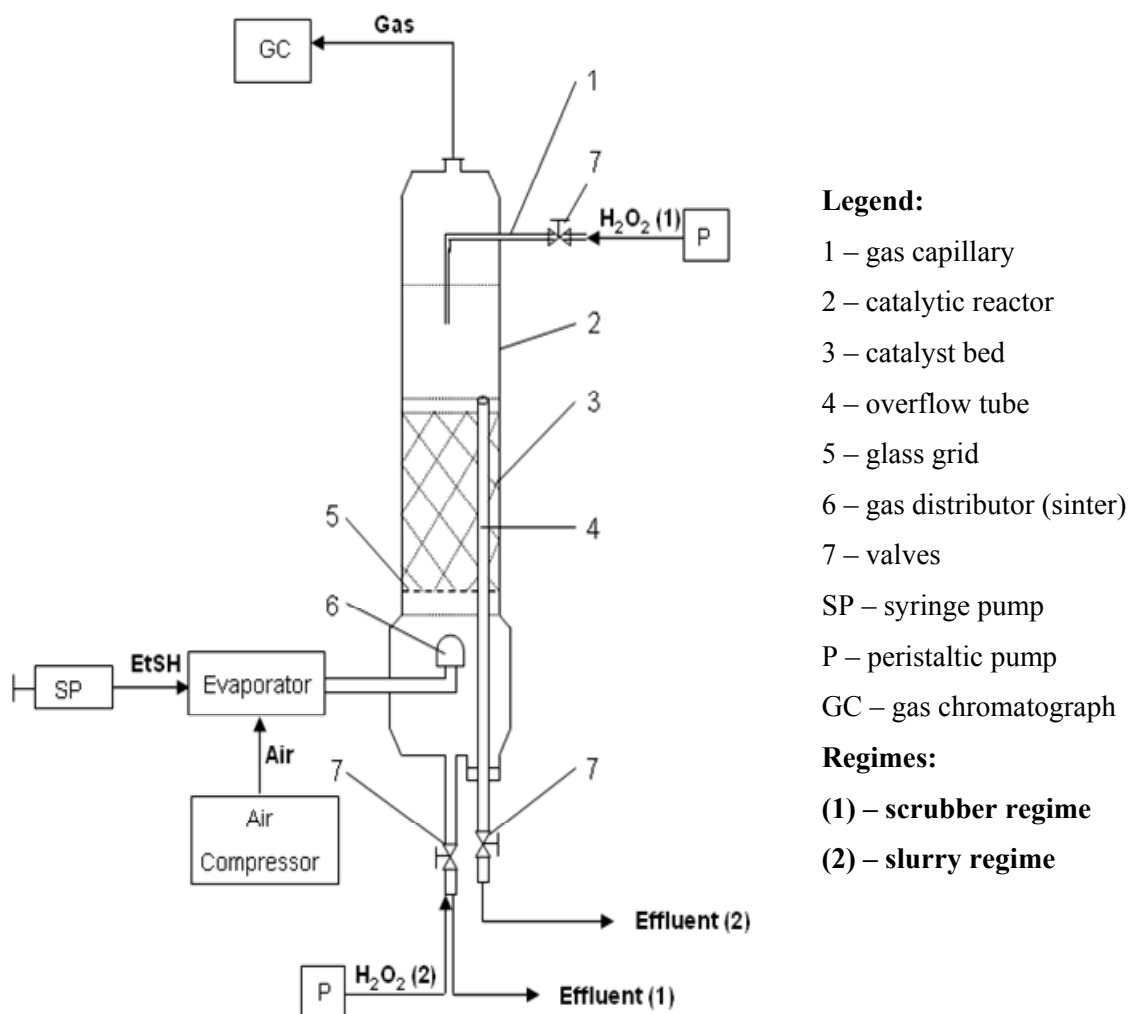
Figure 6.2. Schematic installation of the first version of the experimental rig, including the three-phase catalytic reactor with overflow tube

Operation for the scrubber regime (1)

The scrubber regime ensures a counter flow contact of the gas phase with the liquid H_2O_2 solution. The H_2O_2 solution was fed at the top of the reactor, through a fine capillary (1), and flowed over the fixed bed of catalyst (3) exiting the system at the lower end of the reactor as liquid effluent containing dissolved oxidation products and/or unreacted EtSH. The gas phase was fed at the bottom of the reactor through the sintered part of the gas distributor (6), passed the catalyst bed (3), where it also came into contact with the H_2O_2 solution and where the catalytic reaction took place. The gas phase left the reactor at its upper part, together with any gaseous reaction products and/or unreacted EtSH.

Operation for the slurry regime (2)

The slurry regime ensures a concurrent flow of liquid and gas phase in the catalytic reactor. Both H_2O_2 solution and gas were fed at the bottom of the reactor (the gas through the sintered gas distributor (6) and the liquid through the pipe fed by the peristaltic pump). Both liquid and gas phases passed the catalyst bed (3) in order to exit the reactor, and the catalyst was totally immersed in the liquid phase. The gas effluent exited the system at the top part of the reactor, containing any gaseous oxidation products and/or unreacted EtSH. The liquid effluent left the system through the glass overflow tube (4), containing any dissolved reaction products and/or unreacted EtSH. The level of liquid in the reactor was controlled with the overflow tube, with adjustable height. The overflow tube offered the advantage that the amount of catalyst (and thus

the volume of the reactor) could be varied, ensuring at the same time that the catalyst was covered by liquid at all times, and there was no excess of liquid in the reactor.

The liquid organic compound (EtSH) sent from the syringe pump (SP, model KDS100, KD Scientific Inc., UK) and the air from the compressor (Jun-Air 6-25, 25 L tank, work cycle 50%; Jun-Air International, Denmark) were mixed in the evaporator. The airflow was measured and adjusted using the valve fitted to a flow meter. The desired ratio of air/pollutant was achieved by altering the air flow and using different flow rates for the syringe pump (SP). The reaction mixture was then sent to the catalytic reactor (2), where it came into contact with the catalyst (3) and the H_2O_2 solution introduced into the system via the peristaltic pump (P). The catalyst ([Fe] = 0.52 mmol Fe/g threads) was produced by modification and impregnation of raw PAN mesh, resulting in catalytic mesh with 50% impregnated PAN yarn and 50% PP support. The catalytic reactor consisted of a glass tube with the dimensions: length x internal diameter = 200 mm x 36 mm, with a glass grid (5) positioned at the bottom part of the reactor. The glass grid acted as support for the catalyst bed. The catalytic mesh was cut into discs of 36 mm diameter or pieces (15 mm x 10 mm) and was introduced in the reactor as a compact bed positioned on the supporting grid. Before starting the experiment, the catalyst was conditioned by keeping it in the reactor, covered with H_2O_2 solution for 30 minutes. The overflow tube (4) passed the catalyst bed and the supporting glass grid, and facilitated the exit of the liquid effluent at the bottom part of the reactor. The same procedure was followed for the 'scrubber mode' operation of the reactor.

The volume of catalyst bed was calculated as the volume of a cylinder of 36 mm diameter and height (L) equal to the height of the catalytic bed.

$$V_{cat} = \pi \, (D/2)^2 L = 3.14 \times 1.8^2 \text{ cm}^2 \times L \text{ cm} = 10.1736 \times L \text{ cm}^3 \qquad (6.6)$$

The space velocity (SV) and residence time (T) for the gas and liquid phases in the reactor were calculated as:

$$SV_{gas} \, (h^{-1}) = 1/T; \qquad T_{gas}(h) = \frac{\text{Volume of catalyst bed (cm}^3)}{\text{Flowrate of air mixture (cm}^3/h)} \qquad (6.7)$$

$$SV_{liqiuid} \, (h^{-1}) = 1/T; \qquad T_{liquid} \, (h) = \frac{\text{Volume of catalyst bed (cm}^3)}{\text{Flowrate of liquid (cm}^3/h)} \qquad (6.8)$$

In both scrubber and slurry operating regimes, the temperature was kept constant (at 45-47 °C) throughout the experimental rig, using a heating system (temperature controller Horst MC1 in conjunction with an HST Heating cable (5.5 m, 125 W) and a Pt100/250°C temperature sensor), and by wrapping the rig in aluminium foil for better thermal insulation. The temperature sensor was positioned outside the reactor, in intimate contact with the reactor wall, at the middle of catalyst bed length).

The experiments consisted in the continuous passage of a mixture of air and EtSH, in known ratio, and H_2O_2 solution of known concentration through the rig. The gas and liquid effluent were periodically analysed using the GC, IC and GC-MS analytical techniques, as described in sections 3.3 and 3.4.

6.3.1.2. Dynamic experiments in 'scrubber mode' operation of the reactor

Two experiments were performed in order to test the scrubber mode operation for the catalytic reactor. The experiments were conducted in the experimental rig presented in Figure 6.2., operated according to the description presented in section 6.3.1.1.

<u>Experiment 1</u>

EtSH was introduced continuously into the system at a rate of 1 µL/h (0.84 mg EtSH/h), and mixed with the air introduced at 50 cm^3/min (0.003 m^3/h). The gas mixture was fed into the system at the bottom of the reactor, and the theoretical initial concentration of EtSH in air was 280 mg EtSH/m^3 air. H_2O_2 solution of 33 mg/L was introduced continuously in the system at the top of the reactor, at a flow rate of 2.4 cm^3/min. The molar ratio EtSH: H_2O_2 was 1:10, calculated as the stoichiometric amount of H_2O_2 necessary for total mineralization of EtSH. The catalyst (11.37 g mesh) was introduced in the reactor to form a compact bed (60 mm high) of 15 discs, with a volume of V_{cat} = 61 cm^3. The volume of liquid in the reactor was measured at the end of the experiment and was 63 cm^3. These conditions ensured a residence time T_{gas}= 73.25 s (20.3×10^{-3} h) for the gas phase (SV_{gas} = 49.26 h^{-1}), and T_{liquid} = 26.25 min (0.437 h) for the liquid phase (SV_{liquid}= 2.28 h^{-1}). The experiment (245 hours) was performed at 45 °C.

The gas effluent exiting the reactor at its upper part was analysed periodically to check for breakthrough of EtSH and for identification of gas phase reaction products. No breakthrough was noticed in the 245 hours and only very small amounts of DEDS

(reaction product) were identified, starting from analysis at time 2 hours from the start

of the experiment. The results of the gas effluent analysis are presented in Figure 6.3.
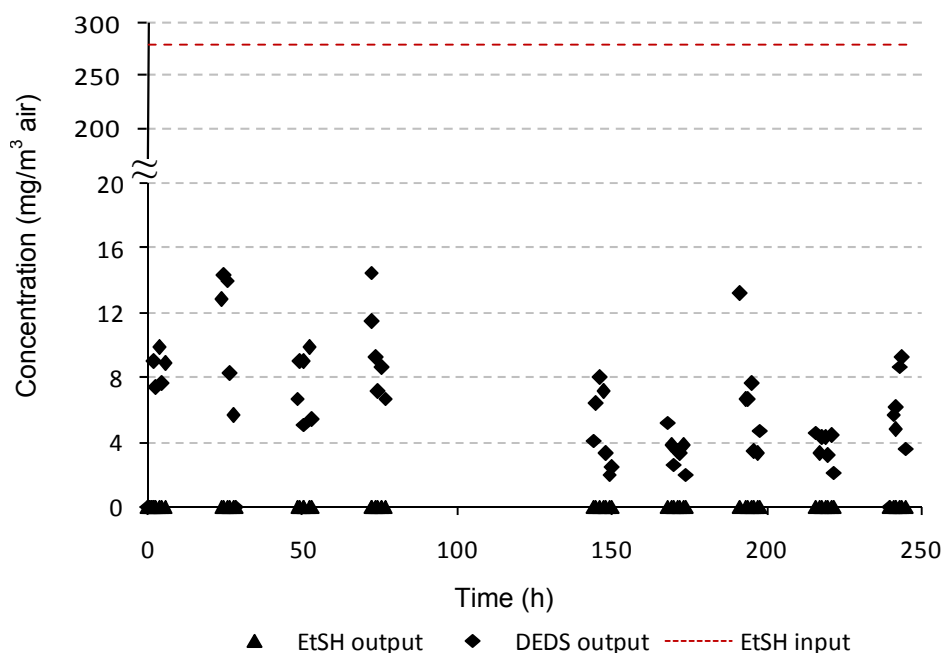
Figure 6.3. Variation of EtSH and DEDS concentration in time (gas effluent) for "scrubber mode" operation of the tri-phase reactor (experiment 1)

Figure 6.3. shows that at any time during the experiment, the concentration of both

EtSH and DEDS are very low in comparison with the continuous input flow of EtSH,

which is 280 mg EtSH/m^3 air. DEDS concentrations are at all times much lower than

those expected according to the results of the preliminary tests. The figure clearly shows

that EtSH concentration in the gas effluent is 0 at all times and DEDS concentration is

varying, with a maximum of 15 mg/m^3 air at some times.

The liquid effluent was also analysed periodically by GC-MS, according to the

procedure presented in section 3.4.1., and no EtSH or DEDS was identified. The limit of

detection for the GC-MS used was 0.5 mg/L for EtSH and DEDS, thus lower concentrations would not be detected. The IC analysis methods for $EtSO_3H$ and organic acids were not developed yet, thus the liquid effluent was not analysed by IC.

As no breakthrough and no significant amounts of reaction products were noticed, the experiment was stopped. A second experiment with increased EtSH concentration in air and with adjusted H_2O_2 solution concentration was planned.

Experiment 2

The experiment (362 hours at 45 °C) was performed with EtSH concentration 10 times higher than in the first experiment (2800 mg EtSH/ m^3 air). This concentration was achieved by using a flow rate of 10 μL EtSH/h (8.4 mg EtSH/h), and keeping the air flow at 50 cm^3/min (0.003 m^3/h). H_2O_2 solution of 320 mg/L was introduced in the system at the top of the reactor, at a flow rate of 2.4 cm^3/min, keeping the molar ratio EtSH: H_2O_2 at 1:10. The mass and volume of the catalytic bed, and thus the residence times for the gas and liquid phases were kept the same as in the first experiment.

GC analysis of the gas effluent showed no identification of EtSH in the 362 hours and only insignificant amounts of reaction products (DEDS). The results are summarized in Figure 6.4.
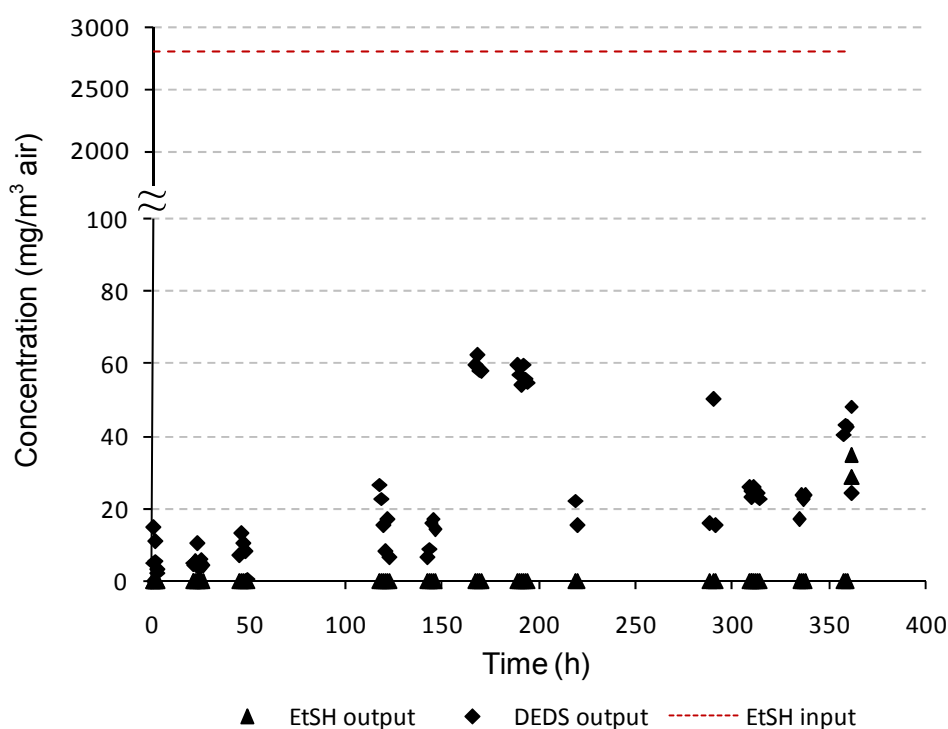
Figure 6.4. Variation of EtSH and DEDS concentration in time (gas effluent) for "scrubber mode" operation of the tri-phase reactor (experiment 2)

Figure 6.4. shows that at any time during the experiment, the concentration of both EtSH and DEDS are very low in comparison with the continuous input flow of EtSH, which in this case is 2800 mg EtSH/m^3 air, 10 times higher than in experiment 1. The values for DEDS concentrations are much lower than those expected according to the results of the preliminary tests. The figure clearly shows that EtSH concentration in the gas effluent is 0 at all times and DEDS concentration is varying, with a maximum of around 60 mg/m^3 air at some times.

The liquid effluent was analysed for identification and quantification of reaction products, using IC and GC-MS and the results are described below:

(i) In the first 168 hours of the experiment, IC analysis was focused on identification of organic acids, according to the procedure presented in section 3.4.2. Formic acid (about 1 mg/L) and acetic acid (less than 0.1 mg/L) were identified; the peak for formic acid increased in time, while the peak for acetic acid was constant at low values, indicating that this was only an intermediate product, being further oxidized to formic acid.

(ii) The last part of the experiment (between hours 168 and 362), IC analysis was focused on identification of $EtSO_3H$ and sulphates in the liquid effluent, as presented in section 3.4.2. A constant level of 4 mg/L $EtSO_3H$ was identified in the liquid effluent during the last 48 hours of the experiment. The peak for SO_4^{2-} was also present on the chromatograms, but as the catalyst production involved the use of $Fe_2(SO_4)_3$, it was not possible to identify how much was originating from the catalyst and how much was due to mineralization of sulphur.

(iii) Small amounts of DEDS and an average of 4 mg/L EtSH were identified during GC-MS analysis of the liquid effluent exiting the reactor.

After 360 hours, as the reaction products were detected at lower levels than expected, a gas sample from the gas exiting the reactor at its lower part (along with the liquid effluent), was collected and analysed to determine whether unreacted EtSH and/or DEDS are present in the sample. The analysis showed that insignificant amounts of DEDS and at least 85% of the EtSH introduced into the system exit the reactor as unreacted, along with the liquid effluent.

Taking into account the amount of EtSH identified as dissolved in the liquid phase and the amount of EtSH exiting as gas along with the liquid effluent it was calculated that only about 8% of the EtSH passes the catalyst and is oxidized in the catalytic reactor. As a consequence it was decided that the reactor design used is not suitable for these experiments. One reason might be that the packing of the catalyst in the reactor is too tight, making it easier for the gas to leave the system at the bottom of the reactor, together with the liquid effluent.

6.3.1.3. Dynamic experiments in 'slurry mode' operation of the reactor

The slurry mode operation of the three-phase reactor was tested in a control experiment with EtSH, H_2O_2 and raw PAN mesh (as discs) and a series of experiments with EtSH, H_2O_2 and catalytic mesh as discs or pieces. The experiments were conducted in the experimental rig presented in Figure 6.2., operated according to the description presented in section 6.3.1.1. The slurry mode operation ensures a concurrent flow of the gas and liquid phases; both liquid and gas are introduced into the system at the bottom of the reactor and are forced to pass the catalyst bed in order to exit the system.

<u>Control experiment</u>

EtSH was introduced continuously into the system at a rate of 5 μL/h (4.2 mg EtSH/h), and mixed with the air introduced at 50 cm^3/min (0.003 m^3/h). The gas mixture was fed into the system at the bottom of the reactor (through the sintered part of the gas distributor), and the theoretical initial concentration of EtSH in air was 1400 mg EtSH/ m^3 air. H_2O_2 solution of 160 mg/L was introduced continuously in the system at the

bottom of the reactor, at a flow rate of 2.4 cm^3/min. The molar ratio EtSH: H$_2$O$_2$ was 1:10, calculated as the stoichiometric amount of H$_2$O$_2$ necessary for total mineralization of EtSH. The PAN mesh (m$_{control}$ = 5.6 g raw PAN mesh, corresponding to 7.26 g catalyst considering the 30% mass gain during the modification and impregnation process), was cut into discs of 36 mm diameter and 10 identical discs were inserted into the reactor as a tightly packed bed (45 mm high), resulting in a bed volume of V$_{control}$ = 45.8 cm^3. The volume of liquid in the reactor was measured at the end of the experiment and was 46 cm^3.These conditions ensured a residence time T$_{gas}$ = 55 s (15.27 × 10^{-3} h) for the gas phase (SV$_{gas}$= 65.48 h^{-1}), and T$_{liquid}$ = 19.1 min (0.318 h) for the liquid phase (SV$_{liquid}$ = 3.14 h^{-1}). Before starting the experiment, the control bed was conditioned by keeping it in the reactor, covered with H$_2$O$_2$ solution for 30 minutes. The control experiment was performed at 45 °C and lasted 24 hours. The liquid left the reactor via the overflow tube.

The GC analysis of the gas effluent (top of reactor) showed instant identification of EtSH and insignificant amounts of DEDS as reaction product in the gas phase. EtSH concentration increased in time rapidly. The results are presented in Figure 6.5.
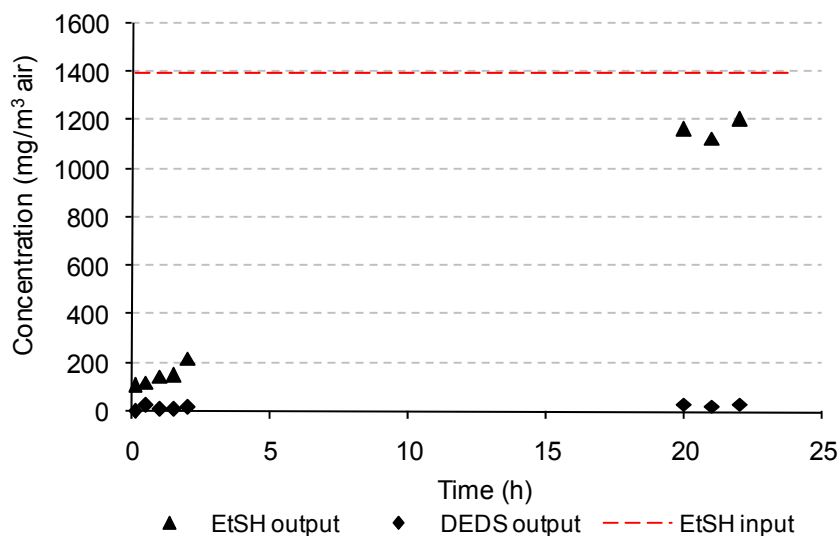
Figure 6.5. Variation of EtSH and DEDS concentration in time (gas effluent) for the "slurry mode" operation of the tri-phase catalytic reactor (control experiment)

Very little DEDS was found in the gas effluent while the concentration of EtSH increased constantly to values close to the input concentration, as shown in Figure 6.5.

The liquid effluent was analyzed for identification of unreacted EtSH and reaction products, using IC and GC-MS. GC-MS analysis of the liquid effluent showed that it contained an average of 2 mg/L EtSH (corresponding to 6.8% of the total amount of EtSH introduced into the system), and insignificant amounts of DEDS. IC analysis of liquid effluent showed that the effluent contained traces of $EtSO_3H$ (less than 0.1 mg/L) and no SO_4^{2-}.

Analysis of the gas carried out of the reactor together with the liquid effluent through the overflow pipe identified large amounts of DEDS and an average of 60.35% of the initial concentration of EtSH introduced into the system.

A mass balance for the EtSH at 22 hours of experiment showed that only 4.8% of the total amount of EtSH introduced into the system reacted, with DEDS being the main reaction product. The rest (95.2%) was detected as unreacted: 28% in the gas effluent (exiting at the top of the reactor), 60.35% identified in the gas carried out of the reactor together with the liquid effluent through the overflow pipe and a further 6.85% identified in the liquid effluent.

This experiment showed that the system PAN mesh/H_2O_2 is not efficient in the decomposition of EtSH from gas samples. When only H_2O_2 is used as oxidant, very little DEDS is produced as main reaction product, along with traces of $EtSO_3H$.

Experiments with catalyst

A series of 5 similar experiments with EtSH, catalytic mesh and H_2O_2 were performed in order to test the performance of the catalytic reactor in slurry mode operation.

EtSH was introduced continuously into the system at a rate between 1 - 5 μL/h (0.84 – 4.2 mg EtSH/h), and mixed with the air introduced at 30 - 50 cm^3/min (1.8 – 3 × 10^{-3} m^3/h). The gas mixture was fed into the system at the bottom of the reactor, and the theoretical initial concentration of EtSH in air ranged between: 466.7 - 1400 mg EtSH/ m^3 air. H_2O_2 solution of 33 -160 mg/L was introduced continuously in the system at the bottom of the reactor, at a flow rate of 2.4 cm^3/min, keeping the molar ratio EtSH: H_2O_2 = 1:10, calculated as necessary for total mineralization of the EtSH. The catalyst (7.36 – 21.6 g mesh) was used as discs or pieces and was packed tightly in the reactor (height between 40 – 110 mm), giving bed volumes between V_{cat} = 40.7 – 112 cm^3. These

conditions ensured a residence time between T_{gas} = 48.8 s – 3.23 min (13.55 × 10^{-3} –

53.83 × 10^{-3} h) for the gas phase (SV_{gas} = 73.8 – 18.57 h^{-1}), and T_{liquid} = 16.95 – 46.66

min (0.282 – 0.777 h) for the liquid phase (SV_{liquid} = 3.54 – 1.28 h^{-1}). The catalytic bed

was conditioned by keeping it in the reactor, covered with H_2O_2 solution for 30 minutes

prior starting the experiment. The experiments were performed at 45 °C and lasted

between 2 and 24 hours, with the catalyst bed being completely covered with H_2O_2

solution at all times and the liquid exiting the reactor via the overflow tube.

In all the experiments, GC analysis of the gas effluent (from the top of the reactor)

showed an instant identification of EtSH and insignificant amounts of DEDS as reaction

product. EtSH concentration in the gas effluent increased rapidly in time. EtSH passed

the catalytic bed covered by liquid via a preferential route, next to the overflow tube,

where the resistance was lower. In this way, the gas bypassed the catalyst bed and the

real residence time was much lower than the theoretical value calculated above. It was

also observed that the gas phase left the system not only at the top of the reactor, but

also via the overflow tube as a mixture of gas and liquid effluent.

GC-MS analysis of the liquid effluent identified no EtSH or DEDS. IC analysis of the

liquid effluent showed the presence of increasing amounts of $EtSO_3H$, indicating that

EtSH undergoes an advanced oxidation process and that the system did not reach the

steady state operation. SO_4^{2-} could not be quantified as the peak corresponding to SO_4^{2-}

was too intense; the catalyst production involves impregnation with $Fe_2(SO_4)_3$.

GC analysis of the gas carried out of the reactor together with the liquid effluent through the overflow tube identified an average of 51% of the total EtSH introduced into the system. The analysis also showed large amounts of DEDS in the gas samples.

A mass balance for EtSH after 3 hours of catalysis showed that only 6.34% of the total amount of EtSH introduced reacted in liquid phase, leading to DEDS and considerable amounts of $EtSO_3H$. The rest (93.66%) was detected as unreacted: 43.23% in the gas effluent (exiting at the top of the reactor) and 53.14% in the gas carried out of the reactor through the overflow pipe, along with the liquid effluent.
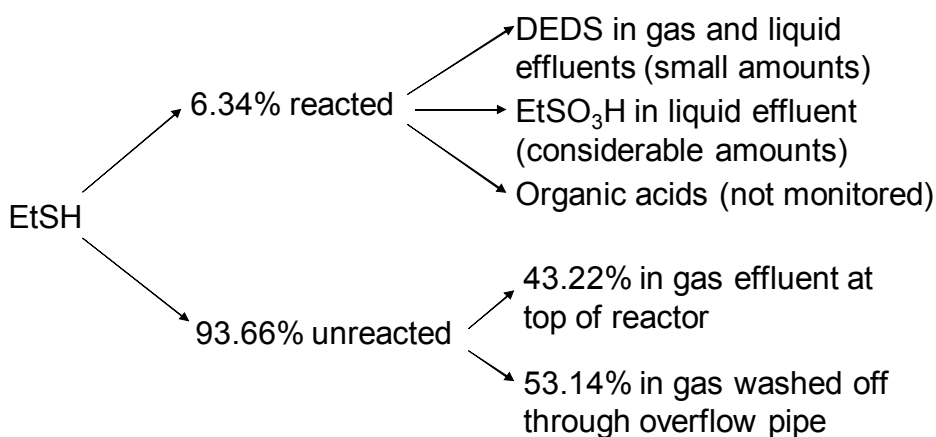
The construction of the reactor with overflow as an internal tube rising on one side from the bottom of the reactor did not permit a packing of the catalyst close enough to the overflow tube and the wall of the reactor. The gas had a preferential path for exiting the reactor in the space between the overflow tube and the wall of the reactor, where the resistance was minimal. As H_2O_2 alone is not able to oxidize EtSH efficiently (as shown by the control experiment), a large amount of EtSH left the system without oxidation. As a consequence, the reactor was redesigned and the overflow tube removed.

6.3.2. Modification of initial design. Catalytic reactor with overflow at the side

6.3.2.1. Redesign of the catalytic reactor

In order to overcome the limitations of the first design and to prevent the formation of a preferential gas pathway next to the overflow tube, the tri-phase reactor was redesigned by replacing the overflow tube by an overflow situated at the side of the reactor, towards its upper end. This design eliminates the possibility of the gas phase bypassing the catalyst, ensuring a longer "real" residence time for the gas in the system.

The new experimental setup, with a close-up of the catalyst packing as discs is shown in Figure 6.6. a and b, and the schematic is shown in Figure 6.7.
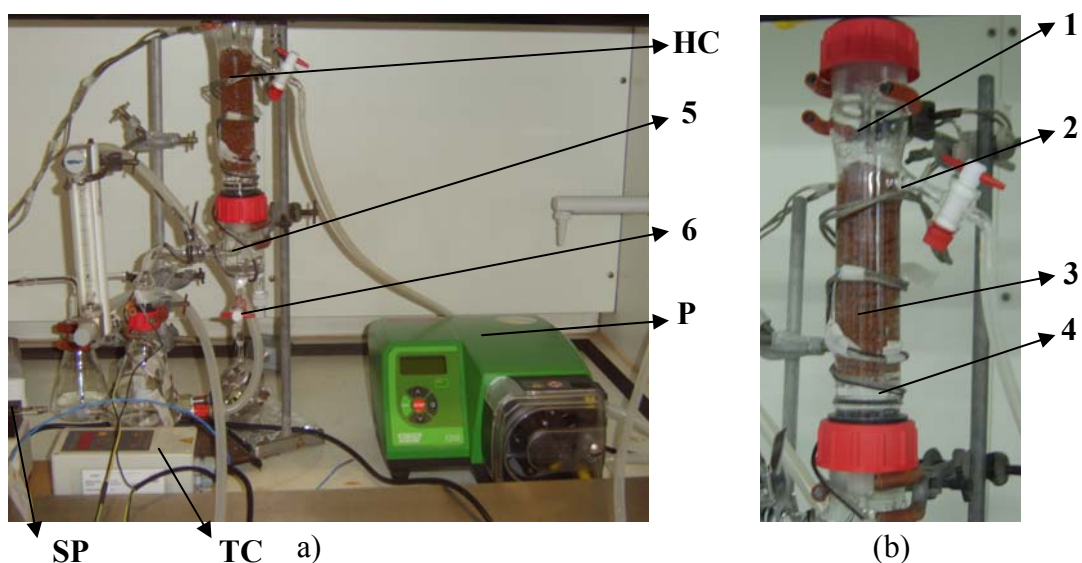
Legend: 1-loaded catalytic reactor, 2-overflow, 3-catalyst bed, 4-glass grid, 5-gas distributor, 6-valve, HC -heating cable, TC –temperature controller, SP –syringe pump, P –peristaltic pump

Figure 6.6. Redesigned slurry reactor with overflow at the side of the reactor (a) and expanded view of the catalyst packed as discs (b)
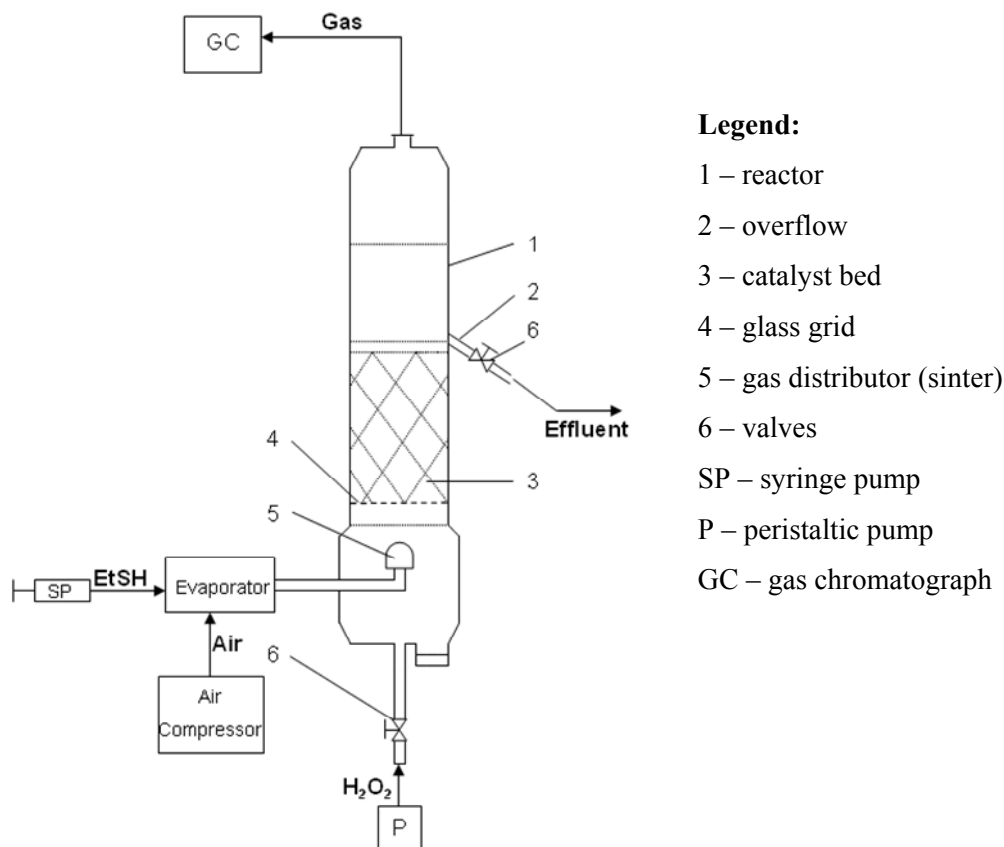
Figure 6.7. Schematic of the experimental setup with the redesigned slurry reactor (with overflow at the side of the reactor)

Operational procedure for the catalytic reactor with overflow at the side

The reactor is operated in slurry regime; this ensures an upward concurrent flow of liquid and gas phases in the catalytic reactor, both H_2O_2 solution and gas being fed at the bottom of the reactor (the gas through the sintered gas distributor and the liquid through the pipe fed by the peristaltic pump). Both liquid and gas phases pass the catalyst bed (which is totally immersed in the liquid phase) in order to exit the reactor. The gas effluent exits the system at the top part of the reactor, while the liquid effluent exits via the overflow (2). The level of liquid in the reactor is not adjustable, being controlled by the position of the overflow.

The experimental procedure is the same as for the slurry mode operation described in section 6.3.1.1., with the only difference that the liquid effluent exits the system through the side overflow, not through the adjustable overflow tube. The temperature is kept constant throughout the experimental rig, using the heating cable and temperature control system described in previous sections. The online analysis of the gas samples was replaced by manual analysis, which consists of injecting 1 cm^3 of gas sample collected from the top of the reactor (using a gas tight syringe with long needle) into the GC and recording the retention times of any organic compounds present in the sample (EtSH, DEDS). The GC method used is presented in section 3.3.1.

The experiments consisted in the passage of a mixture of air and EtSH, in known ratio, and H_2O_2 solution through the experimental setup and analysing the composition of both the gas effluent (GC analysis) and the liquid effluent (IC and GC-MS analyses).

6.3.2.2. Dynamic experiments in the redesigned catalytic reactor

Two experiments were performed in order to test the efficiency of the redesigned catalytic reactor, and these are presented below:

<u>**Experiment 1**</u>

EtSH was introduced continuously into the system at a rate of 1 μL/h (0.84 mg EtSH/h), and mixed with the air introduced at 30 cm^3/min (1.8×10^{-3} m^3/h). The gas mixture was fed into the system at the bottom of the reactor, and the theoretical initial concentration of EtSH in air was 466.7 mg EtSH/ m^3 air. H_2O_2 solution of 33 mg/L was introduced

continuously in the system at the bottom of the reactor, at a flow rate of 2.4 cm³/min, the molar ratio EtSH : H_2O_2 was 1:10, calculated as necessary for total mineralization of the EtSH. The catalyst (20.1 g mesh, [Fe] = 0.52 mmol/g thread) was introduced into the reactor as discs of 36 mm diameter, tightly packed to cover the cross area of the reactor to a height of 115 mm (the maximum height to which the catalyst can be loaded into the reactor due to the position of the overflow). The theoretical volume of the catalyst bed was V_{cat} = 117 cm³; the measured volume of liquid in the reactor was 120 cm³. These conditions ensured a molar ratio Fe:H_2O_2 of 44.9:1, residence times of T_{gas} = 3.9 min (65 × 10⁻³ h) for the gas phase (SV_{gas} = 15.38 h⁻¹), and T_{liquid} = 50 min (0.833 h) for the liquid phase (SV_{liquid} = 1.2 h⁻¹). The catalytic bed was conditioned by keeping it in the reactor, covered with H_2O_2 solution for 30 minutes prior starting the experiment. The experiments were performed at 45 °C and lasted 48 hours. The catalyst bed was completely covered with H_2O_2 solution at all times and the liquid exited the reactor via the overflow.

The GC analysis of the gas effluent (sample collected from the top of the reactor) indicated an instant breakthrough of EtSH, as well as minute concentration of gaseous DEDS. The results are presented in Figure 6.8.

The liquid effluent was analysed by GC-MS, but no reactant or reaction products were identified. The limit of detection for GC-MS is 0.5 mg/L for both EtSH and DEDS, thus lower concentrations would not be detected. IC analysis of the liquid phase was focused on identification and quantification of $EtSO_3H$, according to the method presented in Section 3.4.2. The results are presented in Figure 6.9.
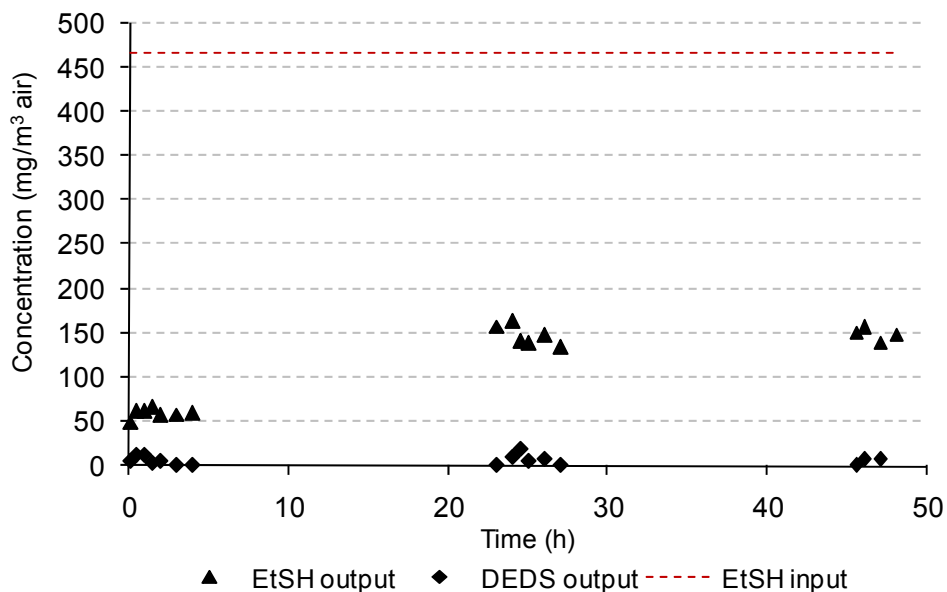
Figure 6.8. Variation of EtSH and DEDS concentrations with time in the gas effluent (catalytic reactor with overflow at the side, first experiment)

Figure 6.8. shows that after a few hours, the system is operated in steady state, with ~70% removal of EtSH from the inlet stream, but very little DEDS is identified in the gas phase.
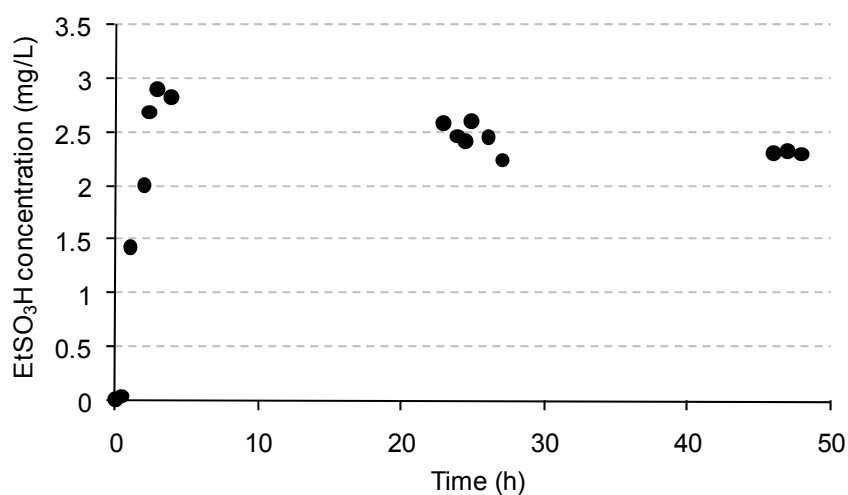
Figure 6.9. Variation of EtSO$_3$H concentration with time in the liquid effluent (catalytic reactor with overflow at the side, first experiment)

Figure 6.9. shows that after a few hours, the system reaches steady state operation, with consistent production of $EtSO_3H$ at a concentration of 2.3 mg/L. This represents 22.2% yield taking into account the total amount of EtSH introduced into the system, or 31.8% yield if the unreacted EtSH (GC analysis) is subtracted from the initial EtSH amount. A mass balance for EtSH at 47 hours of experiment is presented below (see Appendix 1 for a detailed calculation based on the results of GC, GC-MS and IC analysis of gas and liquid effluents):
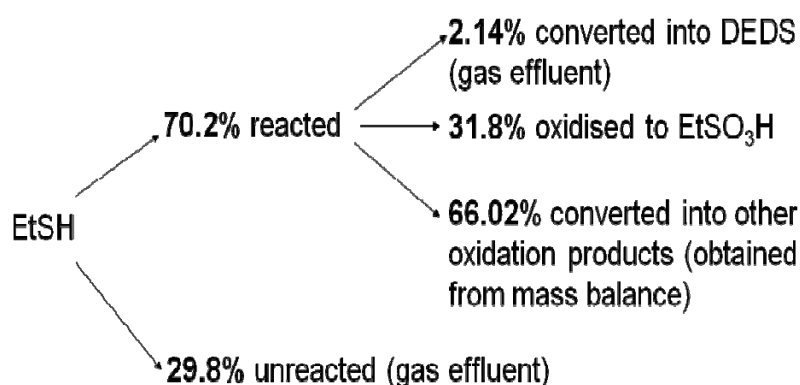
2.14% converted into DEDS (gas effluent)

70.2% reacted ⟶ **31.8% oxidised to EtSO$_3$H**

EtSH

66.02% converted into other oxidation products (obtained from mass balance)

29.8% unreacted (gas effluent)

The modified PAN catalyst/H_2O_2 solution is effective in the advanced oxidation of gas phase EtSH in dynamic mode, but the experimental conditions need to be optimised with regard to amount of catalyst, packing of the catalyst in the reactor, initial flow rates and concentrations of EtSH and H_2O_2. Even though the calculated theoretical residence time is 3.9 minutes, the real residence time is much shorter, as the gas passes the catalytic bed via preferential routes.

Optimisation of experimental conditions

The first step was to vary the initial EtSH concentration in air, as the height of the catalytic bed could not be increased; this is limited by the position of the overflow,

which is fixed. The maximum volume of the catalytic bed was 117 cm^3; this ensured a theoretical residence time of 3.9 minutes for the gas, at a gas flow rate of 30 cm^3/min. It is not possible to lower the gas flow rate due to limitations in the gas flow meter. The only parameters that could be varied without major alterations to the experimental setup were: concentration of EtSH in air, (by varying the flow rate for the syringe pump: minimum rate is 0.1 μL/h, corresponding to 0.084 mg EtSH/h), the H$_2$O$_2$ solution concentration and flow rate at which is fed into the system, and the temperature.

A series of 5 experiments with different EtSH concentrations in air were performed, keeping all other experimental conditions as in the first experiment (see above). The flow rate for EtSH was set between 0.5 and 0.1 μL/h and that for air was kept at 30 cm^3/min. This ensured EtSH concentrations between 233.3 and 46.6 mg EtSH/m^3 air. The experiments lasted between 5 and 30 hours. In all cases GC analysis of the gas effluent showed instant identification of unreacted EtSH, indicating that the experimental setup needs major modification in order to increase the time EtSH is in the system. As the catalytic reaction was expected to take place in the liquid phase, the mass transfer of EtSH from gas to liquid phase needed to be improved.

6.3.3. Experimental rig with absorption column and catalytic reactor

6.3.3.1. Design and operational procedure

The experimental setup was modified to incorporate an absorption column before the catalytic reactor, in order to facilitate the mass transfer of EtSH from gas to liquid phase

and thus to increase the residence time for the pollutant in the system (residence time for the liquid phase is 50 minutes compared to 3.9 minutes for the gas phase). The absorption column was a vertical glass tube of dimensions L x i.d. = 280 mm × 18 mm, having at its lower end a sintered disc (support for the polypropylene (PP) threads used as filling material). PP is an inert material also used as scaffold in the knitting-up of the raw PAN mesh used in the production of the catalyst. The PP threads (7.5 g) were packed tightly in the absorption column and occupied its entire diameter over a length of 250 mm (volume 63.6 cm^3). The gas and liquid phases passed easily through the sintered disc on their way through the system.

The experimental setup with absorption column and catalytic reactor is presented in Figure 6.10. a and b and the schematic is shown in Figure 6.11.
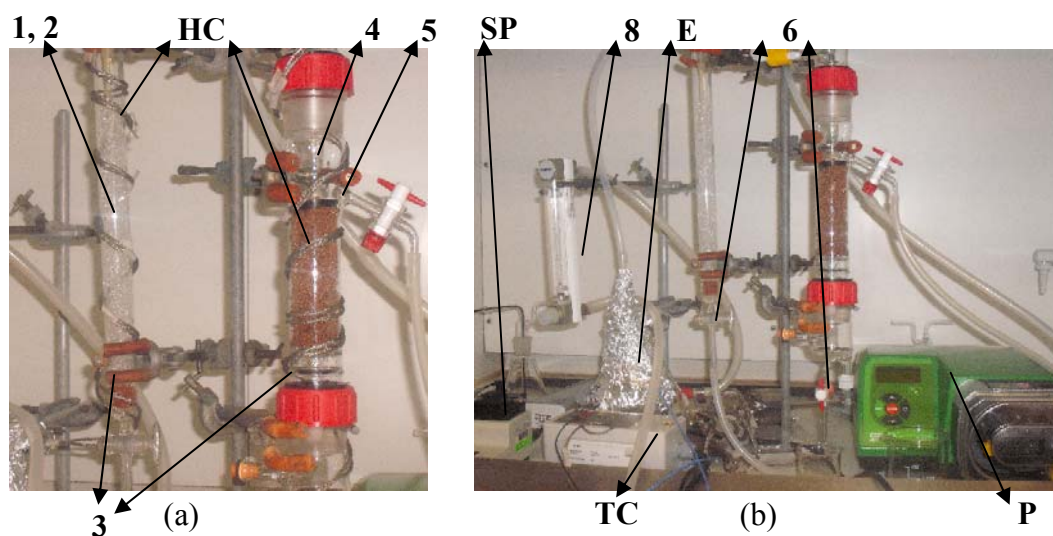
Legend: 1- absorption column 2 - PP threads 3- supportive grid, 4 - loaded catalytic reactor, 5- overflow, 6 - valves, 7 - catalytic bed, 8- gas flow meter, HC - heating cable, TC - temperature controller, SP - syringe pump, E - evaporator, P - peristaltic pump

Figure 6.10. Experimental setup with absorption column and catalytic reactor: (a) - with heating cable, (b) - without heating cable
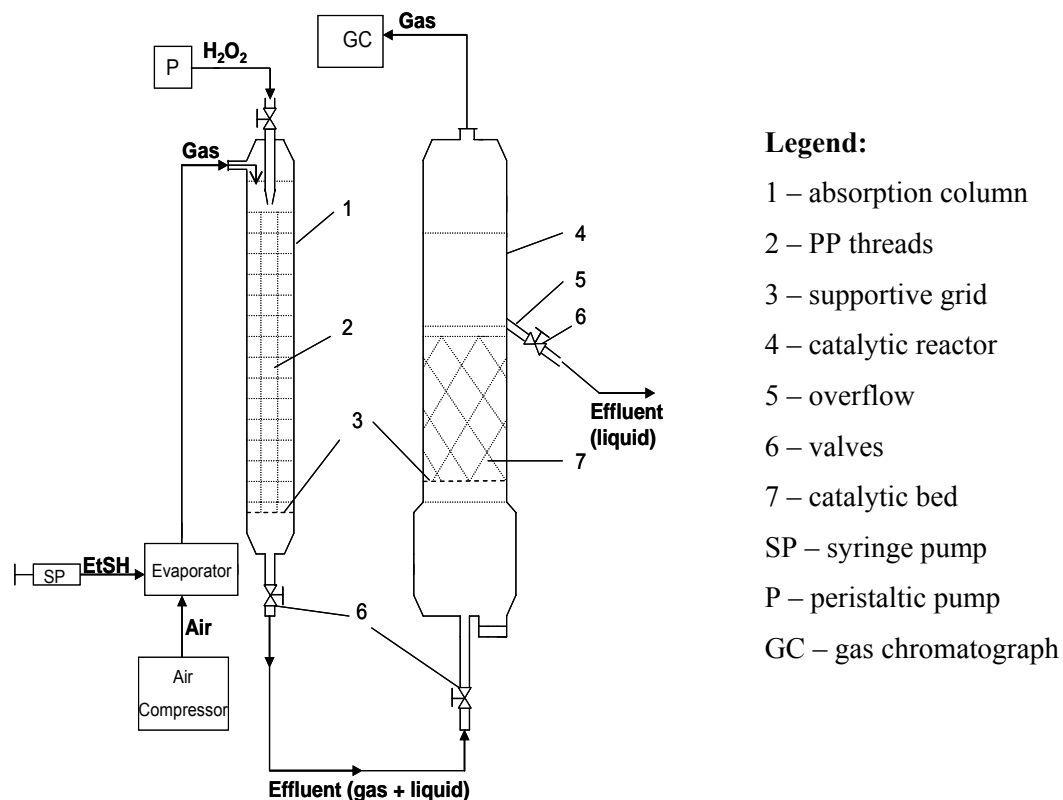
Figure 6.11. Schematic of the experimental setup with absorption column and catalytic reactor

Operational procedure

H_2O_2 solution and the contaminated air enter the system at the top of the absorption column (1), H_2O_2 being fed via a peristaltic pump and the gas phase from the evaporator (air and EtSH are mixed in known proportions in a vessel kept at 45 °C to ensure that EtSH is in gas phase). The H_2O_2 and the gas come into contact and pass the bed of PP threads (2), which ensures a higher physical contact between the two phases and enhances the mass transfer of EtSH from gas to liquid phase. The gas - liquid mixture exits the absorption column and enters the lower part of the catalytic reactor (4), which is operated in slurry regime (upwards concurrent flow of liquid and gas phases). Both liquid and gas phases pass the catalyst bed (7); this is totally immersed in the liquid

phase. The gas effluent exits the system at the top of the reactor, while the liquid effluent exits via the overflow (5), positioned at the upper side of the reactor. The level of liquid in the reactor is controlled by the overflow, which has a fixed position. The experimental rig can be operated at a set temperature (using the heating cable and the temperature controller), or at ambient temperature, when the heating cable is removed from all parts of the setup but the evaporator (see Figure 6.10. b).

The experiments consisted in the passage of H_2O_2 solution and a mixture of air and EtSH, in known ratio, through the experimental rig, and analysing the composition of the gas effluent (GC analysis) and of the liquid effluent (IC and GC-MS analyses). The online analysis of the gas samples was replaced by manual analysis, which consisted of injecting 1 cm^3 of gas sample collected from the top of the reactor into the GC and recording the retention times of the organic compounds present in the sample.

6.3.3.2. Catalytic decomposition of airborne EtSH at 45 °C in the experimental rig with absorption column and catalytic reactor

A series of experiments with initial concentrations of EtSH between 46.6 and 233.3 mg EtSH/m^3 air were performed in order to test the efficiency of the new experimental rig at 45 °C. These concentrations were achieved by keeping the flow rate of air constant (30 cm^3/min) and varying the flow rate for the syringe pump used to feed EtSH into the evaporator (0.1 – 0.5 µL/h). The catalyst (20. 1 g mesh, [Fe]=0.52 mmol/g threads) was used as mesh cut into rectangular pieces of 10 × 15 mm and inserted into the reactor to form a catalytic bed of 117 cm^3 volume (diameter 36 mm, height of bed 115 mm). Prior

to start of the experiment the catalyst was conditioned by keeping it in the reactor, covered with H_2O_2 solution for 30 minutes. The temperature was kept constant at 45 °C throughout the experimental rig. At the end of the experiment the liquid was drained from the reactor and the volume that covered the catalyst was measured to be 120 cm^3.

For concentrations higher than 93.3 mg EtSH/m^3 air, EtSH was instantly identified in the gas effluent (GC analysis), but not in the liquid effluent (GC-MS analysis), indicating that the mass transfer in the absorption column is not complete. To increase the mass transfer, a bigger absorption column or another filling material should be used.

The best results were obtained when the theoretical initial concentration of EtSH was 93.3 mg EtSH/m^3 air, achieved by using an air flow of 30 cm^3/min (1.8×10^{-3} m^3/h) and an EtSH flow of 0.2 µL/h (0.168 mg EtSH/h). H_2O_2 solution of 100 mg/L was continuously introduced into the system at a flow rate of 2.4 cm^3/min. These conditions ensured a molar ratio Fe:H_2O_2 of 14.8:1, and H_2O_2:EtSH of 177.5:1. The residence times were T_{gas}= 3.9 min (65×10^{-3} h) for the gas phase (SV_{gas}= 15.38 h^{-1}), and T_{liquid} = 50 min (0.833 h) for the liquid phase (SV_{liquid} = 1.2 h^{-1}).

The experiment performed using the optimised conditions lasted for 415 hours and no deactivation of the catalyst was noticed in this time. The results of the GC analysis of the gas effluent are presented in Figure 6.12.

Figure 6.12. Variation of EtSH and DEDS concentrations with time in the gas effluent (setup with absorption column and catalytic reactor, optimised conditions) at 45 °C

Figure 6.12. shows that no DEDS was identified in the gas effluent and that sometimes EtSH was identified in small concentrations (less than 2.5 mg/m^3 air); this could be attributed to the working cycle of the air compressor, as small fluctuations in the flow rate occurred and this affected the residence time of the gas in the system. Overall the system was stable; the small amounts of unreacted EtSH identified occasionally were always below the admissible limit of EtSH in air (10 ppmv or 25 mg/m^3 air according to OSHA Ceiling PEL regulations) (OSHA, 2008). The removal efficiency of this system with regard to the EtSH concentration in the inlet stream was calculated to be (93.3 − 2.5)×100/93.3 = 97.3 %. This is comparable with the reported efficiencies of the packed bed wet scrubbers using chemical agents such as ClO_2 or NaOCl, with reported

efficiencies between 85-98% for removal of VOCs including sulphur compounds (Kastner *et al.*, 2003; Chungsiriporn *et al.*, 2005), or even better than the 34% removal performance of the compact scrubber with wire mesh packing system using H_2O_2 and ozone used for the removal of dimethyl disulphide (DMDS) at ambient temperature (Biard *et al.*, 2009).

The liquid effluent was analysed by GC-MS for reaction products, but no reactant or reaction products were identified. The limit of detection for GC-MS is 0.5 mg/L for EtSH and DEDS, thus lower concentrations would not be detected. IC analysis of the liquid phase was focused on identification and quantification of $EtSO_3H$ according to the method presented in Section 3.4.2. The variation of $EtSO_3H$ concentration in time during this experiment is presented in Figure 6.13.

Figure 6.13. Variation of EtSO₃H concentration with time in the liquid effluent (setup with absorption column and catalytic reactor, optimised conditions) at 45 °C

A total amount of 0.2 μL/h × 0.84 mg/μL = 0.168 mg EtSH/h and 2.4 cm^3/min × 60 min/h = 144 cm^3/h H_2O_2 solution are fed into the system in one hour. Considering that all the EtSH was transferred into the liquid phase, the concentration of EtSH would be 1.16 mg EtSH/L. Figure 6.14. shows that after a few hours required for stabilisation of the reactor, the system reaches steady state operation, with consistent production of $EtSO_3H$ at a concentration of ~ 1.75 mg/L. This represents ~86 % yield (86 % of the theoretical 2.05 mg $EtSO_3H$/L that would be produced if all the EtSH were converted to $EtSO_3H$).

Considering that neither EtSH nor DEDS were identified in the liquid or gas effluents, it can be assumed that the rest of the EtSH (~14%) introduced into the system was converted to other oxidation products such as organic acids (acetic acid, formic acid). These products were not monitored as the method of their analysis involves different conditions (column, eluent, and regenerant).

The H_2O_2 consumption was also monitored during the oxidation process, using the instrument and the method presented in Section 3.4.3. The variation of H_2O_2 concentration with time during this experiment is presented in Figure 6.14.

Figure 6.14. Variation of H$_2$O$_2$ concentration with time in the liquid effluent (setup with absorption column and catalytic reactor, optimised conditions) at 45 °C

Figure 6.14. shows that for steady state operation, the residual H$_2$O$_2$ concentration in the liquid effluent is constant at about 24-25 mg/L, indicating that H$_2$O$_2$ is added in excess. Knowing the consumption of H$_2$O$_2$ during the treatment process allows the feed concentration to be adjusted in order to reduce the costs of air treatment. In this particular case H$_2$O$_2$ concentration could be reduced from 100 mg/L to 80 mg/L.

The system modified PAN catalyst/H$_2$O$_2$ solution is effective in the advanced oxidation of gas phase EtSH in dynamic mode, for the conditions presented above. In order to process higher flow rates of contaminated air or air contaminated with higher concentration of EtSH, the system needs to be scaled up. The residence time for EtSH in the system could be increased by increasing the mass transfer from gas to liquid phase, using an absorption column with higher capacity, and other filling materials with different physical properties and characteristics.

The process should be further optimised with regard to operational parameters for the absorption column and catalytic reactor, for cases when the residual concentration of the pollutant (other than EtSH) in the treated air is above the admissible limits set by the Environment Agency.

6.3.3.3. Catalytic decomposition of airborne EtSH at ambient temperature in the experimental rig with absorption column and catalytic reactor

In order to test the efficiency of the system at ambient temperature, the heating system was removed from the main parts of the experimental rig except the evaporator/mixing vessel, which was kept at 45 °C in order to ensure that all EtSH sent through the rig is in gas phase when reaches the absorption column (see section 6.3.1.1., Figure 6.10. b). The heating system was removed while the experiment was still running, and as the catalyst in the reactor did not show any signs of deactivation, the same catalyst was used in the experiment at ambient temperature. The experimental conditions were the same as in the previous experiment, except the temperature has changed from 45 °C to ambient (16 − 18 °C). The experiment lasted 309 hours (from time 416 h to 724 h), and no deactivation of the catalyst was noticed. The results of the GC analysis of the gas effluent are presented in Figure 6.15.
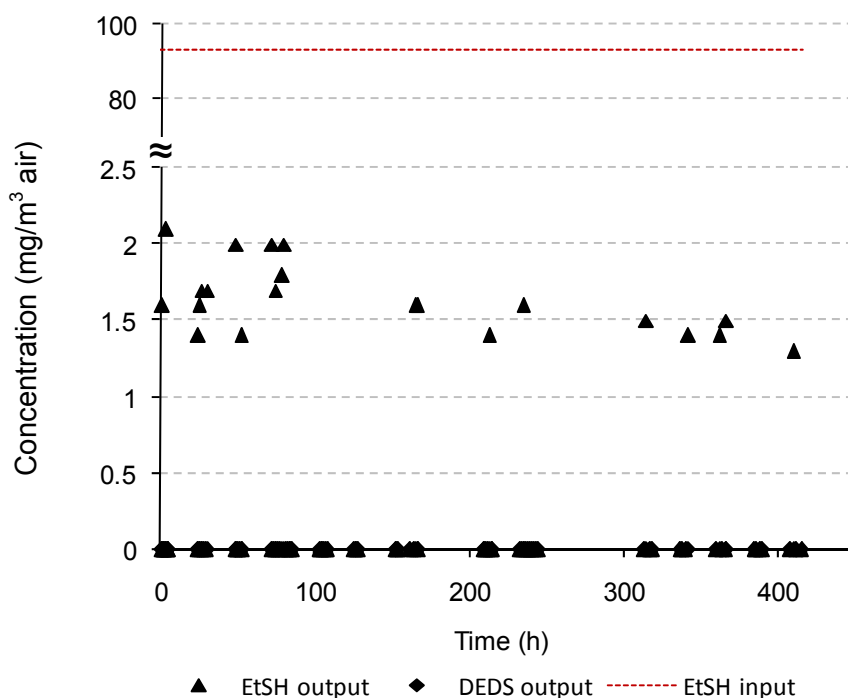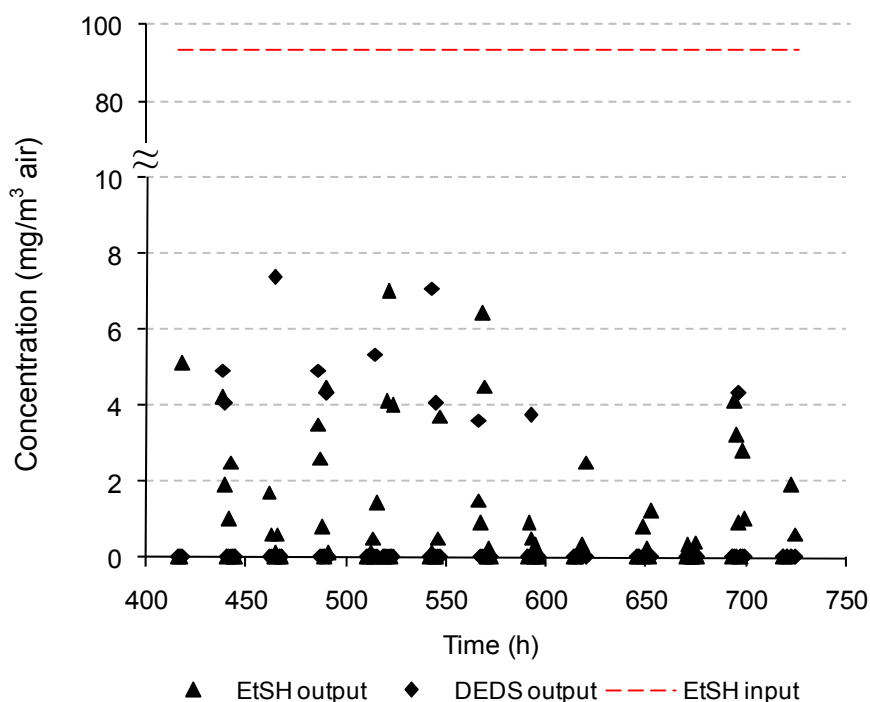
Figure 6.15. Variation of EtSH and DEDS concentration with time in the gas effluent (setup with absorption column and catalytic reactor) at ambient temperature

Figure 6.15. shows that both EtSH and DEDS are occasionally identified in the gas effluent in small concentrations (less than 10 mg/m^3 air, which is the admissible limit in air for EtSH). This can be attributed to the working cycle of the air compressor, as small fluctuations in the flow rate often occurred and these fluctuations affected the residence time of the gas in the system and thus the system's performance. As mentioned in section 6.3.3.2., the process should be further optimised to eliminate or minimize the amount of residual pollutant left untreated in the gas effluent.

The liquid effluent was analysed by GC-MS, but no reactant or reaction products were identified. As mentioned before, the limit of detection for GC-MS is 0.5 mg/L for EtSH

and DEDS, thus lower concentrations would not be detected. IC analysis of the liquid effluent was focused on the identification and quantification of $EtSO_3H$, according to the method presented in section 3.4.2. The results are presented in Figure 6.16.
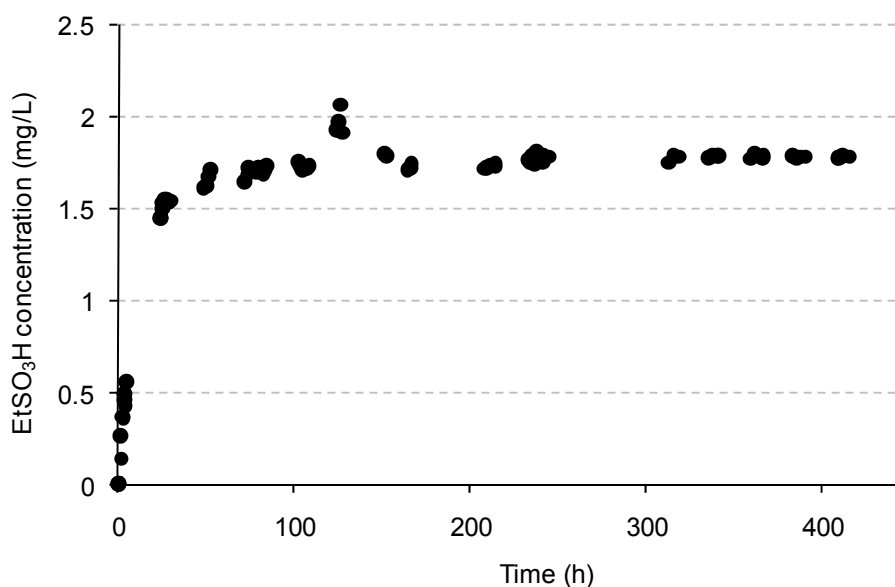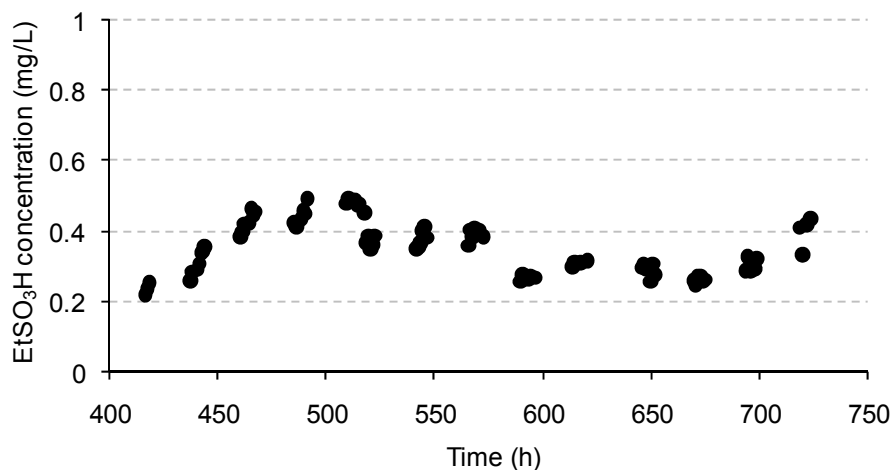

Figure 6.16. Variation of EtSO$_3$H concentration with time in the liquid effluent (setup with absorption column and catalytic reactor) at ambient temperature

Figure 6.16. shows that reducing the temperature from 45 ˚C to room temperature (the temperature oscillated between 16 ˚C and 19 ˚C during the day in winter) significantly reduce the efficiency of the decontamination process. When the experiment was performed at 45 ˚C, $EtSO_3H$ was constantly produced at a calculated concentration of 1.75 mg/L representing 86% yield considering the total amount of EtSH introduced into the system. When the temperature was reduced to an average of 18 ˚C, the concentration of $EtSO_3H$ in the liquid phase was only ~0.36 − 0.48 mg/L, representing an average yield of ~16 − 18%. Even though the GC-MS analysis did not show that EtSH and DEDS are present in the liquid phase, this possibility is not eliminated as they can be present at levels below the limit of quantification (0.5 mg/L). If the mass transfer of

EtSH from gas to liquid phase would be total, the theoretical EtSH concentration in liquid phase would be 1.16 mg/L. Other reaction products (organic acids) were not monitored in time, thus a mass balance for EtSH could not be calculated.

The consumption of H_2O_2 was monitored in time; the results are presented below:
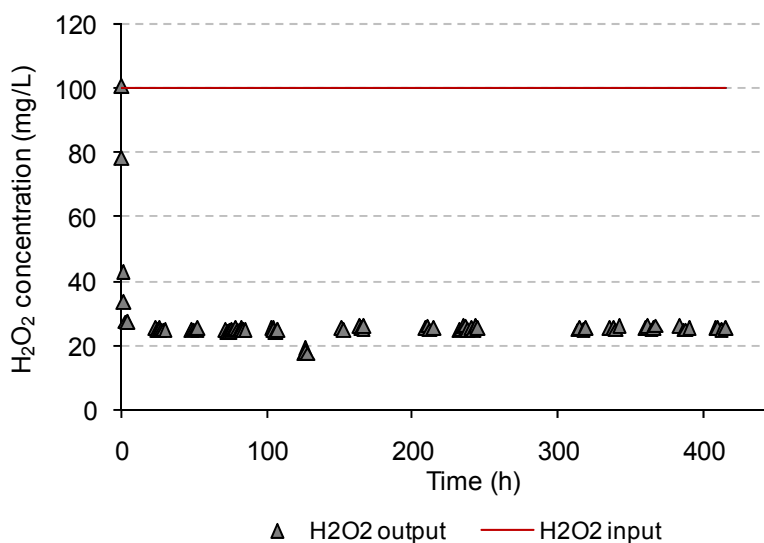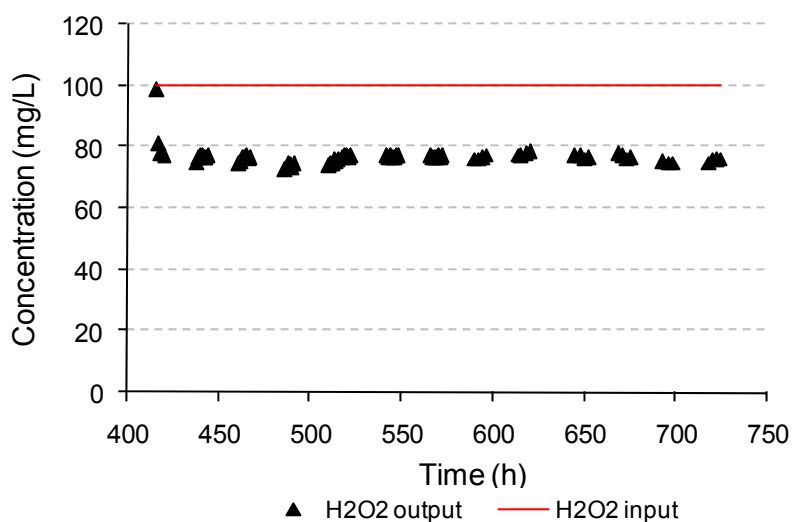

Figure 6.17. Variation in the concentration of H_2O_2 with time in the liquid effluent (setup with absorption column and catalytic reactor) at ambient temperature

Figure 6.17. shows that for steady state operation the residual H_2O_2 concentration in the liquid effluent is constant at about 74 - 77 mg/L, indicating that H_2O_2 is added in excess. Some of the H_2O_2 consumed in during the process must have been used in other oxidation reactions than production of $EtSO_3H$, as the yield in $EtSO_3H$ is ~16 – 18%, whereas the consumption of H_2O_2 is 23-26%. Figure 6.17. also shows that the initial concentration of the H_2O_2 fed into the system could be reduced to ~25 mg/L as the initial value of 100 mg/L proved to be in great excess.

Comparing the results of the experiments at 45 ˚C with those at ambient temperature, one can see that decreasing the temperature from 45 ˚C to ~18 ˚C would seem to have reduced the extent of the advanced oxidation process from 86-90% to ~25% (i.e. the amount of $EtSO_3H$ produced was less), although the efficiency in decontamination of air from EtSH remained similar (i.e. very little EtSH identified in the gas phase).

6.4. Conclusions

A three-phase catalytic reactor was designed and constructed in order to test the capability of the novel fibrous catalyst to decompose airborne organic pollutants in the presence of H_2O_2 solution. The reactor was incorporated into an experimental rig and was tested against EtSH, in both scrubber and slurry modes, using different experimental conditions. The design of the reactor was modified in order to achieve the best performance for the system.

The system that performed the best incorporated an absorption column inserted before a tubular catalytic reactor with a fixed overflow at its upper side, operated in slurry mode, with both the gas and liquid flowing downwards.

The best results were obtained at 45 ˚C, when the catalyst ([Fe] = 0.52 mmol Fe/g thread) was used as mesh pieces, tightly packed in the reactor to form a compact catalytic bed of 115 mm height (V_{cat} = 117 cm^3). The volume of liquid drained from the catalytic reactor was 120 cm^3. The catalyst bed was conditioned before the start of the

experiment. The absorption column was packed with PP threads, readily available, as PP was also used as scaffold in the knitting of the PAN mesh. The PP threads were packed tightly in the column to form a bed of 250 mm height (volume 63.6 cm^3). Liquid EtSH was continuously sent to the mixing vessel/evaporator at a rate of 0.2 µL/h (0.168 mg/h), where it mixed with the air (flow rate: 0.0018 m^3/h). The resulting EtSH concentration in air was 93.33 mg EtSH/m^3 air. H_2O_2 solution of 100 mg/L was continuously supplied into the system at a flowrate of 2.4 cm^3/min. The calculated residence times in the reactor were: 3.9 min for the gas phase and 50 min for the liquid phase and the molar ratios were Fe:H_2O_2 = 14.8:1 and H_2O_2:EtSH = 177.5:1.

The results of this study showed that the novel catalytic system was effective in the oxidation of air borne organic pollutants, namely EtSH. The system was operated in steady state for 415 hours, without deactivation of the catalyst. $EtSO_3H$ was identified in the liquid effluent, and quantified as reaction product; the constant average yield in $EtSO_3H$ was 86%. It was also determined that no DEDS or dissolved EtSH was present in the liquid effluent (at concentrations higher than 0.5 mg/L which was the detection limit for the GC-MS instrument used for analysis). The analysis of the gas effluent showed that DEDS and EtSH were occasionally present in the gas effluent (most probably to the duty cycles of the air compressor used in the experiments), at concentrations below the admissible limit in air according to the OSHA Ceiling PEL regulations. It was assumed that the rest of EtSH was oxidised to other advanced oxidation products such as acetic and formic acids, identified in previous experiments but not monitored as the IC instrument was set for $EtSO_3H$ identification and quantification.

When the efficiency of the modified PAN catalyst/H_2O_2 system was tested at ambient temperature, the system was operated in steady state for an additional 309 hours.

Comparing the results for the experiments with EtSH at 45 ˚C and at ambient temperature, it can be concluded that the rise in temperature from ambient temperature (16-19 ˚C) to 45 ˚C increased the yield in $EtSO_3H$ from ~16-18% (at ambient temperature) to ~86% (at 45 ˚C). This was in good accordance with the consumption of H_2O_2, monitored in the two experiments (~26% for ambient temperature compared to ~80% for 45 ˚C). It is also expected that the temperature would greatly influence the decontamination of any 'real life' effluent. The self decomposition of H_2O_2 was not considered in these studies, as H_2O_2 was used as diluted solution freshly prepared from commercially stabilized solution.

Chapter 7. Gas-liquid-solid catalytic decomposition of a mixture of VOCs in air

7.1. Introduction

This chapter presents the results of a dynamic mode experiment, for a simulated 'real life' incident that required emergency response. The experiment was performed at ambient temperature, with a simulated 'real' contaminated air flow, the novel catalyst (as knitted mesh) and H_2O_2 solution as oxidant. The 'real' contaminated air was simulated by mixing two volatile liquids: EtSH and DMS (50:50 v/v) with air.

The purpose of this study was to determine whether the catalyst/H_2O_2 system was able to efficiently oxidize a continuous flow of air contaminated with more than one organic pollutant (i.e. mixture of EtSH and DMS), at ambient temperature. The experiment was performed in the experimental rig with absorption column and catalytic reactor with overflow at the side (see Figures 6.11. and 6.12.), following the procedure described in section 6.3.3.3., the only difference being that the pollutant was a mixture of EtSH and DMS (50:50 v/v) instead of pure EtSH.

In the presence of the fibrous catalyst/H_2O_2 system, the oxidation of mercaptans (i.e. EtSH) and DMS take place according to the chemical reactions:

$$R\text{-}SH \xrightarrow{[O]} R\text{-}SOH \xrightarrow{[O]} R\text{-}S(O)\text{-}OH \xrightarrow{[O]} R\text{-}S(O)_2\text{-}OH$$

Mercaptan   Sulphenic acid   Sulphinic acid   Sulphonic acid

$$CH_3\text{-}S\text{-}CH_3 \xrightarrow{[O]} CH_3\text{-}SO\text{-}CH_3 \xrightarrow{[O]} CH_3\text{-}SO_2\text{-}CH_3 \xrightarrow{[O]} CH_3\text{-}SO_3H$$

DMS   Dimethyl sulphoxide   Dimethyl sulphone   Methane sulphonic acid
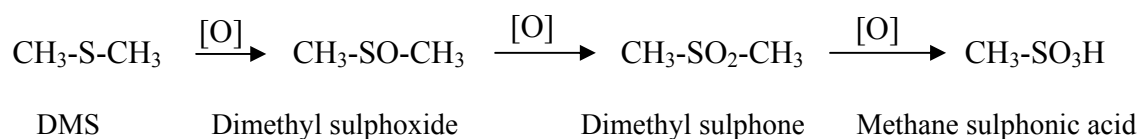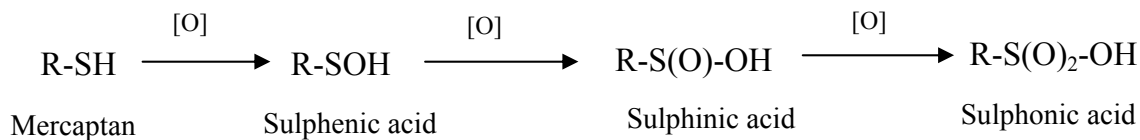
DMS was used to simulate the real effluent because of the compound's physical properties, very similar to those of EtSH, compound intensively used in this research. The physical properties of the two compounds are presented in Section 3.2.2. DMS was also studied in static experiments, the results showing a slight reduction in the concentration of DMS in gas phase, without the addition of H_2O_2 as additional oxidant.

The experiment consisted of sending the simulated contaminated air flow through the experimental rig presented in section 6.3.3. operated at ambient temperature, and analysing the gas effluent (GC analysis), and the liquid effluent (GC-MS and IC analysis), according to the methods presented in Section 3.3 and 3.4. The experiment was conducted in the same conditions as for the study presented in section 6.3.3.3 with regard to the absorption column filling material.

DMS and EtSH were first mixed in 50-50% ratio (v/v) and the mixture was then sent through the experimental rig using the syringe pump at a flow rate of 0.4 µL/h. Air was

sent to the evaporator at a constant flow rate of 30 cm^3/min (0.018 m^3/h). These flow rates ensured a residence time of T_{gas}= 3.9 min (65×10^{-3} h) for the gas phase and a theoretical concentration of the pollutants in air of 93.3 mg EtSH/m^3 air and 100 mg DMS/m^3 air. H_2O_2 solution of 100 mg/L was fed continuously into the system at the top of the absorption column, at a flow rate of 2.4 cm^3/min; this ensured a residence time of 50 minutes (0.833 h) for the liquid phase in the catalytic reactor The molar ratios calculated were: Fe:H_2O_2 = 14.8:1, H_2O_2:EtSH = 177.5:1 and H_2O_2:DMS = 165.7:1. The catalyst used in this experiment was the same catalyst used in the experiments with EtSH at 45 ˚C and with EtSH at ambient temperature (V_{cat} = 117 cm^3). The reason for using the same catalyst was that the catalyst did not show signs of deactivation at the end of those experiments, and also to collect data on the life-time of the novel catalyst. The consumption of H_2O_2 was monitored during the oxidation process using the same method presented in Section 3.4. The experiment lasted for 780 hours, when it was stopped because the catalyst showed signs of deactivation (in the last 240 hours, the consumption of H_2O_2 dropped from ~35% to a level of ~9% of the input concentration).

7.2. Results and discussion

The gas effluent, exiting at the top of the reactor, was analysed periodically (GC analysis) to check for breakthrough of reactants (EtSH and DMS) and for identification of gas phase reaction products. The variation in the concentration of EtSH and DMS with time during this experiment is presented in Figure 7.1.
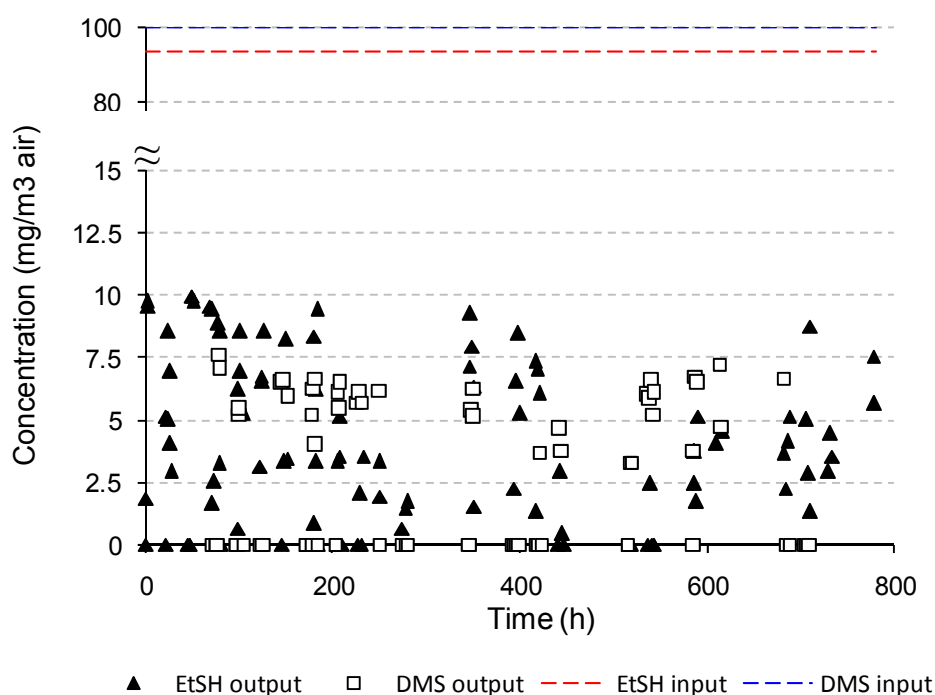
Figure 7.1. Variation of EtSH and DMS concentrations (gas effluent) with time, in the experiment with simulated contaminated air, at ambient temperature

Figure 7.1. shows that both EtSH and DMS are occasionally identified in the gas effluent in concentrations below the admissible limits in air (10 mg/m^3 air for EtSH and 20 mg/m^3 air for DMS) according to OSHA (OSHA, 2008). This could be attributed to the working cycle of the air compressor, as small fluctuations in the flow rate of air occurred during the experiment and these fluctuations affected the residence time of the gas in the system. Also, it was possible that the mass transfer of EtSH and DMS from gas to liquid phase was not total and thus the compounds had a relatively short residence time in the catalytic reactor (3.9 minutes instead of 48.75 minutes). This inconvenience could be overcame by optimising the operating parameters of the absorption column to achieve total mass transfer, and then the amount of catalyst in the reactor to achieve total decomposition of the pollutants in the liquid phase. Overall, the

system was operated in steady state, with a satisfactory level of removal of the contaminants from air.

The liquid effluent was analyzed by GC-MS for reaction products, but no reaction products were identified. EtSH and DMS were identified in the liquid phase, but at levels below the limit of quantification (0.5 mg/L); the peaks were visible but the ratio signal/noise was lower than 2 indicating that the compounds were present in the sample but they could not be quantified. The IC analysis of the liquid effluent was focused on the identification and quantification of $EtSO_3H$ and $MeSO_3H$, according to the method presented in Section 3.4.2. $EtSO_3H$ and $MeSO_3H$ have very similar structures and dissociation constants; their retention times on the IC column (Metrohm 'anion' column AS4A-SC) are very similar (3.48 min for $EtSO_3H$ and 3.52 min for $MeSO_3H$). For this reason, the two peaks could not be separated with the IC system used, the two compounds eluted together as one peak with a retention time of 3.49 minutes. As the proportion of each compound was not known, the peak area was plotted as a function of time and is presented in figure 7.2. For comparison, the variation of peak area of $EtSO_3H$ plotted also as a function of time for the catalysis of EtSH alone at ambient temperature is presented in the same figure. The time scale was adjusted to reflect both experiments (the experiment with simulated 'real' contaminated air was performed after the experiment with EtSH alone).
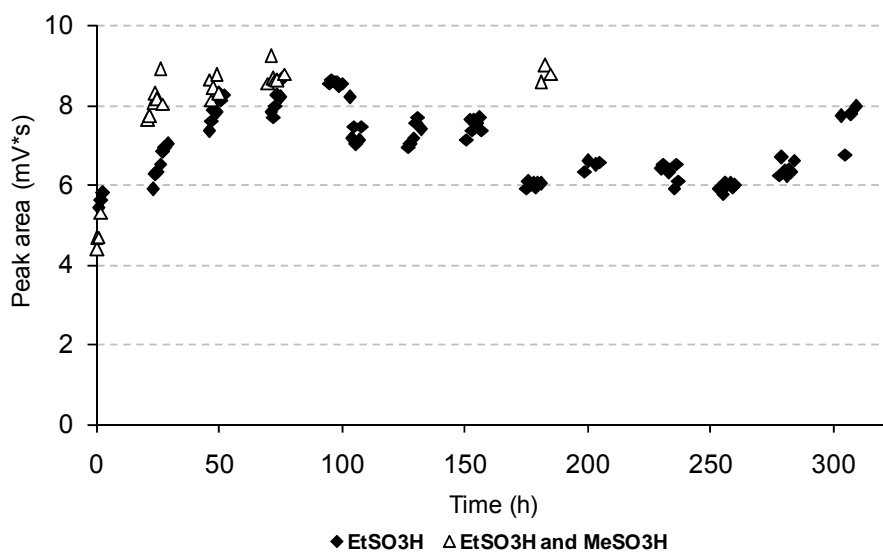
Figure 7.2. Variation of peak area with time for the mixture 'EtSO₃H & MeSO₃H' compared to the previous peak area of EtSO₃H, in the setup with absorption column and catalytic reactor at ambient temperature

Figure 7.2. shows that the peak area for the mixture of $EtSO_3H$ and $MeSO_3H$ originating from the oxidation of the simulated 'real' contaminated air, was slightly higher than that of $EtSO_3H$ originating from the catalysis of EtSH alone at ambient temperature. This indicates that the novel catalytic system was effective in the decomposition of the mixture of EtSH and DMS in air. The difference in the peak areas is small, indicating that perhaps DMS was oxidised to $MeSO_3H$ only to a small extent, probably other less advanced oxidation products (dimethyl sulphoxide and dimethyl sulphone) were produced in higher amounts, but these compounds were not identified/monitored during the experiment.

Further work should concentrate on identification and quantification of these reaction products to have a better understanding of the complex oxidation process that takes

place. Further work should also concentrate on separation of $MeSO_3H$ and $EtSO_3H$ using different matrixes IC column/eluent in order to quantify both sulphonic acids and thus be able to evaluate the efficiency of the catalytic system in the decomposition of EtSH when other competing substrate is present.

The consumption of H_2O_2 was monitored during the oxidation process using the method presented in Section 3.4.3.; the results are presented in Figure 7.3.
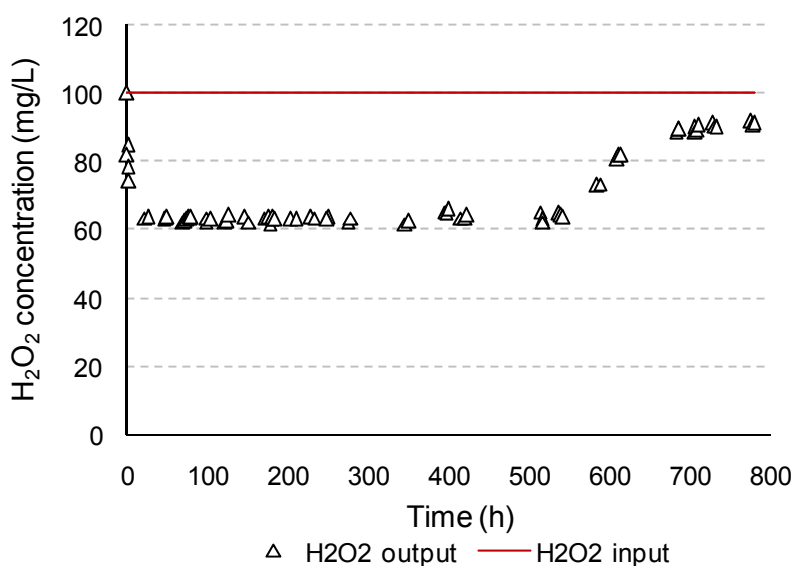
Figure 7.3. Variation of H_2O_2 concentration with time (liquid effluent) during the experiment with simulated contaminated air, at ambient temperature

Figure 7.3. shows that for steady state operation, the residual H_2O_2 concentration in the liquid effluent is constant at about 63-64 mg/L, indicating that H_2O_2 was added in excess. Comparing the H_2O_2 consumption in the catalysis of EtSH alone and 'real' contaminated air at ambient temperature it can be noticed that for the mixture of EtSH and DMS the residual H_2O_2 concentration is about 10 - 12 mg/L less than for EtSH

alone, as seen Figure 6.18 (~36 mg/L compared to ~24 mg/L). This indicates that H_2O_2 was used in oxidising EtSH and also takes part in other oxidation reactions (oxidation of DMS to different oxidation products). The results also indicate that the initial concentration of H_2O_2 could be reduced to about 40 mg/L.

In addition, Figure 7.3. shows that in the last 240 hours (time 542 h -780 h) the residual concentration of H_2O_2 increased from $\sim$ 64 mg/L to $\sim$ 91 mg/L, indicating that the efficiency of the catalyst was reduced and the process should be stopped for catalyst regeneration. The regeneration process consists of washing the catalyst for 2 hours (flow wash) with a dilute HCl solution (1×10^{-3} M), pH 3, containing 5 g/L H_2O_2 (Huddersman, 2011).

7.3. Conclusions

The modified PAN/H_2O_2 solution system was effective in the advanced oxidation of a mixture of EtSH (93.3 mg EtSH/m^3 air) and DMS (100 mg DMS/m^3 air) in air, as tested in the experiment presented above. The results show that both EtSH and DMS were occasionally identified in the gas effluent, at concentrations below the admissible limits in air set by OSHA; in this respect the efficiency of the decontamination process was satisfactory.

Further work should concentrate on the optimisation of the mass transfer in the absorption column (optimisation of flows of gas and liquid, type and size of filling

material for the absorption column, height of column, etc) in order to achieve maximal mass transfer of pollutants from gas to liquid phase, as the oxidation reaction is expected to take place in the liquid phase.

As presented above, the increase in the operating temperature for the experimental rig greatly increased the efficiency of the catalytic system for the oxidation of EtSH alone in air. It is expected that the same influence would be noticed for the oxidation of mixtures of EtSH and DMS.

Chapter 8. Portable decontamination unit for emergency responses, based on the modified PAN/H$_2$O$_2$ catalytic system

8.1. Introduction

This chapter presents some aspects regarding the emergency response procedure in the case of a chemical, biological, radiological or nuclear (CBRN) incident, and a cost estimation for the decontamination of air contaminated with EtSH (93.3 mg EtSH/m^3 air) using a portable unit based on the modified PAN/H$_2$O$_2$ catalytic system, designed as a scaled-up version of the laboratory scale unit used in this research.

The estimated costs for the decontamination of air take into account capital costs, production of the catalyst, other meaterials, heating costs, electricity and regeneration of the catalys. These costs are summarized for portable units incorporating the catalytic reactor housed in modified 20 ft long ISO container. The operating parameters used in the laboratory tests were scaled up and adjusted to the volume of the reactor. The capital costs involved were estimated using quotes from specialized chemical integrators.

8.2. Documentation on emergency response guide

8.2.1. Strategy

In emergency services terminology, any incident involving unidentified substances is considered a CBRN incident, requiring special procedures to protect the public and the personnel involved in the emergency response. These procedures usually involve the use of personal protective equipment such as containment suits, gas masks/respirators and decontamination tents (CBRN incident, 2010).

It is very difficult to make general statements about CBRN substances because of the wide range and variety of effects, toxicity and concentrations that could be deployed. In general terms, the principal challenges of CBRN decontamination of the environment are that: (i) chemicals are easy to find and isolate but difficult to destroy and can generate toxic by-products; (ii) biological substances are easy to destroy but difficult to find and isolate and it is hard to be certain they are fully removed, and (iii) radiation is easy to find and isolate but impossible to destroy, it can only be removed and containerised.

Plans to deal with CBRN incidents include procedures covering the following: identifying the source of the threat, giving advice to victims caught in the area and to others worried about contamination, arranging urgent medical attention for casualties, decontaminating victims and the area itself. A cross-government initiative, called the

CBRN Resilience Programme, aims to ensure a fast and effective response in the event of a terrorist or accidental CBRN incident, trying to minimize the impact and the negative effects on life, properties and environment. The Resilience Programme is also responsible for providing the emergency services with the most appropriate equipment and training necessary for an effective response to a CBRN incident (Home Office, 2008).

Emergency services are facing an increased variety of demanding situations, including major incidents caused by natural disasters, industrial accidents and the threat of terror attacks. As all these incidents could have an impact on our daily lives, the emergency services need to have a high level of preparedness and improved ability to operate effectively. The Resilience Programme provides CBRN response training to emergency service personnel, government staff and other public service staff, through several expert organisations including police, hospitals, universities, colleges, etc.

There are different strategies set by the Home Office that have to be followed in the case of a CBRN incident, depending on the place affected by the incident: closed buildings and infrastructures (Strategic National Guidance, 2008), or the open environment (DEFRA, 2008).

8.2.2. Recovery from a CBRN incident

Recovery from a CBRN incident involves a partnership between the public local authority and private sector organisations. Commercial contractors are likely to undertake decontamination and clean-up operations on behalf of the local authority. The generated wastes are also likely to be managed by commercial organisations.

The factors influencing the recovery strategy are (Communities, 2011):

1. Detection and intervention timelines. Chemical, biological or radiological substances could be dispersed in a number of ways, not necessarily by the use of static containers or explosive devices. The immediate effects caused by the release of a chemical substance are likely to be noticeable more quickly than those of a biological or radiological substance. Biological substances may require an incubation period of several days before people become sick, and therefore the area affected may be greater than initially thought due to the migration of affected individuals. At the same time, exposure to radiological substances may not produce any immediately noticeable health effects, resulting in contamination spread even before its detection.

2. Size of the affected area. The area of land contaminated to a significant degree by a chemical substance will usually stretch only a few hundred metres from the original release point. However, the hazard zone will be larger than the contamination area because of evaporation or re-suspension of the substance into the air. This is especially important for chemical releases of VOCs, which produce a vapour hazard downwind of the contaminated area.

3. Stability and persistence of the substance. The recovery strategy depends on the persistence of the substance in the environment. Although chemical and biological substances vary considerably in their properties and in their effects on humans, substances are not always persistent for long periods of time and may safely break down over a few days when exposed to rain or sunlight or can be destroyed by using simple treatment processes such as spraying with dilute oxidizing solutions. However, most radiological substances and some chemical or biological substances are highly persistent. Additionally, CBRN substances may be absorbed into materials such as rubber and paint, making the decontamination even harder considering that once absorbed they could be released slowly into the atmosphere, resulting in a persistent contact or vapour hazard to people.

4. Nature of the location. Decontamination techniques for urban clean up in towns and cities will be different to those used for rural clean up in the countryside. Also, the cleanup of substances released in the open environment will be different to the clean up procedures used inside a structure. Natural weathering and wet decontamination techniques will be most effective for chemical and biological incidents which take place outdoors either in urban or rural environments.

5. Effectiveness of recovery options. Recovery decisions should take account the expected benefits of different decontamination options and also their contribution to an early return to normal living within the affected population. Potential recovery options may be broadly divided into three categories: **(i)** moderately effective and incur relatively little disruption or require few resources; they can be completed soon after the

incident; (ii) strongly effective - incur significant disruption or require significant resources; usually they can only be carried out over extended periods of times; (iii) either poorly effective or only moderately effective and incur significant disruption or require significant resources . The CBRN recovery strategy should focus initially on the first two options.

6. Health and safety management. Risks to the health and safety of people need to be managed as an integral part of the recovery strategy. This will include local authority staff, clean-up contractors, sewerage company workers, the police and fire services, external advisors, possibly voluntary organisation workers and members of the civic community, who may potentially be exposed to residual levels of CBRN substances during different phases of the clean-up operation.

The role of clean-up contractors is to safely implement the recovery strategy under the direction of the local authority and to provide and operate the decontamination technology. They are required to train and equip their workforce with suitable personal protective equipment and to collaborate with the Environment Agency and with the local sewerage company in order to collect the water used in decontamination and to direct it to containment areas for appropriate treatment. The clean-up contractors also need to manage the solid hazardous waste in an environmentally acceptable and responsible way, minimising the risks to the health and safety of workers, the public and the environment.

7. Persistence of CBRN Substances. The persistence of a CBRN substance is its ability to remain hazardous in the environment over time. The choice of recovery strategy is strongly influenced by the persistence of the substance being cleared up (e.g. substances with low persistence such as sarin or hydrogen cyanide disappear within hours, but a persistent chemical substance might last several months or even a few years under the right conditions). For chemical and biological substances the actual rate of natural deterioration will partly depend on the local weather conditions (e.g. chemical substances evaporate faster on hot days than cold days and biological substances break down faster in direct sunlight than in the shade). For radiological substances, the breakdown may take decades and the rate of decay is not affected by external factors such as the weather.

Irrespective of the precise circumstances of the incident, successful recovery partly depends upon the ready availability of the following local resources that may already be in place to deal with, for example, major chemical incidents:

• *Decontamination solutions.* Chlorine-based bleaching or sterilising solutions are highly effective at removing both chemical and biological contamination. The most widely available sterilising solutions are calcium hypochlorite, sodium hypochlorite and sodium dichloroisocyanurate (FiClor), which are all commonly used to sterilise bacteria in swimming pools. A decontamination solution of 0.5% hypochlorite in water would be effective against many substances.

• *Water supply.* An available water supply is needed both to prepare decontamination solutions and to rinse decontaminated surfaces. In rural or coastal environments

freshwater from watercourses or saltwater from the sea provide a readily available water supply. In urban environments water is usually supplied via fire hydrants, which should be properly maintained and periodically tested, especially near buildings that may be a target for terrorists. Fire hydrants are owned by water companies and tested by the Fire Service.

- *Drainage management equipment.* Run-off water and rinse water from decontamination may contain high concentrations of chlorine if bleach has been used. The wastewater may need to be intercepted and treated to neutralise its chlorine content that is hazardous to the environment. In urban areas the road drainage system is particularly vulnerable. Storm water drains may need to be blocked or their effluents diverted to holding tanks before decontamination is carried out, in accordance with the Water UK Protocol for Disposal of Contaminated Water.

- *ISO containers.* Decontamination methods for dealing with persistent CBRN substances tend to generate large amounts of solid waste. These will normally require temporary storage in ISO containers, especially in the case of radioactive wastes.

8.3. Decontamination after a major chemical incident using the modified PAN catalyst/H₂O₂ system

As presented in the previous chapters, the novel modified PAN/H₂O₂ catalytic system tested in this work proved efficient in the catalytic decomposition of VOCs from air (e.g. sulphur compounds such as EtSH and DMS). The best results were obtained when

the contaminated gas passed through an absorption column before entering the catalytic reactor. The same catalytic system has proved efficient in the decomposition of a large variety of organic compounds in water, such as phenol and azo-dyes (Ishtchenko, 2002, Ishtchenko *et al*, 2003a), 4-nonylphenol (Chi and Huddersman, 2007), real textile effluent from a dyeing factory (Ishtchenko *et al*, 2003a) and effluent from the photographic industry (Yang *et al*, 2006).

In case of a CBRN incident, the technology developed in this work could be used in the recovery phase, namely clean-up phase, towards the efficient decontamination of air (and water) affected by the incident. As mentioned above, commercial contractors are likely to undertake decontamination and clean-up operations on behalf of the local authorities. The modified PAN catalyst/H$_2$O$_2$ treatment system could be used as a stand-alone technology or it could be integrated with other treatment technologies (e.g. biological treatment) in order to achieve effective and timely decontamination.

Figure 8.1. presents the main steps to be followed in the decontamination process of contaminated air in the case of a CBRN incident (specifically a chemical incident affecting the air quality). The decisions involved in this flow chart have to be taken by trained personnel(s). The same applies to the operation of the decontamination units and analysis of gas and water samples.
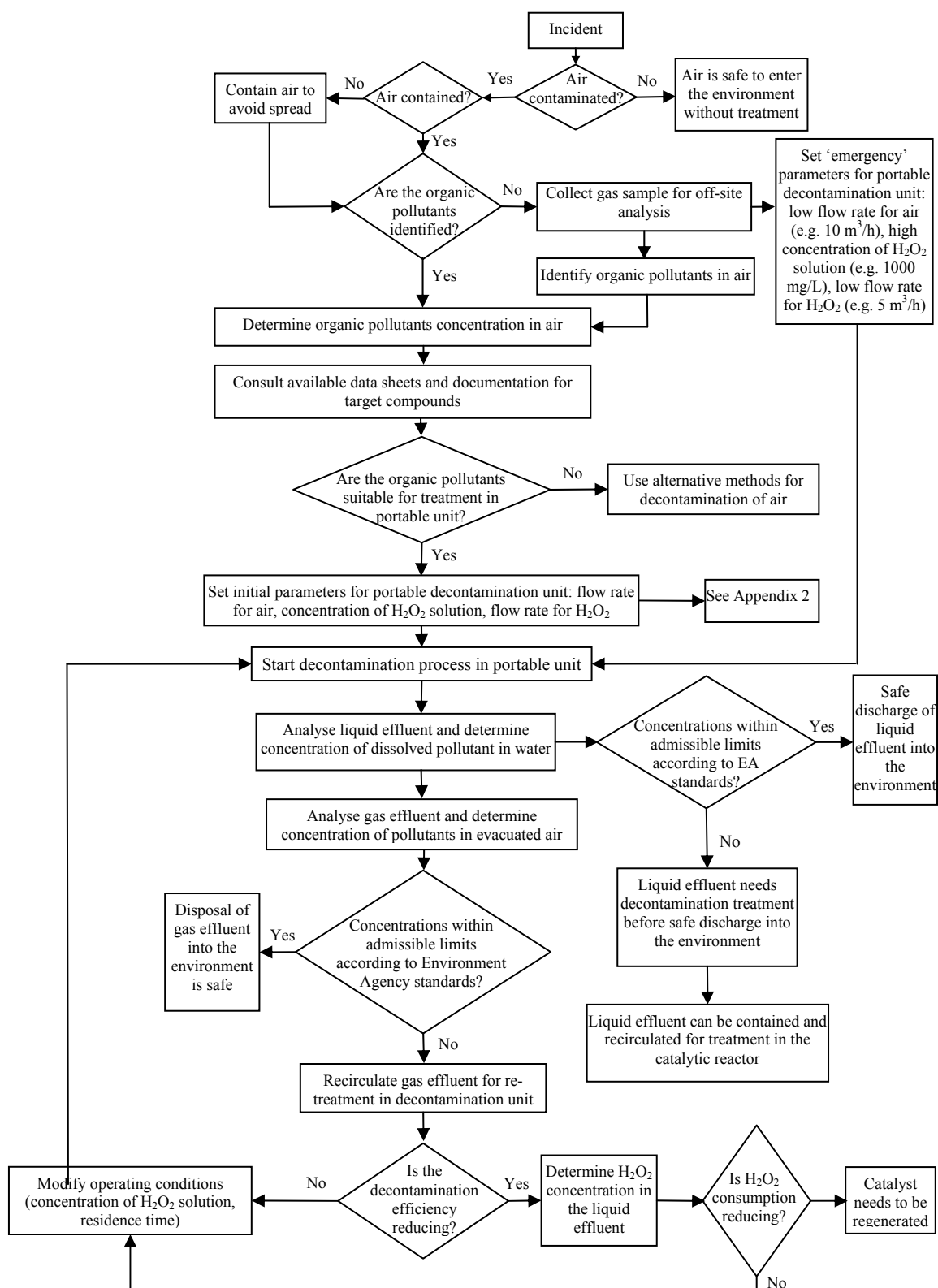
Figure 8.1. Emergency response steps in a CBRN incident with air contamination. Treatment is performed in a 33 m³ catalytic reactor housed in a 20 ft long ISO container.

8. 4. Economics of commercial scale-up

This section gives costing information on a process of decontamination of air using the novel modified PAN/H_2O_2 catalytic system. The total estimated cost includes capital cost, production of the catalytic mesh, other materials, costs related to the heating of gas and liquid phases, electricity used and regeneration of the catalyst. Other costs (e.g. with personnel, transport, chemical analyses, instruments, etc) were not taken into account.

According to the manufacturer (Huddersman, 2010), the fibrous modified PAN catalyst (mesh with 50% catalytic threads, 50% PP support, [Fe] = 0.52 mmol Fe/g threads) can be produced at an estimated cost of £ 35/kg catalyst, including materials, electricity, costs with labour, etc. The PP threads used as filing material for the absorption column is a mixture of equal lengths of PP mono-threads of 0.3 mm diameter and 0.15 mm diameter (priced per tonne at £5.28/kg (0.3 mm) and £3.94/kg (0.15 mm)); the same combination was used in the knitting of the PAN mesh in the catalyst production.

For the scale-up of the laboratory setup, the following assumptions are made: the large scale unit (incorporating an absorption column and a plug flow catalytic reactor with overflow at the side) is designed as a portable decontamination unit, to be used in the clean-up phase of an emergency response after a CBRN incident involving chemicals (i.e. EtSH) and affecting the quality of the air. Keeping the pollutant concentration 93.3 mg EtSH/m^3 air as used in the laboratory scale experiments (see section 6.3.3.2. and 6.3.3.3.), and assuming the same residence times for the gas and liquid phases (3.9

minutes for gas and 50 minutes for liquid), the treatment of contaminated air is scaled up to the dimensions suitable for the catalytic reactor instalment within a 20 ft long ISO container (total internal volume of 33 m^3). The catalyst is packed in the reactor as rectangular pieces, as a compact bed that provides the same density of the catalytic bed as in the laboratory scale reactor ($d_{catalyst\ bed}$ = m_{cat}/V_{cat} = 20.1 g/117 cm^3 = 0.172 g/cm^3 = 172 kg catalyst/m^3 bed). The ratio catalyst volume: liquid volume in the reactor is assumed to be the same as in the laboratory scale reactor (V_{liquid}/V_{cat} = 120 cm^3/117 cm^3 = 1.025). For the absorption column, the same PP threads filling material and the same density of the filling bed as in the laboratory scale unit is assumed ($d_{PP\ bed}$= m_{PP}/V_{PP} = 7.5 g/63.6 cm^3 = 0.118 g/cm^3 = 118 kg PP/m^3 bed). It is also considered that the level of the liquid in the catalytic reactor is set by the position of the overflow, which ensures a volume of 30 m^3 liquid in the reactor and a headspace volume of 3 m^3 above the liquid. In order to fulfil these conditions, the volume of the catalytic bed will be V_{cat} = 30/1.025 = 29.25 m^3 (5031 kg catalytic mesh). The gas and liquid flows are adjusted accordingly to 7.5 m^3/min (450 m^3/h) for the gas phase and 600 L/min (36 m^3/h) for the liquid phase. It is also considered that the operating temperature for the decontamination unit is 45 °C, and that only the liquid phase is heated to this value (from ambient temperature, considered 15 °C).

The capital cost of the equipment was estimated using quotes from suppliers of pumps (for H₂O₂ solution and air) and 'Forbes Group', a well-established UK company specialized in the design and manufacture of custom made or standard tanks, vessels, scrubbers, degassers and other chemical plant units for different industries such as

chemicals, water and wastewater treatment, environmental, oil and gas, dairy and food, pharmaceuticals, etc. They offer a choice of materials for the construction of their products, including thermoplastics, glass fibre reinforced materials or metal. The company advised (Forbes Group, 2010) that due to pressures built in big reactors and safety problems, the design of the reactor should be as a series of smaller vertical reactors rather than a single horizontal unit. Their option was to have 4 vertical units of 2.4 m diameter and 2 m height (volume of 9 m^3) connected in series, with pumps sending the liquid from one unit to the next one. This was considered a good option as each unit could be operated individually, offering the possibility of operating as many units as necessary depending on the circumstances. The individual units could be easily fitted in an ISO container. For this option the capital cost increases, as the effluent needs to be passed from one unit to the next one using pumps.

The only electricity cost considered was the electricity used to operate the pumps.

The regeneration process is only required when the catalyst shows signs of deactivation (e.g. concentration of target compounds treated exceeds admissible limit in air or water), when the treatment process is stopped. The regeneration of the catalyst can be conducted in the same reactor used for decontamination, following the procedure: flow washing for 2 hours with dilute HCl solution (1×10^{-3} M), pH 3, containing 5 g/L H_2O_2.

The summary of the estimated costs for air treatment using a 33 m^3 catalytic reactor are presented in table 8.1., with the detailed mathematical calculations presented in Appendix 3.

Table 8.1. Summary of estimated costs for decontamination of air in a 33 m³ catalytic reactor

Type of cost	Item	Quantity	Unit price (£/unit)	Subtotal (£)
Capital cost	Catalytic reactor*			
	- number of tanks	4	~£ 4,000	£ 16,000
	Absorption column	1	~£ 12,000	£ 12,000
	Water pump	4	£ 679	£ 2,716
	Air pump	1	£ 972	£ 972
	Subtotal			*~£ 31,688*
Materials	Catalyst	5031 kg	£ 35/kg	£ 176,085
	Absorption column filling			
	PP threads mixture[a]	1876.2 kg		
	- 40% (d=0.15 mm)	750.48 kg	£5.28/kg (1 t)	£ 3,962.5
	- 60% (d=0.3 mm))	1125.72 kg	£3.94/kg (1 t)	£ 4,435.4
	Subtotal			**£ 184,482.9**
Running costs	**Solution H₂O₂ 100 mg/L**			
	- H₂O₂(35%)	222.24 L/day	£ 268/1000L	£ 59.5/day
	- water	~863.77 m³/day	free from river	0
	Subtotal:	**864 m³**		**£ 59.5/day[b]**
	Heating[c]: (H₂O₂ solution)	**1319.5 kWh/day**	**£ 0.06983/kWh**	**£ 2,211.1/day**
	Electricity (for pumps)			
	- air pump	52.8 kWh/day	£ 0.1019/kWh	£ 5.4/day
	- water pumps (4 pumps)	105.6 kWh/day	£ 0.1019/kWh	£ 10.7/day
	Subtotal:	**158.4 kWh/day**	**£ 0.1019/kWh**	**£ 16.1/day**
	Total running cost:			**£ 2,280.7/day[d]**
[e]Catalyst regeneration	H₂O₂(35%)	1312.8 L	£ 268/1000L	£ 351.8
	HCl (36%)	~ 8.8 L	£ 0.403/L (1 t)	£ 3.6
	Subtotal			**£ 355.4**

[*, a-e] See notes below

*The cost of the catalytic reactor was estimated as the cost of 4 individual vertical units, as advised by the 'Forbes Group' consultant. The number of water pumps was thus adjusted to 4.

a) The cost of the absorption column packing material could be reduced to £ 7,392.2 by using only PP thread of 0.3 mm diameter instead of mixture of two diameter sizes. Different filling materials should also be tested in order to improve the mass transfer and to reduce costs.

b) Considering that only 75-80% of the initial H_2O_2 was consumed during the decontamination process, this cost could be reduced by 20%, to £ 46.7/day.

c) Heating with gas is 45.9% cheaper than heating with electricity (British Gas, 2010(a,b)), therefore the total running cost includes this option. The cost included in the table takes into account a 95% efficiency of the heating system.

d) The running costs could be significantly reduced to £ 75.6/day if the heating were eliminated and the reactor were operated at longer residence times for liquid.

e) The regeneration procedure was not fully determined, but is likely to be according to the procedure described above and in Appendix 3.

In table 8.1. the cost of the catalyst is high as the catalyst was densely packed and consequently a large amount was used in the reactor. The amount of catalyst needs to be optimised to lower the costs.

The regeneration of the catalyst is only needed when the catalyst shows signs of deactivation (i.e. H_2O_2 consumption drops to 80% of the steady state operation value). The regeneration method proposed is quick and easy and can be used on-site, in the same reactor/reactor series as the decontamination process. As the procedure is not fully optimised and could possibly be achieved at lower cost.

The capital cost could be reduced by having the catalytic reactor as one unit, not as 4 individual units. The price of the reactor might not change, but the number of water pumps will be reduced to one, therefore the capital cost could be reduced by £ 2,037. The costs with electricity (for the operation of pumps) would also be reduced.

Considering that the proposed decontamination unit is used continuously, the total amount of air treated would be: 450 m³/h × 24 h/day = 10,800 m³ air/day (the volume of approximately 25 average size 3 bedroom detached houses in UK, with dimension of width × depth × height = 8 m × 9 m × 6 m), or 3,942 × 10³ m³ air/year. Not taking into account the capital cost and the costs with materials, and further considering that in a year the maximum number of regenerations needed is 5 (using the data collected in the laboratory testing), the cost of treating 1 m³ air contaminated with EtSH (93 mg/m³ air) would be £0.21/m³ air, calculated as following: ((£2280.7/day × 365day/year) + 5 × £355.4/regeneration)/(3942×10³ m³ air treated/year) = £8342325/year/3942000 m³ air treated/year = £0.21/m³ air treated.

8.5. Conclusions

The role of the proposed technology in the recovery phase after a CBRN incident with chemicals affecting the quality of air, was identified as being in the clean-up phase, along with other contractors. A logical, step-by-step sequence of activities to be followed when using a portable decontamination unit based on this technology was also proposed as a flow chart.

Assuming that the experimental setup with absorption column and catalytic reactor tested in section 6.3.3.2. and 6.3.3.3., including the experimental conditions, are scaled-up to a decontamination unit fitted in a modified 20 ft long ISO container, a simplified cost estimation for the scale-up was presented. This calculation only took into account costs with part of the capital equipment, catalyst, filling material for the absorption column, running costs that were limited to some materials (H_2O_2 solution, heating of the liquid phase to the operating temperature and electricity used to operate the pumps) and cost of chemicals needed for one catalyst regeneration process. A more comprehensive scale-up costing should also take into account other factors, such as: costs with personnel, instruments needed for gas and liquid sample analysis, reagents, overall energy requirements. The treatment costs were not compared to other suitable and competitive technologies (biofiltration, activated and impregnated activated carbon, scrubbers with chemical reaction, etc), as the comparison would not be realistic.

The costs presented in Table 8.1. could be reduced after further optimisation with regard to amount of catalyst used, operating parameters for the absorption column including type and amount of packing material, residence times for gas and liquid in the catalytic reactor, flow rates processed per unit time, etc. Some recommendations were already proposed (see notes [a] to [e] below Table 8.1.) in order to reduce the costs presented in this section.

Chapter 9. Conclusions and recommendations

9.1. Conclusions

The aim of this research was to test the capability of a novel modified PAN catalyst, in the physical form of knitted mesh or yarn, to decompose a range of air borne toxic VOCs, under mild conditions: ambient pressure and moderate temperature (up to 45 °C). The study also extended to gas-liquid-solid heterogeneous catalytic reactions, where aqueous H_2O_2 was added into the system. The possibility of incorporating the catalytic system into gas-liquid-solid flow reactors which can be fitted into modified ISO Containers to provide mobile decontamination units in the case of a CBRN incident with chemicals that affect the quality of air was also considered.

The novel modified PAN/H_2O_2 catalytic system proved to be effective in the decontamination of air from sulphur VOCs such as mercaptans and sulphides, at moderate (45 °C) and ambient temperature (16 – 18 °C). The best results were obtained when the gas phase passed through an absorption column before entering the catalytic reactor.

The catalyst was also able to oxidize sulphur VOCs (e.g. mercaptans) in the gaseous phase without addition of H_2O_2, but the system did not ensure an advanced oxidation process, towards complete mineralization.

The research was divided into two distinct areas, namely gas phase catalysis, in both static and dynamic modes, and gas absorption into H_2O_2 solution followed by liquid phase catalysis in dynamic mode.

Static, batch experiments showed that the novel fibrous modified PAN catalyst was active in the removal of some VOCs from contaminated air samples, without addition of H_2O_2 into the system. Decrease in the initial concentration of all studied compounds (DMS, MeCN, EtSH and CP) was observed when the catalyst was used either as threads or as mesh. The decrease in concentration was more significant when the catalyst was used as threads, as the threads were more dispersed within the vials than the mesh and thus insured a better contact between catalyst and pollutant.

Dynamic experiments in dry conditions (without addition of H_2O_2) showed that the catalyst was active (regardless of its physical form) in the decomposition of EtSH, with the DEDS dimer as the only reaction product identified in the gas phase.

The results also showed that the physical form, but mainly the packing of the catalyst in reactor was responsible for differences in breakthrough time, which increased from 2.5 hours for catalyst used as threads to 29 hours for catalyst used as mesh. It is likely that the gas passes the catalyst bed easier when the catalyst is used as threads packed loosely

in the reactor. The turnover frequency for the catalyst was similar for both cases: catalyst as threads and as mesh.

 Increasing the humidity of the air fed into the reactor reduced the catalyst efficiency towards EtSH decomposition, presumably because the water flattened the catalytic fibres, facilitating the passage of gas through preferential routes and thus lowering the chances of physical contact between the EtSH in air and the active sites on the catalyst.

Unmodified PAN threads were not active in the removal of EtSH from air and little sorption of EtSH on the PAN threads was observed during control experiments.

To study the oxidation of EtSH in wet conditions (in the presence of H_2O_2 solution), a three phase (gas-liquid-solid) catalytic reactor was designed, constructed and incorporated into an experimental setup with the possibility of on-line GC analysis of the gas samples. The catalytic reactor can be operated in scrubber and slurry regimes, ensuring the simultaneous presence of catalyst, gas phase pollutant (e.g. EtSH) and H_2O_2 in the system. The design of the reactor was modified to improve its efficiency, and the system that performed the best consists of an absorption column inserted before the tri-phase catalytic reactor operated in slurry mode (concurrent flow of liquid and gas phases, both fed at the bottom of the reactor).

The efficiency of this system was evaluated at 45 °C in experiments with EtSH (93.3 mg/m^3 air) and at ambient temperature in experiments with EtSH (93.3 mg/m^3 air) and a mixture of EtSH (93.3 mg/m^3 air) and DMS (100 mg/m^3 air). The catalytic system proved to be efficient in the oxidation of both EtSH and DMS. EtSO$_3$H was identified

and quantified for the oxidation of EtSH both at 45 °C and at ambient temperature and the mixture of ethane and methane sulphonic acids was identified but not quantified for the oxidation of the mixture of EtSH and DMS. The system was operated in steady state, with the main reaction products being the sulphonic acids.

For the experiment with EtSH at 45 °C it was determined that 86% of the EtSH introduced into the system was converted to $EtSO_3H$. Very low amounts of EtSH and DEDS (both well below the admissible limits in air according to OSHA regulations) were occasionally identified in the gas effluent. It was assumed that the rest was oxidized to other products, such as organic acids, as no EtSH or DEDS were identified as dissolved in the liquid effluent.

Reducing the temperature from 45 ˚C to room temperature (16 – 19˚C during the day in winter) significantly reduced the efficiency of the decontamination process (calculated yields in $EtSO_3H$ were 86% at 45 ˚C and only ~16 – 18% at ambient temperature) and the consumption of H_2O_2 (from ~80% at 45 ˚C to ~26% for ambient temperature). This indicates a less advanced oxidation process at room temperature than at 45˚C.

When a mixture of pollutants was used (50% v/v EtSH, 50% v/v DMS), the observed oxidation products ($EtSO_3H$ and $MeSO_3H$) could not be quantified. The two sulphonic acids had similar retention times and eluted together, as a single peak during the IC analysis.

The modified PAN catalyst (20.1 g mesh with 50% catalytic threads and [Fe] = 0.52 mmol Fe/g threads) was used in the presence of 100 mg/L H_2O_2 solution (2.4 mL/min)

for a total of 1504 hours (415 hours in the experiment with EtSH at 45 °C, 309 hours in the experiment with EtSH at ambient temperature and 780 hours in the experiment with mixture of EtSH and DMS). The total amount of air treated in these experiments was 45.12 L, total amount of contaminants passing through the experimental setup was 252.67 mg EtSH and 140.4 mg DMS. Advanced oxidation products were identified and quantified for the experiments with EtSH, for the experiment with the mixture of pollutants the quantification was not possible.

The novel catalytic system can be incorporated in a mobile decontamination unit with the absorption column and catalytic reactor housed in modified ISO Containers that can be easily transported on ISO Trucks to the affected site after a CBRN incident for air decontamination.

A simplified cost estimation for the scale-up to the mobile decontamination unit mentioned above was calculated, taking into account costs with part of the capital equipment, catalyst, filling material for the absorption column, running costs limited to H_2O_2 solution, heating of the liquid phase to the operating temperature and electricity used to operate the pumps and cost of chemicals needed for one catalyst regeneration process. These costs could be reduced by optimizing the operating conditions for the decontamination unit. Some additional recommendations were made with regard to possible ways to reduce the running costs.

Running the decontamination process at ambient temperature instead of 45 °C would reduce the daily running costs, but will also reduce the efficiency of the treatment.

Assuming a residence time of 3.9 minutes for the gas phase and 50 minutes for the liquid phase, about 10,800 m^3 air (a volume of approximately 25 average size 3 bedroom detached properties) could be decontaminated in a day using a catalytic reactor housed in a 33 m^3 modified ISO Container. Considering the maximum number of regenerations needed to be 5 and limiting the calculations to the running costs, the treatment cost would be £0.21/ m^3 air.

9.2. Recommendations

It was noticed that lengthy storage before use has a negative effect on the catalyst performance. The storage conditions and an eventual reactivation of the catalyst before use should be investigated, as in practice is not always possible to have freshly prepared catalyst ready to use.

This study was limited to sulphur VOCs. The efficiency of the fibrous catalyst/H_2O_2 system should be tested towards other classes of VOCs, as single pollutants or as mixtures and a database of the tested compounds (or classes of compounds) should be developed.

The used catalyst should be further investigated in order to elucidate the causes of deactivation. A suitable method for this would be thermogravimetry (TGA).

A suitable method of analysis should be developed for the quantification of all sulphonic acids in the liquid effluent.

In order to improve the efficiency of the decontamination unit, the following recommendations are made:

The mass transfer of contaminants from gas to liquid phase needs to be maximized by optimising the operating conditions for the absorption column with regard to dimensions of absorption column (length, diameter), packing material (type, size, etc), flow rates for gas and liquid.

The operating conditions for the catalytic reactor should be optimised with regard to the amount of catalyst used. It is expected that once the mass transfer of the organic pollutant from gas to liquid phase is maximised, the decontamination process will need less catalyst to achieve at least the same or even better efficiency.

The lifetime of the catalyst, the regeneration process and the re-use of the catalyst after regeneration should be investigated. A quick and easy in-situ regeneration procedure was proposed in this work. As proposed, the regeneration process can be used on-site, in the same reactor (reactor series) as the decontamination process. The regeneration procedure is not fully optimised yet and could possibly be achieved at lower cost.

References

1. Abdul Galil, MS; Yogendra-Kumar, MS and Nagendrappa, G; 2007 – 'A simple and rapid spectrophotometric method for the determination of nitrite by its decolorizing effect on peroxovanadate complex', Spectrochimica Acta Part A 67, pp 76-82

2. Addamo, M; Augugliaro, V; Coluccia, S; Faga, MG; Garcia-Lopez, E; Loddo, V; Marci, G; Martra, G and, Palmisano, L; 2005 – 'Photocatalytic oxidation of acetonitrile in gas-solid and liquid-solid regimes', Journal of Catalysis, 235, pp 209-220

3. Agarwal, SK; Spivey, JJ and Butt, JB; 1992 – 'Catalyst deactivation during deep oxidation of chlorohydrocarbons', Applied Catalysis A: General, 82, pp. 259-275

4. Alcaraz, JJ; Arena, BJ; Gillespie, RD and Holmgren, JS; 1998 – 'Solid base catalysts for mercaptan oxidation', Catalysis Today, 43(1), pp. 89-99

5. Aranzabal, A; Gonzales-Marcos, JA; Ayastuy, JL and Gonzales-Velasco, JR; 2006 – 'Kinetics of Pd/alumina catalysed 1,2-dichloroethane gas-phase oxidation', Chemical Engineering Science, 61, pp. 3564-5376

6. Aranzabal, A; González-Marcos, JA; López-Fonseca, R; Gutiérrez-Ortiz, MA and González-Velasco, JR; 2000 - 'Deep catalytic oxidation of chlorinated VOC mixtures from groundwater stripping emissions', Studies in Surface Science and Catalysis, 130 (Proceedings of the 12th International Congress on Catalysis), pp. 1229-1234

7.   Babich, H and Stotzky, G; 1978 – 'Atmospheric sulfur compounds and microbes', Environmental Research, 15(3), pp. 513-531

8.   Balzhinimaev, BS; Paukshtis, EA; Vanag, SV; Suknev, AP and Zagoruiko, AN; 2010 – 'Glass-fiber catalysts: Novel oxidation catalysts, catalytic technologies for environmental protection', Catalysis Today, 151(1-2), pp. 195-199

9.   Balzhinimaev, BS; Simonova, LG; Barelko, VV; Toktarev, AV; Zaikovskii, VI and Chumachenko, VA; 2003 – 'Pt-containing catalysts on a base of woven glass fiber support: a new alternative for traditional vanadium catalysts in SO2 oxidation process', Chemical Engineering Journal, 91, pp. 175-179

10. Basu, B; Satapathy, S and Bhatnagar AK; 1993 – 'Merox and Related Metal Phthalocyanine Catalyzed Oxidation Processes', Catalysis Reviews, Science and Engineering, 35(4), pp. 571-609

11. Benitez, F; Hereida, J; Acero, J and Rubio, F; 1999 – 'Chemical Decomposition of 2,4,6-Trichlorophenol by Ozone, Fenton's Reagent and UV Radiation', Industrial & Engineering Chemistry Research, 38, pp. 1341-1349

12. Bentley, R and Chasteen, TG; 2004 – 'Environmental VOCs – formation and degradation of dimethyl sulphide, methanethyol and related materials', Chemosphere, 55(3), pp. 291-317

13. Biard, PF; Couvert, A; Renner, C and Lavasseur, JP; 2009 – 'Assessment and optimisation of VOC mass transfer enhancement by advanced oxidation process in a compact wet scrubber', Chemosphere, 77, pp. 182-187

14. Bickle, GM; Suzuki, T and Mitarai, A; 1994 – 'Catalytic destruction of chlorofluorocarbons and toxic chlorinated hydrocarbons', Applied Catalysis B: Environmental, 4(2-3), pp. 141-153

15. Bozzi, A; Yuranova, T; Mielczarski, E; Mielczarski, J; Buffat, PA; Lais, P and Kiwi, J; 2003 – 'Superior biodegradability mediated by immobilized Fe-fabrics of

waste waters compared to Fenton homogeneous reactions', Applied Catalysis B: Environmental, 42(3), pp. 289-303

16. British Gas; 2010(a) – http://www.britishgas.co.uk/pdf/Elec-20Price-20guarantee-202008.pdf - as of February 20, 2010

17. British Gas; 2010(b) – http://www.britishgas.co.uk/pdf/gas-PG-2010.pdf - as of February 20, 2010

18. Calleja, G; Melero, JA; Martinez, F and Molina, R; 2005 – 'Activity and resistance of iron-containing amorphous, zeolitic and mesostructured materials for wet peroxide oxidation of phenol', Water Research, 39, pp. 1741-1750

19. Capozzi, G and Modena, G; 1974 – 'Oxidation of Thiols' in 'The Chemistry of the Thiol Group', part 2, editor S. Patai, John Wiley & Sons, Bristol, pp. 801, ISBN 0-471-66948-2

20. Carriazo, JG; Guelou, E; Barrault, J; Tatibouët, JM; Molina, R and Moreno, S; 2005 – 'Catalytic wet peroxide oxidation of phenol by pillared clays containing Al-Ce-Fe', Water Research, 39, pp. 3891-3899

21. CBRN incident; 2010 – http://www.nationmaster.com/encyclopedia/CBRN - as of Oct. 10, 2010

22. Centi, G; Perathoner, S; Torre, T and Verduna, MG; 2000 – 'Catalytic wet oxidation with H_2O_2 of carboxylic acids on homogeneous and heterogeneous Fenton-type catalysts', Catalysis Today, 55, pp. 61-69

23. Cervini-Silva, J; Wu, J; Larson, RA and Stucki, JW; 2000 – 'Transformation of Chloropicrin in the presence of iron-bearing clay minerals', Environmental Science and Technology, 34(5), pp. 915-917

24. Chamarro, E; Marco, A and Esplugas, S; 2001 – 'Use of Fenton reagent to improve organic chemical biodegradability', Water Research, 35(4), pp. 1047-1051

25. Chauhan, SMS; Kumar, A and Srinivas, KA; 2003 – 'Oxidation of thiols with molecular oxygen catalyzed by cobalt(II)', Chemical Communications, 18, pp. 2348-2349

26. Chen, J and Zhu, L; 2007 – 'Heterogeneous UV-Fenton catalytic degradation of dyestuff in water with hydroxyl-Fe pillared bentonite', Catalysis Today, 126, pp. 463-470

27. Cheng, M; Ma, W; Li, J; Huang, J; Zhao, J; Wen, Y and Xu, Y; 2004 – 'Visible-light-assisted degradation of dye pollutants over Fe(III)-loaded resin in the presence of H_2O_2 at neutral pH values', Environmental Science & Technology, 38, pp. 1569-1575

28. Chi Tangyie, G and Huddersman, KD; 2007 – 'Novel ion chromatography technique for the rapid identification and quantification of saturated and unsaturated low molecular weight organic acids formed during the Fenton oxidation of organic pollutants', Journal of Chromatography A, 1139(1), pp. 95-103

29. Chi Tangyie, G; 2008 – 'Synthesis, chemical characterization and scale-up of a heterogeneous catalyst for the oxidation of organic pollutants in wastewater', Ph.D Thesis, De Montfort University Leicester, UK

30. Chirchi, L and Ghorbel, A; 2002 – 'Use of various Fe-modified montmorillonite sample for 4-nitrophenol degradation by H_2O_2', Applied Clay Science, 21, pp. 271-276

31. Chiron, S; Fernandez-Alba, A; Rodriguez, A and Garcia-Calvo, R; 2000 – 'Pesticide chemical oxidation: state-of-the-art', Water Research, 34(2), pp. 366-377

32. Chou, S and Huang, C; 1999 – 'Application of a supported iron oxyhydroxide catalyst in oxidation of benzoic acid by hydrogen peroxide', Chemosphere, 38, pp. 2719-2731

33. Chu, H and Lee, WT; 1998 – 'The effect of sulphur poisoning of dimethyl disulphide on the catalytic incineration over a Pt/Al_2O_3 catalyst', The Science of the Total Environment, 209, pp. 217-224

34. Chu, H; Hao, GH and Tseng, TK; 2003 – 'Laboratory study of poisoning of a MnO/Fe_2O_3 catalyst by dimethyl sulphide and dimethyl disulphide', Journal of Hazardous Materials, B100, pp. 301-316

35. Chu, H; Lee, WT; Horng, KH and Tseng, TK; 2001 – 'The catalytic incineration of $(CH_3)_2S$ and its mixture with CH_3SH over a Pt/Al_2O_3 catalyst', Journal of Hazardous Materials, 82(1), pp. 43-53

36. Chungsiriporn, J; Bunyakan,Ch and Nikom, R; 2004 – 'Removal of VOCs by Oxidation Reaction in Wet Scrubber', available online at: http://homepage.eng.psu.ac.th/chem/File/polngan/2548/juntima/2.Removal%20of %20VOCs%20by%20oxidation%20reaction%20in%20wet%20scrubber.pdf - (as of Feb.15, 2011)

37. Chungsiriporn, J; Bunyakan,Ch,and Nikom, R; 2005 – 'Treatment of Toluene Using Wet Scrubber With Sodium Hypochlorite Oxidation Reaction', PSU International Conference on Engineering and Environment - ICEE-2005, Novi Sad 19-21 May, 2005, Paper No. T11-3.1, pp. 1-4, available online at: http://www.scribd.com/doc/43158467/3-Treatment-of-Toluene-Using-Wet-Scrubber-With-Sodium-Hypochrolite-Oxidation-Reaction - as of 2 Feb, 2009

38. Coates, J; 2000 – 'Interpretation of Infrared Spectra, a Practical Approach' – in Encyclopedia of Analytical Chemistry, John Wiley & Sons LTD, Chichester, pp. 10815-10837

39. Cole, SK; Cooper, WJ; Fox, RV; Gardinali, PR; Mezyk, SP; Mincher, BJ and O'Shea, KE; 2007 – 'Free Radical Chemistry of Disinfection Byproducts. 2. Rate Constants and Degradation Mechanism of Trichloromethane (Chloropicrin)', Environmental Science & Technology, 41(3), pp. 863-869

40. Communities; 2011 – Precautions to minimise effects of a Chemical, Biological, Radiological or Nuclear Event on Buildings and Infrastructure – retrieved from http://www.communities.gov.uk/documents/fire/pdf/143741.pdf - as of May 20, 2011

41. Cremlyn, RJ; 1996 – 'An Introduction to Organosulphur Chemistry", John Wiley & Sons LTD, ISBN 0-471-95512-4, pp. 164

42. DEFRA; 2008 – 'Strategic National Guidance - The decontamination of the open environment exposed to CBRN substances or material (www.ukresilience.gov.uk/ emergencies/cbrn/defra/ - as of Dec.12, 2008

43. Dionex; 2008 – 'Technical Note 12', available online at: http://www.dionex.com/ en-us/webdocs/4696-tn12.pdf, as of March 1, 2008

44. Dong, Y; Han, Z; Liu C and Du, F; 2010 – 'Preparation and photocatalytic performance of Fe (III)-amidoximated PAN fiber complex for oxidative degradation of azo dye under visible light irradiation', Science of The Total Environment, 408(10), pp. 2245-2253

45. Duguet, JP; Tsutsumi, Y and Bruchet, A; 1988 – 'Chloropicrin in Potable Water: Conditions of Formation and Production During Treatment Processes', Environmental Technology Letters, 9(4), pp. 299-310

46. EA; 2011 – http://www.environment-agency.gov.uk/research/library/position/ 41241.aspx - as of 15 May, 2011

47. EPA; 2011 – http://www.epa.gov/oar/toxicair/newtoxics.html - as of 10 Apr., 2011

48. European Solvents Industry Group; 2009 – 'VOC definition in Europe', http://www.esig.org/uploads/documents/81-518- voc%20definition%20in%20europe.doc - as of 26 June 2009

49. Fajerwerg, K and Debellefontaine, H; 1996 – 'Wet oxidation of phenol by hydrogen peroxide using heterogeneous catalyst Fe-ZSM-5: a promising catalyst', Applied Catalysis B: Environmental, 10, pp. L229-L235

50. Feng, J; Hu, X and Yue, PL; 2003 – 'Degradation of azo-dye Orange II by a photoassisted Fenton reaction using a novel composite of iron oxide and silicate nanoparticles as a catalyst', Industrial Engineering and Chemical Research, 42, pp. 2058-2066

51. Feng, J; Hu, X and Yue, PL; 2006 – 'Effect of initial solution pH on the degradation of Orange II using clay-based Fe nanocomposites as heterogeneous photo-Fenton catalyst', Water Research, 40, pp. 641-646

52. Fenton, HJ; 1894 – 'Oxidation of Tartiaric Acid in the Presence of Iron', Journal of Chemical Society, Transactions, 65, pp. 899-910

53. Fernandez, J; Bandara, J; Lopez, A; Albers, P and Kiwi, J; 1998 – 'Efficient photo-assisted Fenton catalysis mediated by Fe ions on Nafion membranes active in the abatement of non-biodegradable azo-dye', Chemical Communication, 14, pp. 1493-1494

54. Fernandez, J; Bandara, J; Lopez, A; Buffet, Ph and Kiwi, J; 1999 – 'Photoassisted Fenton degradation of nonbiodegradable azo dye (Orange II) in Fe-free solution mediated by cation transfer membranes', Langmuir, 15, pp. 185-192

55. Field, L; 1977 – 'Disulfides ans Polysulfides', in 'Organic Chemistry of Sulphur', editor S. Oae, Plenum Press, New York, pp. 316-351, ISBN: 0-306-30740-5

56. Firouzabadi, H; Iranpoor, N; Kiaeezadeh, F and Toofan, J; 1986 – 'Chromium(VI) based oxidants-1 : Chromium peroxide complexes as versatile, mild, and efficient oxidants in organic synthesis', Tetrahedron, 42(2), pp. 719-725

57. Flores, Y; Flores, R and Gallegos, AA; 2008 – 'Heterogeneous catalysis in the Fenton-type system reactive black5/H_2O_2, Journal of Molecular Catalysis A: Chemical, 281, pp. 184-191

58. Fogler, HS; 1992 – 'Elements of chemical reaction engineering', Second edition, published by Prentice Hall Inc., USA, ISBN: 0-13-263534-8, pp. 246

59. Forbes Group; 2010 – Personal communication with company representative

60. Fritz, JS and Gjerde, DT; 2000 –'Ion Chromatography', Third edition, Wiley-VCH, ISBN-13: 978-3527299140, pp. 5-154

61. Georgi, A and Kopinke, FD; 2005 – 'Interaction of adsorption and catalytic reactions in water decontamination processes part I. Oxidation of organic contaminants with hydrogen peroxide catalyzed by activated carbon', Applied Catalysis B: Environmental, 58, pp. 9-18

62. Golchoubian, H and Hosseinpoor, F; 2007 – 'Aerobic oxidation of thiols to disulfides catalyzed by a manganese(III) Schiff-base complex', Catalysis Communications, 8(4), pp. 697-700

63. Gonzales-Garcia, N; Ayllón, JA; Doménech, X and Peral, J; 2004 – 'TiO$_2$ deactivation during the gas-phase photocatalytic oxidation of dimethyl sulphide', Applied Catalysis B: Environmental, 52(1), pp. 69-77

64. Gonzales-Velasco, JR; Aranzabal, A; Gutierrez-Ortiz, JI; Lopez-Fonseca, R Gutierrez-Ortiz, MA; 1998 – 'Activity and product distribution of alumina supported platinum and palladium catalysts in the gas-phase oxidative decomposition of chlorinated hydrocarbons', Applied Catalysis B: Environmental, 19, pp. 189-197

65. Gumy, D; Fernández-Ibáñez, P; Malato, S; Pulgarin, C; Enea, O and Kiwi, J; 2005 – 'Supported Fe/C and Fe/Nafion/C catalysts for the photo-Fenton

degradation of Orange II under solar irradiation', Catalysis Today, 101, pp. 375-382

66. Haber, F and Weiss, J; 1934 – 'The Catalytic Decomposition of Hydrogen Peroxide by Iron Salts', Proceedings of the Royal Society of London, 147(861), pp. 332-251

67. Han, JW and Hill, CL; 2007 – 'A coordination network that catalyzes O_2-based oxidations', Journal of the American Chemical Society, 129(49), pp. 15094-15095

68. Han, ZB; Dong, YC and Dong, SM; 2010(a) – 'Comparative study on the mechanical and thermal properties of two different modified PAN fibres and their Fe complexes', Materials and Design, 31(6), 2784-2789

69. Han, ZB; Dong, YC and Dong, SM; 2011 – 'Copper–iron bimetal modified PAN fiber complexes as novel heterogeneous Fenton catalysts for degradation of organic dye under visible light irradiation', Journal of Hazardous Materials, 189(1-2), pp.241-248

70. Han, ZB; Dong, YC and Liu, CY; 2010(b) – 'Coordination of Mofified PAN Fibres wit Fe(3+) and Catalytic Activity of Their Complexes for Dye Degradation', Chemical Journal of Chinese Universities, 31(5), pp. 986-993

71. Han, ZB; Dong, YC; Du, F; Zhao, JZ and Liu, CY; 2009 – 'Synthesis of Fe Modified PAN Fibrous Catalyst for Photocatalytic Degradation of Reactive Red 195', Proceedings of the Fiber Society 2009 Spring Conference, Vol I and II, pp. 1488-1491, ISBN: 978-7-5064-5635-7

72. Harkness, AC and Murray, FE; 1970 – 'Oxidation of methyl mercaptan with molecular oxygen in aqueous solution', Atmospheric Environment, 4(4), pp. 417-418

73. Hashemi, MM; Karimi-Jaberi, Z and Ghazanfari, D; 2004 – 'Copper chloride/kieselguhr: an efficient catalyst for oxidation of thiols to disulfides by molecular oxygen or air', Journal of Chemical Research, 5, pp. 364-365

74. Hermosilla, D; Cortijo, M and Huang, CP; 2009 – 'Optimizing the treatment of landfill leachate by conventional Fenton and photo-Fenton processes', Science of The Total Environment, 407(11), pp. 3473-3481

75. Hill, PG and Smith, RM; 2000 – 'Determination of sulphur compounds in beer using headspace solid phase microextraction and gas chromatographic analysis with pulsed flame photometric detection', Journal of Chromatography A, 872, pp. 203-213

76. Hoigne, J and Bader, H; 1994 – 'Kinetics of Reactions of Chlorine Dioxide (OCIO) in Water-I. Rate Constants for Inorganic and Organic Compounds', Water Research, 28(1), pp. 45-55

77. Home Office; 2008 – http://www.homeoffice.gov.uk /security/protecting-the-uk/preparing-for-incidents/ - as of Dec. 10, 2008

78. Howard, PH; 1997 – 'Handbook of environmental Fate and Exposure Data for Organic Chemistry. 3', ISBN: 087371976X , pp. 126

79. HPA; 2011 – retrieved from http://www.hpa.org.uk/NewsCentre/NationalPressReleases/2010PressReleases/100915Healtheffetsofairpollution/ - contents as of 20 May, 2011

80. http://www.arkema-inc.com/msds/999.pdf - contents as of December 3, 2008

81. Huddersman, KD and Ishtchenko, VV; 2007, 2008 – 'Improvements in the Method for the Production of Fibrous Catalysts', International Patent Application No. PCT /GB2007/000612, Patent No WO 2007/099293 (2007), European Patent Application No. 07705244.7 and as US Patent Application No.12/224,399 (2008)

82. Huddersman, KD; 2009 – 'Selection Method in Production of Fibrous Catalyst', Patent No. WO 2009/027655

83. Huddersman, KD; 2010 – Personal communication

84. Huddersman, KD; 2011 – Personal communication

85. Huebner, KD; 2008 – 'CBRNE – Lung damaging agents, Chloropicrin', published on 'e-medicine from WebMD' content as of Feb. 13, 2008

86. Iliev, V; Alexiev, V and Bilyarska, L; 1999 – 'Effect of metal phthalocyanine complex aggregation on the catalytic and photocatalytic oxidation of sulfur containing compounds', Journal of Molecular Catalysis A: Chemical, 137(1-3), pp. 15-22

87. Infrared Spectroscopy; 2008 – 'Infrared spectroscopy' – retrieved from http://www2.chemistry.msu.edu/faculty/reusch/VirtTxtJml/Spectrpy/InfraRed/infrared.htm; contents as of Oct. 3, 2008

88. Ishtchenko, VV; 2002 – 'Novel Heterogeneous Oxidation Catalyst for Organic Compounds', Ph.D Thesis, De Montfort University Leicester, UK

89. Ishtchenko, VV; Huddersman, KD and Vitkovskaya, RF; 2003a – 'Part 1. Production of a modified PAN fibrous catalyst and its optimisation towards the decomposition of hydrogen peroxide', Applied Catalysis A: General, 242(1), pp. 123-137

90. Ishtchenko, VV; Vitkovskaya, RF and Huddersman, KD; 2003b – 'Investigation of the mechanical and physico-chemical properties of a modified PAN fibrous catalyst', Applied Catalysis A: General, 242(2), pp. 221-31

91. Kachina, A; Preis, S and Kallas, J; 2006 – 'Catalytic TiO_2 oxidation of ethanethiol for environmentally benign air pollution control of sulphur compounds', Environmental Chemistry Letters, 4(2), pp. 107-110

92. Karaivanova, S and Badev, A; 1986 – 'Modification of polyacrylonitrile fibers with hydrazine and hydroxylamine in aqueous medium', Die Angewandte Makromolekulare Chemie, 140, pp.1-32

93. Kastner, JR and Das, KC; 2002 – 'Wet scrubber analysis of volatile organic compound removal in the rendering industry', Journal of the Air and Waste Management, 52, pp. 459-469

94. Kastner, JR and Das, KC; 2005 – 'Comparison of chemical wet scrubbers and biofiltration for control of volatile organic compounds using GC/MS techniques and kinetic analysis', Journal of Chemical Technology and Biotechnology, 80, pp. 1170-1179

95. Kastner, JR; Das, KC and Melear, ND; 2002 – 'Catalytic oxidation of reduced sulphur compounds using coal fly ash', Journal of Hazardous Materials, 95(1-2), pp. 81-90

96. Kastner, JR; Das, KC; Buquoi, Q and Melear, ND; 2003 – 'Low Temperature Catalytic Oxidation of Hydrogen Sulfide and Methanethiol Using Wood and Coal Fly Ash', Environmental Science & Technology, 37(11), pp. 2568-2574

97. Kavitha, V and Palanivelu, K; 2004 – 'The role of ferrous ion in Fenton and photo-Fenton processes for the degradation of phenol', Chemosphere, 55(9), pp. 1235-1243

98. Kozlov, DV; Vorontsov, AV; Smirniotis, PG and Savinov, EN; 2003 – 'Gas-phase photocatalytic oxidation of diethyl sulphide over TiO_2: kinetic investigations and catalyst deactivation', Applied Catalysis B: Environmental, 42, pp. 77-87

99. Kuptsov, AH and Zhizhin, GN; 1998 – 'Handbook of Fourier Transform Raman and Infrared Spectra of Polymers' – Elsevier, ISBN 0-444-82620-3

100. Kusic, K; Koprivanac, N and Selanec, I; 2006 – 'Fe-exchanged zeolite as the effective hetenogeneous Fenton-type catalytic for the organic pollutant minimization: UV irradiation assistance', Chemosphere, 65, pp. 65-73

101. Lawrence, NS; Davis, J and Compton, RG; 2000 – 'Analytical strategies for the detection of sulfide: a review', Talanta, 52, pp. 771-784

102. Lee, JM; Kim, JH; Chang, YY and Chang, YS; 2009 – 'Steel dust catalysis for Fenton-like oxidation of polychlorinated dibenzo-p-dioxins', Journal of Hazardous Materials, 163(1), pp. 222-230

103. Leitão, A and Rodrigues, A; 1989 – 'Studies on the Merox process: kinetics of N-butyl mercaptan oxidation', Chemical Engineering Science, 44(5), pp. 1245-1253

104. Leitão, A and Rodrigues, A; 1990 – 'Fixed-bed reactor for gasoline sweetening: Kinetics of mercaptan oxidation and simulation of the Merox reactor unit', Chemical Engineering Science, 45(3), pp. 679-685

105. Lestremau, F; Desauziers, V; Roux, JC and Fanio, JL; 2003 – 'Development of a quantification method for the analysis of malodorous compounds in gaseous industrial effluents by solid-phase microextraction and gas chromatography-pulsed flame photometric detection', Journal of Chromatography A, 999, pp. 71-80

106. Lichtin, NN and Avudaithai, M; 1996 – 'TiO_2-photocatalysed oxidative degradation of CH_3CN, CH_3OH, C_2HCl_3, and CH_2Cl_2 supplied as vapors and in aqueous solution under similar conditions', Environmental Science and Technology, 30, pp. 2014-2020

107. Lide, DR; 1992 – 'Handbook of Chemistry and Physics', 73rd Edition, CRC Press, ISBN: 0-8493-0566-7

108. Liou, RM; Chen, SH; Hung, MY and Hsu, CS; 2004 – 'Catalytic oxidation of pentachlorophenol in contaminated soil suspension by Fe^{3+}-resin/H_2O_2', Chemosphere, 55, pp. 1271-1280

109. Liou, RM; Chen, SH; Hung, MY; Hsu, CS and Lai, JY; 2005 – 'Fe (III) supported on resin as effective catalyst for the heterogeneous oxidation of phenol in aqueous solution', Chemosphere, 59, pp. 117-125

110. López, C; Gonzalez, A; Cossio, AP and Palomo, C; 1985 – '3-Carboxypyridinium Dichromate (NDC) and 4-Carboxypyridinium Dichromate (INDC). Two New Mild, Stable, Efficient, and Inexpensive Chromium (VI) Oxidation Reagents', Synthetic Communications,15(13), pp. 1197-1211

111. López-Fonseca, R; Gutiérrez-Ortiz, JI; Ayastui, JL; Gutiérrez-Ortiz, MA and González-Velasco, JR; 2003 – 'Gas-phase catalytic combustion of chlorinated VOC binary mixtures', Applied Catalysis B: Environmental, 45(1), pp. 13-21

112. Mallik, D. and Chaudhuri, SK; 1999 – 'Air oxidation of aqueous sodium sulfide solutions with coal fly ash', Water Research, 33(2), pp. 585-590

113. Martinez, F; Calleja, G; Melero, JA and Molina, R; 2005 – 'Heterogeneous photo-Fenton degradation of phenolic aqueous solutions over iron-containing SBA-15 catalyst', Applied Catalysis B: Environmental, 60, pp. 181-190

114. Martinez, F; Calleja, G; Melero, JA and Molina, R; 2007 – 'Iron species incorporated over different silica supports for the heterogeneous photo-Fenton oxidation of phenol', Applied Catalysis B: Environmental, 70, pp. 452-460

115. Maurya, MR; Titinchi, SJJ; Chand, S and Mishra, IM; 2002 – 'Zeolite-encapsulated Cr(III), Fe(III), Ni(II), Zn(II) and Bi(III) complexes as catalysts for the decomposition of H_2O_2 and oxidation of phenol', Journal of Molecular Catalysis A: Chemical, 180, pp. 201-209

116. Mayer, RA; 2003 – 'Sulphur Compound Extraction and Sweetening' in 'Handbook of Petroleum Refining Process 3rd Edition', McGraw-Hill Company, ISBN: 0071391096

117. Menini, L; Pereira, MC; Ferreira, AC; Fabris, JD and Gusevskaya, EV; 2011 – 'Cobalt–iron magnetic composites as heterogeneous catalysts for the aerobic oxidation of thiols under alkali free conditions', Applied Catalysis A: General, 392(1-2), pp. 151-157

118. Micaroni, RC; Bueno, MIMS and Jardim, WF; 2004 – 'Degradation of Acetonitrile Residues Using Oxidation Processes' – Journal of Brazilian Chemical Society, 15(4), pp. 509-513

119. Moilanen, KW; Crosby, DJ and Humphrey, J; 1978 – 'Vapor-Phase Photodecomposition of Chloropicrin', Tetrahedron, 34, pp. 3345-3349

120. Nakagawa, K; Shiba, S; Horikawa, M; Sato, K; Nakamura, H; Harada, N and Harada, F; 1980 – 'Oxidation with Nickel Peroxide. XIII. Oxidation of Thiols to Disulfides', Synthetic Communications, 10, pp. 305-309

121. Nemykin, VN; Polshyna, AE; Borisenkova, SA and Strelko, VV; 2007 – 'Preparation, characterization, and catalytic activity of synthetic carbon-supported (phthalocyaninato)cobalt-containing complexes in dodecane-1-thiol oxidation reaction', Journal of Molecular Catalysis A, 264(1-2), pp. 103-109

122. NHS; 2011 – Retrieved from http://www.nhs.uk/news/2009/01January/Pages/ Pollutionandlifeexpectancy.aspx - as of 25 May, 2011

123. Noordally, E; Richmond, JR and Drumm, KJ; 1994 – 'Catalytic Oxidation Processes for Odour and VOC Control', Studies in Environmental Science, 61, pp. 459-467

124. Noorjaha, M; Kumari, VD; Subrahmanyam, M and Panda, L; 2005 – 'Immobilized Fe(III)–HY: an efficient and stable photo-Fenton catalyst, Applied Catalysis B: Environmental, 57, pp. 291-298

125. Ohno, A and Oae, S; 1977 – 'Thiols', in 'Organic Chemistry of Sulphur', editor S. Oae, Plenum Press, New York, pp. 155-156, ISBN: 0-306-30740-5

126. Oppenlander, T; 2003 – 'Photocemical Purification of Water and Air. Advanced Oxidation Processes (AOPs): Principles, Reaction Mechanisms, Reactor Concepts', WILEY-VCH, Weinheim, ISBN: 3-527-30563-7

127. OSHA; 2008 – Occupational Safety and Health Administration, United States Department of Labour, Toxic and Hazardous Substances, Table Z-1: Limits for Air Contaminants (available on-line at: http://www.osha.gov/pls/oshaweb/ owadisp.show_document?p_table=standards&p_id=9992, as of 15 Dec, 2008)

128. Parra, S; Henao, L and Mielczarski, E; 2004 – 'Synthesis, testing, and characterization of a novel Nafion membrane with superior performance in photoassisted immobilized Fenton catalysis', Langmuir, 20, pp. 5621-5629

129. Parsons, SA; 2004 – 'Advanced Oxidation Processes for Water and Wastewater Treatment', IWA Publishing, London, ISBN: 978-1843390176

130. Pigantello, J; 1992 – 'Dark and Photoassisted Fe^{3+} - Catalysed Degradation of Chlorophenoxyl Herbicides by Hydrogen Peroxide', Environmental Science and Technology, 26, pp. 944-951

131. Pignatello, JJ; Oliveros, E and MacKay, A; 2006 – 'Advanced oxidation processes for organic contaminant destruction based on the Fenton reaction and related chemistry', Critical Reviews in Environmental Science and Technology, 36(1), pp. 1-84

132. Poplawski, K; Lichtenberger, J; Keil, FJ; Schnitzlein, K and Amiridis, MD; 2000 – 'Catalytic oxidation of 1,2-dichlorobenzene over ABO$_3$-type perovskites', Catalysis Today, 62(4), pp. 329-336

133. Prage, JL and Cocke, DL; 2001 – 'Oxidation of cyanide in a hydrocyclone reactor by chlorine dioxide', Desalination, 140(3), pp. 289-293

134. Radojevic, M and Bashkin, VN; 2006 – 'Practical Environmental Analysis', Second Eddition, ISBN 0-85404-679-8, RSC Publishing, Cambridge, UK, pp.85-86

135. Ramirez, JH; Maldonado-Hodar, FJ and Perez-Cadenas, AF; 2007 – 'Azo-dye Orange II degradation by heterogeneous Fenton-like reaction using carbon–Fe catalysts', Applied Catalysis B: Environmental, 75, pp. 312-323

136. Rav-Acha, C and Choshen, E; 1987 – 'Aqueous Reactions of Chlorine Dioxide with Hydrocarbons', Environmental Science and Technology, 21, pp. 1069-1074

137. Rossin, JA and Farris, MM; 1993 – 'Catalytic-oxidation of chloroform over a 2-percent platinum alumina catalyst', Industrial & Engineering Chemistry Research, 32, pp. 1024-1029

138. Sarbak, Z; 1996 – 'Desulfurization of ethanethiol over cadmium and mercury modified zeolite NaX', Applied Catalysis A: General, 147(19), pp. 47-54

139. Savige, WE and Maclaren, JA; 1966 – 'Oxidation of disulfides with special reference to Cystine', in 'The Chemistry of Organic Sulfur Compounds', vol.2, editors Kharasch, N and Mayers, CY; Pergamon Press, pp. 368-371

140. Saxena, A; Kumar, A and Mozumdar, S; 2007 – 'Ni-nanoparticles: An efficient green catalyst for chemo-selective oxidative coupling of thiols', Journal of Molecular Catalysis A, 269(1-2), pp. 35-40

141. Schneider, R; Kießling, D and Wendt, G; 2000 – 'Cordierite monolith supported perovskite-type oxides — catalysts for the total oxidation of chlorinated hydrocarbons', Applied Catalysis B: Environmental, 28(3-4), pp. 187-195

142. Shaabani, A and Lee, DG; 2001 – 'Solvent Free Permanganate Oxidations', Thetrahedron Letters, 42(34), pp. 5833-5836

143. Shirini,F; Zolfigol, MA and Khaleghi, M; 2004 – 'Oxidative coupling of thiols in solution and under solvent-free conditions', Mendeleev Communications, 14(1), pp. 34-35

144. Siegel, H and Siegel, A; 1999 – 'Interrelations between free radicals and metal ions in life processes', CRC Press, ISBN: 0824719565

145. Silveira, CC and Mendes, SR; 2007 – 'Catalytic oxidation of thiols to disulfides using iodine and $CeCl_3 \cdot 7H_2O$ in graphite', Tetrahedron Letters, 48(42), pp. 7469-7471

146. Sinquin, G; Petit, C; Libs, S; Hindermann, JP and Kiennemann, A; 2001 – 'Catalytic destruction of chlorinated C_2 compounds on a $LaMnO_{3+\delta}$ perovskite catalyst', Applied Catalysis B: Environmental, 32, pp. 37–47

147. Skoog, A; Holler, FJ and Niemann, TA; 2006 –'Principles of Instrumental Analysis', Brooks/Cole Publishing, New York, 6th Edition, ISBN-13: 978-0495125709

148. Spivey, JJ; 1987 – 'Complete catalytic oxidation of volatile organics', Industrial & Engineering Chemistry Research, 26(11), pp. 2165-2180

149. Spokas, K; Wang, D; Venterea, R and Sadowsky, M; 2006 – 'Mechanism of N_2O production following chloropicrin fumigation', Applied Soil Ecology, 31(1-2), pp. 101-109

150. Strategic National Guidance; 2008 – The decontamination of buildings and infrastructure exposed to CBRN substances or material. Version 1, 2004 – retrieved from http://www.homeoffice.gov.uk/security/ - as of Dec. 10, 2008

151. Tereschenko, LY; Vitkovskaya, RF; Dahm, RH; Huddersman, KD and Ishtchenko, VV; 2000 – 'Method for the Production of Fibrous Catalysts', British Patent No. 99307811

152. Tidal volume; 2011 – In Encyclopædia Britannica. Retrieved from http://www.britannica.com/EBchecked/topic/595145/tidal-volume - as of 25 May, 2011

153. Tony, MA; Zhao, YQ and Taye, AM; 2009 – 'Exploitation of Fenton and Fenton-like reagents as alternative conditioners for alum sludge conditioning', Journal of Environmental Sciences, 21(1), pp. 101-105

154. Van de Vusse, IrJG; 1958 – 'Engineering aspects of the oxidation of mercaptans in caustic solutions: Reaction kinetics and design of reactor', Chemical Engineering Science, 8(1-2), pp. 72-80

155. Van der Braken, AM; – 'VOC treatment', available online at: www.safetynet.de/Publications/articles/VOCtreat.PDF, as of May 20, 2008

156. Venkatadri, R and Peters, RW; 1993 – 'Chemical Oxidation Technologies: Ultraviolet Light/Hydrogen Peroxide, Fenton's Reagent, and Titanium Dioxide-Assisted Photocatalysis', Hazardous Waste and Hazardous Materials, 10(2), pp. 107-149

157. Vorontsov, AV; Savinov, EV; Davydov, L and Smirniotis, PG; 2001 – 'Photocatalytic destruction of gaseous diethyl sulphide over TiO_2', Applied Catalysis B: Environmental, 32, pp. 11-24

158. Wade, EA; Reak, KE; Parsons, BF; Clemes, TP and Singmaster, KA; 2002 – 'Photochemistry of chloropicrin in cryogenic matrices', Chemical Physics Letters, 365, pp. 473-479

159. Wallace, TJ and Schriesheim, A; 1965 – 'The Base-Catalysed Oxidation of Aliphatic and Aromatic Thiols and Disulphides to Sulphonic Acids', Tetrahedron, 21, pp. 2271-2280

160. Wallace, TJ; 1966 – 'Reactions of Thiols with Metals. II. Low-Temperature Oxidation by Soluble Metal Salts', Journal of Organic Chemistry, 31(10), pp. 3071-3074

161. Wallace, TJ; Schriesheim, A; Hurwitz, H and Glosser, MB; 1964 –'Base-Catalyzed Oxidation of Mercaptans in Presence of Inorganic Transition Metal Complexes', Industrial and Engineering Chemistry Process Design and Development, 3(3), pp. 237-241

162. Walling, C; 1974 – 'Fenton's Reagent Revised', Accounts of Chemical Research, 8, pp. 125-131

163. Wardencki, W; 1998 – 'Problems with the determination of environmental sulphur compounds by gas chromatography', Journal of Chromatography A, 793, pp. 1-19

164. Wilson, MV; Ingersoll, CA and Thies, WG; 1999 – 'Testing for effects of stump fumigation with chloropicrin on vegetation in an early seral Douglas-fir stand', Canadian Journal of Forrest Research, 29(8), pp. 1254-1258

165. Xiaobing, L; Farooq, S and Viswanathan, S; 2003 – 'Evaluation of a novel reactor–biofilter system', Industrial & Engineering Chemistry Research, 42(4), pp. 752-763

166. Xiong, C; Chen, Q; Lu, W; Gao, H; Lu, W and Gao, Z; 2000 – 'Novel Fe-based complex oxide catalysts for hydroxylation of phenol', Catalysis Letters, 69, pp. 231-236

167. Yang, Zh; Ishtchenko, VV and Huddersman, KD; 2006 – 'Novel fibrous catalyst in advanced oxidation of photographic processing effluent', Journal of Environmental Science and Health, Part A: Toxic/Hazardous Substances and Environmental Engineering, 41(2), pp.129-141

168. Yuranova, T; Enea, O; Mielczarski E and Mielczarski, J; 2004 – 'Fenton immobilized photo-assisted catalysis through a Fe/C structured fabric', Applied Catalysis B: Environmental, 49, pp. 39-50

169. Zhang, M; Zhou, B and Chuang, KT; 1997 – 'Catalytic deep oxidation of volatile organic compounds over fluorinated carbon supported platinum catalysts at low temperatures', Applied Catalysis B: Environmental, 13, pp. 123-130

170. Zheng, W; Papiernik, SK; Guo, M and Yates, SR; 2003 – 'Competitive degradation between the fumigants Chloropicrin and 1,3-Dichloropropene in unnamed and amended soils', Journal of Environmental Quality, 32, pp. 1735-1742

171. Zhuang, J; Rusu, CN and Yates Jr., JT; 1999 – 'Adsorption and photooxidation of CH_3CN on TiO_2', Journal of Physical Chemistry B, 103, pp. 6957 – 6967

Appendix 1

Calculation of mass balance at 47 hours in the catalytic reactor with overflow at the side, first experiment (see section 6.3.2.2.)

Initial conditions:

Air flow: 30 cm^3/min

EtSH concentration in air: 466.7 mgEtSH/m^3 air

Flow of liquid (H$_2$O$_2$ solution) = 2.4 cm^3/min

Concentration of organic compounds calculated from instruments readings (47 h):

GC analysis (gas phase): [EtSH] = 139.1 mg/m^3 air; [DEDS] = 6.9 mg/m^3 air

IC analysis (liquid phase): [EtSO$_3$H] = 2.31 mg/L

GC-MS analysis (liquid phase): [EtSH] = 0; [DEDS] = 0 (neither of them identified)

The reactor is operated in steady state and the mass balance will be calculated considering the time unit as 1 minute.

Initial mass of EtSH in the reactor feed:

$$m_{EtSH(0)} = 466.7 \frac{mg}{m^3 \ air} \times 30 \times 10^{-6} m^3 \ air = 14 \times 10^{-3} \ mg \ EtSH$$

Mass of EtSH unconverted:

$$m_{EtSH} = 139.1 \frac{mg}{m^3 \ air} \times 30 \times 10^{-6} m^3 \ air = 4.173 \times 10^{-3} \ mg \ EtSH$$

Therefore, the percentage of EtSH unreacted is:

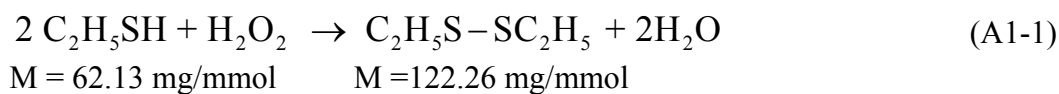$$EtSH \ unreacted \ (\%) \ = \ \frac{4.17 \times 10^{-3} \ mg}{14 \times 10^{-3} \ mg} \times 100 = 29.8\%$$

Mass of EtSH converted into reaction products:

$$m_{EtSH} = 14 \times 10^{-3} \ mg - 4.17 \times 10^{-3} \ mg = 9.83 \times 10^{-3} \ mg \ EtSH$$

Therefore, the percentage of EtSH converted is:

$$EtSH \ reacted \ (\%) \ = \ \frac{9.83 \times 10^{-3} \ mg}{14 \times 10^{-3} \ mg} \times 100 = \ 70.2\%$$

The oxidation of EtSH to DEDS proceeds according to the chemical reaction:

$$2 \ C_2H_5SH + H_2O_2 \ \rightarrow \ C_2H_5S-SC_2H_5 + 2H_2O \qquad (A1\text{-}1)$$
$$M = 62.13 \ mg/mmol \qquad M = 122.26 \ mg/mmol$$

The mass of DEDS in the gas effluent is:

$$m_{DEDS} = 6.9 \frac{mg}{m^3 \ air} \times 30 \times 10^{-6} m^3 \ air = 0.207 \times 10^{-3} \ mg \ DEDS$$
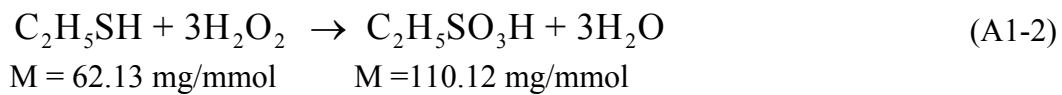
According to the chemical reaction (A1-1), this mass of DEDS is obtained from:

$$\text{EtSH}_{\text{(converted into DEDS)}} = \frac{0.207 \times 10^{-3} \text{ mg} \times 2 \times 62.13 \text{ mg/mmol}}{122.26 \text{ mg/mmol}} = 0.21 \times 10^{-3} \text{ mg EtSH}$$

Therefore, the percentage of EtSH converted into DEDS is:

$$\text{EtSH}_{\text{(converted into DEDS)}}(\%) = \frac{0.21 \times 10^{-3} \text{ mg}}{9.83 \times 10^{-3} \text{ mg}} \times 100 = 2.14\%$$

The oxidation of EtSH to EtSO$_3$H proceeds according to the chemical reaction:

$$C_2H_5SH + 3H_2O_2 \rightarrow C_2H_5SO_3H + 3H_2O \quad\quad\quad \text{(A1-2)}$$
M = 62.13 mg/mmol   M = 110.12 mg/mmol

The mass of EtSO$_3$H in the liquid effluent is:

$$m_{\text{EtSO}_3\text{H}} = 2.3 \frac{\text{mg}}{\text{L}} \times 2.4 \times 10^{-3} \text{ L} = 5.54 \times 10^{-3} \text{ mg EtSO}_3\text{H}$$

According to the chemical reaction (A1-2), this mass of EtSO$_3$H is obtained from:

$$\text{EtSH}_{\text{(converted into EtSO}_3\text{H)}} = \frac{5.54 \times 10^{-3} \text{ mg} \times 62.13 \text{ mg/mmol}}{110.12 \text{ mg/mmol}} = 3.13 \times 10^{-3} \text{ mg EtSH}$$

Therefore, the percentage of EtSH converted into EtSO$_3$H is:

$$\text{EtSH}_{\text{(converted into EtSO}_3\text{H)}}(\%) = \frac{3.13 \times 10^{-3} \text{ mg}}{9.83 \times 10^{-3} \text{ mg}} \times 100 = 31.84\%$$
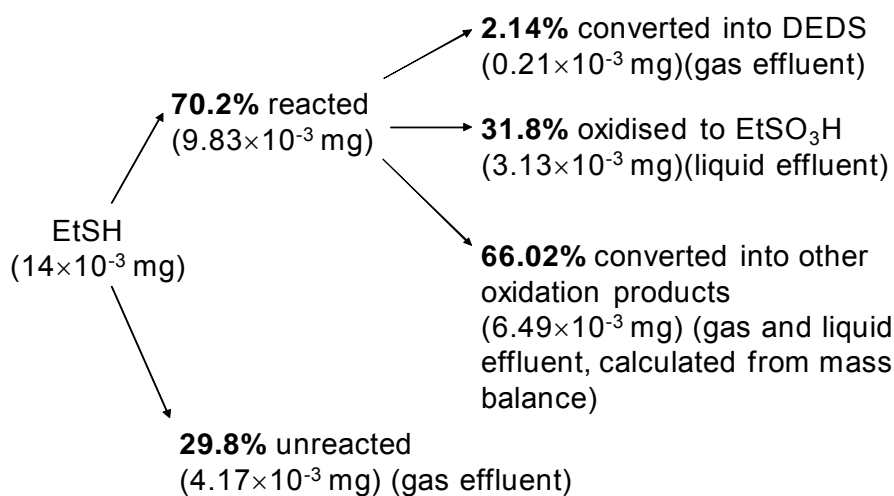
Considering that the rest of EtSH is converted to other oxidation products, the mass of EtSH converted to unidentified reaction products is:

$$m_{EtSH} = 9.83 \times 10^{-3} \text{ mg} - (0.21 \times 10^{-3} \text{ mg} + 3.13 \times 10^{-3} \text{ mg}) = 6.49 \times 10^{-3} \text{ mg EtSH}$$

Therefore, the percentage of EtSH converted to unidentified reaction products is:

$$EtSH_{(converted\ into\ other\ products)}(\%) = \frac{6.49 \times 10^{-3} \text{ mg}}{9.83 \times 10^{-3} \text{ mg}} \times 100 = 66.02\%$$

A summary of the mass balance for EtSH calculated above (experiment time 47 hours) is presented schematic below:

2.14% converted into DEDS
(0.21×10^{-3} mg)(gas effluent)

70.2% reacted
(9.83×10^{-3} mg)

31.8% oxidised to EtSO$_3$H
(3.13×10^{-3} mg)(liquid effluent)

EtSH
(14×10^{-3} mg)

66.02% converted into other oxidation products
(6.49×10^{-3} mg) (gas and liquid effluent, calculated from mass balance)

29.8% unreacted
(4.17×10^{-3} mg) (gas effluent)

Appendix 2

Table A1. Initial conditions for decontamination of air in the case of a CBRN incident (using a 33 m^3 catalytic reactor housed in a 20 ft long ISO Container)

Pollutant*	Conc. of pollutant (mg/m^3 air)	Catalyst amount (kg)	[H$_2$O$_2$] (mg/L)	H$_2$O$_2$ flow (L/min)	Air flow (m^3/min)	Residence time, gas (min)	Residence time, liquid (min)
Sulphur compounds	Up to 100	5031	100	600	7.5	3.9	50

* The range of pollutants needs to be extended and eventually developed into a database.

Appendix 3

Cost estimation of commercial scale-up

This appendix contains the detailed calculation used for the estimation of commercial scale-up of the setup with absorption column and catalytic reactor used in the laboratory trials, to a portable decontamination unit including a catalytic reactor of 33 m^3 volume. The assumptions made in section 8.3. are considered true.

1. Capital cost estimation

Air pump: Zepher air blower Model RT-5026-2: **£ 972** (quote from Zepher UK Ltd)

Absorption column including pipes and filling: ~**£ 12,000** (estimate: *'Forbes Group'*)

Water pump: Lowara water pump model DOMO10/B: 4 x £ 679 = **£ 2716** (quote from Anchor Pumps Ltd, UK)

Catalytic reactor and pipes: ~**£ 16,000 (**estimate: *'Forbes Group'*; catalytic reactor with 4 vertical units in cascade).

2. Materials

catalyst: From laboratory scale the density of the catalyst bed packed tightly in the reactor is: $d_{catalyst\ bed}$ = 20.1 g/117 cm^3 = 0.172 g/cm^3 = 172 kg/m^3. The calculated

volume of the catalyst bed in the catalytic reactor is 29.25 m^3, mass will be: m$_{cat}$ = 29.25 m^3×172 kg/m^3 = 5031 kg. The cost with the catalyst is: 5031 kg × £35/kg = **£ 176,085**

PP threads: From laboratory scale, the density of the PP threads packed tightly in the absorption column is: d$_{PP\ bed}$ = 7.5 g/63.6 cm^3 = 0.118 g/cm^3 = 118 kg/m^3 (mixture: 40% of 0.15 mm diameter, priced at £5.28/kg (for 1 tonne) and 60% of 0.3 mm diameter, priced at £ 3.94/kg (for a tonne)). Scaling up proportionally the volume of PP threads used in laboratory, the total volume of PP threads necessary is: (7.5 m^{3}air/min × 63.6 ×10^{-6} m^3)/(30 × 10^{-6} m^3 air/min) = 15.9 m^3 PP threads. The mass will be: 15.9 m^3 × 118 kg/m^3 = 1876.2 kg. The cost with PP threads as filling for the absorption column is: 1876.2 kg × (5.28 × 0.4 + 3.94 × 0.6) £/kg = **£ 8397.9.** *This cost could be reduced to £ 7392.2 if only PP thread of 0.3 mm diameter were used.*

Hydrogen peroxide: H$_2$O$_2$ is used as 100 mg/L solution at a flow rate of 600 L/min = 36000 L/h. This is prepared by using water (could be free if river water is used) and commercial H$_2$O$_2$ solution of 35% (w/w, d = 1.11 kg/L), priced at £268/1000L. The volume of H$_2$O$_2$ 35% used per hour will be: (36000L/h × 100 mg/L)/0.35 kg/kg/1.11 kg/L = 9.26 L/h. The cost with H$_2$O$_2$ is: 9.26 L/h × £268/1000L = **£ 2.48/h = £ 59.52/day (864 m^3 solution 100 mg/L)**. *Considering that only ~ 75-80 % of the initial H$_2$O$_2$ solution is consumed, the cost could be reduced by 20%, to £ 47.6/day.*

3. Cost of heating (based on theoretical calculations)

In the normal operation of the decontamination unit, the air will not be heated; in the laboratory the gas phase was only heated in order to ensure that the entire amount of model pollutant is in the gas phase (EtSH is a volatile liquid, boiling point of 38 °C). The cost of heating the liquid is calculated according to the equation A-1:

$$Q = c_p \cdot F \cdot (T_2 - T_1); \quad P(W) = Q(J/h)/t(s), \quad 1W = 1J/1s \quad \text{(A3-1)}$$

Where: Q – energy flux used in 1h to raise the temperature of liquid from T_1 to T_2 (kJ/h)

c_p – specific heat capacity for water: 4.181 kJ/kgK (at 15 °C), 4.181 kJ/kgK (at 45 °C)

F – flow of liquid heated (kg/h): 35931.6 kg/h (density of water at 15 °C: 998.1 kg/m^3)

T_1, T_2 – temperature (K): T_1 = 15 °C (inlet), T_2 = 45 °C (outlet)

P – power (kW), t – time (s)

The physical properties of the H_2O_2 solution (100 mg/L) are approximated to those of water. For each hour of heating the flow of liquid, the energy consumed will be:

$$\mathbf{Q} = c_p \times F \times (T_2 - T_1) = 4.186 \text{ kJ/kgK} \times 35931.6 \text{ kg/h} \times (318.15K - 288.15K) = \mathbf{4512290.3 \ kJ/h}$$

The power for 1 hour of heating will be: **P** = 4512290.3 kJ/3600 s = **1253.4 kW**

The energy consumption is: 1253.4 kW·1h = **1253.4 kWh**. Depending on the heating method used, the price will vary:

- For heating using **electricity** (price for **1 kWh is £ 0.1019**, according to British Gas pricing – (British Gas, 2010(a)), the price per day will be: 1253.4 kWh × 0.1019 £/kWh × 24h = **£ 3065.3/day**

- For heating using **gas** (price for **1kWh is £ 0.06983**, according to British Gas pricing (British Gas, 2010(b)), the price per day will be: 1253.4 kWh × 0.06983 £/kWh × 24h = **£ 2100.6/day**

- Heating with gas is 45.9 % cheaper than with electricity and this is used if possible.

The efficiency of heating water is usually 93-95 %, meaning that the actual cost with heating will be higher (~ £ 3226.6/day using electricity or £ 2211.1/day using gas). This cost can be eliminated if the reactor offers a long enough residence time in order to decompose the target compounds. The rise in temperature speeds up the oxidation reaction.

4. Cost with electricity to operate the pumps

Cost of 1 kWh of energy (British Gas, 2010(a)) = 10.91 pence = **£ 0.1091/kWh.**

- **Air pump** (air blower Zephler): Power: 2.2 kW. Energy consumption: 2.2 kW x 1h = 2.2 kWh. Price per day: 2.2 x 0.1091 x 24 = **£ 5.38/day**

- **Water pump** (Lowara): Power: 1.1 kW. Energy consumption: 4 x 1.1 kW x 1h = 4.4 kWh. Price per day: 4.4 x 0.1091 x 24 = **£ 10.76/day**

The total estimated cost of electricity used with the air and water pumps is: ~**£ 16.14/day.**

5. Regeneration of the deactivated catalyst

The regeneration process is required only when the catalyst shows signs of deactivation (e.g. concentration of target compounds treated exceeds admissible limit in air or water). At this point the treatment process is stopped. The regeneration of the catalyst can be conducted in the same reactor used for decontamination, following the procedure: flow washing for 2 hours with dilute HCl solution (1×10^{-3} M), pH 3, containing 5 g/L H_2O_2.

Parameters: flow rate = 36 m^3/hour; reactor capacity = 30 m^3

Total volume of regenerating solution: V = 30 m^3 + 2 × 36 m^3 = 102 m^3

H_2O_2 used (35 %, d =1.11 kg/L): 1312.8 L solution 35% to make 102 m^3 solution 5 g/L

Cost with H_2O_2 for regeneration: 1312.8 L × £ 0.268/L = **£ 351.8**

Hydrochloric acid (36 %, d =1.18 kg/L): ~8.8 L HCl concentrate to make 102 m^3 solution 10^{-3} mol/L.

Cost with HCl for regeneration: 8.8 L × £ 0.403/L = **£ 3.6**

Total cost with chemicals used in the regeneration process: **£ 355.4**

Summary of costs

The estimated costs for scale-up to a decontamination unit incorporating a 33 m^3 catalytic reactor are presented in Table A2

Table A2. Summarised cost for decontamination of air (93.3 mg EtSH/m^3 air) using the modified PAN/H$_2$O$_2$ catalytic system in the scaled-up unit

Item	Cost of treatment in a 33 m^3 reactor
Capital cost	**£ 31,688**
Materials	**£ 184,482**
- Catalyst	£176,085
- PP threads	£ 8397.9
Total running costs	**£ 2,280.7/day**
- H$_2$O$_2$ solution	£ 59.5/day
- Heating	£ 2211.1/day
- Electricity for pumps	£ 16.1/day
Catalyst regeneration (H$_2$O$_2$ + HCl)	**£ 355.4**